Delta-like 4 – Notch Signalling in Angiogenesis and Tumour Biology



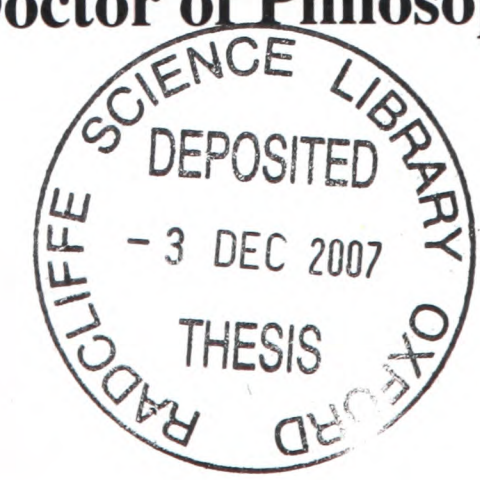
Thesis submitted by

Wen Shi

Magdalen College

for the degree of

Doctor of Philosophy



Delta-like 4 – Notch Signalling in Angiogenesis and Tumour Biology

Wen Shi
Magdalen College
University of Oxford

D.Phil.
Trinity Term
August 2007

Abstract

Notch signalling plays a key role in physiological development and tumourigenesis. The recent discovery and characterisation of Notch ligand Delta-like 4 (Dll4), which is predominantly expressed in endothelial cells, have underscored the role of Notch signalling in angiogenesis. This thesis investigates the regulation and function of Dll4-Notch signalling in angiogenesis and tumourigenesis.

First, the Dll4-Notch pathway interacted with the cellular hypoxia-sensing pathway. In human umbilical vein endothelial cells (HUVECs), Dll4 overexpression repressed hypoxic induction, and the repression was mediated by Notch target gene Hey2. In the breast cancer cell line MCF7, hypoxia induced Notch target gene Hey1 and ligand Jagged2 via hypoxia inducible factor 1. The hypoxic induction of Hey1 was also dependent on Notch signalling.

Second, Dll4 expression in HUVECs was up-regulated by several pathways. Notch signalling, activated by receptor overexpression, ligand stimulation or cell-cell contact, induced Dll4 expression. Treatment with vascular endothelial growth factor (VEGF) or hypoxia also induced Dll4 expression via Notch signalling. In addition, VEGF promoted Notch signalling and Dll4 expression in tumours.

Third, Dll4 expression in HUVECs was up-regulated by co-culturing with cancer cells. B16 mouse melanoma cells and human breast cancer cell lines induced Dll4 expression in HUVECs via Notch signalling. B16 cells also induced Dll4 expression via soluble factors independent of Notch signalling.

Finally, Dll4-Notch signalling regulated tumour growth *in vivo*. Dll4 overexpression in cancer cell lines activated Notch signalling in the stroma of xenograft tumours, and promoted the growth of human U87 (glioblastoma) and PC3 (prostate cancer) xenografts. In addition, Dll4-overexpressing U87 tumours were resistant to anti-VEGF treatment during later stages; however, they did respond to anti-Notch treatment.

Altogether, the Dll4-Notch pathway is tightly regulated and plays an important role in physiological and tumour angiogenesis. Inhibiting this pathway may be a viable therapy for cancers resistant to VEGF inhibition.

Acknowledgements

Studying towards a DPhil degree in the past three years has been the most challenging and fulfilling experience of my life. I could not have done it without the generous help and support from many individuals and organisations.

I am very grateful to Professor Adrian Harris for accepting me as a student in his lab and supporting my application for the Rhodes Scholarship. For the past three years, Adrian has offered me valuable guidance and support, on topics ranging from experimental design and data analysis to publications and career choices. I would also like to thank Dr Ji-Liang Li, who has co-supervised my work in the lab and provided helpful advice on how to complete my degree on time. In addition, Professor David Jackson and Dr Stephan Feller, who examined my transfer to DPhil status, offered constructive feedback on how I could improve my research.

Next, I would like to thank my colleagues in the lab. Richard Sainson has spent much time helping me design experiments and troubleshoot results, and has always been forthcoming with honest appraisals of my work. Laura Harrington is always kind and generous with her time and expertise, and also a great source of laughter. I appreciate Emily Heikamp for her humour and her perspective as the only other American in the lab. Other current and former lab members have taught me techniques, provided samples, helped with equipment and offered feedback on my results. An incomplete list includes Simon Wigfield, Howard Mellor, Helen Sheldon, Sarah Lowndes, Shalini Patiar, Francesca Buffa, Russell Leek, John Moore, Nilay Patel, Cassin Williams and Daniele Generali.

Outside the lab, I have enjoyed the friendship of fellow DPhil students Anthony Yeh, John Yuen, Alex Billioux, Camille Koppen, Hajar Masri, Samira Lakhal among others. It has always been beneficial for us to discuss problems, share tips and motivate each other. In addition, David Graham and Jane Rudman, successive Graduate Studies Officers, have unfailingly provided answers whenever I contacted them.

I am hugely indebted to the Rhodes Trust, and the Rhodes selection committees in the State of Michigan and District V, for giving me the opportunity to study at Oxford and believing in my abilities. Being a Rhodes Scholar is a great honour, and I hope I will do you proud. Among the Rhodes Trust staff, I would like to thank Sir Colin Lucas and Eliot Gerson for their generous help and advice, and Mary Eaton, Catherine King and Sheila Partridge for their assistance. I am also fortunate to have known fellow Rhodies, such as Lara Anderson, Ye Chen, Gary Huang, Jeff Ishizuka, Julia James, Renee Lee, Rick Malins, Eugene Shenderov and Paul Taylor.

In addition to the Rhodes Trust, Magdalen College has also been supportive of my DPhil studies. In particular, I would like to thank President Clary and Rev Piret for their kindness, and Nancy Cowell and Susan Burton for their assistance.

I am grateful to friends at the Oxford Speakers Club and mentors at the Johns Hopkins University. Your support and encouragement make my DPhil possible.

Most importantly, I want to thank my family. I would like to thank my Grandparents for raising me and always caring for me. I would like to thank my Mother, whose brave struggle against breast cancer provided the inspiration for my research. And I would like to thank my Father, who always believes in me more than I believe in myself, and motivates me to achieve bigger and better things.

Abbreviations

aa	Amino acid
AMP	Adenosine monophosphate
ANOVA	Analysis of variance
ARNT	Aryl hydrocarbon nuclear translocator
bFGF	Basic fibroblast growth factor
bp	Base pairs
BSA	Bovine serum albumin
cDNA	Complementary DNA
ChIP	Chromatin immunoprecipitation
CRUK	Cancer Research UK
Ct	Threshold cycle
DAPT	N-[N-(3,5-difluorophenacetyl)-L-alanyl]-S-phenylglycine t-butyl ester
DBZ	(S,S)-2-[2-(3,5-Difluorophenyl)acetylamino]-N-(5-methyl-6-oxo-6,7-dihydro-5H-dibenzo[b,d]azepin-7-yl)propionamide
DEPC	Diethylpyrocarbonate
Dll4	Delta-like 4
DMSO	Dimethylsulphoxide
DNA	Deoxyribonucleic acid
dNTP	Deoxyribonucleotide triphosphate
EC	Endothelial cells
ECD	Extracellular domain
ECGS	Endothelial cell growth supplement
ECL	Enhanced chemiluminescence
ECM	Extracellular matrix
EDTA	Ethylenediaminetetraacetic acid
ELISA	Enzyme-linked immunosorbent assay
FCS	Foetal calf serum
g	Gravitational acceleration
GFP	Green fluorescence protein
GSI	γ-secretase inhibitor
Hes	Hairy/enhancer of split
Hey	Hairy/enhancer of split related with YRPW motif
HIF	Hypoxia-inducible factor
HRE	Hypoxia response element
HRP	Horseradish peroxidase
HUVEC	Human umbilical cord endothelial cell
ICD	Intracellular Domain
Jag1	Jagged1
kb	Kilo bases
kDa	Kilo Daltons
KDR	Kinase domain region
mAb	Monoclonal antibody
MAPK	Mitogen-activated protein kinase
mRNA	Messenger RNA

mTOR	Mammalian target of rapamycin
NICD	Notch intracellular domain
PAGE	Polyacrylamide gel electrophoresis
PBS	Phosphate-buffered saline
PCR	Polymerase chain reaction
PI3K	Phosphatidylinositol 3-kinase
RAM	RBP-jκ associated module
RBP	Recombination-signal binding protein
rhDll4	Recombinant human Dll4 protein
RNA	Ribonucleic acid
RNAi	RNA interference
rrJag1	Recombinant rat Jag1 protein
SD	Standard deviation
SDS	Sodium dodecyl sulphate
SEM	Standard error of the mean
siRNA	Small interfering RNA
TACE	TNFα-converting enzyme
TM	Transmembrane
UTR	Untranslated region
VEGF	Vascular endothelial growth factor
VHL	von Hippel-Lindau

Abstract I

Acknowledgements II

Abbreviations VI

Chapter One: Introduction 1
1.1 Introduction 2
1.2 Notch signalling overview 3
1.3 Notch signalling in cancer 11
1.4 Notch signalling in angiogenesis 26
1.5 Notch ligand Dll4 37
1.6 Research aims 44

Chapter Two: Materials and Methods 45
2.1 Materials 46
2.2 General laboratory methods 52
2.3 Experimental methods 67
2.4 Mouse models 74
2.5 Statistical methods 75

Chapter Three: Functional Crosstalk between Notch and Hypoxia Pathways 76
3.1 Introduction 77
3.2 Notch-hypoxia crosstalk in HUVECs 78
3.3 Notch-hypoxia crosstalk in MCF7 cells 94
3.4 Summary 102

Chapter Four: Regulation of Dll4 Expression by Notch, VEGF and Hypoxia Signalling 104
4.1 Introduction 105
4.2 Notch signalling induced Dll4 expression 107
4.3 VEGF induced Dll4 expression 122
4.4 Hypoxia induced Dll4 expression 135
4.5 Summary 146

Chapter Five: Regulation of Dll4 Expression by Co-culturing with Cancer Cells 150
5.1 Introduction 151
5.2 HUVECs co-culture with B16 mouse melanoma cells 152
5.3 HUVECs co-culture with human breast cancer cell lines 170
5.4 Summary 177

Chapter Six: Effect of Dll4 Overexpression on Tumour Growth *in Vivo* 180
6.1 Introduction 181
6.2 Dll4 overexpression induced Notch signalling *in vitro* 183
6.3 Dll4 overexpression promoted U87 and PC3 tumour growth 186
6.4 VEGF inhibition retarded the growth of Dll4-overexpressing tumours 192

6.5 VEGF inhibition and Notch inhibition synergistically retarded the growth of Dll4-overexpressing tumours 198
6.6 Summary 204

Chapter Seven: Discussions and Conclusions **207**
7.1 Summary 208
7.2 Functional crosstalk between Notch and hypoxia pathways 209
7.3 Regulation of Dll4 expression by Notch, VEGF and hypoxia signalling 214
7.4 Regulation of Dll4 expression by co-culturing with cancer cells 217
7.5 Effect of Dll4 overexpression on tumour growth *in vivo* 220

References **224**

Appendices **241**

CHAPTER ONE

Introduction

1.1 Introduction

Angiogenesis, the growth of new blood vessels from pre-existing vessels, plays a key role in both embryogenesis and tumourigenesis. Early during embryonic development, blood vessels form *de novo* in a process termed vasculogenesis. These immature vessels then undergo angiogenesis to form a fully functional vascular network (Carmeliet, 2000). Physiological angiogenesis is a multi-step process tightly regulated by pro- and anti-angiogenic factors (Bergers and Benjamin, 2003). One of the best studied pro-angiogenic molecules is vascular endothelial growth factor (VEGF), which can be up-regulated under hypoxia, or low oxygen tensions (Ferrara et al., 2003).

Angiogenesis is also a hallmark of cancer (Hanahan and Weinberg, 2000). As tumours grow to a few millimetres in size, they lack blood supply and suffer from hypoxia. A subset of these tumours secretes pro-angiogenic factors such as VEGF, enabling blood vessel formation and exponential tumour growth (Bergers and Benjamin, 2003). A number of anti-angiogenic, especially anti-VEGF, treatments have been developed as cancer therapy (Ferrara and Kerbel, 2005).

Recently, the Notch signalling pathway has been implicated in both physiological and tumour angiogenesis. The Notch pathway is ubiquitously expressed and regulates a variety of cellular processes including differentiation, proliferation and apoptosis (Artavanis-Tsakonas et al., 1999). Notch signalling dysregulation has been reported in numerous cancer types (Radtke and Raj, 2003).

Notch signalling also plays an important role in angiogenesis. Deletion of several Notch pathway components caused angiogenic defects and embryonic lethality in mice (Iso et al., 2003a). In particular, the Notch ligand Delta-like 4 (Dll4) is expressed predominantly in the endothelium of developing vessels (Shutter et al., 2000). Several recent reports demonstrated that Dll4-Notch acts downstream of VEGF signals to prevent excessive angiogenesis (Sainson and Harris, 2007). Dll4-Notch signalling is also involved in tumour angiogenesis. Dll4 expression is up-regulated in the tumour vasculature (Rehman and Wang, 2006), and anti-Dll4 treatment led to excessive and non-functional angiogenesis, and reduced tumour growth *in vivo* (Thurston et al., 2007).

This chapter presents an overview of Notch signalling (Section 1.2) and reviews current literature on Notch signalling in cancer (Section 1.3), Notch signalling in angiogenesis (Section 1.4) and the Notch ligand Dll4 (Section 1.5). It ends with the research aims of this thesis (Section 1.6).

1.2 Notch signalling overview

1.2.1 Notch receptors and ligands

The Notch gene was originally discovered in *Drosophila* because flies heterozygous for this gene displayed notches at their wing margins. Further analyses in flies indicated that loss-of-function mutations of Notch produced a lethal "neurogenic" phenotype, in which cells destined to become epidermis switched fate and gave rise to neural tissue (Artavanis-

Tsakonas et al., 1999). Notch signalling has also been studied in a variety of other organisms, including *C. elegans*, zebrafish and mammals, and the pathway is conserved from flies to humans.

There is a single Notch receptor and two ligands (Delta and Serrate) in *Drosophila*. In mammals, there are four receptors and five ligands. Notch1-4 are homologues of *Drosophila* Notch; Delta-like-1, -3 and -4 (Dll1, Dll3, Dll4) are homologues of Delta; Jagged1 and Jagged2 (Jag1 and Jag2) are homologues of Serrate (Radtke and Raj, 2003).

Each Notch receptor is synthesized as a full-length precursor protein consisting of extracellular, transmembrane and intracellular domains. Within the Golgi apparatus, the precursor protein is cleaved by a furin-like convertase at site S1 within the extracellular domain and subsequently presented on the cell surface as a heterodimer. One subunit of the heterodimer contains the majority of the extracellular domain; the other contains the remainder of the extracellular domain, the transmembrane domain and the intracellular domain. The two subunits are linked non-covalently by calcium binding (Blaumueller et al., 1997).

All four Notch receptors contain conserved sequences (Figure 1.1). Within the extracellular domain are a number of epidermal-growth-factor (EGF)-like repeats, followed by three calcium-binding Lin12/Notch (LN) repeats. EGF-like repeats 11 and 12 are involved in ligand binding, and the LN repeats are necessary for interaction with the intracellular domain. The intracellular domain contains a RAM (RBP-jκ associated module) domain, six Ankyrin (also

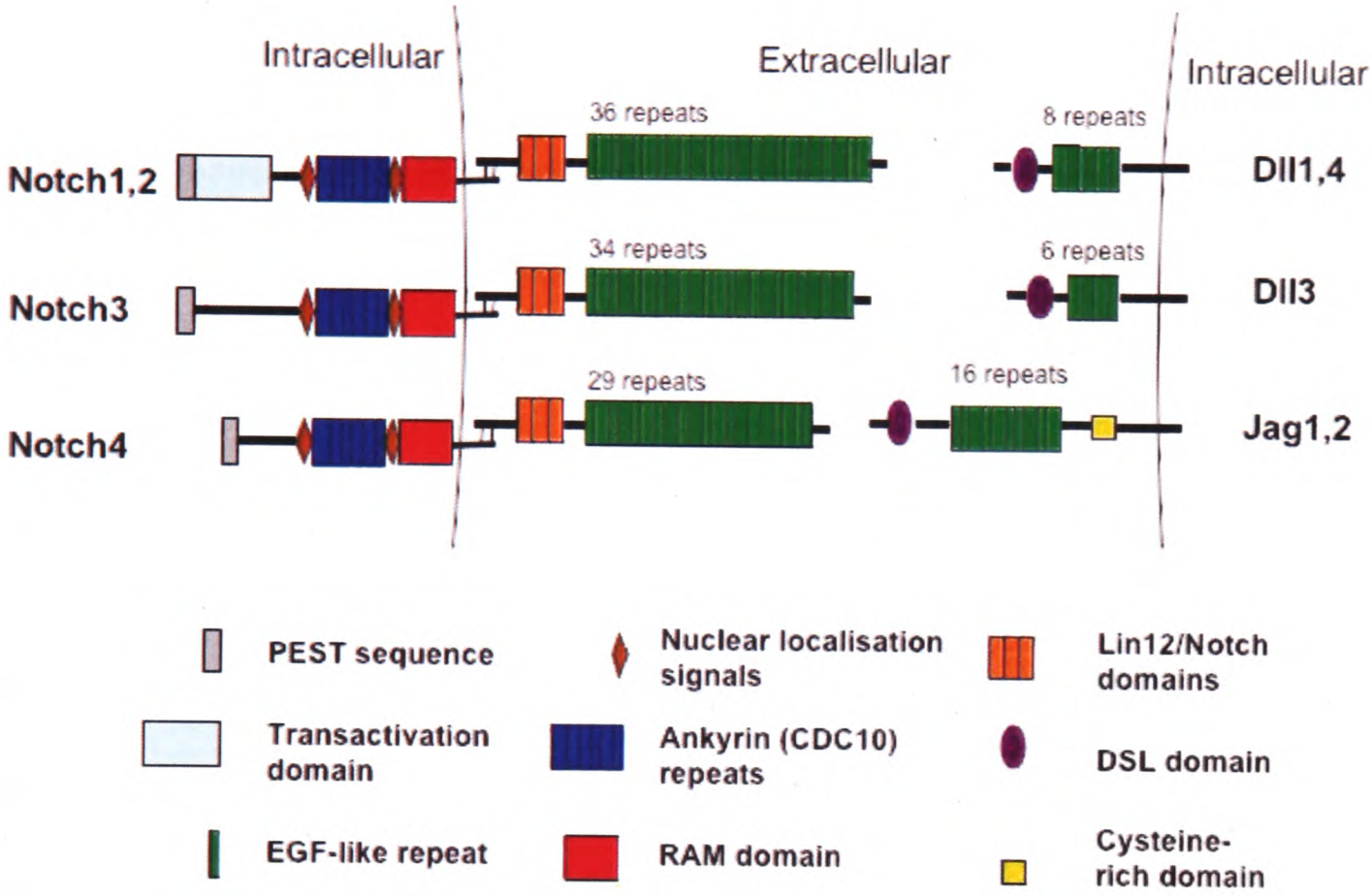


Figure 1.1. Mammalian Notch receptors and ligands.
The extracellular domains of Notch receptors contain a number of EGF-like repeats followed by three Lin12/Notch domains. The extracellular domains are connected to the transmembrane domains non-covalently. Within the intracellular domains, there is a RAM domain, six Ankyrin repeats flanked by nuclear localisation sequences, and transactivation domains (in Notch1 and Notch2 only). Finally, the receptors contain a conserved PEST sequence near the C-terminus. Both the Delta-like and Jagged ligands contain a DSL domain followed by EGF-like repeats. Jagged ligands also contain a cysteine-rich domain.

known as CDC10) repeats flanked by nuclear localisation signals, a transactivation domain and a PEST (proline, glutamic acid, serine and threonine) degradation sequence near the C-terminus. The intracellular domain is responsible for transducing Notch signalling to the nucleus (Radtke and Raj, 2003).

Similar to the receptors, Notch ligands are also Type I transmembrane proteins (Figure 1.1). All five ligands possess the conserved N-terminal structure named DSL (Delta, Serrate or LAG-2 from *C. elegans*), followed by EGF-like repeats. Jagged ligands also contain a cysteine-rich domain that is not present in Delta-like ligands (Radtke and Raj, 2003).

1.2.2 Notch signalling activation

Notch signalling is normally activated by ligand-receptor binding between two neighbouring cells (Figure 1.2). This interaction induces a conformational change in the receptor, exposing a cleavage site, S2, just extracellular to the cell membrane. After cleavage by the metalloprotease ADAM10 or TACE (TNF-α converting enzyme), the Notch receptor undergoes intramembrane proteolysis at site S3. This final cleavage, mediated by the γ-secretase complex, liberates the Notch intracellular domain (NICD), which then translocates into the nucleus to activate Notch target genes. Inhibiting γ-secretase function prevents the final cleavage of the Notch receptor, blocking Notch signal transduction.

In the absence of NICD cleavage, transcription of Notch target genes is inhibited by a repressor complex mediated by the DNA-binding protein RBP-jκ (also known as CBF1, CSL

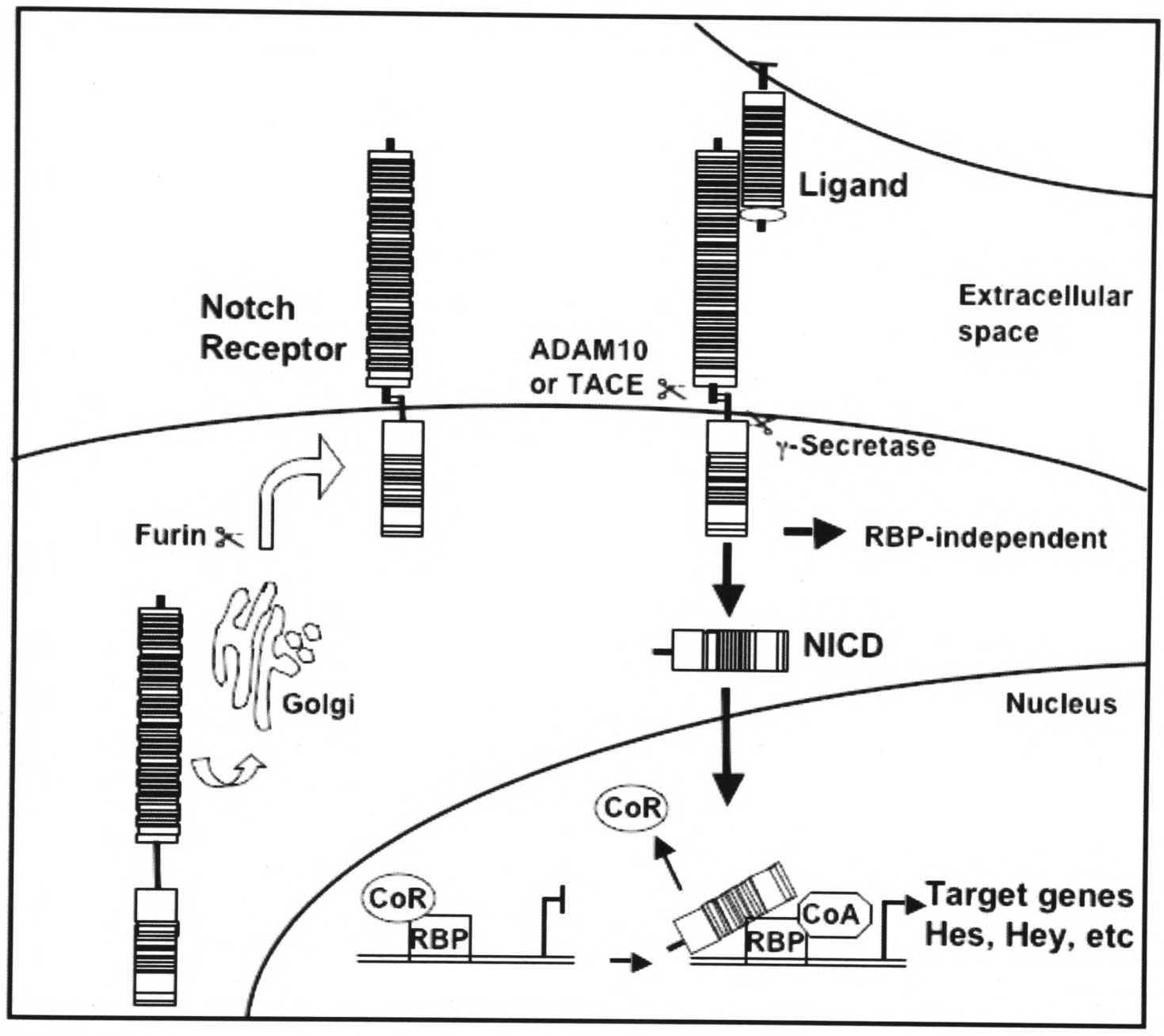


Figure 1.2. Ligand-activated Notch signalling.
Each Notch receptor is synthesized as a single precursor protein, cleaved by a furin-like convertase within the Golgi apparatus and presented on the cell surface as a heterodimer. Upon ligand binding, the receptor undergoes a conformational change that allows cleavage by ADAM10 or TACE. Next, the Notch receptor undergoes an intramembrane cleavage, mediated by γ-secretase, that liberates the Notch intercellular domain (NICD). NICD translocates into the nucleus, interacts with the transcription factor RBP-jκ and co-activators and activates target genes.

or Suppressor of Hairless in *Drosophila*, see Table 1.1). When NICD enters the nucleus, it disrupts the repressor complex and recruits co-activators such as Mastermind-like (MAML) 1 and the histone acetyltransferase p300/CBP. Together, NICD, RBP-jκ and MAML1 form a DNA-binding ternary complex that activates Notch target gene transcription (Wu and Griffin, 2004).

Table 1.1. Nomenclature for Notch pathway components

Name used in this thesis	Other names	Function	References
Notch1	TAN1	Receptor	(Dievart et al., 1999)
Notch4	INT3	Receptor	(Gallahan and Callahan, 1997)
RBP-jκ	CBF1, CSL, Suppressor of Hairless (*Drosophila*)	Transcriptional co-activator	(Leong and Karsan, 2006)
Hey1	Hesr1, Hrt1, Herp2, Chf2	Downstream target	(Iso et al., 2003b)
Hey2	Hesr2, Hrt2, Herp1, Chf1, Gridlock (Zebrafish)	Downstream target	(Iso et al., 2003b)
HeyL	Hesr3, Hrt3, Herp3	Downstream target	(Iso et al., 2003b)

1.2.3 Notch target genes

The best-characterised Notch target genes are transcriptional repressors of the Hes and Hey (also known as Herp, Hesr, Hrt or Chf) families (see Table 1.1). Notch signalling directly activates the transcription of Hes-1, -5, -7 and Hey-1, -2, -L via RBP-jκ binding sites in their promoters (Iso et al., 2003b). Moreover, Hes and Hey proteins are physiological effectors of Notch. Mice doubly deficient for *Hes1* and *Hes5* replicated the neurogenic phenotype of *Notch1* knockout mice (Kageyama and Ohtsuka, 1999), while mice doubly deficient for *Hey1* and *Hey2* replicated the angiogenic phenotype of *Notch1* knockout mice (Fischer et al., 2004).

Recent studies have yielded additional direct targets of Notch signalling in a variety of cellular contexts. The list includes oncogenes c-Myc (Klinakis et al., 2006), Cyclin D1 (Ronchini and Capobianco, 2001) and erbB2 (Chen et al., 1997); tumour suppressors PTEN (Whelan et al., 2007) and p21 (Rangarajan et al., 2001); arterial endothelial marker ephrin B2 (Iso et al., 2006); smooth muscle marker α-SMA (Noseda et al., 2006); and Nrarp (Pirot et al., 2004), a negative regulator of Notch signalling.

Recent studies in *Drosophila* have suggested that Notch can signal independently of the canonical Suppressor of Hairless (RBP-jκ homologue) pathway. However, it is unclear if this is the case in vertebrates. Some early evidence from myogenic cell lines and the developing avian neural crest has suggested that Notch signalling can occur in the presence of dominant negative RBP-jκ, but additional characterisation is needed to establish alternative downstream pathways in vertebrates (Martinez Arias et al., 2002).

1.2.4 Notch signalling modulation

Notch signalling is modulated by enzymes that control glycosylation of the receptors and ligands. One such enzyme is the protein O-fucosyltransferase 1 (POFUT1), which transfers O-linked fucose to EGF-like repeats (Shi and Stanley, 2003). Additionally, Fringe enzymes add N-acetyl-glucosamines to the O-linked fucose and thus affect the binding affinity of Notch receptors and ligands (Haltiwanger and Stanley, 2002).

Notch signalling is also regulated by ubiquitination and proteolysis. Several E3 ubiquitin ligases transfer ubiquitin to Notch receptors or ligands, targeting them for degradation (Lai, 2002). Su(dx)/Itch and Cbl both target membrane-bound Notch receptors for endocytosis and degradation in the lysosome. In contrast, Sel-10 ubiquitinates NICD in the nucleus, thereby limiting Notch signalling following receptor activation. Mindbomb and Neuralized interact with the intracellular domain of Delta-like ligands to promote their ubiquitination and internalization, which are necessary for Notch activation in adjacent cells (Callahan and Egan, 2004).

1.2.5 Physiological Notch signalling

The Notch signalling pathway is ubiquitously expressed in mammalian cells and regulates a variety of cellular processes, including stem cell maintenance, differentiation, cell-fate specification, proliferation and apoptosis. Notch signalling inhibits differentiation and promotes a stem-cell-like phenotype in the developing nervous system, muscles, intestines and T-cells; in contrast, it induces differentiation in the skin (Radtke and Raj, 2003). Notch signalling also participates in cell-fate decisions during development, via either lateral inhibition or lateral induction. In lateral inhibition, a group of equipotent cells start to express Notch ligands or receptors exclusively, thus adopting different cell fates. This phenomenon is best studied in neurogenesis in *Drosophila* (Artavanis-Tsakonas et al., 1999) but also observed in cochlear hair cell development in mammals (Lanford et al., 1999). In lateral induction, Notch ligands expressed in one cell type signals to Notch receptors in another cell type, inducing the recipient cells to differentiate into a particular lineage. For example, during

mouse lymphopoiesis, thymic epithelial cells expressing Notch ligands induce lymphocyte precursors to adopt the T-cell fate; in the absence of such signals, the precursors adopt the B-cell fate as the default pathway (Pear and Radtke, 2003).

Due to its role in regulating cellular differentiation and specifying cell fate, Notch signalling is critical in the development of multicellular organisms. In mammals, loss of Notch signalling leads to embryonic lethality due to severe defects in somitogenesis, angiogenesis, cardiogenesis and neurogenesis (Leong and Karsan, 2006). Notch signalling also regulates the development of postnatal and adult tissues (Artavanis-Tsakonas et al., 1999).

1.3 Notch signalling in cancer

1.3.1 Cancer overview

Cancer, characterised by uncontrolled cell growth, results from changes in the genome, especially mutations in oncogenes and tumour suppressors. According to Hanahan and Weinberg, all tumours accumulate six common characteristics in the multi-step process of tumourigenesis (Hanahan and Weinberg, 2000).

First, tumour cells demonstrate reduced dependence on external growth stimulation. Oncogenes such as Ras and c-Myc are frequently mutated in human cancers, promoting cell proliferation in the absence of growth signals (Field and Spandidos, 1990).

Second, tumour cells are insensitive to anti-growth signals. Normally, the TGFβ pathway suppresses the phosphorylation of Rb protein, preventing entry into S phase of the cell cycle. Members of this pathway are also frequently mutated in cancer (Fynan and Reiss, 1993).

Third, tumour cells acquire the ability to escape apoptosis, or programmed cell death. The p53 tumour suppressor protein can elicit apoptosis in response to DNA damage; *p53* gene mutation is observed in more than 50% of human cancers (Harris, 1996).

Fourth, tumour cells exhibit limitless replicative potential. Most normal cells have the capacity for 60-70 replications; however, stem cells and tumour cells have unlimited replicative potentials. It has been suggested that tumour cells may derive from normal stem cells or that cancers may harbour "cancer stem cells" that are resistant to treatment (Reya et al., 2001).

Fifth, tumours cells induce and sustain angiogenesis by secreting pro-angiogenic factors such as VEGF and fibroblast growth factors (FGF). Because the oxygen and nutrients supplied by the vasculature are critical for cell survival, neovascularisation is a prerequisite to the formation of macroscopic tumours. For a detailed discussion on tumour angiogenesis, refer to Section 1.4.2.

Sixth, tumours invade adjacent tissues and metastasise to distant sites. Invasion and metastasis depend on the process of epithelial-mesenchymal transition (EMT), in which

epithelial cells acquire mesenchymal properties such as reduced intercellular adhesion, degraded extracellular matrix and increased motility (Huber et al., 2005).

Hypoxia is yet another characteristic of cancers (Harris, 2002). As tumours grow beyond a few millimetres in size, simple diffusion of oxygen is not sufficient to reach all tumour cells. The resulting decrease in oxygen tensions activates the cellular hypoxia-sensing mechanisms, which are regulated by the transcription factor hypoxia inducible factor (HIF)-1. HIF1 consists of alpha and beta subunits. Under normoxia, or normal oxygen tensions, HIF1α is hydroxylated at two proline residues and ubiquitinated by the von Hippel-Lindau (VHL) complex, targeting it for proteasomal degradation. Under hypoxia, hydroxylation and subsequent degradation are reduced, and HIF1α translocates to the nucleus where it interacts with the HIF1β subunit, also know as ARNT (Aryl hydrocarbon nuclear translocator). The resultant protein complex activates transcription by binding to hypoxia response elements (HREs) in promoters. A schematic diagram of HIF1α activation under hypoxia is shown in Figure 1.3. A related protein, HIF2α, also interacts with HIF1β, binds to the HREs and up-regulates a different set of genes (Lofstedt et al., 2007). Hypoxia-regulated genes promote tumour growth, survival, angiogenesis and metastasis (Semenza, 2003).

Notch signalling impinges upon all major steps of tumourigenesis described above, by interacting with Ras, c-Myc, TGFβ, p53 and hypoxia signalling (see Table 1.2 for references), and by regulating tumour stem cells (Dontu et al., 2003, Fan et al., 2006), angiogenesis

(Rehman and Wang, 2006) and EMT (Zavadil et al., 2004). Not surprisingly, abnormal Notch signalling has been reported in numerous cancer types, including T-cell leukaemia and

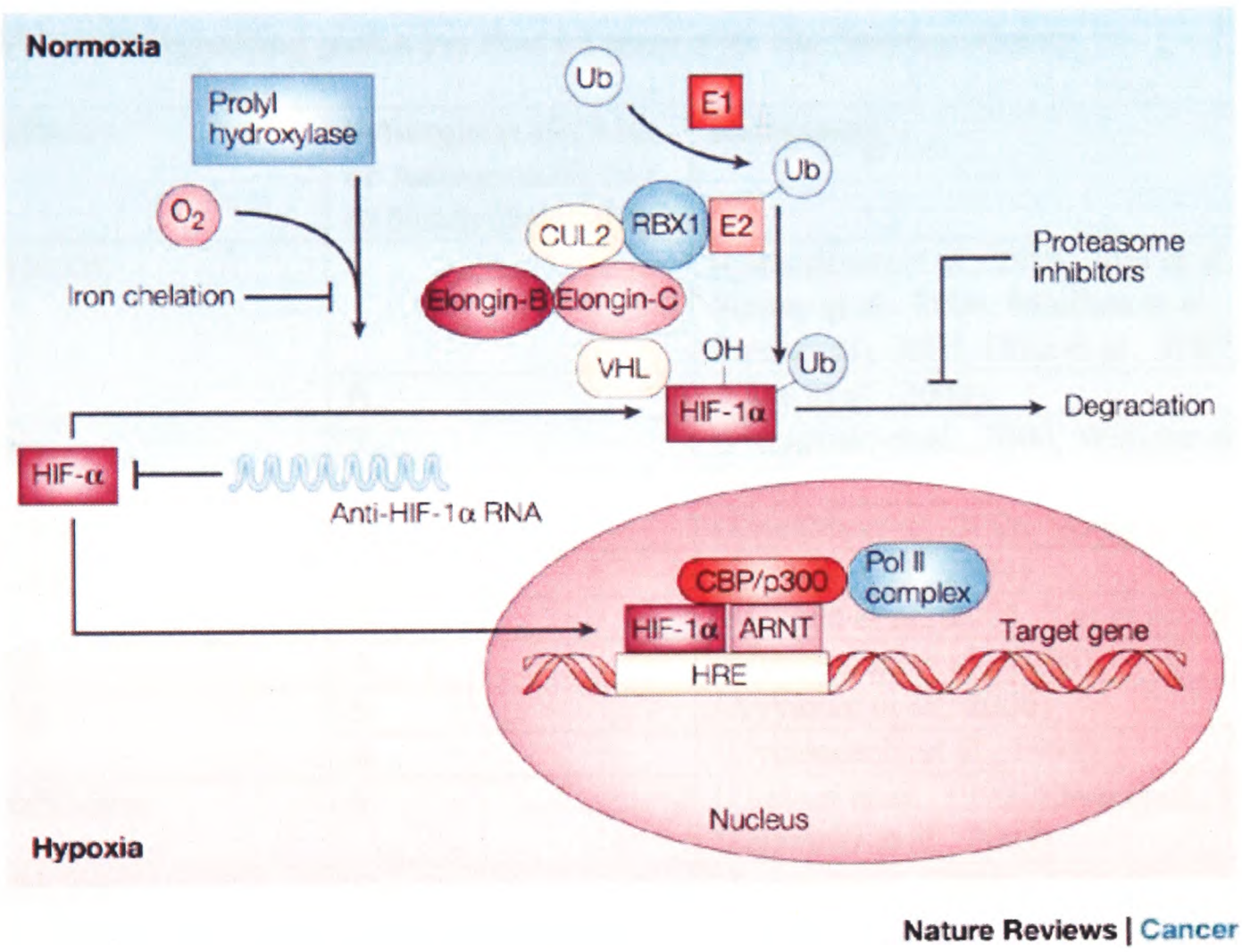


Figure 1.3. The HIF1 pathway under normoxia and hypoxia.
HIF1 is a heterodimeric transcription factor consisting of an alpha subunit and a beta subunit (also known as ARNT). Under normoxia, HIF1α is hydroxylated by prolyl hydroxylases and then ubiquitinated by VHL for proteasomal degradation. Under hypoxia, HIF1α is not hydroxylated or degraded; instead, it translocates into the nucleus, dimerises with ARNT and activates the transcription of hypoxia-regulated genes. The HIF1 binding sites in the promoters of such genes are called hypoxia response elements (HREs). This figure is from a published review (Harris, 2002).

lymphoma, as well as cancers of the breast, kidney, pancreas, prostate, cervix, endometrium, brain, intestine, lung and skin (Radtke and Raj, 2003, Leong and Karsan, 2006). Notch may play either a tumour-suppressive or an oncogenic role, depending on the cancer type, other signalling pathways present and the type of Notch receptors activated.

Table 1.2. Signalling pathways that interact with the Notch pathway

Pathway	**Synergistic (S) with or Antagonistic (A) to Notch Signalling**	**References**
Hypoxia	S	(Gustafsson et al., 2005, Jogi et al., 2002, Soares et al., 2004, Mailhos et al., 2001, Patel et al., 2005, Diez et al., 2007)
	A	(Chin et al., 2000)
Ras	S	(Fitzgerald et al., 2000, Weijzen et al., 2002)
c-Myc	S	(Klinakis et al., 2006, Weng et al., 2006)
TGFβ	S	(Zavadil et al., 2004)
	A	(Masuda et al., 2005, Sun et al., 2005)
p53	A	(Mungamuri et al., 2006)
Wnt	S	(Ayyanan et al., 2006)
	A	(Uyttendaele et al., 1998)
ErbB2/Neu	S	(Dievart et al., 1999, Chen et al., 1997, Sakamaki et al., 2005)
Estrogen	S	(Soares et al., 2004)

1.3.2 Notch as a tumour suppressor

Notch is a tumour suppressor in certain contexts including two types of skin cancer. Mice with Notch1-deficient skin developed basal cell carcinoma-like tumours (Nicolas et al., 2003). In another study, transgenic mice expressing a dominant negative form of MAML1, a pan-Notch inhibitor, developed cutaneous squamous cell carcinomas (Proweller et al., 2006). The

tumour-suppressive functions of Notch have also been reported in cervical cancer (Talora et al., 2002) and small cell lung carcinoma (Sriuranpong et al., 2001).

Two distinct mechanisms may contribute to the tumour-suppressive effects of Notch in the skin. First, N1ICD directly targets p21, a negative regulator of Rb phosphorylation and thus cell cycle progression in keratinocytes (Rangarajan et al., 2001). Second, Notch signalling induced differentiation by inhibiting p63, a molecule implicated in keratinocyte self-renewal and overexpressed in skin cancers (Nguyen et al., 2006).

1.3.3. Notch as an oncogene

The oncogenic role of Notch signalling is best documented in T-cell acute lymphoblastic leukaemia and lymphoma (T-ALL) (Roy et al., 2007). In a subset of T-ALL tumour cells, a t(7;9) chromosomal translocation fuses the 3' portion of Notch1 to the T-cell receptor Jβ locus. This results in a truncated Notch1 protein, which is constitutively active and aberrantly expressed (Ellisen et al., 1991) (Figure 1.4). In addition, activating mutations in Notch1 independent of the t(7;9) translocation were found in more than 55-60% of human T-ALL cases (Weng et al., 2004).

Beyond T-ALL, Notch signals are oncogenic in solid tumours including melanoma (Balint et al., 2005), medulloblastoma (Hallahan et al., 2004), as well as prostate (Santagata et al., 2004)

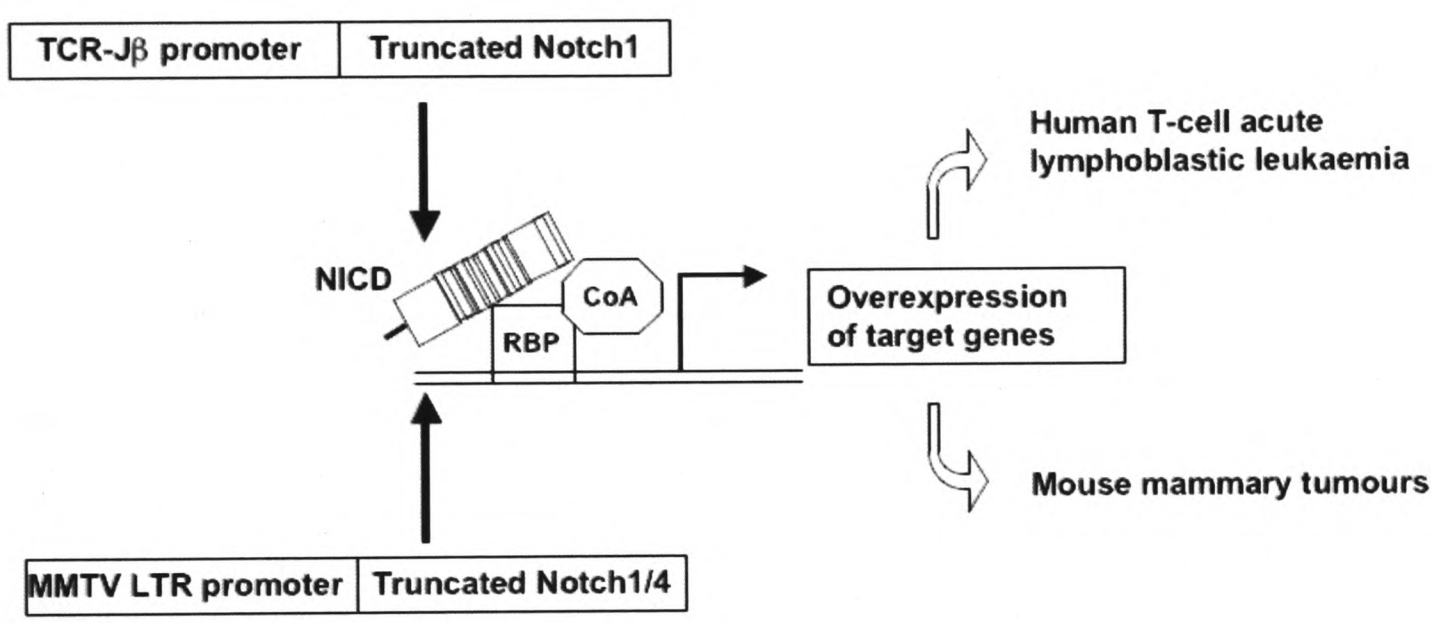


Figure 1.4. Oncogenic activation of Notch signalling.
Chromosomal translocation t(7;9) in humans juxtaposes the 3' portion of *Notch1* with the T-cell receptor Jβ locus. This results in constitutive activation of N1ICD, leading to T-cell acute lymphoblastic leukaemia. The mouse mammary tumour virus may insert into the *Notch1* or *Notch4* locus and lead to truncated Notch1 or Notch4 proteins. These constitutively active Notch intracellular domains can cause mouse mammary tumours.

and ovarian (Park et al., 2006) cancers. The role of Notch signalling in breast cancer is detailed in Section 1.3.4.

One mechanism for the oncogenic role of Notch may derive from its ability to regulate the stem cell phenotype (Androutsellis-Theotokis et al., 2006). As mentioned before, stem cells and cancer cells share common characteristics such as unlimited replication and undifferentiation. It has been proposed that tumours may originate from normal stem cells or contain "cancer stem cells" (Reya et al., 2001).

The role of Notch signalling in stem cells and cancer cells has been elucidated in the intestine. The intestinal epithelium consists of differentiated villi and proliferative crypts. The maintenance of stem cells, located in the crypts, depends on both Wnt and Notch signals. Overexpression of N1ICD in murine intestinal epithelium prevented the differentiation of crypt cells (Fre et al., 2005). In contrast, blocking Notch signalling by a γ-secretase inhibitor (GSI) converted proliferative crypt cells into differentiated goblet cells. Significantly, γ-secretase inhibition also led to decreased proliferation and increased differentiation in murine intestinal adenomas (van Es et al., 2005).

Notch signalling may play similar roles in stem cells of the breast. In an *in vitro* mammosphere model, Notch induced mammary stem cells to self-renew and early progenitor cells to proliferate. This effect was inhibited by a Notch4 neutralising antibody or GSI treatment (Dontu et al., 2003). Notch regulation of mammary stem cells may involve the protein Musashi1 (Msi1). Msi1 activates Notch signalling by translationally repressing the

Notch antagonist Numb (Okano et al., 2002). A recent report identified Msi1 as a marker for mammary stem cells with a role in breast tumourigenesis (Clarke et al., 2005).

Notch signalling may interact with the hypoxia-sensing pathway to synergistically promote the stem cell phenotype. In neuronal stem cells and muscle precursor cells, hypoxia activated Notch target genes and promoted the undifferentiated state in a Notch-dependent manner, as shown in Figure 1.5. Under hypoxia, HIF1α interacted with N1ICD, increasing its stability and enhancing the transcription of Notch target gene Hey2 (Gustafsson et al., 2005). This interaction may have implications for tumour growth. As mentioned in Section 1.3.1, hypoxia up-regulates a number of pathways conducive for tumour growth, such as angiogenesis, cell survival, glucose metabolism and metastasis. Inhibiting the hypoxia pathway has been explored as a cancer therapy (Semenza, 2003).

Indeed, evidence suggests that Notch-hypoxia crosstalk applies to cancer cells. In neuroblastomas, hypoxia up-regulated Notch1 and Hes1, resulting in de-differentiation and more aggressive tumours (Jogi et al., 2002). Another study reported that in the cervical cancer cell line HeLa, hypoxia induced γ-secretase activity and Notch cleavage (Wang et al., 2006).

Notch signalling impinges on the hypoxia pathway as well. In a study involving the breast cancer cell line MCF7, overexpression of full-length Notch1 or N1ICD up-regulated HIF1α protein level (Soares et al., 2004). Additionally, Hey2 was shown to block the induction of VEGF by HIF2α in NIH3T3 cells (Chin et al., 2000). Taken together, the relationship

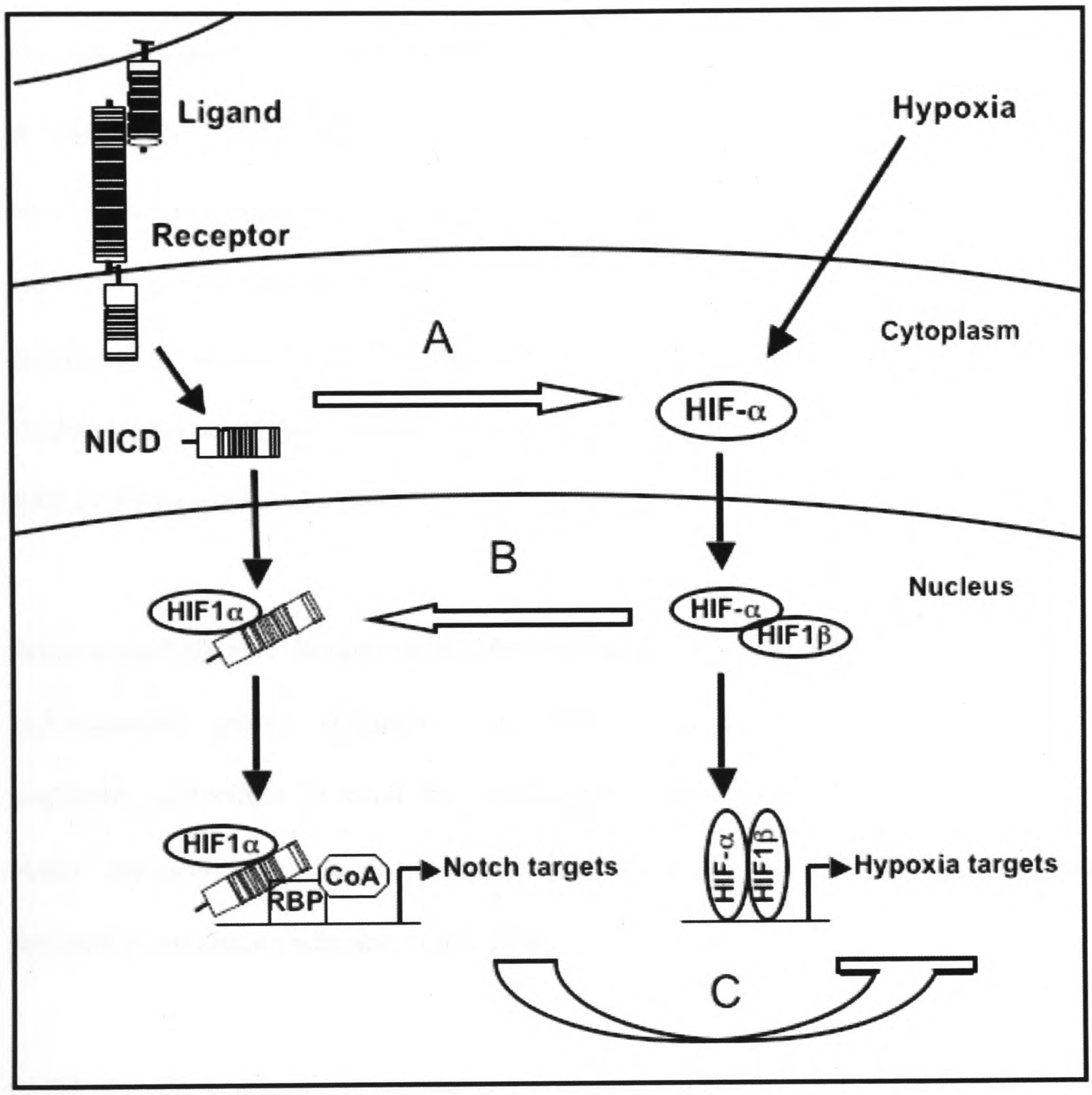


Figure 1.5. Notch and hypoxia signalling crosstalk.
Notch signalling (depicted on the left) and hypoxia signalling (depicted on the right) may interact both synergistically and antagonistically. (A) In MCF7 cells, overexpression of Notch1 or N1ICD increased HIF1α protein levels. (B) In stem and precursor cells, HIF1α was recruited to the promoter of Notch downstream genes, and promoted Notch signalling and the stem cell phenotype. Hypoxia also up-regulated Notch pathway components in neuroblastoma and cervical cancer cell lines. (C) Notch target gene Hey2 may interact with HIF1β and block the hypoxic induction of VEGF by HIF2α.

between Notch and hypoxia signalling may be synergistic or antagonistic, depending on the HIF protein involved and cellular context.

The Notch pathway interacts with other signalling pathways involved in tumourigenesis, such as Ras, c-Myc, p53, TGFβ and Wnt. Notch and Ras signalling synergize for oncogenic activity. In Ras-transformed fibroblasts, inhibiting Notch signalling reduced proliferation *in vitro* and tumour-formation ability *in vivo* (Weijzen et al., 2002). On the other hand, Ras signalling is required for Notch4-induced transformation. Treatment with Ras pathway inhibitors decreased the colony-formation ability of mammary tumour cells overexpressing N4ICD (Fitzgerald et al., 2000).

Notch signalling also directly targets the oncogene c-Myc, in both T-ALL (Weng et al., 2006) and mammary tumours (Klinakis et al., 2006). Conditional knockout of *c-Myc* in the mouse mammary epithelium blocked the tumourigenic effect of N1ICD. In 128 cases of human breast carcinomas, immunohistochemistry showed that N1ICD and Myc expression was positively correlated (Klinakis et al., 2006).

Notch signalling negatively regulates the tumour suppressor p53. Overexpression of N1ICD inhibited p53-mediated apoptosis and conferred chemoresistance to cancer cell lines (Mungamuri et al., 2006).

Notch signalling also interacts with the TGFβ pathway, which plays a dual role in tumour development. During early stages, TGFβ acts as a tumour suppressor by inhibiting

proliferation; during later stages, it functions as an oncogene by promoting invasion and metastasis through the process of EMT (Leong and Karsan, 2006). Notch signalling is involved in both these roles. The cervical cancer cell line CaSki, which spontaneously activates Notch1, did not show growth inhibition in response to TGFβ signalling (Masuda et al., 2005). Similarly, the MCF7 cell line expresses Notch4 and was resistant to the growth-inhibitory effects of TGFβ; blocking Notch receptor processing by GSI restored growth inhibition (Sun et al., 2005). However, Notch and TGFβ signalling may also act synergistically. At the onset of EMT, TGFβ induced Hey1 in mammary epithelial cells. Treatment with Hey1 antisense RNA or GSI blocked TGFβ-induced EMT (Zavadil et al., 2004). Thus, Notch signalling antagonizes or synergizes with TGFβ, but promotes tumour growth in either case.

Complex crosstalk also occurs between Notch and Wnt pathways. In primary human mammary epithelial cells overexpressing Wnt1 (Wnt1-HMECs), the expression of Dll1, Dll4, Notch3, Notch4, Hes1 and Hes5 was all up-regulated. Wnt1-HMECs formed tumours when injected into murine mammary glands; inhibiting Notch signalling suppressed tumour formation (Ayyanan et al., 2006). Other evidence suggests an antagonistic relationship between Notch and Wnt pathways. Wnt1 promoted branching morphogenesis of the murine mammary epithelial cell line TAC-2 while N4ICD inhibited branching (Uyttendaele et al., 1998).

For a list of major signalling pathways known to interact with Notch, see Table 1.2.

1.3.4. Notch signalling in breast cancer

The role of Notch signalling in breast cancer deserves special emphasis, as it is a focus of this thesis. The causal link between Notch signalling and breast tumourigenesis was established by a series of experiments in mouse models (Callahan and Egan, 2004, Politi et al., 2004). The first indication came from a study of the mouse mammary tumour virus (MMTV). MMTV insertion into the mouse genome may activate flanking proto-oncogenes and cause malignant transformation of the mammary gland. According to one study, in 20% of the mammary tumours thus developed, MMTV was inserted into the *Notch4* locus, originally referred to as *int3* (Gallahan and Callahan, 1987). These insertions resulted in truncated Notch4/Int3 proteins that were constitutively active (Figure 1.4). The gain-of-function mutation profoundly altered mammary growth and differentiation, resulting in spontaneous mammary tumours (Gallahan and Callahan, 1997).

Transgenic studies also confirmed the oncogenic activity of Notch4 in the murine mammary gland. Truncated Notch4/Int3 was expressed in mice under the control of the MMTV long terminal repeat. As a result, mammary glands did not develop normally, and mammary carcinomas were formed (Jhappan et al., 1992).

Besides Notch4, Notch1 is also involved in mammary tumourigenesis. Mice overexpressing the oncogene erbB2/neu were infected with MMTV, and among the tumours developed, 2 out of 24 had MMTV insertions into the *Notch1* locus. Similar to Notch4/Int3, the resulting

Notch1 proteins were also truncated and constitutively active (Dievart et al., 1999). This result suggests that Notch1 may cooperate with erbB2/neu in tumourigenesis.

The evidence is still accumulating for the involvement of Notch signalling in human breast cancer. One study reported that stably expressing N1ICD in the "normal" human mammary epithelial cell line MCF10A led to increased expression of Hey1 and cellular transformation *in vitro*. Further, in seven human breast cancer cell lines surveyed, the authors observed a clear accumulation of N1ICD, overexpression of Hey1, and loss of Notch antagonist Numb expression (Stylianou et al., 2006).

Callahan and colleagues identified a truncated form of Notch4, named h-Int3sh, in several human cancer cell lines (Imatani and Callahan, 2000). The short form, consisting of only partial Ankyrin repeats and the transactivation domain, transformed MCF10A cells *in vitro*. In a follow-up study, mice overexpressing h-Int3sh developed mammary tumours, but with a longer latency than mice overexpressing murine Notch4/Int3 (Raafat et al., 2004). Recently, Artavanis-Tsakonas and colleagues developed a transgenic mouse model expressing human N1ICD controlled by the MMTV long terminal repeat. These mice developed lactation-dependent tumours that evolved into adenocarcinomas (Kiaris et al., 2004).

Other studies have investigated the expression of Notch pathway components in human breast cancer samples (Shi and Harris, 2006). In one study, all seven tumours expressed Notch1 protein, while normal samples expressed little or no Notch1 protein (Weijzen et al., 2002). Similarly, accumulation of N1ICD and loss of Numb expression were observed in 20 breast

carcinoma samples of varying grade and hormonal status, indicating aberrantly activated Notch signalling (Stylianou et al., 2006). In a third study examining 97 samples, Notch1 mRNA level was higher in more aggressive tumours while Notch2 mRNA level was higher in less aggressive tumours (Parr et al., 2004). This is the only evidence to date suggesting that a Notch receptor might play a tumour-suppressive role in breast cancer.

A recent study demonstrated that the Notch antagonist Numb plays a role in breast tumourigenesis (Pece et al., 2004). Normal breast tissues expressed Numb; however, 50% of human breast tumours exhibited reduced levels of Numb. In primary cultures of breast cancer cells, introduction of Numb expression decreased Notch signalling and colony-formation ability; RNAi-mediated knockdown of Numb had the opposite effect.

The expression levels of certain Notch genes may also be a prognostic marker for breast cancer patient survival. In 184 tumours, high Notch1 or Jag1 expression predicted poor overall survival for the patient. Tumours expressing high levels of both Notch1 and Jag1 predicted even worse survival (Reedijk et al., 2005, Dickson et al., 2007). In another study, positive N1ICD expression in tumours correlated with shorter disease-free survival in patients (Farnie et al., 2007).

Overall evidence suggests that Notch signalling plays an oncogenic role in human breast cancer. This may be facilitated by Notch cooperating with two signalling pathways important in breast tumourigenesis: erbB2/neu and estrogen. N1ICD directly targets the erbB2 promoter, inducing its transcription (Chen et al., 1997). On the other hand, several breast

cancer cell lines that overexpress erbB2 exhibited marked activation of Notch1, which was abrogated by an erbB2 antagonist (Sakamaki et al., 2005). Estrogen is another crucial player in breast cancer. In the estrogen-sensitive cell line MCF7, 17β-estradiol treatment up-regulated Notch1 and Jag1, and promoted Jag1-induced Notch signalling (Soares et al., 2004).

1.4 Notch signalling in angiogenesis

1.4.1 Physiological angiogenesis

Almost all mammalian tissues require adequate supply of oxygen and nutrients delivered through blood vessels. Not surprisingly, blood vessels form early in embryonic development, in a process termed vasculogenesis. During this process, precursor cells (angioblasts) differentiate into endothelial cells (ECs) that assemble into a primary capillary plexus, which is immature and poorly functional. In the subsequent process of angiogenesis, the vasculature undergoes sprouting and remodelling to form a fully functional network (Carmeliet, 2000).

Angiogenesis is tightly regulated by activators and inhibitors. Activators of angiogenesis are mainly receptor tyrosine kinase ligands, such as VEGF, acidic and basic FGF, platelet-derived growth factor and epidermal growth factor. Inhibitors of angiogenesis include thrombospondin-1 and the statins (*e.g.* angiostatin, endostatin). An increase in activators or decrease in inhibitors triggers the "angiogenic switch" and activates endothelial cells for angiogenesis (Bergers and Benjamin, 2003). The angiogenic switch is depicted in Figure 1.6.

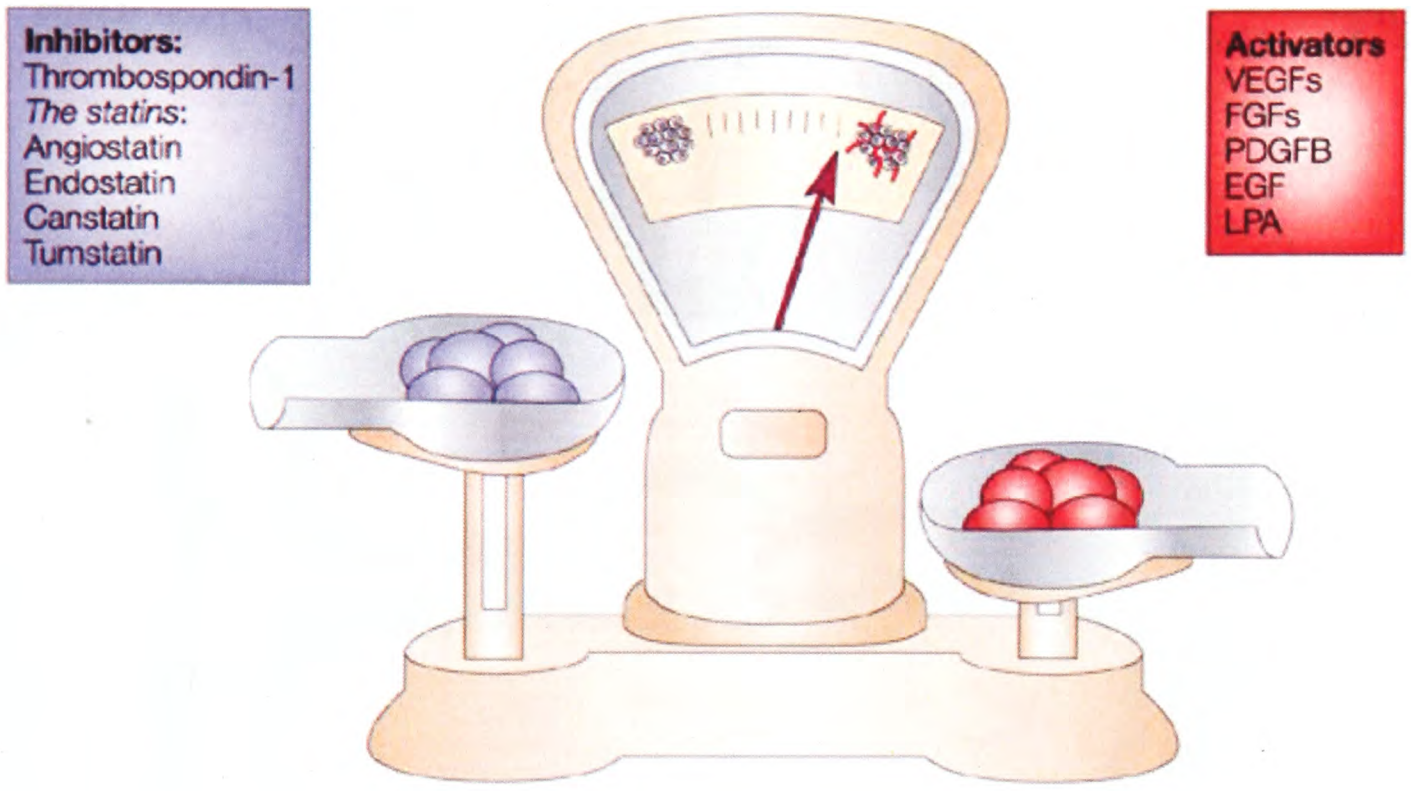


Figure 1.6. The angiogenic switch.
Angiogenesis is orchestrated by a variety of activators and inhibitors, a few of which are listed above. Angiogenic activators are mainly receptor tyrosine kinase ligands, such as vascular endothelial growth factor (VEGF), fibroblast growth factors (FGFs), platelet-derived growth factor (PDGF) and epidermal growth factor (EGF). The first described angiogenic inhibitor was thrombospondin-1. Many inhibitory molecules, such as statins, are derived from larger proteins that have no effect on angiogenesis. In general, the levels of activators and inhibitors dictate whether an endothelial cell will be in a quiescent or an angiogenic state. Changes in the angiogenic balance mediate the angiogenic switch. This figure is from a published review (Bergers and Benjamin, 2003).

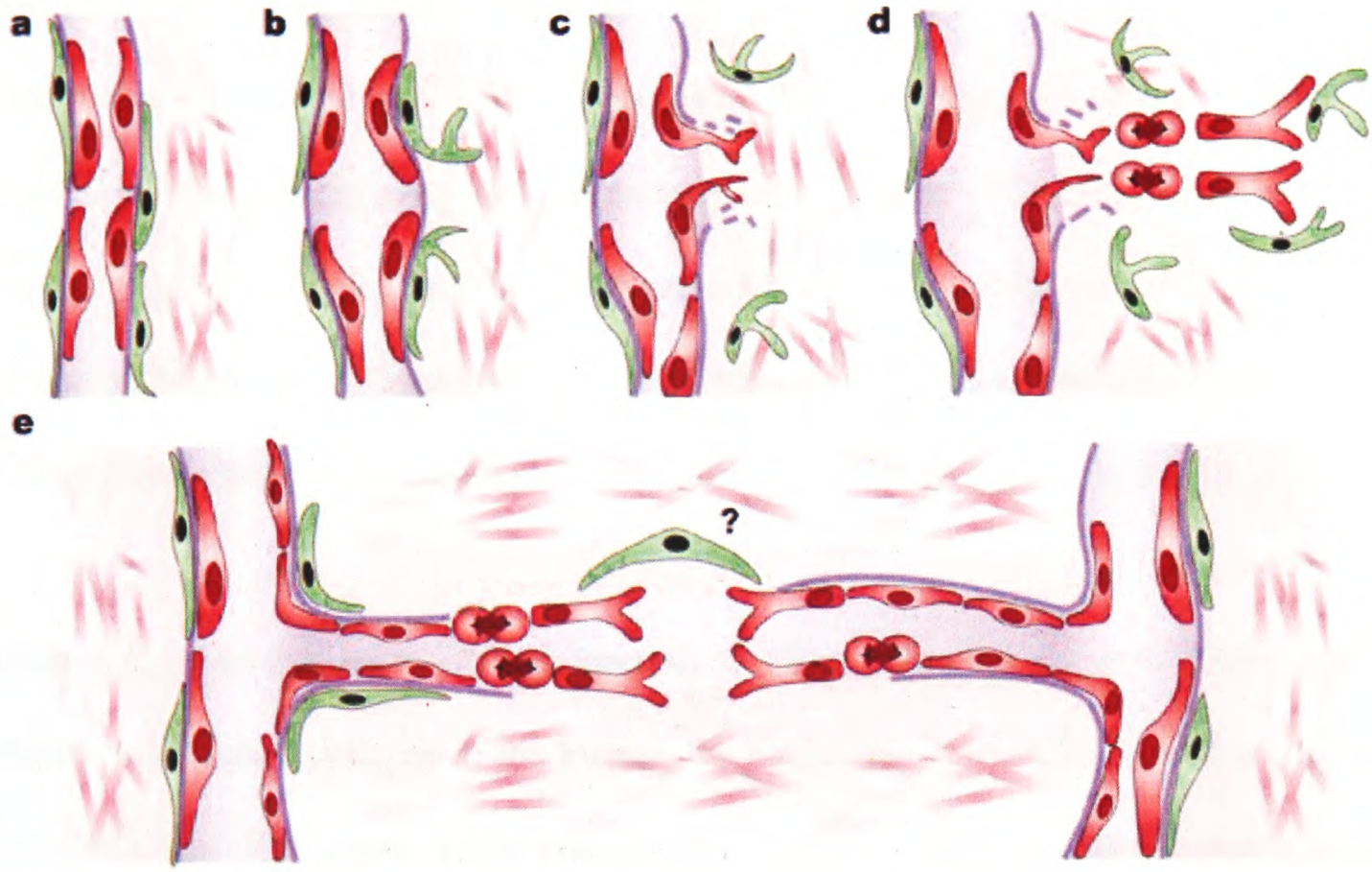


Figure 1.7. Steps of sprouting angiogenesis.
Blood vessels arise from pre-existing capillaries after activation of the angiogenic switch (a). (b) First, mural cells (green) detach, and the basement membrane and extracellular matrix are degraded. (c) This allows endothelial cells (red) to form sprouts towards angiogenic stimuli. (d) Tip cells control the direction of sprouting, and stalk cells proliferate to lengthen the sprouts. Stalk cells become polarised to create a lumen, which is accompanied by basement-membrane formation and mural cell attachment. (e) Finally, blood-vessel sprouts fuse with each other to build new circulatory systems. This figure is from a published review (Bergers and Benjamin, 2003).

Once endothelial cells become activated, they go through several steps to form new blood vessels (Figure 1.7). First, inter-endothelial cell contacts are loosened, and the surrounding basement membrane and extracellular matrix are degraded. This allows activated ECs to form sprouts consisting of "tip cells" and "stalk cells" (Gerhardt et al., 2003). The non-proliferative tip cells extend filopodia into the surrounding environment to screen for angiogenic stimuli, which dictate the direction of sprout migration. Sprout elongation requires proliferation in the stalk cells that subsequently become polarised to form the vessel lumina. Nascent vessels are coated with mural cells, including pericytes and smooth muscle cells, which are essential for vessel stabilisation and maturation. Finally, through fusion to an existing vessel, angiogenesis is completed and continuous blood flow is initiated (Sainson and Harris, 2007).

One of the key regulators of angiogenesis is VEGF, also known as VEGFA (Ferrara et al., 2003). Alternative splicing of the human *Vegf* gene produces three main isoforms containing 121, 165 and 189 amino acids respectively. $VEGF_{121}$ does not bind heparin and is freely diffusible. $VEGF_{189}$ binds to heparin with high affinity and is almost completely sequestered in the extracellular matrix. $VEGF_{165}$, the predominant isoform, has intermediary properties. VEGF binds to two related receptor tyrosine kinases, VEGFR1 (Flt1) and VEGFR2 (Flk1 or KDR). VEGFR2 is the major mediator of VEGF signalling and widely distributed in human tissues (Stewart et al., 2003). On the other hand, VEGFR1 may function as a decoy receptor by preventing VEGF binding to VEGFR2. A soluble form of VEGFR1 is an inhibitor of VEGF activity (Kendall and Thomas, 1993). In addition to VEGFR1 and 2, $VEGF_{165}$ also interacts with Neuropilin 1 and 2 (NRP1/2) receptors. In 1996, two studies showed that inactivation of a single *Vegf* allele in mice resulted in embryonic lethality by E11.5 due to

vascular defects (Carmeliet et al., 1996, Ferrara et al., 1996), emphasising the crucial role of VEGF signalling in physiological angiogenesis.

VEGF signalling is in turn regulated by the hypoxia-sensing pathway. HIF1 and HIF2 induce expression of VEGF, VEGFR1, VEGFR2 and other angiogenic activators. Targeted inactivation of either *Hif1α* or *Hif1β* in the mouse resulted in abnormal vascular development and embryonic lethality (Pugh and Ratcliffe, 2003).

Although angiogenesis occurs mainly during embryonic development, it is also observed in adults where both physiological (*e.g.* wound healing) and pathological (*e.g.* age-related macular degeneration, psoriasis and solid tumour growth) neo-vascularisation occurs.

1.4.2 Tumour angiogenesis

The ability to induce and sustain angiogenesis is a hallmark of cancer (Hanahan and Weinberg, 2000). When tumours first form, they are avascular and lack angiogenic ability. Due to a lack of oxygen and nutrients, tumour cells undergo a high rate of apoptosis, reaching a steady state with cell proliferation. As a result, these tumours lay dormant and cannot grow beyond a few millimetres in diameter. Later, a small subset of dormant tumours activates the angiogenic switch by secreting pro-angiogenic molecules such as VEGF and FGFs. Various studies of animal models and human tumours have demonstrated that angiogenesis is a prerequisite for exponential tumour growth (Bergers and Benjamin, 2003).

Although it is based on physiological angiogenesis, tumour angiogenesis is poorly regulated, without the proper balance of pro- and anti-angiogenic signals. The resulting tumour blood vessels are architecturally distinct from their normal counterparts. They are irregularly shaped, dilated, and often leaky and haemorrhagic. Mural cells, which are normally in close contact with the endothelium, frequently become more loosely attached or less abundant. Tumour vessels have also been reported to have cancer cells integrated into the vessel wall. Blood flows irregularly in tumour vessels, moving more slowly and sometimes even oscillating. Thus, the structural and functional abnormalities of the tumour vasculature reflect the pathological nature of their induction (Bergers and Benjamin, 2003).

VEGF, a key regulator of physiological angiogenesis, also play an important role in tumour angiogenesis. VEGF mRNA was up-regulated in numerous tumour types (Ferrara et al., 2003), and VEGFR2 protein was also present in various tumours (Stewart et al., 2003). Moreover, many cancer cell lines were inhibited *in vivo* by anti-VEGF treatments, including blocking antibodies, siRNA or small molecule inhibitors targeting VEGF or its receptors (Ferrara et al., 2003). Bevacizumab, a monoclonal antibody against human VEGF, has shown efficacy in treating several types of cancers by inhibiting angiogenesis (Ferrara and Kerbel, 2005). Although anti-VEGF treatments are promising, a growing number of cancer types do not respond or become resistant to VEGF blockade (Kerbel et al., 2001, Casanovas et al., 2005), necessitating the development of alternative approaches targeting angiogenesis.

In tumours, the VEGF gene can be induced by activation of oncogenes (*e.g.* Ras), loss of tumour suppressors (*e.g.* VHL) and hypoxia. Tumours exhibit elevated HIF and VEGF levels

at the rim of necrotic and hypoxic tissue, promoting new vessel sprouting to relieve the hypoxia (Bergers and Benjamin, 2003). The tumour suppressor VHL is a key component of the hypoxia-sensing pathway, targeting HIF-α subunits for proteasomal degradation (Figure 1.3). Inactivation of VHL resulted in constitutive stabilisation of HIF-α, upregulation of VEGF and increased angiogenesis (Pugh and Ratcliffe, 2003).

1.4.3 Notch signalling in physiological angiogenesis

The role of Notch signalling in both physiological and pathological angiogenesis has long been recognised. Notch pathway mutations have been linked to several vascular diseases (Shawber and Kitajewski, 2004). One is the neurovascular disorder, Cerebral Autosomal Dominant Arteriopathy with Subcortical Infarcts and Leukoencephalopathy (CADASIL). Patients suffer from neurological symptoms resulting from the loss of vascular smooth muscle cells surrounding cerebral arteries. The CADASIL phenotype correlates with missense mutations in Notch3 in a majority of patients, suggesting a role for Notch3 in maintaining vascular smooth muscle cells. In addition, the Notch ligand Jag1 has been implicated in Alagille syndrome (AGS). Mutations in Jag1 have been identified in 60-70% cases of AGS, a multi-organ developmental disorder with notable vascular phenotypes.

Direct evidence of Notch signal transduction in angiogenesis has come from a variety of *in vivo* and *in vitro* studies manipulating the expression levels of Notch pathway components. Homozygous deletion of *Notch1* in mice, either globally or endothelial-specifically, caused vascular remodelling defects in the yolk sac, placenta and embryo proper, leading to

embryonic lethality by day E10.5 (Krebs et al., 2000, Limbourg et al., 2005). Notch4 is specifically expressed in arterial endothelial cells (Uyttendaele et al., 1996); however, *Notch4*-null mice developed normally and were fertile. Interestingly, homozygous deletions of both *Notch1* and *Notch4* had a synergistic effect, as the doubly mutant mice exhibited more severe vascular defects than *Notch1*-null mice (Krebs et al., 2000). Overexpression of Notch4 also caused vascular abnormalities. Expression of activated Notch4 in the mouse embryonic vasculature led to angiogenic defects similar to that of the *Notch1/4* double knockout mice (Uyttendaele et al., 2001). Taken together, these results indicate that either abrogation or forced activation of Notch signalling disrupts blood vessel development, suggesting an optimal range is required for angiogenesis.

The angiogenic role of Notch signalling extends beyond embryonic development. Expression of activated Notch4 in adult mice using a tetracycline-repressible system led to arteriovenous malformations (AVM) in the liver and lethality within weeks. Notch4 overexpression induced hepatic vascular shunting, arterialisation and induction of other Notch pathway genes. The AVM was reversible in moribund mice after suppression of Notch4 expression with doxycycline (Carlson et al., 2005).

A number of *in vitro* studies have shed light on the mechanisms of Notch signalling in angiogenesis. One study showed that $VEGF_{165}$ treatment of human umbilical vein endothelial cells (HUVECs) induced Notch1 cleavage and Hes1 expression within 15 to 30 minutes. This effect was dependent on γ-secretase activity, as the γ-secretase inhibitor DAPT blocked VEGF-induced Notch1 cleavage (Takeshita et al., 2007). Another study showed that VEGF

treatment up-regulated the mRNA levels of both ADAM10, responsible for Notch cleavage at S2, and presenilin1, a component of γ-secretase responsible for cleavage at S3. Western blotting and immunostaining also showed that VEGF induced the N4ICD accumulation in the nucleus (Hainaud et al., 2006). Thus, Notch signalling is a downstream target of VEGF signalling.

Other studies have suggested that Notch signalling may antagonise VEGF signalling. Overexpression of Hey1 in endothelial cells down-regulated VEGFR2 mRNA levels and blocked proliferation, migration and network formation (Henderson et al., 2001). Further, overexpression of either N1ICD or N4ICD induced Hey1, down-regulated VEGFR2 and decreased EC proliferation in response to VEGF (Taylor et al., 2002).

VEGF promotes EC proliferation by activating MAPK/Erk and PI3K/Akt pathways. Endothelial cells overexpressing N1ICD showed reduced phosphorylation of Erk1/2 and Akt after VEGF stimulation (Liu et al., 2006). Another study showed that N4ICD overexpression inhibited EC proliferation by inducing G_0/G_1 cell cycle arrest (Noseda et al., 2004). Additionally, overexpression of N4ICD inhibited sprouting in human dermal microvascular endothelial cells (Leong et al., 2002). On the other hand, Sainson et al. showed that inhibiting Notch signalling increased vessel diameter and VEGF-induced sprouting by promoting proliferation in stalk cell and tip cells, respectively (Sainson et al., 2005). Taken together, Notch signalling may act downstream of VEGF and antagonise VEGF signalling to modulate angiogenesis. Further evidence of the role of Notch ligand Dll4 in angiogenesis will be reviewed in Section 1.5.3.

1.4.4 Notch signalling in tumour angiogenesis

Notch signalling is also involved in tumour angiogenesis, as demonstrated by recent evidence from human tumour samples and mouse xenograft studies. One of the best-characterised examples involves the Notch ligand Jag1 in head and neck cancer. Wang and colleagues demonstrated that Jag1 expressed in head and neck squamous cell carcinoma (HNSCC) cells triggered Notch activation in neighbouring endothelial cells and promoted EC network formation. This effect was abolished by blocking Notch signalling through γ-secretase inhibition, soluble Jag1 treatment or dominant negative RBP-jκ expression in the ECs. In xenograft models, HNSCC cells overexpressing Jag1 formed larger tumours with increased vascularisation. Moreover, Jag1 protein levels were significantly higher in human HNSCC samples compared with normal samples. Jag1 protein levels correlated with vascular density in tumours (Zeng et al., 2005). These results provided the first causal link between Notch signalling and tumour angiogenesis, and described a novel mechanism of juxtacrine signalling from tumours to the surrounding vasculature (Li and Harris, 2005).

Due to its important role in tumourigenesis and tumour angiogenesis, the Notch pathway may be a viable target for cancer treatment. Tools to block Notch signalling include γ-secretase inhibitors, soluble ligands and monoclonal antibodies. Of these, small-molecule GSIs have been developed to treat Alzheimer's disease, since γ-secretase also cleaves the amyloid precursor protein to form β-amyloid peptides, a key component of plaques (Kopan and Goate, 2000).

A number of studies have used GSIs to inhibit Notch signalling in tumour models. Kaposi's sarcoma (KS) is a type of tumour that derives from endothelial cells. Activated forms of Notch-1, -2, -4 as well as Hey1 and Hey2 were markedly overexpressed in KS tumour samples and cell lines compared with endothelial cells. GSI treatment reduced Notch signalling and caused apoptosis of KS cells *in vitro*. In xenograft models, intratumoural injection of GSI inhibited KS tumour growth by decreasing proliferation and increasing apoptosis (Curry et al., 2005).

Notch blockade may also target the tumour vasculature. Several different types of GSIs reduced endothelial cell proliferation, tube formation and sprouting *in vitro*. In mouse models of human glioblastomas and lung adenocarcinomas, both highly vascularised tumours, DAPT potently reduced tumour growth and vascularisation (Paris et al., 2005).

While GSIs are well developed and effective, they target all Notch receptors (and an increasing list of other transmembrane proteins). Since Notch signalling is required for many physiological processes, GSI treatment may cause widespread toxicity. Tumour- or tumour vessel-specific Notch pathway components may represent superior targets for anti-cancer therapy. The Notch ligand Dll4 is one such target.

1.5 Notch ligand Dll4

1.5.1 Discovery and expression

The discovery of Dll4 as an endothelial-specific Notch ligand (Shutter et al., 2000) has expanded our understanding of the role of Notch signalling in angiogenesis. The *Dll4* gene is located on chromosome 15q21.1 and encodes a 686-aa single-pass Type I transmembrane protein. Dll4 is conserved during evolution, with the human and mouse proteins sharing 87% sequence identity. The extracellular domain of human Dll4 contains a DSL domain necessary for Notch receptor activation, followed by eight EGF-like repeats (Figure 1.1). Dll4 is a ligand for Notch1 and Notch4 (Shutter et al., 2000).

In mouse embryogenesis, Dll4 expression is largely restricted to the endothelium of developing vessels and a small number of additional tissues (*e.g.* the thymus, the retina and intestinal crypts). Endothelial expression of Dll4 is confined to arteries, arterioles and capillaries, and is absent in veins (Shutter et al., 2000, Benedito and Duarte, 2005). Most interestingly, Dll4, which is not widely expressed in the adult vasculature, was found to be up-regulated in vessels in a variety of solid tumours (Mailhos et al., 2001, Patel et al., 2005, Patel et al., 2006).

1.5.2 Regulation of Dll4 expression

Dll4 expression in endothelial cells is regulated by several factors important in angiogenesis, including VEGF, basic FGF (bFGF), HIF1α, Notch and Foxc proteins. VEGF induced Dll4 expression in HUVECs and several arterial endothelial cell types (Liu et al., 2003, Patel et al.,

2005). The induction was dependent on PI3K/Akt signalling and mediated by both VEGFR1 and VEGFR2 (Liu et al., 2003). In another study, VEGF induction of Dll4 was augmented by 8bromo-cyclic AMP treatment (Yurugi-Kobayashi et al., 2006). Similarly, bFGF, another pro-angiogenic molecule, has been shown to induce Dll4 expression in HUVECs (Patel et al., 2005).

Hypoxia also induced Dll4 expression in a variety of endothelial cell types (Mailhos et al., 2001, Patel et al., 2005, Diez et al., 2007). The induction was mediated by HIF1α and not HIF2α (Patel et al., 2005). Several putative HREs have been identified within the *Dll4* promoter; however, a promoter fragment not containing any HRE was still inducible by HIF1α (Diez et al., 2007).

Interestingly, Dll4 expression is also regulated by Notch signalling. Overexpression of the constitutively active N4ICD induced Dll4 expression in human microvascular endothelial cells (Shawber et al., 2003). Similar results were obtained when HUVECs were stimulated by immobilised Dll4 ligands (Ridgway et al., 2006).

Finally, Foxc1 and Foxc2, two closely related transcription factors of the forkhead family, directly bind to the *Dll4* promoter and activate its transcription. Foxc1 and Foxc2 double heterozygous mice die *in utero* due to arteriovenous malformations, with reduced or lost expression of Dll4, Notch1, Notch4 and Hey2 (Seo et al., 2006).

1.5.3 Dll4 signalling in physiological angiogenesis

A number of *in vitro* and *in vivo* studies have underscored the important role of Dll4 in endothelial cell function and angiogenesis. In a co-culture experiment, stimulation by Dll4 but not Jag1 induced the expression of arterial marker ephrin B2 in HUVECs, and the induction was blocked by DAPT treatment (Iso et al., 2006). VEGF treatment also induced Dll4 and ephrin B2 and repressed EphB4, a venous marker (Hainaud et al., 2006). These two studies suggest that Dll4-Notch signalling may play a role in arterial differentiation.

A recent microarray study from our laboratory identified additional target genes of Dll4-Notch signalling in HUVECs (Harrington et al., 2007). In particular, Dll4 overexpression down-regulated VEGFR2 and VEGF co-receptors NRP1/2, and up-regulated decoy receptor VEGFR1. In addition, Dll4 signalling promoted the secretion of soluble VEGFR1, an inhibitor of VEGF signalling. As a result, VEGF signalling was reduced, and sprouting angiogenesis was inhibited in a three-dimensional tubulogenesis assay. Thus, Dll4-Notch may act downstream of VEGF as a negative feedback to limit VEGF signalling.

Because of the important roles of Dll4-Notch signalling, it is not surprising that Dll4 expression level is crucial for EC function. Previous work in our laboratory has demonstrated that either RNAi-mediated downregulation or retroviral overexpression of Dll4 in endothelial cells inhibited proliferation, migration and network formation, all crucial processes in angiogenesis (Patel et al., 2005, Williams et al., 2006). These results indicate that an optimal window of Dll4 expression is essential for EC function.

The dosage sensitivity of Dll4 expression was also observed in developmental angiogenesis. Single allele deletion of *Dll4* in mice resulted in embryonic lethality by E10.5 in most genetic backgrounds tested (Krebs et al., 2004, Duarte et al., 2004, Gale et al., 2004). Heterozygous lethality had previously been described for *VEGF* haploinsufficient mice (Carmeliet et al., 1996, Ferrara et al., 1996). Anatomical analysis of Dll4+/- embryos demonstrated that lethality was due to angiogenic defects such as abnormal constriction of the aorta, lack of well-defined major arteries and increased vessel branching and sprouting. Notably, the heterozygous lethal phenotype depended on the genetic background of the mice, ranging from 100% (fully lethal) to approximately 60% (Thurston et al., 2007). Some Dll4+/- mice of the outbred ICR strain survived without apparent defects; however, none of the Dll4-/- mice survived beyond E10.5 (Duarte et al., 2004).

Recent studies on the mouse retina have further elucidated the role of Dll4-Notch signalling in physiological angiogenesis. The mouse retina is avascular at birth. During the first three postnatal weeks, the retinal vasculature develops as an expanding network from the optic nerve to the periphery of the retina, with a characteristic pattern of radially alternating arteries and veins. Dll4 mRNA expression was observed in tip cells at the leading edge of the growing vascular network, and in a subset of stalk cells in immature arteries (Claxton and Fruttiger, 2004). Intraocular injection of $VEGF_{165}$ increased Dll4 expression in tip cells, while VEGF trap or VEGFR2-blocking antibody markedly inhibited Dll4 expression (Lobov et al., 2007, Suchting et al., 2007).

Various strategies have been used to inhibit Dll4 signalling in the retinal model, including genetic insufficiency (in Dll4+/- mice of the outbred ICR strain), soluble Dll4 protein, Dll4-blocking antibodies and γ-secretase inhibitors. Despite the difference in approaches, the studies all reported that Dll4 inhibition increased EC proliferation and sprouting, leading to a dense network of highly interconnected vessels (Hellstrom et al., 2007, Lobov et al., 2007, Ridgway et al., 2006, Suchting et al., 2007). Notably, VEGF gradients were not affected in Dll4+/- retinas. Rather, increased sprouting may be explained by the upregulation of VEGFR2 and downregulation of the decoy receptor VEGFR1 in Dll4+/- endothelial cells, increasing their responsiveness to VEGF (Suchting et al., 2007). In summary, VEGF induces Dll4-Notch signalling, which in turn suppresses excessive sprouting angiogenesis. Dll4-Notch signalling acts as a negative feedback mechanism to modulate VEGF signalling *in vivo*, consistent with the role of Dll4-Notch signalling in angiogenic models *in vitro* (Harrington et al., 2007).

1.5.4 Dll4 signalling in tumour angiogenesis

Studies of tumours in humans and mice have shown that Dll4 is expressed in the tumour vasculature. Dll4 mRNA levels were markedly induced in the vessels of human breast, kidney and bladder cancers (Mailhos et al., 2001, Patel et al., 2005, Patel et al., 2006). In the kidney and bladder cancer samples, Dll4 expression positively correlated with VEGF expression at the mRNA level (Patel et al., 2005, Patel et al., 2006).

In a xenograft study, the human MCF7 cell line formed tumours expressing high levels of mouse Dll4 within their vasculature (Mailhos et al., 2001). Similarly, Lewis lung carcinoma allograft tumours specifically induced Dll4 expression in tumour vessels. Treatment with a VEGF-trap decreased Dll4 mRNA expression in the vessels (Noguera-Troise et al., 2006). In a mouse transgenic model of hepatocarcinoma characterised by strong remodelling of tumour vessels and increased VEGF expression, Dll4 and Notch4 levels increased in transgenic livers compared with normal livers. Double immunostaining showed co-expression of Dll4 and Notch4 in endothelial cells (Hainaud et al., 2006). Altogether, Dll4 expression is restricted to the tumour vasculature and under the control of VEGF.

Several studies have manipulated Dll4-Notch signalling in tumour models with striking effects on angiogenesis and tumour growth. One study transduced rat C6 glioma cells with retroviral vectors encoding either full-length Dll4 (Fl Dll4) or soluble Dll4 (sDll4), and then implanted the cells into mice (Noguera-Troise et al., 2006). In the resulting tumours, C6-Fl Dll4 cells activated host Notch signalling, whereas C6-sDll4 cells repressed host Notch signalling. The vasculature of C6-Fl Dll4 tumours showed fewer branches and sprouts compared with control tumours, leading to better vessel perfusion but no difference in tumour size. In contrast, the vasculature of C6-sDll4 tumours was much more branched compared with control tumours. Despite increased vascular density, C6-sDll4 tumours were poorly perfused and smaller in size (Noguera-Troise et al., 2006). In a similar study, HT29 (human colon cancer) and KS-SLK (human Kaposi's sarcoma) cells were transfected with vectors to produce Fl Dll4 or sDll4. In this case, Fl Dll4 did not have obvious effects on the tumour vasculature. However, tumours expressing sDll4 showed vessels with more branches and

poorer perfusion (Scehnet et al., 2007). In the same study the murine sarcoma cell line S180 was implanted into adult Dll4+/- mice. Vessels in the allograft tumours showed a lack of structure and deficiency in pericyte recruitment (Scehnet et al., 2007). Hence, the Dll4-Notch pathway normally serves as a negative regulator of vessel sprouting and branching. Blockade of this pathway results in increased but non-productive angiogenesis, leading to reduced tumour growth.

Effort is afoot to develop clinically useful agents targeting Dll4-Notch signalling. Intratumoural or systemic injection of soluble Dll4 or a Dll4-blocking antibody reduced tumour growth, by 50% to more than 90%, in a variety of xenograft models. Reducing Dll4 expression resulted in increased angiogenesis but reduced vessel perfusion and tumour growth (Noguera-Troise et al., 2006, Ridgway et al., 2006).

Interestingly, anti-Dll4 treatment and anti-VEGF treatment act by different mechanisms to inhibit tumour growth. Anti-VEGF treatment results in a regression of tumour vessels, leading to decreased tumour perfusion. In contrast, anti-Dll4 treatment results in increased angiogenesis but poorly functional vessels, also leading to decreased tumour perfusion (Thurston et al., 2007). Inhibiting Dll4 signalling reduced the growth of xenograft tumours resistant to VEGF inhibition, including human sarcomas HT1080 and MMT and murine leukaemia WEHI3 (Noguera-Troise et al., 2006, Ridgway et al., 2006). In xenograft tumours of MV-522 lung carcinoma, co-treatment with anti-Dll4 and anti-VEGF antibodies synergistically inhibited tumour growth (Ridgway et al., 2006). Simultaneously blocking Dll4 and VEGF signalling may prove efficacious in treating a wide range of cancers in the clinic.

1.6 Research aims

This thesis investigates the regulation and function of Dll4-Notch signalling in angiogenesis and tumourigenesis.

Chapter 3 examines the functional crosstalk between Notch and hypoxia pathways in both HUVECS and MCF7 cells.

Chapter 4 studies the regulation of Dll4 expression in HUVECs by other pathways, including Notch, VEGF and hypoxia signalling.

Chapter 5 builds upon the results of Chapter 4 and studies the regulation of Dll4 expression in HUVECs by co-culturing with cancer cell lines.

Chapter 6 extends the *in vitro* results *in vivo*, and investigates the effect of Dll4 overexpression on tumour growth in xenograft models.

CHAPTER TWO

Materials and Methods

2.1 Materials

2.1.1 Chemicals

Chemicals used in this research were purchased from Sigma (Dorset) unless otherwise stated.

2.1.2 DEPC-treated water

All experiments were performed using diethylpyrocarbonate (DEPC)-treated distilled water. DEPC treatment eliminates DNase and RNase. In a fume hood, 1 ml of DEPC was added per litre of distilled water and left to incubate at room temperature overnight. DEPC was then removed by autoclaving treated water for 20 minutes.

2.1.3 Bacteria, bacterial culture and transformation

Top10 competent *Escherichia coli* (*E. coli*) bacteria (Invitrogen, Paisley) were used to clone the Dll4 promoter. *E. coli* was grown in LB (Luria-Bertani) growth medium (Cancer Research UK, London) or on LB agar dishes (Cancer Research UK, Oxford) supplemented with 50 μg/ml of ampicillin. Dll4 promoter fragments were cloned into the pGL3-enhancer (pGL3e) plasmid (Promega, Southampton), which encodes a Firefly luciferase gene.

2.1.4 Cell Lines

Human umbilical vein endothelial cells (HUVECs) were isolated from umbilical cords (Women's Centre, John Radcliffe Hospital, Oxford). MCF7, SKBR3, T47D, MDA-MB-231

breast cancer cells; U87 glioblastoma cells; PC3 prostate cancer cells; HT1080 fibrosarcoma cells; and B16 mouse melanoma cells were purchased from Cancer Research UK's Cell Services (London). The Phoenix viral packaging cell line was purchased from Orbigen (San Diego, USA). Porcine aortic endothelial (PAE) cells (Landgren et al., 1998) were a gift of Prof. Yihai Cao at the Karolinska Institutet, Sweden. Murine L-cells overexpressing rat Jag1 (Lindsell et al., 1995) were a gift of Dr Geraldine Weinmaster at the University of California, Los Angeles, USA.

2.1.5 Cell culture reagents

HUVECs were cultured in M199 medium supplemented with 10% foetal calf serum (FCS), 50 μg/ml endothelial cell growth supplement (ECGS; BD Biosciences, Oxford), 5 IU/ml heparin, 100 IU/ml penicillin, 100 μg/ml streptomycin and 2 mM glutamine (Cancer Research UK, Oxford).

MCF7, MDA-MB-231, SKBR3, U87, HT1080, Phoenix, PAE and L cells were cultured in Dulbecco's Modified Eagle's Medium (DMEM) supplemented with 10% FCS and 2 mM glutamine.

T47D, PC3 and B16 cells were cultured in RPMI-2% glucose medium supplemented with 10% FCS and 2 mM glutamine.

Transfection of all cell types was performed using OptiMEM medium. Cells were removed

from culture plates using Trypsin/EDTA. The formulation of the solutions used in this research is listed below.

Solution	**Source**	**Formulation**
M199	Cancer Research UK	Standard formulation
DMEM	Cancer Research UK	Standard formulation
RPMI-2% glucose	Cancer Research UK	Standard formulation
FCS	Sigma	Fraction V
OptiMEM	Invitrogen	Proprietary composition; contains Glutamax-1
PBS	Cancer Research UK	137 mM NaCl, 2.7 mM KCl, 4.3 mM Na_2HPO_4, 1.4 mM KH_2PO_4, pH 7.3
Trypsin/EDTA	Cancer Research UK	20 mg/ml trypsin, 1 mM ethylenediaminetetraacetic acid (EDTA), in PBS

All cells were cultured on tissue-culture grade polystyrene plasticware (BD Biosciences), including 100 mm dishes, 75 cm^2 flasks, 25 cm^2 flasks, 6-well plates and 24-well plates.

2.1.6 Real-time PCR primers and probes

The following primer-probe sets were designed using the Probe Library Assay Design Centre website (Roche Applied Science, Burgess Hill). The primers were synthesised by Invitrogen, and the Probe Library was purchased from Roche Applied Science.

Gene	**Forward primer**	**Reverse primer**	**Probe**
Flot2	cctcagcttcaccatcaagg	tcagcatctctctgcaccac	61
ActB	cccagcacaatgaagatcaa	cgatccacacggagtacttg	63
HIF1α	cagctatttgcgtgtgagga	tgtgctttcatgtcatcttcaa	89
HIF2α	aatcagcttcctgcgaacac	ttcggactcgttttcagagc	55
BNIP3	tgctgctctctcatttgctg	gactccagttcttcatcaaaaggt	22
GLUT1	ggttgtgccatactcatgacc	cagataggacatccagggtagc	67

PFKFB4	tcatagctgccaacatcgtg	cactgtcgcggttgacatag	44
VEGF	cattggagccttgccttg	atgattctgccctcctcctt	22
ADM	gcctgcccagacccttat	gtagcgcttgactcggatg	57
Notch1	ggcctttactgcgacgtg	acagagccctccatgctg	83
Notch2	aaagtcaatcgtttccagtgc	caatatcaatctggcaaactgg	79
Notch3	caatgctgtggatgagcttg	aagtggcttccacgttgttc	26
Notch4	tgtttgatggctacgactgtg	atggcagtactggtcataggc	19
Jag1	gaatggcaacaaaacttgcat	agccttgtcggcaaatagc	42
Jag2	ctgctggtgttgctttgc	gctgctgtcaggcaggtc	10
Dll1	ctctcggccttgctgtgt	ctcctgcagcttcagttcg	50
Dll3	aaggacgcaggagggttc	ctacctcccgagcgtagatg	68
Dll4-ECD	ccctggcaatgtacttgtgat	tggtgggtgcagtagttgag	23
Dll4-ICD	acagcaaaaccacacattgg	atccgacactctggcttttc	57
Dll4-3'UTR	tcatatgcaacgtgctgctc	tcacagtctgtccggttcct	63
CD31	agagtaccagctgttggtgga	caccttggatggcctcttt	47
Hey1	cgagctggacgagaccat	ggaacctagagccgaactca	39
Hey2	gtaccatccagcagtgcatc	agagaattcagtcagggcattt	60
Hes1	agtgaagcacctccggaac	cgttcatgcactcgctga	60
mActB	aaggccaaccgtgaaaagat	gtggtacgaccagaggcatac	56
mJag1	tggccgaggtcctacactt	gccttttcaattatgctatcagg	22
mDll1	ttcaactgtgagaagaagatggat	gccgaggtccacacactt	103
mDll4	aggtgccacttcggttacac	gggagagcaaatggctgata	106
mCD31	cggtgttcagcgagatcc	cgacaggatggaaatcacaa	45
mHey1	catgaagagagctcacccaga	cgccgaactcaagtttcc	17
mHey2	gaggaaacgacctccgaaa	gacctcatcactgagcttgtagc	85
mHes1	acaccggacaaaccaaagac	cgcctcttctccatgatagg	99
mEfnb2	acacaccagaagacgtggagt	taagcgctggggtcacttta	77
mVEGFR2	cagtggtactggcagctagaag	acaagcatacgggcttgttt	68

2.1.7 Primers for the cloning of Dll4 promoter

The following primers, synthesised by Invitrogen, were used to clone the human Dll4 promoter. All forward primers contain the restriction site for NheI (GCTAGC), and the reverse primer contains the restriction site for HindIII (AAGCTT). The first column indicates the position of the first nucleotide 3' to the restriction site, relative to the translational start site ATG.

Position relative to ATG	Forward or Reverse	Sequence
-3967 bp	Forward	aagGCTAGCggaagctgctgcattaaattgtaa
-2244 bp	Forward	aagGCTAGCcaggatttggagttgagagaggacag
-1086 bp	Forward	aagGCTAGCtgggtctctggcacgcgccaagccc
-500 bp	Forward	aagGCTAGCactggctgacggggaggggggagcg
-97 bp	Reverse	atgAAGCTTaaagaggcgctcctctcgggacgctg

2.1.8 Small interfering RNAs

The following small interfering RNAs (siRNAs) were designed using the siDESIGN Center website (Dharmacon, Lafayette, USA) and synthesised by Eurogentec (Southampton). siRNA oligonucleotides were re-suspended in annealing buffer (100 mM NaCl, 50 mM Tris, pH 7.5-8.0). Working solutions (10 μM) of siRNA were stored at -20°C, and stocks (100 μM) were stored at -80°C.

Gene	Sense	Antisense
Scrambled control	ucugaaaagcacgcuugacTT	gucaagcgugcuuuucagaTT
HIF1α	cugaugaccagcaacuugaTT	ucaaguugcuggucaucagTT
HIF2α	cagcaucuuugauagcaguTT	acugcuaucaaagaugcugTT
Dll4	cuacuauggagacaacugcTT	gcaguugucuccauaguagTT
Hey2 #1	gagagggauuauagagaaaTT	uuucucuauaaucccucucTT
Hey2 #2	gauuauggcaagaaagaaaTT	uuucuuucuugccauaaucTT
Hey2 #3	uaacagaaguugcgcgguaTT	uaccgcgcaacuucuguuaTT

2.1.9 Antibodies

The following primary antibodies were used for Western blotting.

Protein	Company	Monoclonal or polyclonal	Secondary	Dilution
β-Tubulin	Sigma	M	Anti-mouse	1:2000

β-Actin	Sigma	M	Anti-mouse	1:1000
HIF1α	BD Bioscience	M	Anti-mouse	1:1000
N1ICD	Cell Signaling, Boston, USA	P	Anti-rabbit	1:500
Dll4 (R3)	In house	P	Anti-rabbit	1:1500
Hes1	Toray, Tokyo, Japan	P	Anti-rabbit	1:1600

Secondary antibodies against mouse or rabbit immunoglobulin conjugated to horseradish peroxidase (HRP) were obtained from Dako (Ely).

2.1.10 Molecular weight markers

For agarose gel electrophoresis, 1 kb ladders (New England Biolabs, Hitchin) were used to ascertain the molecular weight of DNA fragments from 0.5 to 10 kb. For Western blotting, rainbow markers (GE Healthcare, Chalfont St Giles) were used to determine the molecular weight of proteins from 10 to 250 kDa.

2.1.11 Xenograft and allograft mouse models

Female BALB/c mice with severe combined immune deficiency (SCID) were purchased from Harlan UK (Bicester). All mice were housed in the Clare Hall facility of Cancer Research UK, and all procedures were carried out by trained technicians under a Home Office licence. Bevacizumab was produced by Genentech (San Francisco, USA). DBZ was produced by Syncom (Groningen, the Netherlands).

2.1.12 Mouse tumours expressing VEGF isoforms

Mouse fibrosarcoma tumours expressing only single isoforms of murine VEGF (120, 164 or 188 aa) or wild-type VEGF were a gift of Prof. Gillian Tozer at the University of Sheffield. First, primary mouse fibroblasts were isolated from 13.5-day embryos produced by heterozygous breeding pairs of single VEGF isoform-expressing mice. Fibroblasts were then genotyped to identify cells homozygous for $VEGF_{120}$, $VEGF_{164}$ or $VEGF_{188}$. In addition, fibroblasts expressing wild-type VEGF were isolated from 13.5-day wild-type embryos. Next, cells expressing single VEGF isoforms or wild-type VEGF were transformed with SV40 and h-Ras. The resulting fibrosarcoma cell lines were injected subcutaneously ($1x10^6$ cells in 50 μl) into the rear dorsum of female SCID mice, three mice per cell line. The tumours were excised when they reached 6 mm in diameter and snap frozen. Cell line generation and animal studies were conducted by Chryso Kanthou, Sheila Harris and Simon Akerman in the Tozer Laboratory.

2.2 General laboratory methods

2.2.1 Bacterial cell culture

2.2.1.1 General culture conditions

Top10 *E. coli* (Invitrogen) was grown in LB growth medium supplemented with 50 μg/ml ampicillin in a 37°C shaking incubator set to 225 rpm. Alternatively, it was grown on LB agar dishes containing 50 μg/ml ampicillin in a 37°C incubator.

2.2.1.2 Bacterial transformation

Top10 *E. coli* (Invitrogen) was transformed with DNA according to the manufacturer's protocol. Briefly, one vial of Top10 cells for each DNA plasmid was thawed on ice. Next, 1 µl of DNA plasmid was pipetted directly into the bacteria and mixed by tapping gently. The vials were incubated for 30 minutes on ice, and then for exactly 30 seconds in a 42°C water bath. Next, 250 µl of pre-warmed LB medium (without ampicillin) was added to each vial. The vials were incubated at 37°C for 1 hour in a shaking incubator set to 225 rpm. Afterwards, 20-200 µl from each vial was spread on a separate LB agar dish (containing ampicillin), which was then inverted and incubated at 37°C overnight. The next morning, several colonies were selected from each dish, inoculated into 15 ml centrifuge tubes containing 10 ml LB-ampicillin medium each, and incubated at 37°C in a shaking incubator. In late afternoon, 5 ml medium was removed from each tube and transferred into 200 ml of LB-ampicillin medium in a large flask. Both the 15 ml tube and the flask were incubated overnight in a shaking incubator. The next day, medium in the tube and the flask was centrifuged at 6000 g for 15 minutes at 4°C, and the pellet was frozen for Miniprep and Maxiprep, respectively.

2.2.2 DNA extraction and analysis

2.2.2.1 DNA extraction from bacteria

Either Mini-preparation or Maxi-preparation was performed depending on the volume of the bacterial culture.

Mini-preparation

Small-scale extraction of plasmid DNA from bacteria was performed using the QIAprep Spin Miniprep Kit (Qiagen, Crawley) following manufacturer's protocol. Briefly, the bacteria pellet from a 5 ml overnight culture was re-suspended in 250 µl Buffer P1 and lysed with 250 µl Buffer P2. After neutralisation with 350 µl Buffer N3, the lysis mixture was centrifuged for 10 minutes at 18,000 g at room temperature to pellet genomic DNA, protein and cell debris. The supernatant was then applied to a QIAprep spin column and centrifuged for 30-60 seconds at top speed in a bench-top centrifuge at room temperature. The bound plasmid DNA was washed with 750 µl Buffer PE and eluted with 50 µl Buffer EB (10 mM Tris-HCl, pH 8.0).

Maxi-preparation

Large-scale extraction of plasmid DNA from bacteria was performed using the HiSpeed Plasmid Maxi Kit (Qiagen) following manufacturer's protocol. Briefly, the bacteria pellet from a 200 ml overnight culture was re-suspended in 10 ml Buffer P1 and lysed with 10 ml Buffer P2 for 5 minutes at room temperature. After neutralisation with 10 ml Buffer P3, the lysis mixture was transferred into the barrel of a QIAfilter Cartridge and incubated for 10 minutes at room temperature. During the incubation, genomic DNA, protein and cell debris precipitated, and the supernatant was filtered into a HiSpeed Tip column. The bound plasmid DNA was washed with 60 ml Buffer QC and eluted with Buffer QF. To further increase purity and concentration of the plasmid DNA, isopropanol precipitation was carried out in a QIAprecipitator, which was then eluted with 1 ml Buffer TE (10 mM Tris-HCl, pH 8.0; 1 mM

EDTA).

2.2.2.2 DNA quantification

DNA was quantified using the ND-1000 spectrophotometer (NanoDrop Technologies, Wilmington, USA). The sample pedestal was cleaned with DEPC-treated water and dried before use. A 1.5 µl sample of DEPC-treated water was used to blank the spectrophotometer. DNA was quantified using the DNA-50 presets (DNA concentration equals 50 times the absorbance at 260 nm, or A260). A 1.5 µl sample of DNA was pipetted onto the pedestal for a reading of concentration in ng/µl.

2.2.2.3 Hot-start polymerase chain reaction

All polymerase chain reactions (PCR) were performed using the HotStarTaq DNA Polymerase kit (Qiagen). Each reaction mixture contained 100 ng of template DNA, 5 µl of 10x PCR Buffer, 1 µl of dNTP mix (10 µM of each dNTP), 1 µl each of forward and reverse primers (10 µM) and 0.5 µl of DNA Polymerase, in a total volume of 50 µl.

In a Peltier thermal cycler (GRI, Braintree), the PCR samples were initially incubated for 15 minutes at 94°C to activate the HotStarTaq DNA Polymerase. PCR was performed with 30 cycles. Each cycle consisted of 30 seconds at 94°C for template DNA denaturation, 30 seconds at 50°C-68°C (5°C below the melting temperature, or T_m, of primers) for primer annealing, and 1 minute per kb of PCR product at 72°C for DNA synthesis. After cycling, samples were incubated at 72°C for another 10 minutes for final extension of the PCR

products. PCR products were then incubated at 4°C until use or stored at -20°C.

2.2.2.4 Agarose gel electrophoresis

DNA was separated according to molecular weight by agarose gel electrophoresis. Briefly, 1% gels were prepared by dissolving 1 g electrophoresis-grade agarose (Invitrogen) in 100 ml tris-borate-EDTA buffer (TBE; 90 mM tris-borate, 2 mM Na_2EDTA, pH 8.0). The solution was then heated in a microwave until the agarose was completely dissolved. Next, the solution was cooled at room temperature for 10 minutes before 3 µl ethidium bromide (Bio-Rad, Hemel Hempstead) was added. After thorough mixing, the agarose solution was poured into a gel casting rack to solidify, with a comb inserted.

After the gel solidified, the comb was removed and the gel placed in a mini-sub gel electrophoresis unit (Bio-Rad) containing TBE. DNA samples dissolved in gel loading buffer (0.04% bromophenol blue and 5% glycerol in water) were loaded into the gel. Samples were separated by a constant voltage of 100 V. Following electrophoresis, DNA bands were visualized under trans-UV lighting in a MultiImage Light Cabinet (Alpha Innotech, San Leandro, USA) and pictures were taken. When necessary, DNA bands were excised from the gel using a scalpel and extracted using a Gel Extraction Kit (Qiagen).

2.2.2.5 DNA storage

DNA samples were stored in DEPC-treated water at -20°C.

2.2.3 Isolation of HUVECs

HUVECs were isolated from fresh human umbilical cords by infusion with 0.2% collagenase (Worthington Biochemical Corporation, Lakewood, USA) in PBS. Briefly, a 21-gauge Safety-Lok blood collection needle (BD Biosciences) was inserted into the umbilical vein and clamped in place with a haemostat. Through the needle, 50 ml PBS solution was injected into the umbilical vein to remove any blood and blood clots. Next, 10 ml warm collagenase solution was slowly pushed into the umbilical vein with a syringe, and the bottom end of the umbilical cord was clamped with another haemostat. The cord, filled with collagenase, was then submerged in PBS and incubated at 37°C for 15 minutes. After incubation, the bottom haemostat was removed and the collagenase solution containing dissociated HUVECs was collected in a 30 ml Sterilin tube (Barloworld Scientific, Stone). The tube was centrifuged at 160 g for 4 minutes, and the pellet was re-suspended in 5 ml HUVEC culture medium and plated in a 25 cm^2 culture flask. Freshly isolated HUVECs were designated passage 0 (P0).

After HUVECs reached confluence in the flask, they were trypsinized and re-plated in a 75 cm^2 flask, previously covered with 0.2% porcine gelatin (VWR, Lutterworth) in PBS. Each trypsinization increased HUVEC passage number by one. HUVECs up to passage 6 were used in experiments.

2.2.4 Mammalian cell culture

2.2.4.1 General culture conditions

Cells were cultured in incubators maintaining a temperature of 37°C and atmosphere containing 5% CO_2. Cells were grown in 10 ml medium in 100 mm dishes or 75 cm^2 flasks, 5 ml medium in 25 cm^2 flasks, 2 ml medium per well in 6-well plates, and 1 ml medium per well in 24-well plates.

2.2.4.2 Recovery of cryo-preserved cells

The appropriate cell culture medium was warmed up to 37°C in a water bath. For HUVECs, cell culture flasks were pre-coated with 0.2% gelatin in PBS for 30 minutes. Then, a vial of cryo-preserved cells was retrieved from liquid nitrogen and thawed at 37°C. As soon as the cells appeared thawed, they were transferred to a Sterilin tube and centrifuged at 160 g for 4 minutes to remove any dimethyl sulfoxide (DMSO) used for cryo-preserving cells. After centrifugation, the pellet was re-suspended in the appropriate medium and plated in 75 cm^2 culture flasks. The flasks were then incubated at 37°C.

2.2.4.3 Subculturing

HUVECs were routinely split 1 in 3, while other cell types were split 1 in 5. Cells were sub-cultured when they had reached 90-100% confluence. Cell culture medium, PBS and trypsin/EDTA solutions were all pre-incubated in a 37°C water bath. Medium was removed from cells, which were then washed with PBS. Next, trypsin/EDTA was added to detach the cells (1 ml was added to 100 mm dishes or 75 cm^2 flasks, and 500 µl to 25 cm^2 flasks or each well of 6-well plates). Upon cell detachment, 5 ml of medium for every 1 ml of trypsin/EDTA

was added to deactivate trypsin.

The cell suspension was then transferred to a 30 ml Sterilin tube and centrifuged at 160 g for 4 minutes. After centrifugation, the cell pellet was re-suspended in an appropriate volume of medium and plated in tissue-culture ware.

2.2.4.4 Cell counting

Cell suspension (400 µl) was diluted in 19.6 ml ISOTON diluent (Beckman Coulter, High Wycombe), and the cell number per millilitre of the original cell suspension was measured using a Z2 Coulter Counter (Beckman Coulter).

2.2.4.5 Preparation of frozen cell stocks

Cells stocks were prepared for cryo-preservation. Cells were trypsinized and centrifuged as in Section 2.2.4.3. After centrifugation, cell pellets were re-suspended in freezing solution containing 90% FCS and 10% DMSO. Cells in freezing solution were dispensed into Corning 2 ml round-bottom cryogenic vials (Fisher Scientific, Loughborough). Vials were cooled slowly overnight at -80°C and transferred to liquid nitrogen (-140°C) the next day for long-term storage.

2.2.5 RNA extraction and analysis

2.2.5.1 RNA extraction from cultured cells

All RNA work was performed using filtered and aerosol-resistant pipette tips, sterile microcentrifuge tubes and DEPC-treated water. RNA extraction from cultured cells was performed using TRI Reagent according to the manufacturer's protocol. Briefly, cell culture medium was aspirated, and the cell monolayer was washed with PBS. After PBS was removed, an appropriate volume of TRI Reagent was added (1 ml per 100 mm dish, or 150 µl per well of a 6-well plate). Cells were then scraped with a Costar cell scraper (Fisher Scientific) to facilitate lysis. The cell lysate was then transferred to 1.7 ml microcentrifuge tubes (Axygen Scientific, Union City, USA). At this stage, RNA samples may be stored at -80°C for up to a month; otherwise, RNA extraction was performed immediately.

Five minutes after cell lysis, 0.2 ml chloroform per 1 ml TRI reagent was added to the samples. Samples were then vortexed for 15 seconds, incubated at room temperature for 10 minutes, and then centrifuged at 12,000 g for 15 minutes at 4°C. The centrifugation separated the mixture into three phases, and the top aqueous phase containing RNA was transferred into a new microcentrifuge tube. To the new tube, 0.5 ml isopropanol per 1 ml TRI reagent was added and mixed. After standing at room temperature for 5 minutes, the samples were centrifuged at 12,000 g for 10 minutes at 4°C. After centrifugation, an RNA pellet formed at the bottom of the tube. Pellets were then washed with 1 ml 75% ethanol per 1 ml TRI reagent, vortexed, and centrifuged at 12,000 g for 5 minutes at 4°C. The supernatant was removed and the pellet was air-dried for 10 minutes. RNA was re-suspended in 25-50 µl of DEPC-treated water, depending on the size of the pellet.

2.2.5.2 RNA extraction from tumour samples

RNA extraction from tumour samples was performed using the FastPrep instrument (Qbiogene, Irvine, USA) and TRI reagent according to a modified protocol. Briefly, 1 ml of TRI reagent was added to each green-cap tube containing Lysing Matrix D (Qbiogene). A piece of tumour sample weighing approximately 25 mg was removed with a scalpel and cut into small pieces. The tumour sample was then transferred into TRI reagent within a green-cap tube. After all samples were cut and transferred into tubes, the tubes were processed in the FastPrep instrument for 40 seconds at a setting of 6.0. Afterwards, the tubes were centrifuged at 12,000 g for 5 minutes at 4°C. The supernatant (~750 µl) was transferred into a new microcentrifuge tube. From this point on, the protocol for TRI reagent as described in Section 2.2.5.1 was followed.

2.2.5.3 DNase treatment

All RNA samples were treated with DNase in the DNA-free kit (Ambion, Austin, USA) according to manufacturer's protocol. Briefly, 0.1 volume of DNase I Buffer and 1 µl rDNase were added to each RNA sample and mixed. The sample was then incubated at 37°C for 25 minutes. Next, 0.1 volume of DNase Inactivation Reagent was added per sample. The samples were mixed, incubated at room temperature for 2 minutes and centrifuged at 10,000 g for 2 minutes. The supernatant containing DNA-free RNA was transferred into a new tube.

2.2.5.4 RNA quantification

RNA was quantified using the ND-1000 spectrophotometer (NanoDrop Technologies). The procedures were similar to those for DNA quantification, except that the RNA-40 presets were used. RNA concentration, in ng/μl, equals 40 times the absorbance at 260 nm, or A260.

2.2.5.5 Reverse transcription

Reverse transcription was performed using the High Capacity cDNA Reverse Transcription Kit (Applied Biosystems, Warrington). Briefly, 1 μg of RNA was diluted in 71 μl of DEPC-treated water in a 0.2 ml thermo-tube (ABgene, Epsom). To the RNA sample, 10 μl 10x RT Buffer, 10 μl 10x Random Primers, 4 μl 25x dNTP mixture, and 5 μl MultiScribe Reverse Transcriptase were added, making the final volume 100 μl. The sample was then incubated at 25°C for 10 minutes, 37°C for 2 hours, and 4°C for up to 12 hours before use. The cDNA concentration is taken to be 10 ng/μl (1 μg per 100 μl) assuming 100% efficiency of reverse transcription.

2.2.5.6 Real-time quantitative PCR

Real-time PCR quantitative (qPCR) was performed using the Exiqon system (Roche Applied Science) (Mouritzen et al., 2003). Briefly, a master mix for each gene to be tested was prepared containing the following: 12.5 μl ABsolute QPCR Mix (ABgene), 1 μl forward primer (10 μM), 1 μl reverse primer (10 μM), 0.25 μl probe from the Probe Library (Roche Applied Science), and 0.25 μl DEPC-treated water. Reactions were prepared in 0.1 ml tubes by a CAS-1200 robot (Corbett Research, Cambridge). In triplicates, 15 μl master mix was

added to each reaction tube, followed by 10 ng cDNA in 10 µl. Upon completion of the robot run, reaction tubes were capped and placed in the 72-well rotor of a Rotor-Gene RG-3000 qPCR thermocycler (Corbett Research). The samples were then incubated at 50°C for 2 minutes followed by 95°C for 10 minutes to activate the Taq polymerase in the QPCR Mix. Afterwards, the cDNA samples went through 40 cycles of amplification at 95°C for 15 seconds followed by 60°C for 1 minute.

Two housekeeping genes (HKGs) were used to normalise the expression of genes of interest (GOIs). Human flotillin2 (Flot2) was used for cDNA derived from HUVECs (Andersen et al., 2004). Human or mouse β-actin (ActB) was used for cDNA derived from cell lines and tumours (Castello et al., 2002). Data were analyzed using the comparative Ct method (Livak and Schmittgen, 2001). Briefly, the threshold cycle (Ct) values for each GOI and HKG were converted to raw expression values by performing the operation 2^{-Ct}. The raw expression value of each GOI was then divided by that of the HKG to account for different amounts of cDNA in each sample. Finally, the normalised values were then rescaled to set the expression in the control sample to 1. Error propagation was calculated throughout the operations, and final results were reported as mean ± standard error of the mean (SEM) to reflect the triplicate measurements.

2.2.5.7 RNA storage

RNA was re-suspended in DEPC-treated water and stored at -80°C.

2.2.6 Protein extraction and analysis

2.2.6.1 Protein extraction from cultured cells

Protein extraction from cultured cells was performed using a lysis buffer consisting of 10% glycerol, 10 mM Tris-HCl (pH 6.8), 5 mM dithiothreitol, 1% sodium dodecyl sulphate (SDS) and 8 M urea. Briefly, medium was removed from cultured cells, which were then washed with PBS. To each 100 mm dish of cells, 1 ml of the lysis buffer and 10 µl of Protease Inhibitor Cocktail were added. Cells were then scraped off with a cell scraper, and cell lysates transferred to microcentrifuge tubes.

2.2.6.2 Protein quantification

Protein concentration was quantified using the Bio-Rad DC Protein Assay (Bio-Rad). Briefly, 25 µl reagent A'—prepared by adding 20 µl Reagent S to 1 ml Reagent A—was added to each well of a 96-well plate as needed. To this, 5 µl protein samples or standards of known concentration were added in triplicate. Finally, 200 µl of Reagent B was added to each well, and the plate was incubated at room temperature for 45 minutes. Absorbance at 690 nm was measured using a µQuant Microplate Spectrophotometer (BioTek Instruments, Winooski, USA). The absorbance of the standards was plotted against their concentration to create a standard curve, and the concentration of unknown samples was derived from the standard curve.

2.2.6.3 Western blotting

Western blotting of protein samples was performed as described by Burnette (Burnette, 1981) with modifications. First, protein samples were separated according to molecular weight by SDS polyacrylamide gel electrophoresis (SDS-PAGE). All reagents and apparatuses were obtained from Invitrogen. Protein samples (25 μg) were diluted in lysis buffer to a volume of 19.5 μl, and 7.5 μl 4x LDS Sample Buffer and 3 μl 10x Reducing Agent were added. The samples were then heated at 70°C for 10 minutes and loaded into NuPAGE 10% Bis-Tris gels in an XCell SureLock Mini-Cell. The upper chamber of the Mini-Cell was filled with 200 ml 1x MOPS SDS Running Buffer containing 500 μl Antioxidant, and the lower chamber was filled with 600 ml 1x Running Buffer. Gels were run at a constant voltage of 200 V for 50 minutes.

Proteins were then transferred from the gel to an Immobilon-PVDF transfer membrane (Millipore, Watford). Both the membrane and the gel were sandwiched between six layers of filter paper, with the membrane between the gel and the anode. The membrane and filter paper had been pre-soaked in transfer buffer (25 mM Tris base, 192 mM glycine, 15% methanol). The transfer assembly was placed in a semi-dry transfer apparatus (WEP, Seattle, USA). Protein was transferred at a constant current of 130 mA per gel for 40 minutes.

After transferring, non-specific binding sites on the membrane were blocked for 1 hour at room temperature in blocking solution (5% milk powder, 0.1% Tween-20 in PBS). After blocking, the membrane was probed with a primary antibody in blocking solution overnight at 4°C. The membrane was then washed in PBS with 0.1% Tween-20 three times for 10 minutes each. Next, the membrane was probed with an appropriate HRP-conjugated secondary

antibody in blocking solution for 1 hour at room temperature. Following this step, the membrane was again washed as before. Finally, the membrane was covered with Enhanced Chemiluminescence (ECL) reagent (GE Healthcare) for 1 minute and placed in a film cassette. In a dark room, the membrane was exposed to ECL Hyperfilm (GE Healthcare) for 10 seconds, 1 minute, 10 minutes or longer as needed, and the films were then developed using an X-ray film processor (Xograph, Tetbury).

In certain cases, membranes were stripped for re-blotting with a different antibody. Membranes were incubated in stripping buffer (62.5 mM Tris-HCl, 2% SDS, 100 mM β-mercaptoethanol) at 60°C for 30 minutes, and washed in PBS with 0.1% Tween-20 three times for 10 minutes each. Membranes were then re-blocked and probed with different primary and secondary antibodies.

2.2.6.4 Protein storage

Protein samples were stored in lysis buffer at -80°C.

2.2.7 Websites

Genome Browser: http://genome.ucsc.edu/

NCBI: http://www.ncbi.nlm.nih.gov/

Probe Library Assay Design Center: http://www.roche-applied-science.com/sis/rtpcr/upl/adc.jsp

PubMed: http://www.ncbi.nlm.nih.gov/entrez/query.fcgi

siDESIGN™ Center: http://www.dharmacon.com/sidesign/

2.3 Experimental methods

2.3.1 Cloning of the Dll4 promoter

Human Dll4 promoters of varying lengths were cloned into pGL3e plasmids, which encode the Firefly luciferase gene. Briefly, Dll4 promoters of 4 kb, 2.2 kb, 1 kb and 500 bp were cloned from human genomic DNA (Promega) using forward and reverse primers (Section 2.1.7) and hot-start PCR (Section 2.2.2.3). The PCR products were run on an agarose gel (Section 2.2.2.4) to ensure they were of correct sizes. Next, the PCR products and pGL3e plasmids were each digested with 1 μl NheI, 1 μl HindIII, 3 μl 10x Buffer 2 and 0.3 μl 100x BSA (all from New England Biolabs) at 37°C for 2 hours. After digestion, 15 μl PCR product and 2 μl plasmid were ligated with 1 μl T4 DNA ligase and 2 μl 10x ligation buffer (New England Biolabs) at 16°C overnight. The next morning, the ligation products were used to transform Top10 *E. coli* cells (Section 2.2.1.2) for plasmid amplification, and Miniprep and Maxiprep were performed to extract plasmid DNA (Section 2.2.2.1). Samples of the extracted plasmids were digested with NheI and HindIII to check for the expected size of inserts as revealed by agarose gel electrophoresis. They were also sequenced to ensure the correct promoter fragments had been cloned.

Dll4 promoter of 1.6 kb was obtained by digesting the promoter of 2.2 kb with a SacI restriction enzyme. The SacI restriction site GAGCTC is located at -1592 bp upstream of the

translational start site. The 1.6 kb promoter fragment was then cloned into a pGL3e plasmid as described above.

2.3.2 Transient plasmid transfection into PAE cells

To measure Dll4 promoter activation, the pGL3e plasmid was co-transfected with the pRL plasmid (Promega) into PAE cells. The pRL plasmid encodes a Renilla luciferase gene driven by an SV40 promoter. PAE cells were used due to their ease of transfection.

One million PAE cells per dish were cultured in 100 mm dishes for 40 hours. Cells in each dish were then co-transfected with pGL3e and pRL plasmids using Lipofectamine 2000 (Invitrogen). A different mass for each pGL3e plasmid was used to ensure that the same molar amount of plasmid was added to each dish, as shown in the table below.

Plasmid	**Size (kb)**	**Plasmid added (μg)**	**Lipofectamine added (μl)**
pGL3e + 4 kb promoter	9	1.8	4.5
pGL3e + 2.2 kb promoter	7.2	1.44	3.6
pGL3e + 1.6 kb promoter	6.6	1.32	3.3
pGL3e + 1 kb promoter	6	1.2	3
pGL3e + 500 bp promoter	5.5	1.1	2.75
pGL3e (empty vector)	5	1	2.5

The pGL3e plasmids, plus 50 ng of pRL plasmids, were added to polystyrene round-bottom tubes (BD Bioscience) containing 1 ml of OptiMEM each. Next, Lipofectamine 2000 (volume as indicated in the table above) was added to separate round-bottom tubes containing 1 ml of OptiMEM each. After 5 minutes, the solutions for each plasmid were mixed to achieve a 1:2.5

plasmid: Lipofectamine ratio. After another 15 minutes, PAE cells were gently washed with PBS, and 5 ml of DMEM plus 0.5% FCS without antibiotics was added to each dish. In addition, 2 ml of plasmid-Lipofectamine mixture was added to each dish. After 2-hour incubation, PAE cells were washed with PBS again and cultured in 7 ml of DMEM plus 10% FCS without antibiotics.

The next morning, transfected PAE cells were split 1:40 and plated in triplicate for each treatment condition in 24-well plates. The cells were then exposed to various treatments such as rhDll4, VEGF and hypoxia.

2.3.3 Luciferase assay

Luciferase assay was performed using the Dual-Luciferase Reporter 1000 Assay System (Promega) according to the manufacturer's protocol. Briefly, culture medium was removed from PAE cells, which were then washed with PBS. The 5x Passive Lysis Buffer was diluted to 1x in distilled water, and 100 µl was added to each well of a 24-well plate. The plate was then placed on a shaker for 30 minutes to ensure complete lysis of the cells. Afterwards, the plate containing cell lysates was frozen at –80°C until ready to perform the assay.

To perform the luciferase assay, cell lysates were thawed and 20 µl was added into each well of a 96-well Optical Bottom Plate (Nunc, Roskilde, Denmark). Meanwhile, the FLUOstar OPTIMA microplate reader (BMG Labtech, Aylesbury) was set up to dispense 100 µl of Luciferase Assay Reagent II (LAR II) and measure Firefly luciferase activity, and then

dispense 100 μl of Stop & Glo Reagent and measure Renilla luciferase activity. Next, the 96-well plate containing cell lysates was inserted into the microplate reader to initiate the run. The ratio of Firefly and Renilla luciferase activities was calculated for each well, and data were presented as mean ± SEM for each treatment condition as previously described (Ameri et al., 2002).

2.3.4 Transient plasmid transfection into HUVECs

The pcDNA plasmids containing N1ICD or GFP control were a kind gift of Dr Richard Sainson, a postdoctoral fellow in our laboratory.

HUVECs were plated, $1x10^5$ cells per well, in a 6-well plate pre-coated with 0.2% gelatin. After 24 hours, cells were transfected with Lipofectamine 2000. Briefly, 1 μg of pcDNA-N1ICD or pcDNA-GFP was added to 100 μl of OptiMEM in a polystyrene round-bottom tube. Next, 2.5 μl of Lipofectamine 2000 was added to 100 μl of OptiMEM in another round-bottom tube. (All the numbers above are for 1 well only.) After 5 minutes, the solutions were mixed to achieve a 1:2.5 plasmid: Lipofectamine ratio. After another 15 minutes, HUVECs were gently washed with PBS, and 2 ml of M199 medium plus 0.5% FCS without ECGS or antibiotics was added per well. In addition, 200 μl of plasmid-Lipofectamine mixture was added per well. After 4-hour incubation, HUVECs were washed with PBS again and cultured in 2 ml of M199 plus 10% FCS and ECGS without antibiotics overnight. Regular culture medium was replaced the next morning.

2.3.5 RNA interference

The transfection of siRNAs into cells was performed using Lipofectamine 2000 as described (Patel et al., 2005).

Briefly, $1x10^5$ HUVECs or $3x10^5$ MCF7 cells per well were plated in a 6-well plate and cultured for 24 hours. The transfection volume was 1 ml per well, and the siRNA concentration was 20 nM. Therefore, 2 µl of the siRNA working solution (10 µM) was added to 98 µl of OptiMEM in a round-bottom tube. A scrambled control siRNA was used to control for non-specific RNAi-related effects. Next, 5 µl of Lipofectamine was added to 95 µl of OptiMEM. (All the numbers above are for 1 well only.) After 5 minutes, the siRNA and Lipofectamine solutions were mixed. After another 15 minutes, cells were gently washed with PBS, and 800 µl of medium plus 0.5% FCS without antibiotics was added per well. In addition, 200 µl of siRNA-Lipofectamine mixture was added per well. After 4-hour incubation, cells were washed with PBS again and cultured in 2 ml medium without antibiotics overnight. Regular culture medium was replaced the next morning.

2.3.6 Retroviral infection

The cDNA of human full-length Dll4 was cloned into the retroviral expression vector LZRSpBMN-linker-IRES-eGFP (gift of Dr Maarten van Lohuizen, The Netherlands Cancer Institute) as described (Williams et al., 2006). This vector contains an internal ribosomal entry site (IRES) that allows cap-independent translation of the enhanced green fluorescence protein (eGFP) marker. The vector also contains a puromycin resistance gene.

Phoenix cells grown on 100 mm dishes to 50% confluence were transfected with retroviral vectors containing full-length Dll4 or empty vector control. Briefly, 18 µl FuGENE6 (Roche) was added to 580 µl OptiMEM (Invitrogen). After 5 minutes, 6 mg vector was added. After another 15 minutes, the transfection mix was added to Phoenix cells together with 9.4 ml DMEM + 10% FCS for 24 hours. After transfection, fresh medium was added containing 2 µg/ml puromycin to select for transfected cells.

Transfected phoenix cells were then transferred into T75 flasks. After reaching 70% confluence, cells were carefully washed with PBS and cultured in 10 ml OptiMEM per flask for 40 hours at 37°C and another 24 hours at 32°C. The virus-containing OptiMEM was filtered (0.4 µm) and added with polybrene (4 µg/ml) to 50% confluent HUVECs at passage 2. After 5 hours at 37°C, 5 ml regular HUVEC medium was added. The infection process was repeated on two subsequent days, and then the HUVECs were cultured under standard conditions.

2.3.7 Coating plates with recombinant Dll4 or Jag1 protein

Recombinant human Dll4-ECD (rhDll4) and rat Jag1-ECD (rrJag1) proteins were purchased from R&D Systems (Abingdon). For rhDll4, 50 µg of protein was re-suspended in 500 µl of 0.1% BSA in PBS. The stock solution, of concentration 100 µg/ml, was aliquoted and stored at -20°C. One day before use in cell culture, the stock solution was diluted 1:100 to 1 µg/ml (or 18 µM), and 330 µl of the diluted solution was used to cover one well of a 6-well plate.

For control, 330 μl of 0.1% BSA in PBS was used per well of a 6-well plate. The plate was then kept at 4°C overnight. The next day, protein solutions were removed, and cell culture was performed on the plate as usual.

In another experiment, rrJag1 protein of the same molar concentration (18 μM) was used to cover the 6-well plates.

2.3.8 Human VEGF ELISA

Human VEGF enzyme-linked immunosorbent assay (ELISA) was performed using the Human VEGF DuoSet ELISA kit (R&D Systems) according to the manufacturer's protocol. Briefly, 100 μl Capture Antibody (180 μg/ml of mouse anti-human VEGF in PBS) was added to each well of a 96-well plate and incubated overnight. The next morning, each well was aspirated and washed with 400 μl Wash Buffer (0.05% Tween-20 in PBS) for three times, and the Wash Buffer was completely removed afterwards. Next, the plate was blocked for 1 hour by adding 300 μl Reagent Diluent (1% BSA in PBS) per well. The aspiration/wash step was repeated, and 100 μl of cell culture medium or standards (made from serial dilution of recombinant human VEGF of 2 ng/ml) was added per well in triplicate and incubated for 2 hours. The aspiration/wash step was repeated, and 100 μl Detection Antibody (9 μg/ml of biotinylated goat anti-human VEGF in Reagent Diluent) was added per well and incubated for 2 hours. The aspiration/wash step was repeated, and 100 μl Streptavidin-HRP working solution was added per well and incubated for 20 minutes. The aspiration/wash step was repeated, and 100 μl Substrate Solution (1:1 mixture of tetramethylbenzidine and H_2O_2) was

added per well and incubated for 20 minutes. To stop the reaction, 50 µl of 1 M H_2SO_4 solution was added per well and mixed gently. The absorbance of each well was determined using a µQuant Microplate Spectrophotometer set to 450 nm. The absorbance of the standards was plotted against their VEGF concentration to create a standard curve, and the VEGF concentration of unknown samples was derived from the standard curve. Data were presented as mean ± SEM for each sample.

2.4 Mouse models

Six- to eight-week-old female BALB/c SCID mice were injected subcutaneously with 100 µl cell suspension containing $1x10^7$ U87, $5x10^6$ PC3, $1x10^7$ HT1080 or $1x10^7$ MDA-MB-231 cells, together with 100 µl Matrigel (BD Bioscience). Alternatively, the mice were injected subcutaneously with 100 µl cell suspension containing $2x10^4$ B16 cells, without Matrigel. Each treatment group consisted of five mice. Tumour growth was monitored two to three times per week by measuring the length (L), width (W) and height (H) of each tumour with a calliper. Tumour volumes (V) were then calculated from the formula ($V = 1/6 \bullet \pi \bullet L \bullet W \bullet H$). When the tumour reached the maximum size permitted by the Home Office license, the mouse was sacrificed and the tumour excised. Half the tumour was frozen in liquid nitrogen for RNA isolation, and the other half fixed in formalin for immunohistochemical analysis.

For antibody experiments, bevacizumab (10 mg/kg) was given intraperitoneally every three days, for a total of five injections (U87) or seven injections (PC3), starting from day 0 when the tumour cells were implanted.

For combined antibody and DBZ experiments, bevacizumab (10 mg/kg) or DBZ (5.4 μmol/kg) or both was given intraperitoneally every three days, starting from day 11 until the mice were sacrificed. Bevacizumab and DBZ were given on separate days.

2.5 Statistical methods

The statistical analysis and graphing software Excel (Microsoft, USA) and Prism (GraphPad, USA) were used to analyse data. The unpaired t-test was used to compare mean values between two unpaired data sets. The analysis of variance (ANOVA) test was used to compare mean values among three or more data sets, and the Bonferroni's post-test was used to compare any two data sets among the three or more sets. A minimum of 95% confidence interval (i.e., $p<0.05$) was used in all statistical tests. In the figures, one star (*) denotes $p<0.05$, two stars (**) denote $p<0.01$, and three stars (***) denote $p<0.001$. The ^ symbol denotes $p\geq0.05$ (no significance). All error bars depict SEM.

CHAPTER THREE

Functional Crosstalk between Dll4-Notch and Hypoxia Pathways

3.1 Introduction

As described in Sections 1.3.1 and 1.4.2, hypoxia is a key regulator of both tumorigenesis and tumour angiogenesis (Harris, 2002, Pugh and Ratcliffe, 2003). Since oxygen can only diffuse approximately 180 μm from capillaries to cells, tumour cells located more than this distance away from vessels become hypoxic. Hypoxia induces the transcription of genes involved in glucose uptake, glycolysis, oxygen transport and angiogenesis, promoting cell survival. Tumour hypoxia is associated with poor prognosis and resistance to radiotherapy (Harris, 2002).

The cellular response to hypoxia is mainly mediated by the transcription factors HIF1 and HIF2. Each protein consists of alpha and beta subunits. Under normoxia, the alpha subunit is ubiquitinated and degraded in the proteasome. Under hypoxia, degradation is markedly reduced, and HIF-α translocates into the nucleus, interacts with the beta subunit (also know as ARNT) and activates gene transcription. HIF1 and HIF2 regulate two overlapping but different sets of genes (Lofstedt et al., 2007).

Recently, a number of experiments have suggested that the hypoxia pathway interacts with the Notch pathway. In neural stem cells and muscle precursors, hypoxia activated Notch target genes and helped maintain an undifferentiated state. The effect was dependent on HIF1α, which interacted with N1ICD at the promoter of the Notch target gene Hey2, enhancing transcription (Gustafsson et al., 2005). Another study showed that hypoxia up-regulated Notch1 and Hes1 in neuroblastomas, resulting in de-differentiation and a more aggressive phenotype (Jogi et al., 2002).

In addition, Notch signalling impinges on the hypoxia pathway. Overexpression of full-length Notch1 or N1ICD up-regulated HIF1α protein level in MCF7 breast cancer cells (Soares et al., 2004). On the other hand, Hey2 blocked the induction of VEGF by HIF2α in NIH3T3 cells (Chin et al., 2000).

Experiments in this chapter seek to elucidate the mechanisms of Notch-hypoxia signalling crosstalk, which may have implications for both angiogenesis and tumourigenesis. The chapter has two results sections. The first section focuses on HUVECs. The expression level of Notch ligand Dll4 was manipulated, and the induction of hypoxia-regulated genes was measured. The second section focuses on MCF7 cells. The hypoxic induction of Notch pathway components was examined. In all experiments, cells were cultured under 0.1% oxygen tension.

3.2 Notch-hypoxia crosstalk in HUVECs

Previously we have shown that hypoxia induces Dll4 expression in HUVECs (Mailhos et al., 2001, Patel et al., 2005). The level of Dll4 expression may in turn affect the cellular hypoxia response. Here, two methods were used to manipulate the level of Dll4 expression in HUVECs: RNAi-mediated knockdown and retrovirus-mediated overexpression.

3.2.1 Dll4 knockdown did not affect hypoxia-regulated gene induction

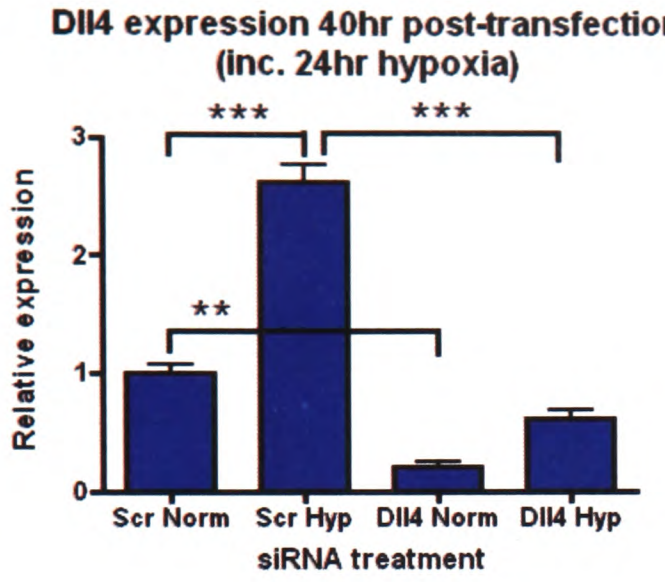
First, small-interfering RNAs (siRNAs) were used to knock down Dll4 expression in HUVECs, as described previously (Patel et al., 2005). HUVECs were transfected with scrambled (Scr) or Dll4 siRNA. Twenty-four hours post-transfection, HUVECs were cultured under normoxia or 0.1% hypoxia for 16 hours, and total RNA was isolated for real-time PCR.

As shown in Figure 3.1A, hypoxia induced Dll4 expression by 2.6-fold in the absence of Dll4 siRNA ($p<0.001$, ANOVA with Bonferroni's post-test). This agrees with published results (Mailhos et al., 2001, Patel et al., 2005). Dll4 siRNA reduced Dll4 mRNA expression by 80% under normoxia ($p<0.01$) and by 77% under hypoxia ($p<0.001$), confirming the effectiveness of the siRNA.

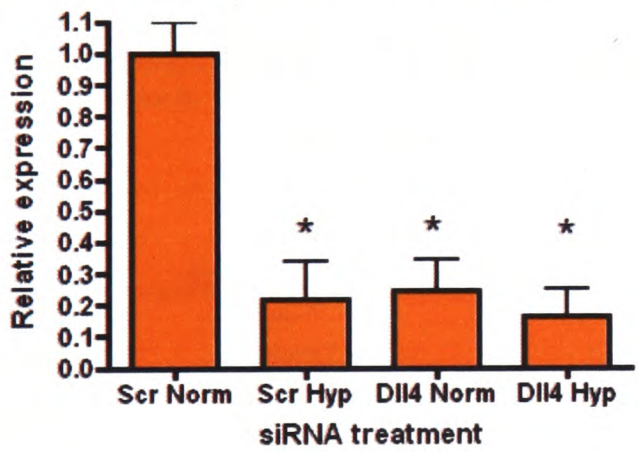
The expression of Notch target genes Hey1 and Hey2 was also measured. Both genes were repressed by hypoxia in the absence of Dll4 siRNA (for both genes, $p<0.05$, ANOVA with Bonferroni's post-test; Figure 3.1B-C). Dll4 siRNA reduced Hey1 mRNA level by 76% ($p<0.05$; Figure 3.1B) but did not affect Hey2 mRNA level (Figure 3.1C), in agreement with (Patel et al., 2005).

Next, the expression of four known hypoxia-regulated genes was examined: BNIP3, GLUT1, PFKFB4 and VEGF. BNIP3 (BCL-2/adenovirus E1B-19 kDa-interacting protein 3) is a HIF1α target gene and regulator of hypoxic cell death (Bacon et al., 2007). GLUT1 (glucose transporter 1) is also induced by HIF1α to increase glucose uptake under hypoxia (Chen et al., 2001). PFKFB4 (6-phosphofructo-2-kinase/fructose-2,6-bisphosphatase 4) is up-regulated by

A



B



C

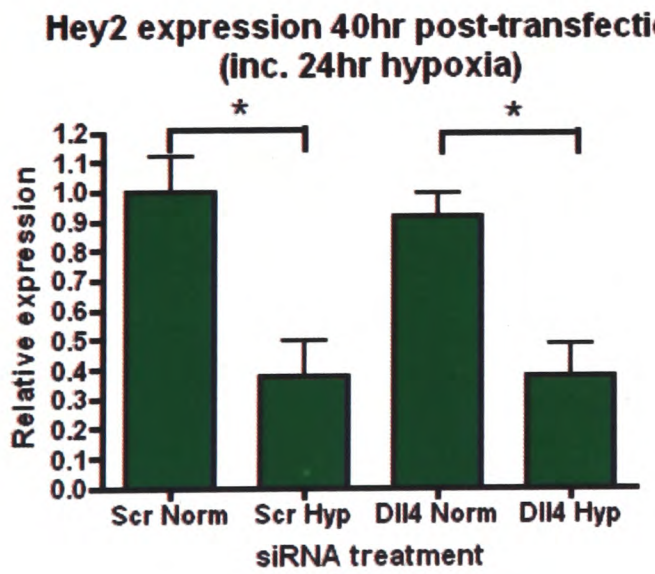


Figure 3.1. Dll4 knockdown reduced the expression of Hey1 but not Hey2.
HUVECs were transfected with Scr or Dll4 siRNA. Twenty-four hours post-transfection, cells were cultured under normoxia or 0.1% hypoxia for 16 hours. Real-time PCR was used to measure the expression of Dll4 (A), Hey1 (B) and Hey2 (C) (*$p<0.05$, **$p<0.01$, ***$p<0.001$, ANOVA with Bonferroni's post-test, n=3). In (B), stars indicate significant differences with the Scr Norm sample.

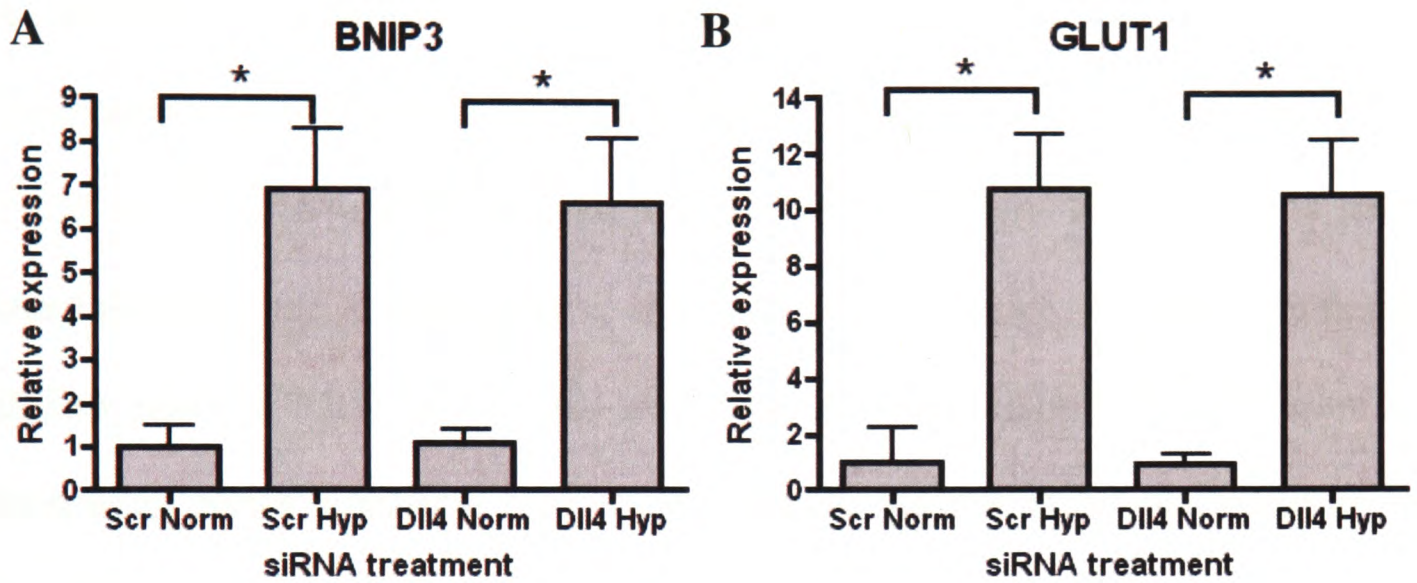


Figure 3.2. Dll4 knockdown did not affect hypoxia-regulated gene induction.
In the Dll4 knockdown experiment, real-time PCR was used to measure the normoxic and hypoxic expression of hypoxia-regulated genes BNIP3 (A), GLUT1 (B), PFKFB4 (C) and VEGF (D) (^$p \geq 0.05$, *$p < 0.05$, ***$p < 0.001$, ANOVA with Bonferroni's post-test, n=3).

HIF1α in mammary gland cancer cell lines (Minchenko et al., 2005). Finally, VEGF, the pro-angiogenic molecule, is induced by both HIF1α and HIF2α (Forsythe et al., 1996, Maemura et al., 1999).

As shown in Figure 3.2, hypoxia induced BNIP3 by 6.9-fold ($p<0.05$, ANOVA with Bonferroni's post-test), GLUT1 by 10.8-fold ($p<0.05$), PFKFB4 by 31.0-fold ($p<0.001$) and VEGF by 3.6-fold ($p<0.05$) in cells treated with Scr siRNA. However, Dll4 siRNA did not affect the normoxic or hypoxic level of any of the genes tested. Hypoxia significantly induced all four genes ($p<0.05$) even as Dll4 expression was reduced by 77% (see Figure 3.1A). Thus, decreasing Notch signalling by Dll4 knockdown did not affect the induction of hypoxia-regulated genes.

Two possible explanations may account for these results. First, Dll4-induced Notch signalling did not affect hypoxia-regulated gene induction in HUVECs. Second, since Dll4 expression is low in HUVECs compared with other endothelial cell types (Patel et al., 2005), further reduction by siRNA may not significantly affect Dll4-induced Notch signalling. Indeed Dll4 knockdown did not reduce the expression of Notch target gene Hey2. To address both possibilities, the alternative approach of Dll4 overexpression was utilised.

3.2.2 Dll4 overexpression repressed hypoxia-regulated gene induction

Dll4 was overexpressed in HUVECs using retrovirus-mediated transduction as described previously (Williams et al., 2006). Briefly, the phoenix viral packaging cell line was transfected with an IRES-GFP retroviral vector containing full-length human Dll4 (Fl Dll4) or

with an empty vector (EV) as control. The culture medium of transfected phoenix cells, which contain viruses, was then used to infect HUVECs three times. Approximately 90% of HUVECs infected with Fl Dll4 viruses or EV control viruses expressed GFP the day after the last infection (data not shown).

To confirm Dll4 overexpression, protein was isolated from infected HUVECs, separated by SDS-PAGE and immunoblotted with antibodies recognising Dll4, cleaved N1ICD and β-tubulin (loading control). The Dll4 antibody detected a band at approximately 70 kDa in protein samples from cells transduced with Fl Dll4, while the endogenous Dll4 protein level from the control cells was too low to be detected (Figure 3.3A). The predicted molecular weight of Dll4 is 75 kDa. Additionally, the overexpressed Dll4 ligand was functional and induced Notch signalling, as indicated by the accumulation of the cleaved, and thus activated, N1ICD (Figure 3.3A). Taken together, retrovirus-mediated Dll4 overexpression in HUVECs promoted Notch signalling.

The effect of Dll4 overexpression on hypoxia signalling was then examined. Twenty-four hours after the last infection, Fl Dll4 HUVECs and EV control HUVECs were cultured under normoxia or 0.1% hypoxia for 16 hours, and total RNA was isolated for real-time PCR.

As shown in Figure 3.3B, Dll4 mRNA level was 50.9-fold higher in Fl Dll4 cells than in EV control cells under normoxia ($p<0.001$, ANOVA with Bonferroni's post-test), consistent with protein-level results (Figure 3.3A). Hypoxia induced Dll4 expression by 2.7-fold in EV control cells ($p<0.05$) and by 1.4-fold in Fl Dll4 cells ($p<0.05$).

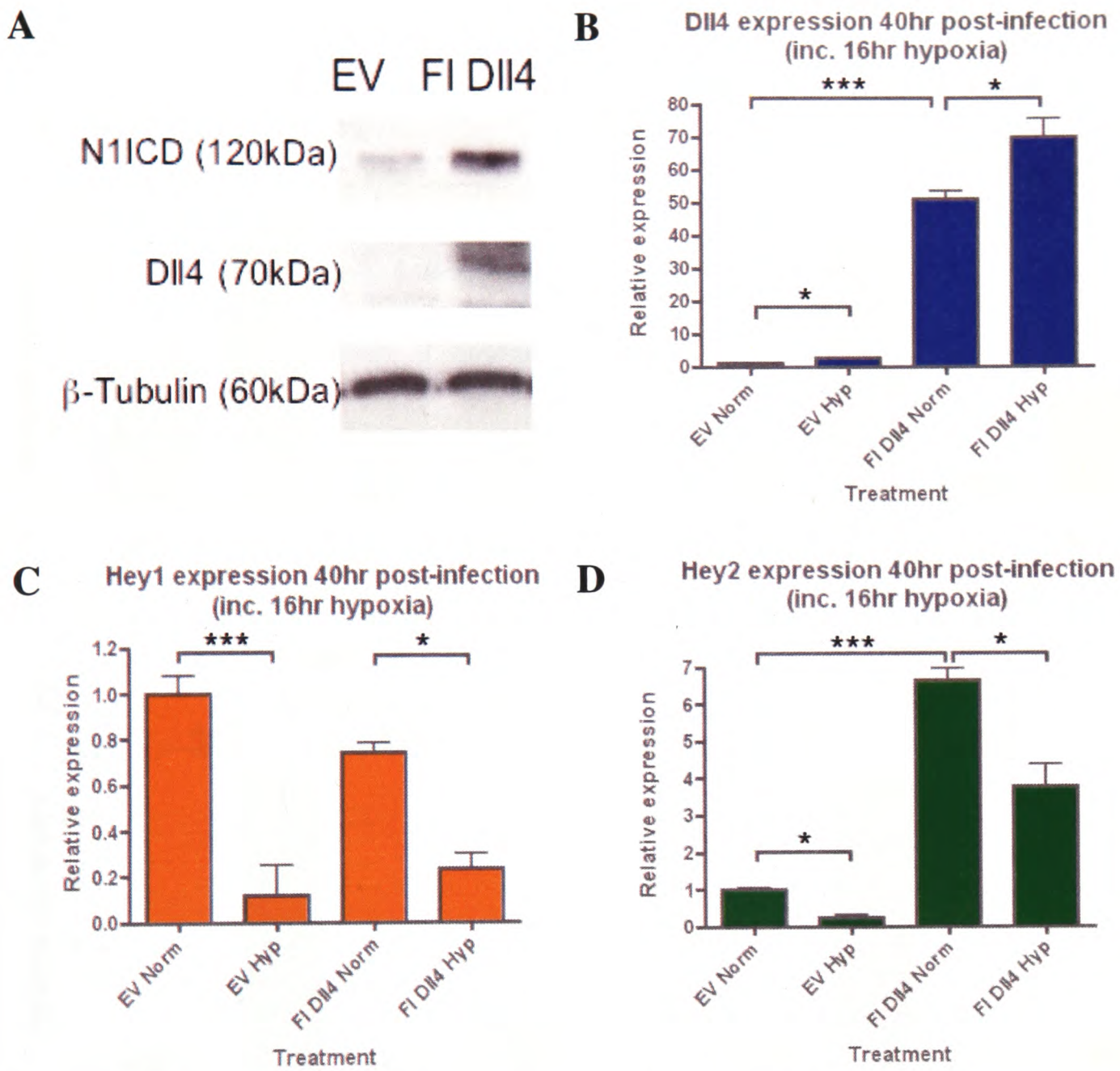


Figure 3.3. Dll4 overexpression induced the expression of Hey2 but not Hey1.
HUVECs were infected with EV control retroviruses or Fl Dll4 retroviruses. (A) Protein samples were isolated from each cell type, separated by SDS-PAGE and blotted with antibodies against Dll4, N1ICD and β-tubulin (n=2). (B-D) Twenty-four hours after infection, cells were cultured under normoxia or 0.1% hypoxia for 16 hours. Real-time PCR was used to measure the expression of Dll4 (B), Hey1 (C) and Hey2 (D) (*$p<0.05$, ***$p<0.001$, ANOVA with Bonferroni's post-test, n=3).

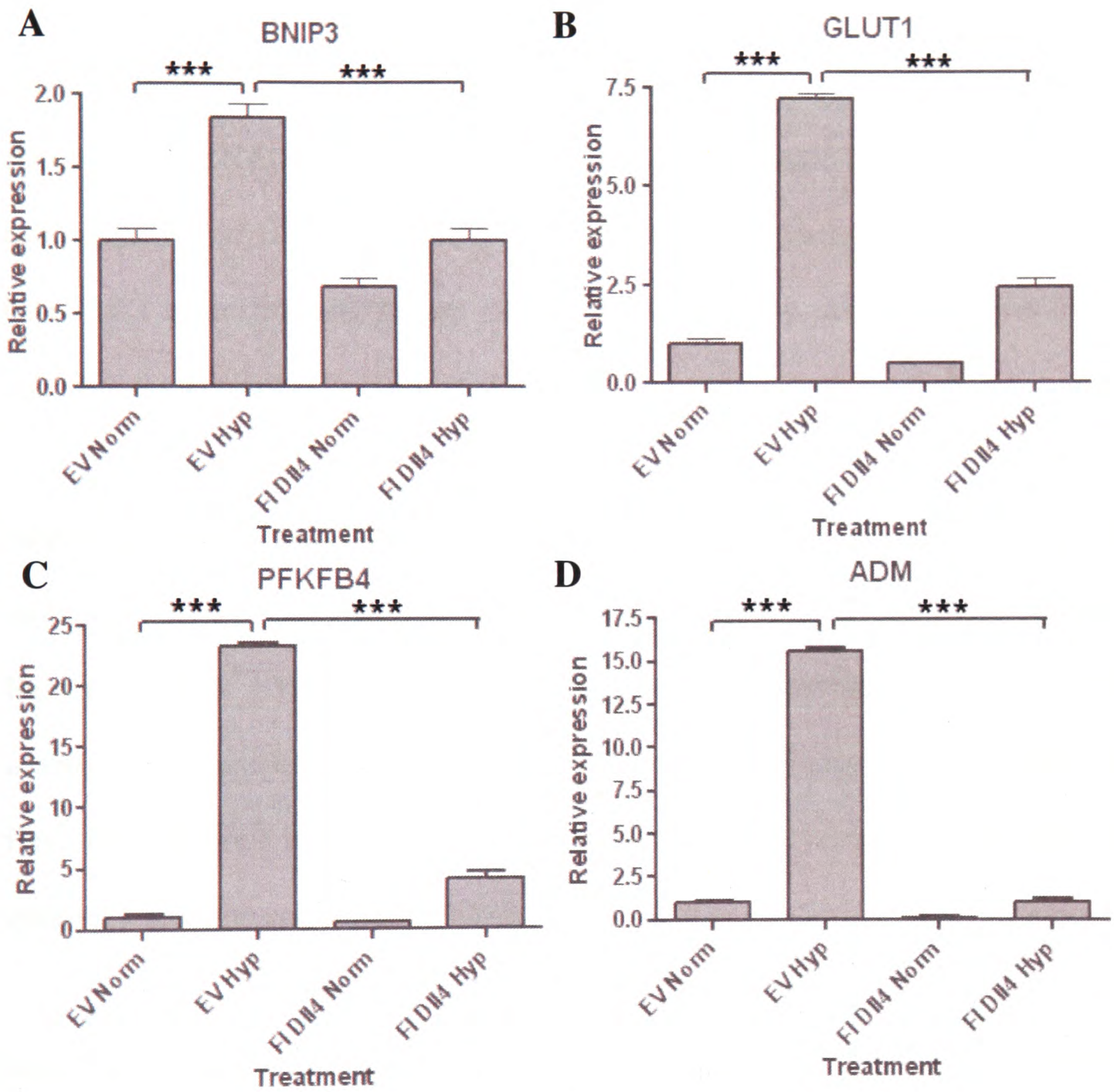


Figure 3.4. Dll4 overexpression repressed hypoxia-regulated gene induction.
In the Dll4 overexpression experiment, real-time PCR was used to measure the normoxic and hypoxic expression of hypoxia-regulated genes BNIP3 (A),. GLUT1 (B), PFKFB4 (C) and ADM (D) (***$p<0.001$, ANOVA with Bonferroni's post-test, n=3).

The expression of Notch target genes Hey1 and Hey2 was also measured. Hypoxia repressed Hey1 in both EV ($p<0.001$, ANOVA with Bonferroni's post-test) and Fl Dll4 ($p<0.05$) cells (Figure 3.3C). Similarly, hypoxia repressed Hey2 in both EV ($p<0.05$, ANOVA with Bonferroni's post-test) and Fl Dll4 ($p<0.05$) cells (Figure 3.3D). In addition, Dll4 overexpression induced Hey2 mRNA level by 6.6-fold ($p<0.001$; Figure 3.3D) but did not affect Hey1 mRNA level (Figure 3.3C). This is in agreement with published results of Dll4 overexpression in HUVECs (Williams et al., 2006). Similarly, another study reported that CHO cells overexpressing human Dll4 induced Hey2 but not Hey1 expression in murine endothelial precursor cells (Diez et al., 2007).

Interestingly, Dll4 knockdown by siRNA reduced Hey1 expression but did not affect Hey2 (see Figure 3.1B-C), whereas Dll4 overexpression induced Hey2 expression but did not affect Hey1 (see Figure 3.3C-D). It is possible that Hey1 is more sensitive to Dll4-Notch signalling at the lower, basal level; thus, Dll4 knockdown reduced its expression. On the other hand, Hey2 may require a higher level of Dll4-Notch signalling for its induction; thus, it was only induced when Dll4 was overexpressed.

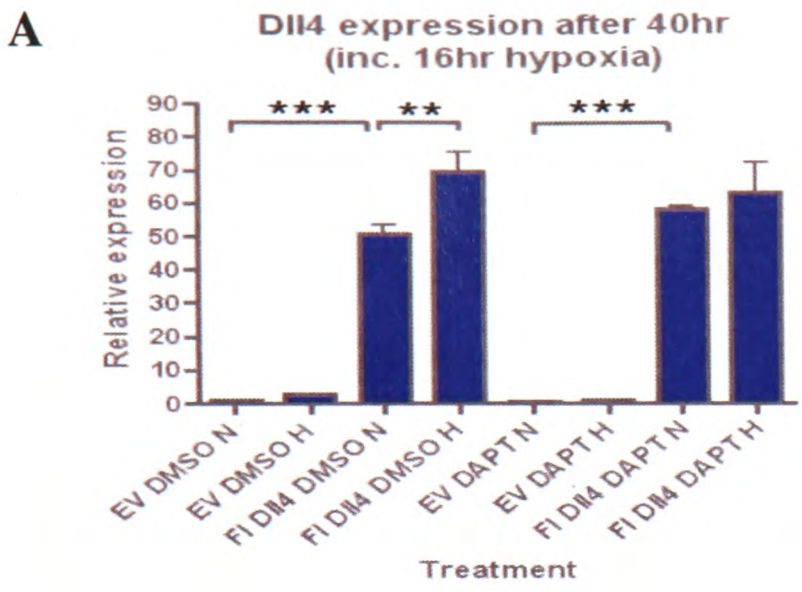
Next, the expression of four known hypoxia-regulated genes was examined: BNIP3, GLUT1, PFKFB4 and ADM. ADM (adrenomedullin) is another HIF1α target and regulator of angiogenesis (Garayoa et al., 2000).

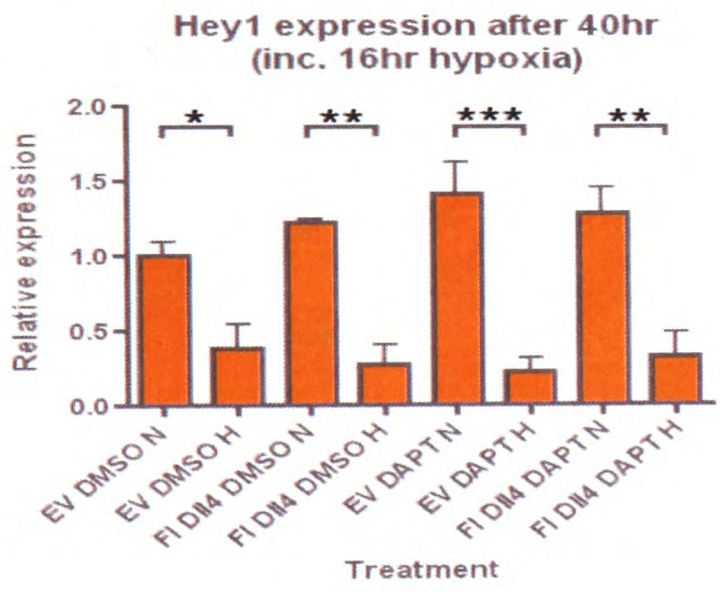
As shown in Figure 3.4, hypoxia induced BNIP3 by 1.8-fold ($p<0.001$, ANOVA with Bonferroni's post-test), GLUT1 by 7.2-fold ($p<0.001$), PFKFB4 by 23.3-fold ($p<0.001$) and

ADM by 15.6-fold ($p<0.001$) in EV cells. For all four genes, the hypoxic induction was significantly reduced in Fl Dll4 cells (for all genes, $p<0.001$, ANOVA with Bonferroni's post-test). Thus, increasing Notch signalling by Dll4 overexpression repressed the induction of hypoxia-regulated genes.

To confirm the role of Notch signalling in the repression of hypoxic induction, the γ-secretase inhibitor DAPT was used to block Notch cleavage. Fl Dll4 or EV-transduced HUVECs were treated with 2 μM DAPT or DMSO for 40 hours, the last 16 of which under normoxia or 0.1% hypoxia. Total RNA was isolated for real-time PCR.

As shown in Figure 3.5A, Dll4 expression was induced by hypoxia in both EV control cells and Fl Dll4 cells. DAPT treatment did not affect the overexpression of Dll4. The expression pattern of Hey1 and Hey2 with DMSO was similar to that in the previous experiment (see Figure 3.3C-D). Hypoxia repressed both genes in EV and Fl Dll4 cells, and Dll4 overexpression induced Hey2 but not Hey1 (Figure 3.5B-C). DAPT did not affect Hey1 expression under any of the four conditions (Figure 3.5B). On the other hand, DAPT significantly reduced Hey2 expression in Fl Dll4 cells under both normoxia (column 3 vs. column 7, $p<0.001$, ANOVA with Bonferroni's post-test; Figure 3.5C) and hypoxia (column 4 vs. column 8, $p<0.05$). Hey2 expression was not significantly different among the four conditions with DAPT ($p\geq0.05$). Thus, Dll4 overexpression induced Hey2 expression, which was repressed by DAPT treatment.





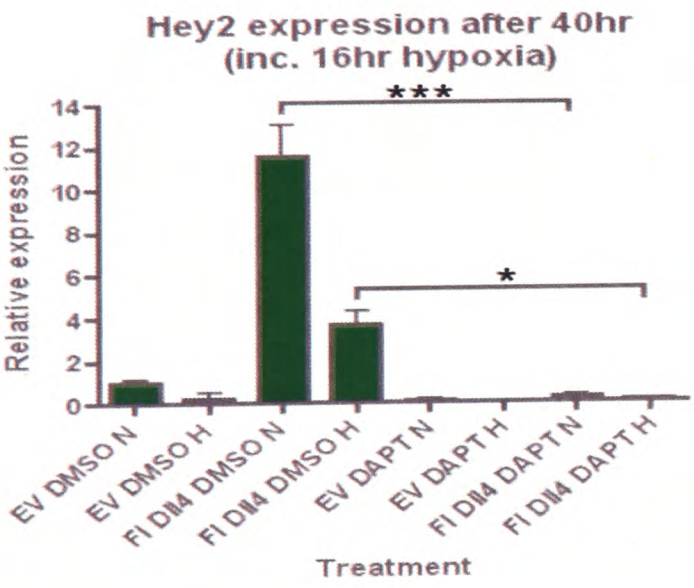


Figure 3.5. DAPT treatment reduced Hey2 induction by Dll4 overexpression.
EV or Fl Dll4-transduced HUVECs were treated with DMSO or 2 μM DAPT for 40 hours, the last 16 of which under normoxia or 0.1% hypoxia. Real-time PCR was used to measure the expression of Dll4 (A), Hey1 (B) and Hey2 (C) (*$p<0.05$, **$p<0.01$, ***$p<0.001$, ANOVA with Bonferroni's post-test, n=3).

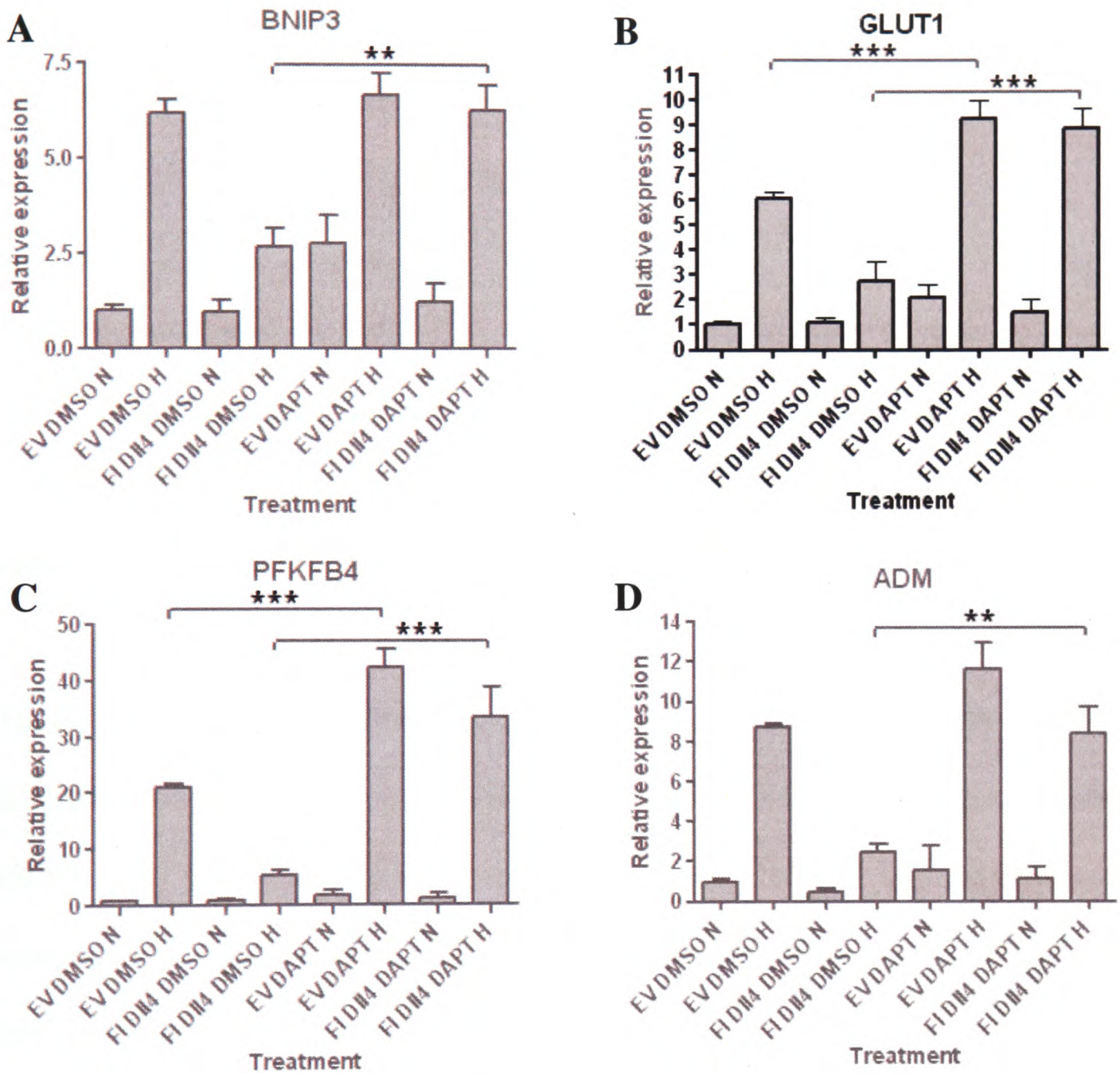


Figure 3.6. DAPT treatment restored hypoxia-regulated gene induction in Fl Dll4 cells.
In the Dll4 overexpression plus DAPT experiment, real-time PCR was used to measure the normoxic and hypoxic expression of hypoxia-regulated genes BNIP3 (A), GLUT1 (B), PFKFB4 (C) and ADM (D) (**$p<0.01$, ***$p<0.001$, ANOVA with Bonferroni's post-test, n=3).

The expression of the hypoxia-regulated genes was also measured in this experiment. As in the previous experiment (see Figure 3.4), Dll4 overexpression repressed the hypoxic induction of the four genes tested (Figure 3.6). DAPT treatment, which inhibited Notch signalling and Hey2 expression, restored the hypoxic induction of the four genes. Thus, for each gene, Fl Dll4 cells treated with DAPT (column 8) had similar expression under hypoxia to EV cells treated with DMSO (column 2).

Taken together, Dll4 overexpression induced Hey2 expression and repressed the induction of hypoxia-regulated genes; DAPT treatment reduced Hey2 expression and restored hypoxic induction in cells overexpressing Dll4. Hence, it was hypothesized that Hey2 may mediate the repression of hypoxic induction by Dll4-Notch signalling.

To test this hypothesis, siRNA was used to knock down Hey2 expression in HUVECs. Three different siRNA duplexes were designed and transfected into HUVECs; a scrambled (Scr) siRNA was also transfected. As shown in Figure 3.7A, all three duplexes significantly reduced Hey2 expression, to 19%, 19% and 6% of the control level, respectively ($p<0.01$, ANOVA with Bonferroni's post-test). Duplex #3 was used in the subsequent experiment, as it was the most effective.

Fl Dll4 or EV-transduced HUVECs were transfected with Hey2 siRNA #3 or Scr siRNA. Twenty-four hours post-transfection, HUVECs were cultured under normoxia or 0.1% hypoxia for 16 hours, and total RNA was isolated for real-time PCR.

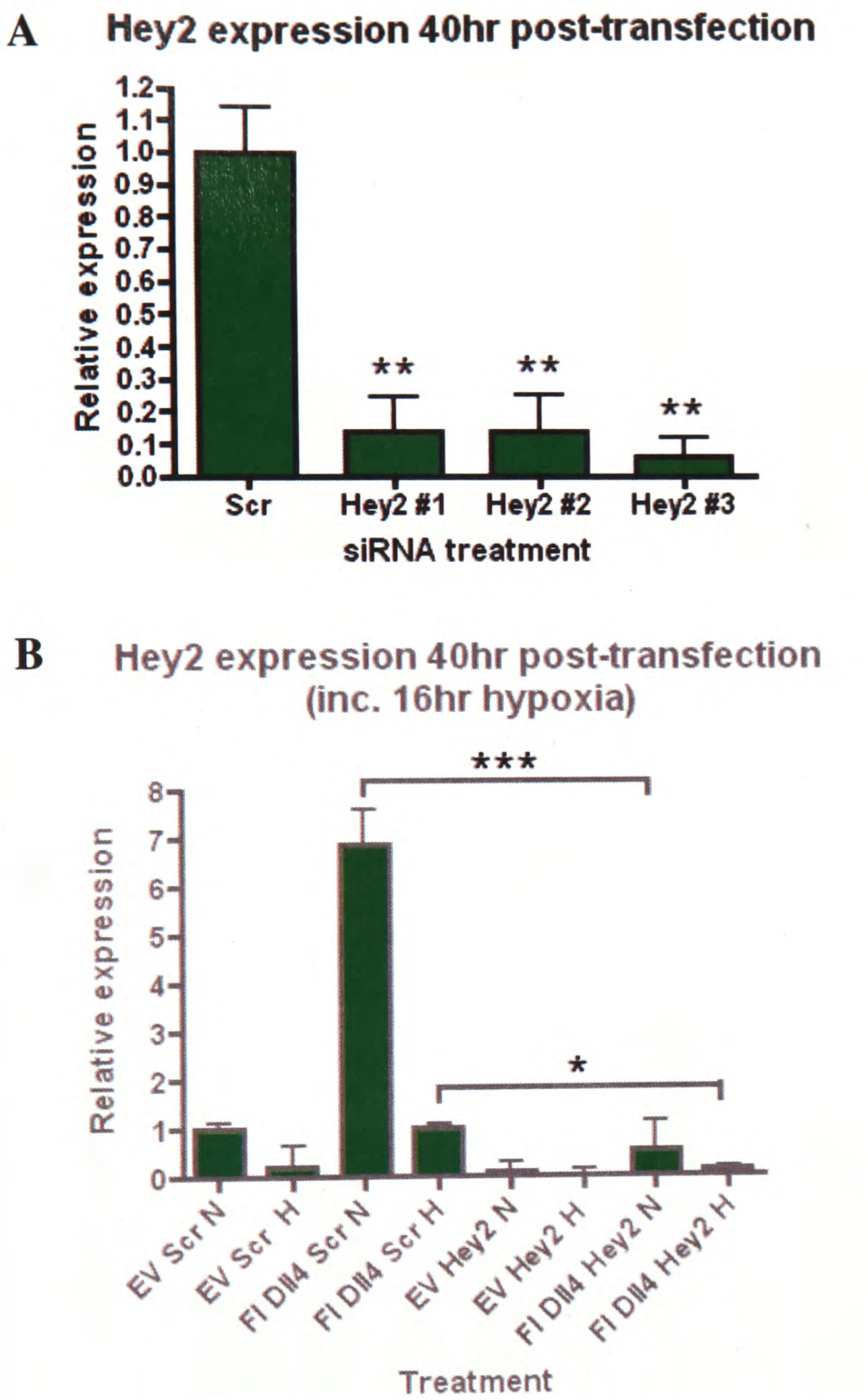
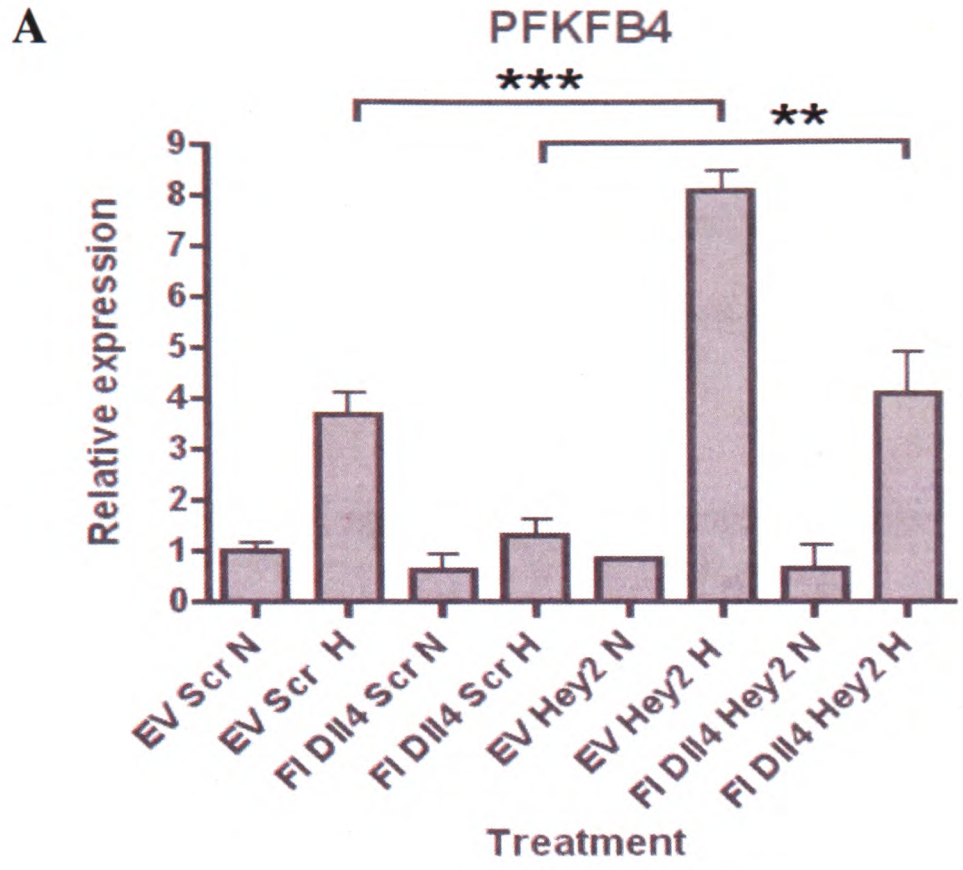


Figure 3.7. Hey2 siRNA reduced Hey2 expression.
(A) HUVECs were transfected with Scr siRNA or one of three Hey2 siRNAs. Hey2 expression was measured by real-time PCR 40 hours post-transfection (**$p<0.01$, ANOVA with Bonferroni's post-test, n=3). Stars indicate significant differences with the Scr sample. (B) EV or Fl Dll4-transduced HUVECs were transfected with Scr or Hey2 siRNA #3. Twenty-four hours post-transfection, cells were cultured under normoxia or 0.1% hypoxia for 16 hours. Hey2 expression was measured by real-time PCR (*$p<0.05$, ***$p<0.001$, ANOVA with Bonferroni's post-test, n=3).



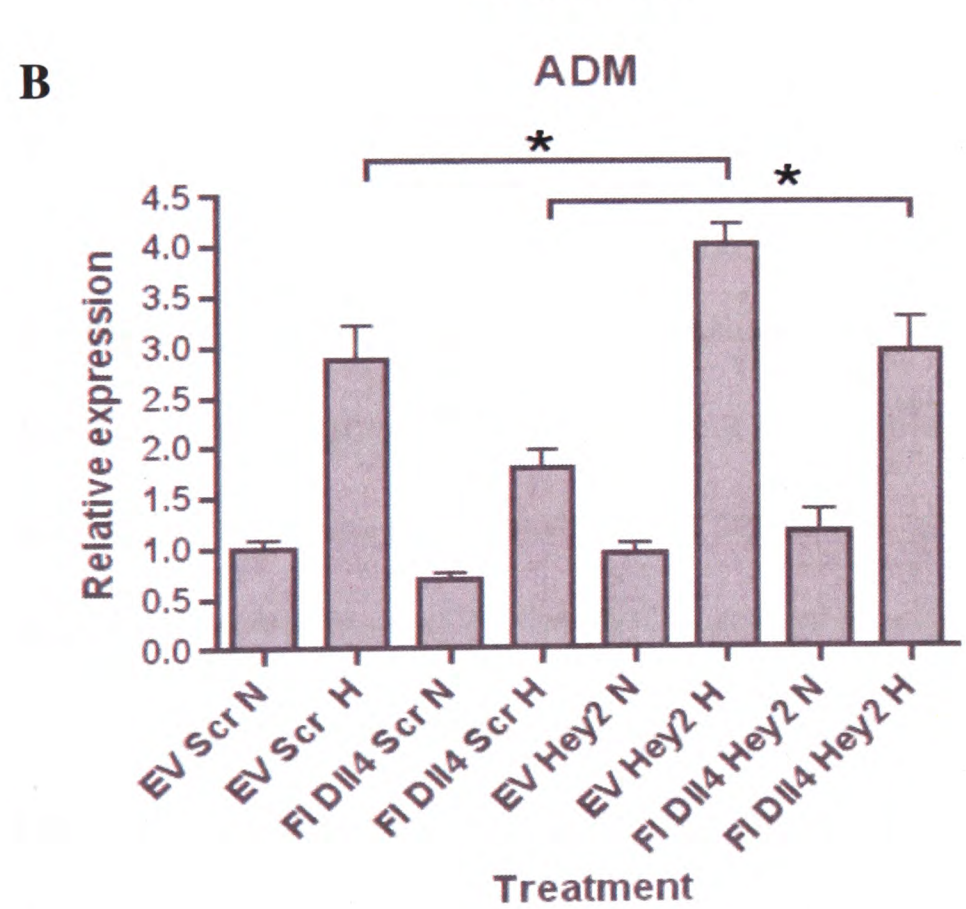


Figure 3.8. Hey2 siRNA restored hypoxia-regulated gene induction in Fl Dll4 cells.
In the Dll4 overexpression plus Hey2 siRNA experiment, real-time PCR was used to measure the normoxic and hypoxic expression of hypoxia-regulated genes PFKFB4 (A) and ADM (B) (*$p<0.05$, **$p<0.01$, ***$p<0.001$, ANOVA with Bonferroni's post-test, n=3).

As shown in Figure 3.7B, hypoxia repressed Hey2 expression while Dll4 overexpression induced Hey2 expression, as expected. Hey2 siRNA significantly reduced Hey2 expression in Fl Dll4 cells under both normoxia (column 3 vs. column 7, $p<0.001$, ANOVA with Bonferroni's post-test) and hypoxia (column 4 vs. column 8, $p<0.05$). The effect of Hey2 siRNA on Hey2 expression was similar to that of DAPT treatment (see Figure 3.5C).

The expression of hypoxia-regulated genes PFKFB4 and ADM is shown in Figure 3.8. Dll4 overexpression repressed the hypoxic induction, as expected. Hey2 siRNA restored the hypoxic induction of both genes. For each gene, Fl Dll4 cells treated with Hey2 siRNA (column 8) had similar expression under hypoxia to EV cells treated with Scr siRNA (column 2). Thus, Hey2 siRNA replicated the effect of DAPT treatment in this experiment, supporting the hypothesis that Hey2 mediates the effect of Dll4-Notch signalling on hypoxic induction.

These results are consistent with published studies. In one study, overexpression of either Hey1 or Hey2 repressed HIF1-dependent transcription (Diez et al., 2007). An earlier study may help explain the mechanism of this repression. In that study, Hey2 interacted with ARNT and inhibited the binding of the HIF2α-ARNT heterodimer to the hypoxia response element. As a result, HIF2-dependent transcription was repressed (Chin et al., 2000). Although most hypoxia-regulated genes studied in this chapter are HIF1 targets, the mechanism may still apply since both HIF1α and HIF2α depend on ARNT to activate transcription. Hey2 may interact with ARNT at the expense of HIFα-ARNT interaction and subsequent hypoxic induction. Altogether, the Dll4-Notch-Hey2 pathway repressed the induction of hypoxia-regulated genes in HUVECs.

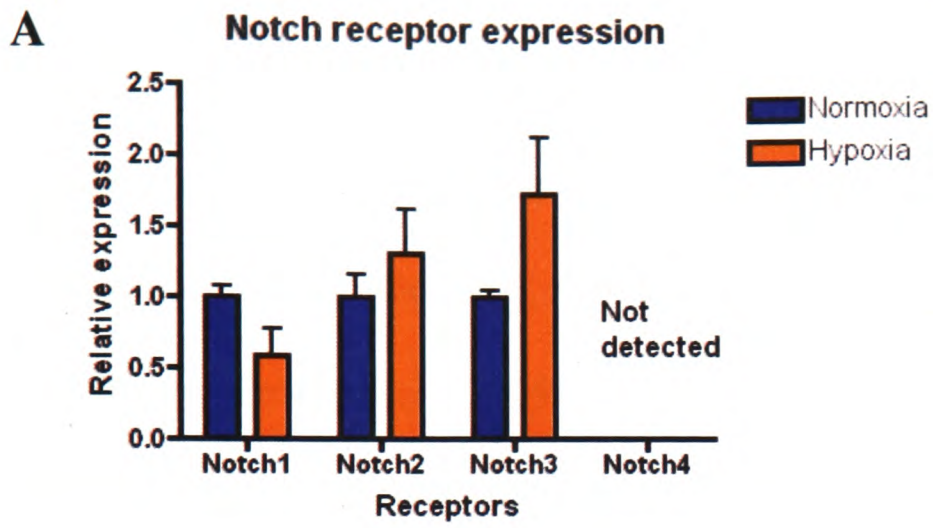
3.3 Notch-hypoxia crosstalk in MCF7 cells

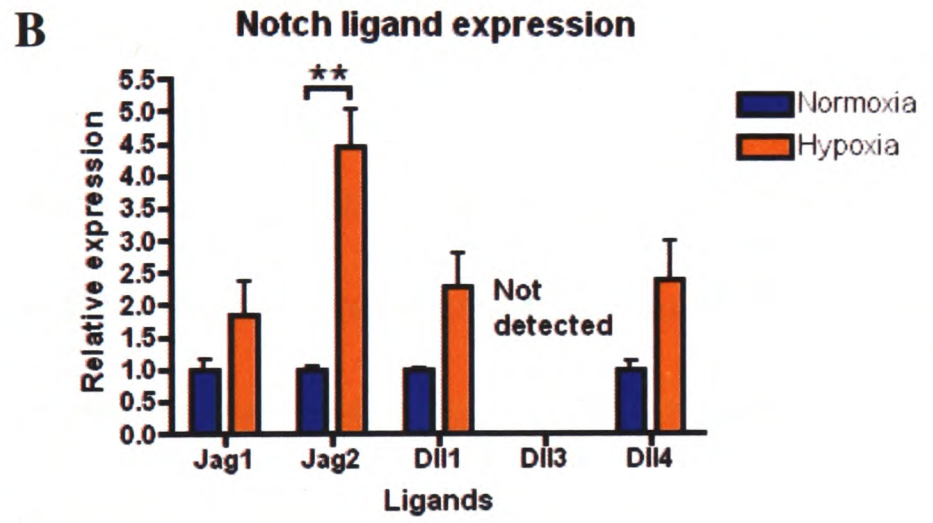
Previous studies have shown that hypoxia activated Notch signalling in neuroblastomas (Jogi et al., 2002) and HeLa cells (Wang et al., 2006). Experiments in this section investigated the effect of hypoxia treatment on Notch signalling in the breast cancer cell line MCF7.

3.3.1 Hypoxia induced Hey1 and Jag2 expression in MCF7 cells

First, MCF7 cells were cultured under normoxia or 0.1% hypoxia for 16 hours. Real-time PCR was used to measure the normoxic and hypoxic expression of Notch receptors 1-4; ligands Dll1, 3, 4 and Jag1, 2; and target genes Hey1, Hey2 and Hes1. As shown in Figure 3.9A, Notch4 mRNA was not detected. However, two published studies reported detecting Notch4 protein in MCF7 cells, by Western blotting (Sun et al., 2005) or immunohistochemistry (Dontu et al., 2004). It is possible that Notch4 mRNA level was too low to be detected by real-time PCR. Unlike Notch4, Notch1, 2 and 3 were detected; however, none of the three receptors was induced by hypoxia.

Among the ligands, Dll3 was not detected, and Jag2 was significantly induced by hypoxia, by 4.5-fold ($p=0.0039$, unpaired t-test; Figure 3.9B). Dll4 was also induced by hypoxia in MCF7 cells, as it was in HUVECs (see Figure 3.1A); however, the induction was not significant ($p=0.094$). All three Notch target genes tested were detected in MCF7 cells; however, only Hey1 was induced by hypoxia, by 20.7-fold ($p=0.0055$, unpaired t-test; Figure 3.9C). Altogether, hypoxia treatment induced Hey1 and Jag2 expression in MCF7 cells.





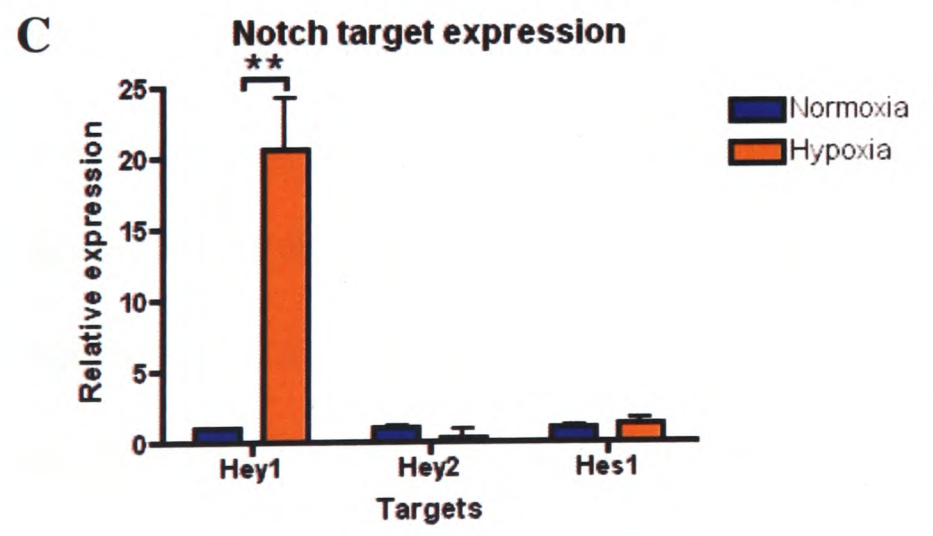


Figure 3.9. Hypoxia induced Hey1 and Jag2 expression in MCF7 cells.
MCF7 cells were cultured under normoxia or 0.1% hypoxia for 16 hours, and the mRNA expression of Notch receptors (A), ligands (B) and target genes (C) was measured by real-time PCR (**$p<0.01$, unpaired t-test, n=3).

3.3.2 Hypoxic induction of Hey1 and Jag2 was HIF1-dependent

Cellular hypoxia response is mediated by two related transcription factors, HIF1α and HIF2α (Harris, 2002). To determine which transcription factor was responsible for the hypoxic induction of Hey1 and Jag2, siRNAs against HIF1α and HIF2α were used, as described previously (Patel et al., 2005). MCF7 cells were transfected with Scr, HIF1α or HIF2α siRNA. Twenty-four hours post-transfection, cells were cultured under normoxia or 0.1% hypoxia for 16 hours, and total RNA was isolated for real-time PCR.

As shown in Figure 3.10A-B, hypoxia did not affect the mRNA expression of either HIF1α or HIF2α. This is consistent with previous studies that the hypoxic induction of HIF signalling occurs at the protein rather than mRNA level (Harris, 2002). HIF1α expression was specifically reduced by HIF1α siRNA, by 80% under normoxia ($p<0.01$, ANOVA with Bonferroni's post-test; Figure 3.10A) and by 83% under hypoxia ($p<0.01$). Similarly, HIF2α expression was specifically reduced by HIF2α siRNA, by 93% under normoxia ($p<0.05$, ANOVA with Bonferroni's post-test; Figure 3.10B) and by 95% under hypoxia ($p<0.01$). Notably, HIF2α expression was induced by HIF1α siRNA, under both normoxia ($p<0.001$) and hypoxia ($p<0.05$). This is consistent with a previous study from our laboratory, in which HIF1α knockdown induced HIF2α mRNA expression in the renal cancer cell line RCC4 (Raval et al., 2005). It is possible that HIF2α expression increased to compensate for the decrease in HIF1α expression by siRNA knockdown.

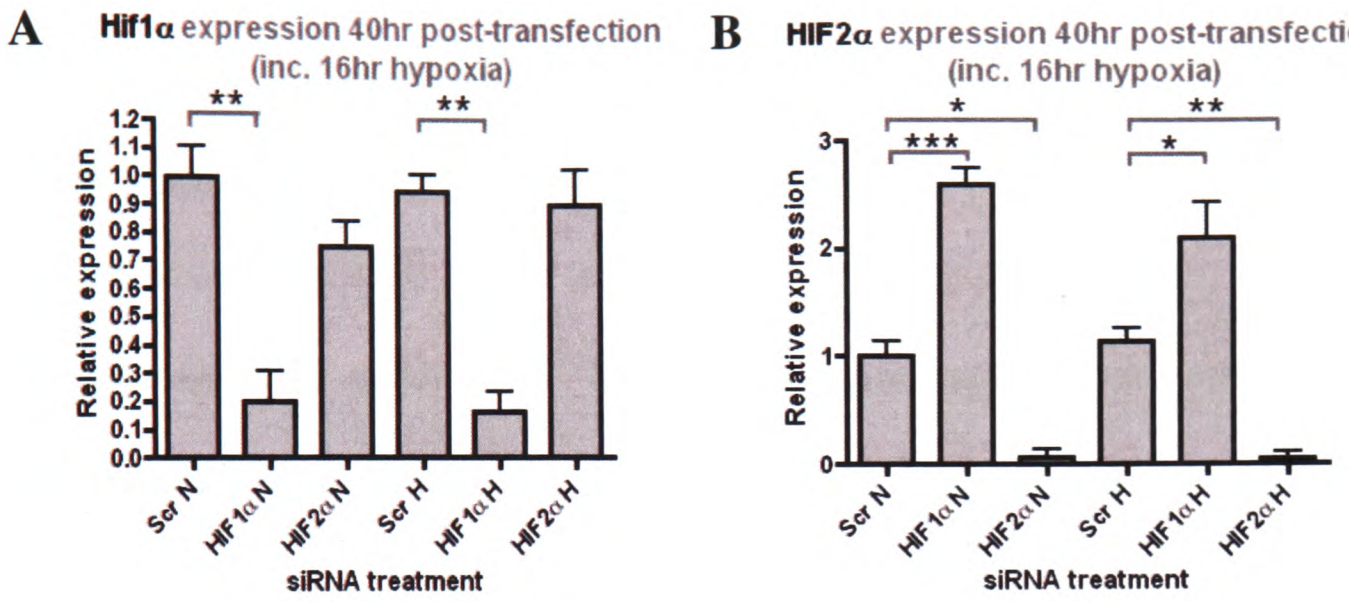


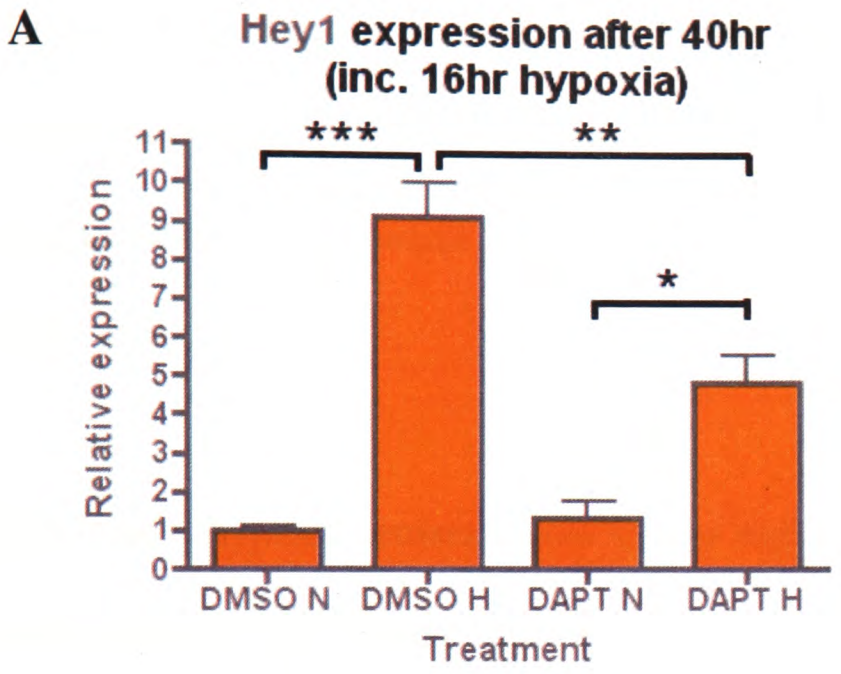
Figure 3.10. Hypoxic induction of Hey1 and Jag2 was HIF1-dependent.
MCF7 cells were transfected with Scr, HIF1α or HIF2α siRNA. Twenty-four hours post-transfection, cells were cultured under normoxia or 0.1% hypoxia for 16 hours. Real-time PCR was used to measure the expression of HIF1α (A), HIF2α (B), Hey1 (C) and Jag2 (D) (*p<0.05, **p<0.01, ***p<0.001, ANOVA with Bonferroni's post-test, n=3).

The expression of Hey1 and Jag2 was measured in the same experiment. Hey1 was induced by hypoxia by 19.3-fold ($p<0.001$, ANOVA with Bonferroni's post-test; Figure 3.10C), and the induction was abolished by HIF1α siRNA ($p<0.001$). Similarly, Jag2 was induced by hypoxia by 2.9-fold ($p<0.001$, ANOVA with Bonferroni's post-test; Figure 3.10D), and the induction was abolished by HIF1α siRNA ($p<0.001$). In contrast, HIF2α siRNA did not affect the expression of either gene. Thus, the hypoxic induction of both Hey1 and Jag2 was specifically HIF1α-dependent.

3.3.3 Hypoxic induction of Hey1 but not Jag2 was Notch-dependent

To determine whether hypoxia induced Hey1 and Jag2 via Notch signalling, the γ-secretase inhibitor DAPT was used. MCF7 cells were treated with 5 μM DAPT or DMSO for 40 hours, the last 16 of which under normoxia or 0.1% hypoxia. Hey1 and Jag2 expression was measured by real-time PCR.

As shown in Figure 3.11A, hypoxia induced Hey1 by 9.1-fold ($p<0.001$, ANOVA with Bonferroni's post-test), and the expression under hypoxia was significantly reduced by DAPT ($p<0.01$). This suggests that the hypoxic induction of Hey1 was Notch-dependent. Notably, DAPT treatment did not completely abolish the induction of Hey1 by hypoxia (3.6-fold, $p<0.05$). This could be explained by the incomplete inhibition of Notch signalling by DAPT. Alternatively, hypoxia may signal through other pathways in addition to Notch to induce Hey1 expression.



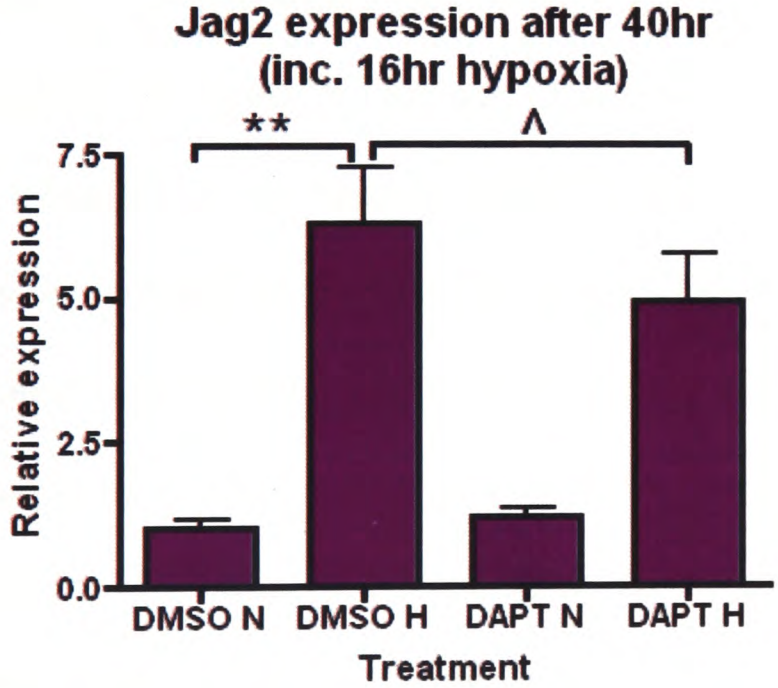
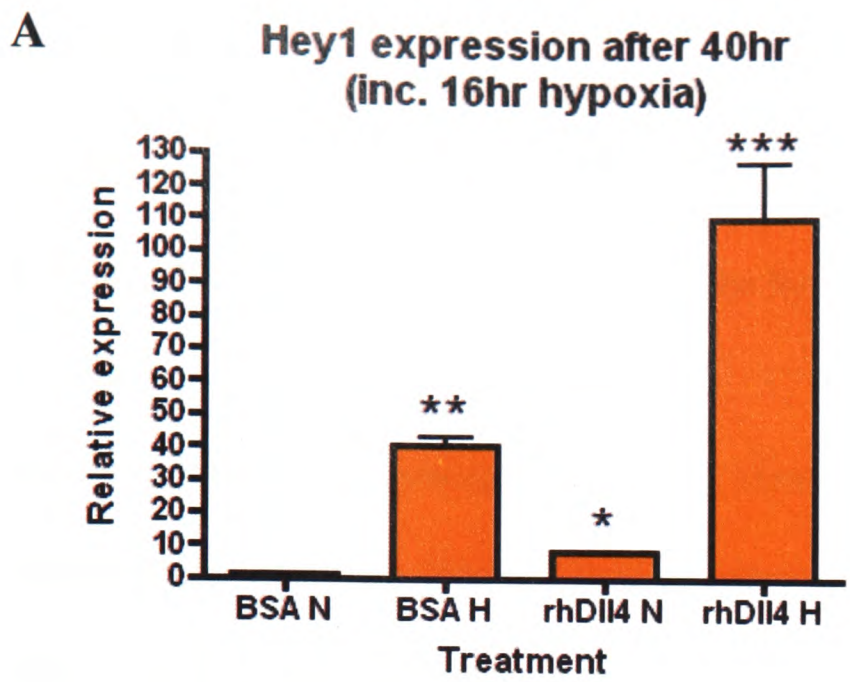


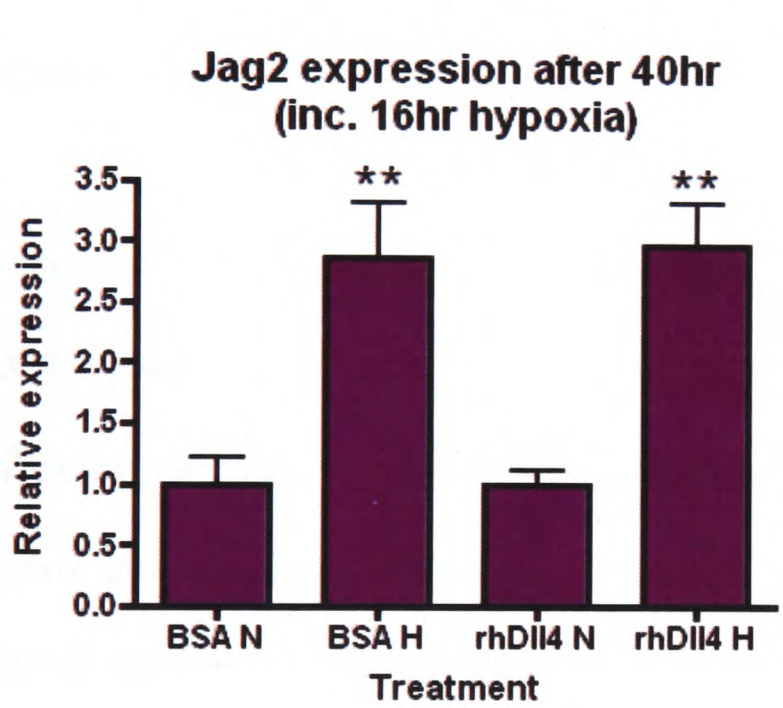
Figure 3.11. DAPT treatment repressed hypoxic induction of Hey1 but not Jag2.
MCF7 cells were treated with 5 μM DAPT or DMSO for 40 hours, the last 16 of which under normoxia or 0.1% hypoxia. Real-time PCR was used to measure the expression of Hey1 (A) and Jag2 (B) (^$p \geq 0.05$, *$p < 0.05$, **$p < 0.01$, ***$p < 0.001$, ANOVA with Bonferroni's post-test, n=3).

Like Hey1, Jag2 was induced by hypoxia by 6.3-fold ($p<0.01$, ANOVA with Bonferroni's post-test; Figure 3.11B). However, the expression under hypoxia was not reduced by DAPT ($p\geq0.05$). To date, no published study has identified Jag2 as a Notch target gene, and its expression does not depend on γ-secretase cleavage. In contrast, Hey1 is a Notch target gene downstream of γ-secretase cleavage. Thus, the induction of Hey1 but not Jag2 was Notch-dependent.

The Notch-hypoxia crosstalk was further explored by culturing MCF7 cells on plates coated with recombinant human Dll4 (rhDll4) before hypoxia treatment. Previous work in our laboratory demonstrated that rhDll4 immobilised on cell culture plates induced Notch signalling, as shown by the accumulation of N1ICD protein (Williams et al., 2006). Here, MCF7 cells were cultured on rhDll4- or BSA-coated plates for 24 hours under normoxia, and then for 16 hours under 0.1% hypoxia or normoxia. As shown in Figure 3.12A, hypoxia alone induced Hey1 by 40.8-fold ($p<0.01$, ANOVA with Bonferroni's post-test), and rhDll4 alone induced Hey1 by 8.0-fold ($p<0.05$). The combined hypoxia and rhDll4 treatment induced Hey1 by 110.7-fold ($p<0.001$). Thus, the hypoxia and Dll4-Notch pathways synergistically induced Hey1 expression in MCF7 cells.

Jag2 expression was measured in the same experiment (Figure 3.12B). Hypoxia induced Jag2 by 2.9-fold in cells grown on BSA-coated plates, and by 3.0-fold in cells grown on rhDll4-coated plates. Thus, promoting Dll4-Notch signalling did not further the hypoxic induction of Jag2.





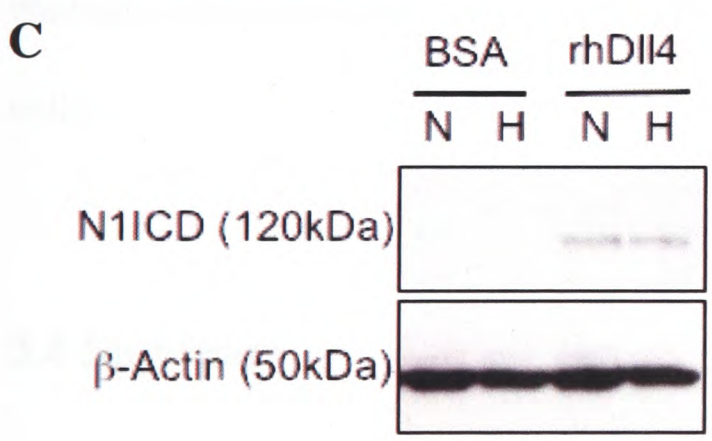


Figure 3.12. Dll4-Notch and hypoxia signalling synergistically induced Hey1 but not Jag2.
MCF7 cells were cultured on rhDll4- or BSA-coated plates for 40 hours, the last 16 of which under normoxia or 0.1% hypoxia. (A-B) Real-time PCR was used to measure the expression of Hey1 and Jag2 (*$p<0.05$, **$p<0.01$, ***$p<0.001$, ANOVA with Bonferroni's post-test, n=3). Stars indicate significant differences with the BSA N sample. (C) Protein samples were isolated from the same experiment, separated by SDS-PAGE and blotted with antibodies against N1ICD and β-actin (n=2).

Taken together, these results show that the hypoxic induction of Hey1 was at least partially Notch-dependent, and the hypoxia and Notch pathways synergised to induce Hey1. In contrast, Notch signalling did not affect the hypoxic induction of Jag2.

The hypoxia-Notch synergy may have several possible mechanisms. First, hypoxia may induce Notch cleavage. Second, hypoxia may stabilise NICD. Third, HIF1α may interact with NICD at the Hey1 promoter to enhance transcription, as described previously in stem and precursor cells (Gustafsson et al., 2005).

To test the first hypothesis, protein samples were isolated from MCF7 cells cultured on rhDll4-coated plates under hypoxia, separated by SDS-PAGE and immunoblotted with antibodies for cleaved N1ICD and β-actin (loading control). As shown in Figure 3.12C, hypoxia did not lead to the accumulation of cleaved N1ICD. However, this result did not preclude the involvement of other Notch receptors. Thus, further experiments are needed to elucidate the mechanism of hypoxia-Notch synergy in inducing Hey1 expression in MCF7 cells.

3.4 Summary

Experiments in this chapter explored two aspects of the Notch-hypoxia signalling crosstalk. First, Dll4 overexpression in HUVECs affected hypoxic induction. Second, hypoxia induced the expression of Hey1 and Jag2 in MCF7 cells.

In HUVECs, siRNA-mediated knockdown of Dll4 expression did not affect the induction of four hypoxia-regulated genes. This may be due to the low expression level of Dll4 in HUVECs so that knockdown did not affect Dll4-Notch signalling.

In contrast, retrovirus-mediated overexpression of Dll4 repressed the induction of the four hypoxia-regulated genes. The repression was Notch-dependent as DAPT treatment, which blocked Notch signalling, restored the hypoxic induction.

In addition, Dll4 overexpression induced Hey2 expression, and DAPT reduced Hey2 expression; thus, Hey2 may mediate the repression of hypoxic induction. Indeed, Hey2 knockdown restored the hypoxic induction, replicating the effect of DAPT. Further experiments are needed to elucidate the mechanism of Hey2 repression of hypoxic induction.

In MCF7 cells, hypoxia induced the expression of Hey1 and Notch ligand Jag2. Specific knockdown of HIF1α and HIF2α showed that the hypoxic induction of both Hey1 and Jag2 was HIF1α-dependent.

DAPT treatment significantly reduced the hypoxic induction of Hey1 but not that of Jag2, suggesting that Hey1 induction by hypoxia was Notch-dependent. In addition, culturing MCF7 cells on rhDll4-coated plates promoted Notch signalling, which synergistically induced Hey1 expression under hypoxia. In contrast, Jag2 expression was not affected by either DAPT treatment or rhDll4-coated plates. The likely explanation is that Hey1 is a Notch target gene, but Jag2 is not. Further experiments are needed to clarify the mechanism of the hypoxic induction of these two genes.

CHAPTER FOUR

Regulation of Dll4 Expression by Notch, VEGF and Hypoxia Signalling

4.1 Introduction

As stated in Sections 1.5.3 and 1.5.4, Dll4-Notch signalling plays a crucial role in both developmental and tumour angiogenesis; therefore, it is important to examine which signalling pathways regulate Dll4 expression *in vitro*. Previous studies have suggested that Dll4 expression is regulated by Notch signalling (Shawber et al., 2003), VEGF (Liu et al., 2003, Patel et al., 2005) and hypoxia (Mailhos et al., 2001, Patel et al., 2005). Experiments in this chapter seek to elucidate the mechanisms of such regulation in cultured endothelial cells.

Two approaches were used to achieve the aim of this chapter. First, Dll4 mRNA expression was measured by real-time PCR. HUVECs were cultured under various conditions, and total RNA was extracted for real-time PCR analysis. While Dll4 is expressed predominantly in the arterial vasculature during development, previous work in our laboratory has shown that Dll4 is expressed in HUVECs (Patel et al., 2005).

Second, the activation of the human Dll4 promoter was measured by luciferase assays. The 4 kb proximal promoter is shown in Figure 4.1, together with known transcription factor binding sites (UC Santa Cruz Genome Browser, June 2005 version). The 4 kb promoter contains one putative HIF binding site, or hypoxia response element (HRE), 1930 bp upstream of the translational start site ATG. Promoter fragments of different lengths (4 kb, 2.2 kb, 1.6 kb, 1 kb and 500 bp) upstream of ATG were cloned into the pGL3e plasmid encoding a Firefly luciferase gene. The pRL plasmid encoding a Renilla luciferase gene was used to control for transfection efficiency. The pGL3e and pRL plasmids were co-transfected

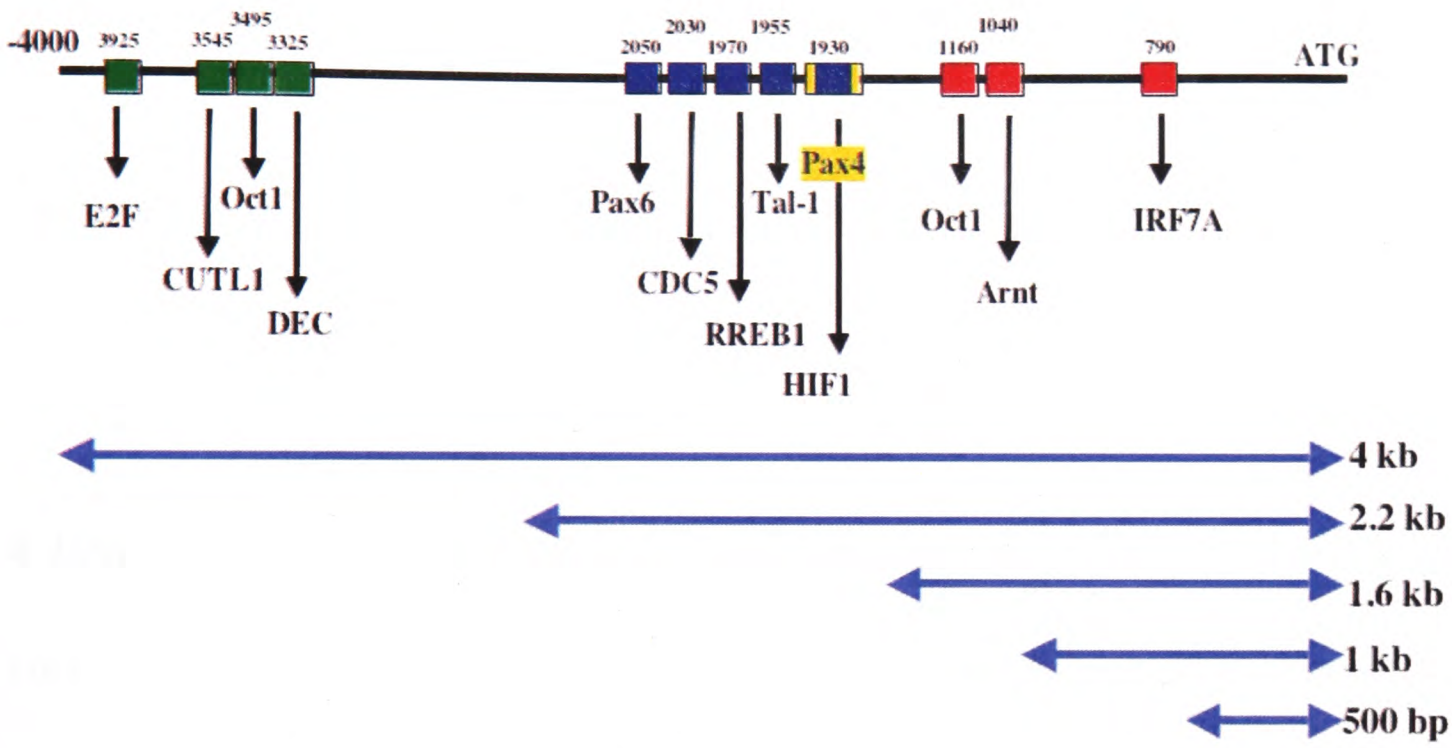


Figure 4.1. Dll4 promoters fragments used in this chapter.
The 4 kb Dll4 proximal promoter is shown with known transcription factor binding sites (UC Santa Cruz Genome Browser, June 2005 version). Dll4 promoter fragments used in this chapter are depicted below.

into immortalised porcine aortic endothelial (PAE) cells, chosen for their arterial origin and ease of transfection (Landgren et al., 1998). Transfected PAE cells were then cultured under various conditions and lysed for luciferase assays to measure the activation of the promoters.

Both real-time PCR and luciferase assays studied Dll4 regulation at the transcriptional level. At the translational level, although there are several antibodies capable of detecting Dll4 protein overexpressed *in vitro* and in tumour samples, none is capable of detecting endogenous Dll4 protein *in vitro*. Therefore, it was not possible to study Dll4 regulation at the protein level.

4.2 Notch signalling induced Dll4 expression

Dll4 is a ligand for Notch1 and Notch4 (Shutter et al., 2000), both of which play crucial roles in angiogenesis. *Notch1*-null mice developed angiogenic defects leading to embryonic lethality. *Notch1/4* double knockout mice exhibited more severe vascular abnormalities than *Notch1*-null mice (Krebs et al., 2000). Expression of activated Notch4 in the mouse embryonic vasculature also led to angiogenic defects (Uyttendaele et al., 2001), suggesting that an optimal range of Notch signalling is necessary for vascular development and function.

Interestingly, recent *in vitro* studies and results presented in this chapter demonstrated that Notch signalling regulates Dll4 expression in endothelial cells, suggesting a positive feedback mechanism.

4.2.1 Notch1 intracellular domain induced Dll4 expression

According to a previous report, transfection of human microvascular endothelial cells with the Notch4 intracellular domain, the activated form of Notch4, resulted in a 16-fold increase in Dll4 mRNA expression (Shawber et al., 2003). Here, I focused on the effect of the Notch1 intracellular domain (N1ICD), the activated form of Notch1, on Dll4 expression. The pcDNA plasmids encoding cDNA for N1ICD and green fluorescent protein (GFP), referred to as pcDNA-N1ICD and pcDNA-GFP, were provided by Dr Richard Sainson.

To measure the effect of N1ICD on Dll4 mRNA expression, HUVECs were transfected with 1 μg of pcDNA-N1ICD or pcDNA-GFP, and total RNA was isolated 48 hours after transfection. Real-time PCR analysis indicated that N1ICD overexpression induced endogenous Dll4 mRNA by 8.6-fold compared with the GFP control ($p=0.0007$, unpaired *t*-test; Figure 4.2A). Expanding on this result, increasing amounts of the pcDNA-N1ICD plasmid (0 μg or pcDNA-GFP, 0.2 μg, 0.5 μg, 1 μg and 2 μg) were used to transfect HUVECs, and total RNA was isolated 48 hours after transfection. N1ICD overexpression induced Dll4 mRNA dose-dependently up to 1 μg, and the results were statistically significant ($p=0.0037$, ANOVA; Figure 4.2B). As expected, Notch target gene Hey1 was similarly induced by N1ICD overexpression ($p=0.013$, ANOVA; Figure 4.2C).

Dll4 induction by Notch signalling was further confirmed using promoter constructs. Briefly, pcDNA-N1ICD or pcDNA-GFP were co-transfected into PAE cells with 1 μg of pGL3e plasmid encoding the Dll4 1.6 kb promoter and 50 ng of pRL plasmid. The plasmid encoding the 1.6 kb promoter was used because it was highly activated by various treatments. PAE

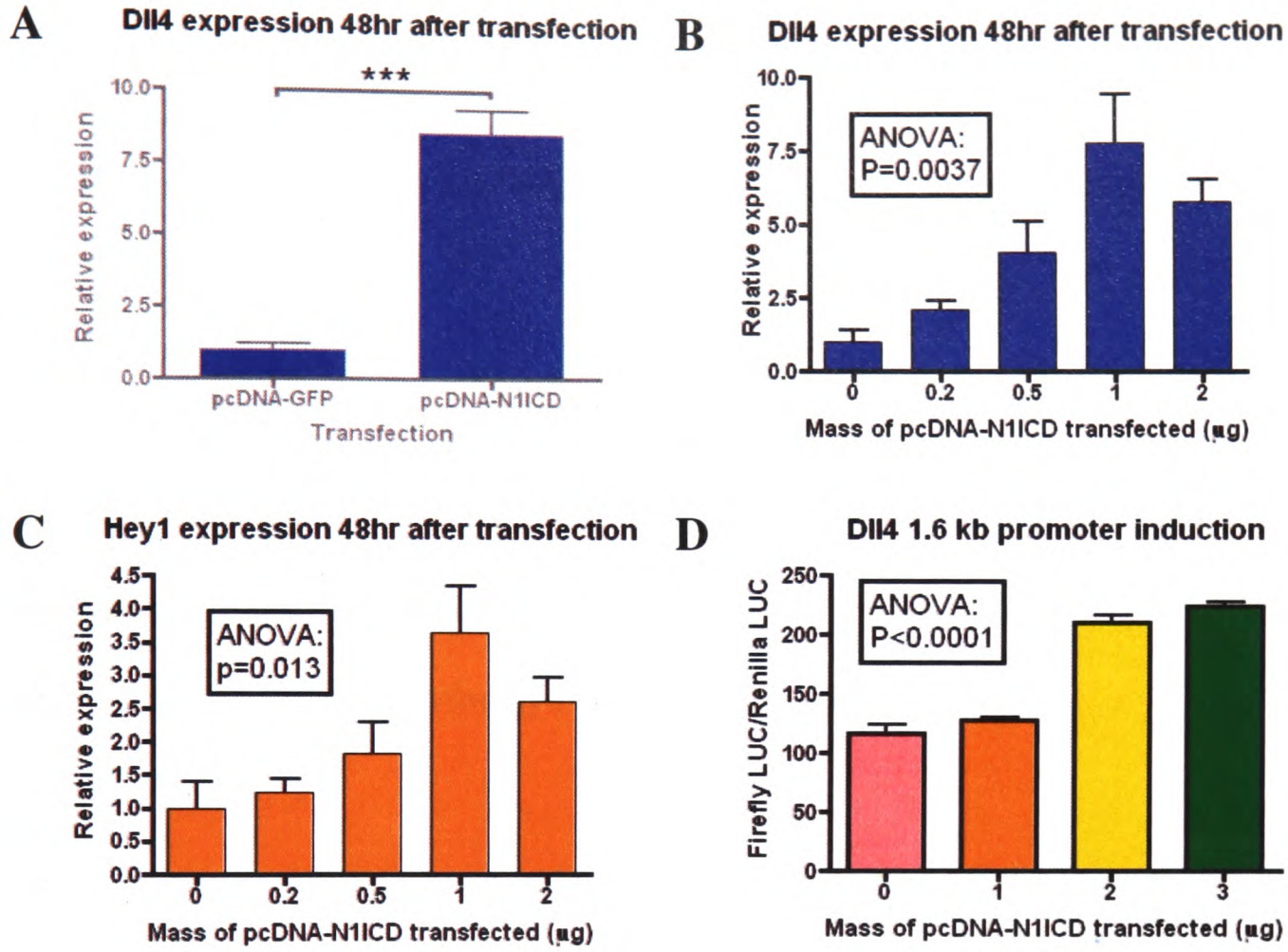


Figure 4.2. Notch1 intracellular domain (N1ICD) induced Dll4 expression.
(A) HUVECs were transfected with 1 µg of pcDNA-N1ICD or pcDNA-GFP plasmid. After 48 hours, Dll4 expression was quantified using real-time PCR (***$p<0.001$, unpaired t-test, n=3). (B-C) HUVECs were transfected with different amounts of pcDNA-N1ICD, and real-time PCR was used to quantify the expression of Dll4 (B) and Hey1 (C) 48 hours post-transfection. The data were analysed with ANOVA (n=3). (D) PAE cells were transfected with different amounts of pcDNA-N1ICD as indicated, together with the pGL3e plasmid encoding the 1.6 kb promoter and the pRL plasmid. Luciferase assay was used to measure promoter activation, and the ratios of Firefly-to-Renilla luciferase are presented. The data were analysed with ANOVA (n=6).

cells were lysed 48 hours post-transfection, and luciferase assays were performed to measure the Firefly and Renilla luciferase (LUC) activities. The ratio of Firefly LUC to Renilla LUC was used to control for the amount of plasmid transfected. As shown in Figure 4.2D, N1ICD overexpression (from 0 to 3 μg) activated the Dll4 promoter dose-dependently ($p<0.0001$, ANOVA). These results confirmed the Dll4 induction by N1ICD at the mRNA level, suggesting that a positive feedback loop exists between Notch1 and Dll4.

4.2.2 Exogenous Dll4 ligands induced Dll4 expression

Beyond overexpression of N1ICD, an alternative approach was used to investigate Notch regulation of Dll4 expression. Recombinant human Dll4 (rhDll4) protein was used for this purpose, as described previously (Williams et al., 2006).

Here, culturing HUVECs on rhDll4-coated plates for 24 hours induced endogenous Dll4 mRNA expression by 4.3-fold ($p<0.001$, ANOVA with Bonferroni's post-test; Figure 4.3A). The induction was abrogated by treatment with 2 μM DAPT, a γ-secretase inhibitor that blocks Notch signalling ($p<0.001$). This is consistent with the hypothesis that the induction of Dll4 was dependent on Notch signalling.

To confirm this result, a dose-response curve of rhDll4, 0 (BSA), 0.2, 0.4, 0.6, 0.8 and 1 μg/ml, was used to coat cell culture plates, on which HUVECs were seeded. Real-time PCR analysis confirmed that endogenous Dll4 mRNA expression was induced dose-dependently by rhDll4 after 24 hours ($p=0.011$, ANOVA; Figure 4.3B). As expected, rhDll4 also dose-

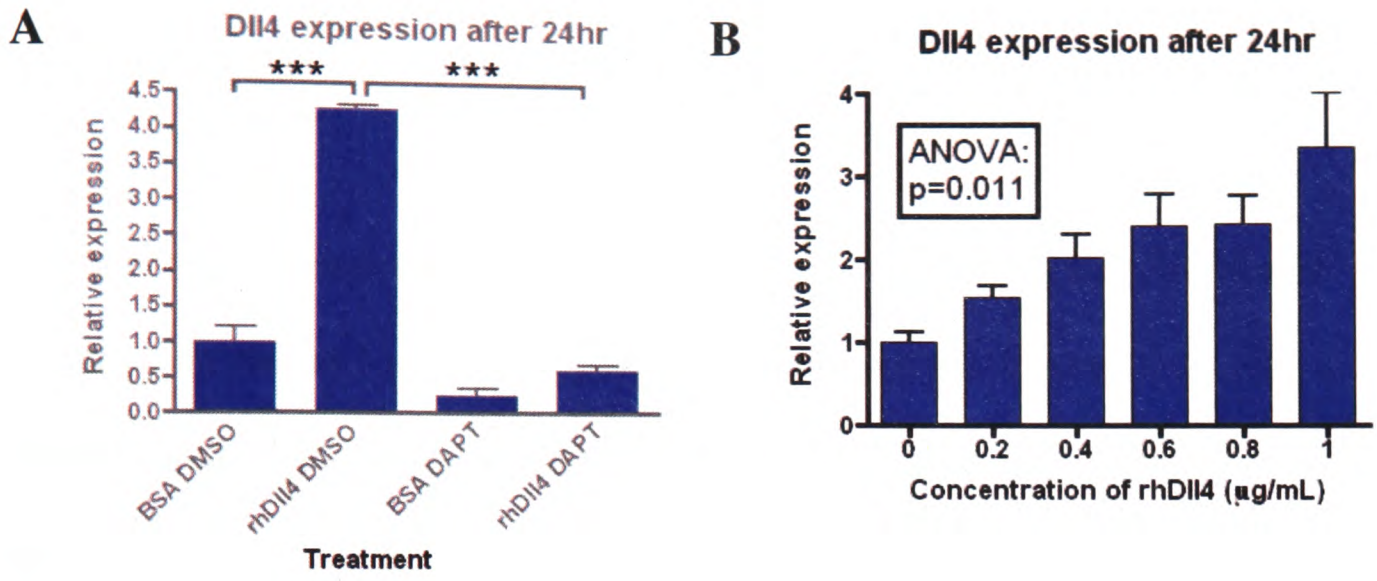


Figure 4.3. Exogenous Dll4 ligands induced Dll4 expression.
(A) HUVECs were cultured on plates coated with rhDll4 (1 μg/ml) or BSA with 2 μM DAPT or DMSO for 24 hours. Dll4 expression was quantified using real-time PCR (***$p<0.001$, ANOVA with Bonferroni's post-test, n=3). (B-D) HUVECs were cultured on plates coated with different concentrations of rhDll4 for 24 hours, and real-time PCR was used to quantify the expression of Dll4 (B), Hey1 (C) and Hey2 (D). The data were analysed with ANOVA (n=3).

dependently induced Notch target genes Hey1 ($p=0.0076$, ANOVA; Figure 4.3C) and Hey2 ($p=0.0006$, ANOVA; Figure 4.3D). These results support the hypothesis that exogenous Dll4 is capable of inducing endogenous Dll4 mRNA expression via Notch signalling. This conclusion is further supported by a recent report that immobilised Dll4 ligands induced endogenous Dll4 protein expression in HUVECs (Ridgway et al., 2006).

A time course experiment of Dll4 induction by rhDll4 was conducted. HUVECs were cultured on rhDll4-coated plates, and RNA was isolated from cells after 0, 4, 8, 16, 24 and 48 hours. As shown in Figure 4.4A, Dll4 mRNA expression was induced by 3.9-fold at 4 hours, peaked at 4.5-fold at 8 hours and then gradually decreased to 2.4-fold at 48 hours. In comparison, Hey1 was induced by 190.0-fold at 4 hours, and the expression decreased to 96.3-fold at 8 hours and 13.1-fold at 24 hours (Figure 4.4B). Both Dll4 and Hey1 were induced after 4 hours of culture on rhDll4, suggesting that both genes are direct targets of Dll4-Notch signalling.

Next, the effect of rhDll4 on Dll4 promoter activation was measured by luciferase assays. First, 1 μg of pGL3e plasmids encoding Dll4 promoters of different lengths, and pGL3e empty vector (EV) control, were co-transfected into PAE cells with 50 ng of pRL plasmid. After 16 hours, PAE cells were re-plated on rhDll4- or BSA-coated plates for 24 hours before being lysed for luciferase assays. The normalised luciferase activities (Firefly LUC/Renilla LUC) are shown in Figure 4.5A, and the ratios of induction by rhDll4 compared with BSA are shown in Figure 4.5B. As expected, there was no induction in EV control cells. Among the five Dll4 promoters, the 1.6 kb and 500 bp promoters were significantly activated by

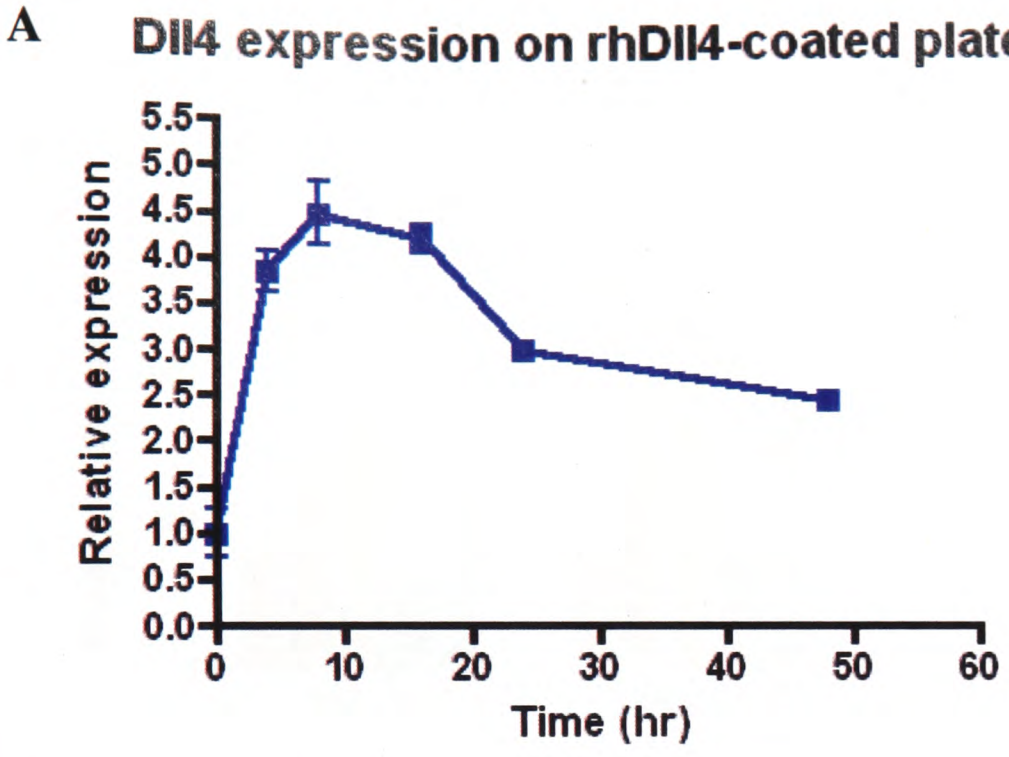
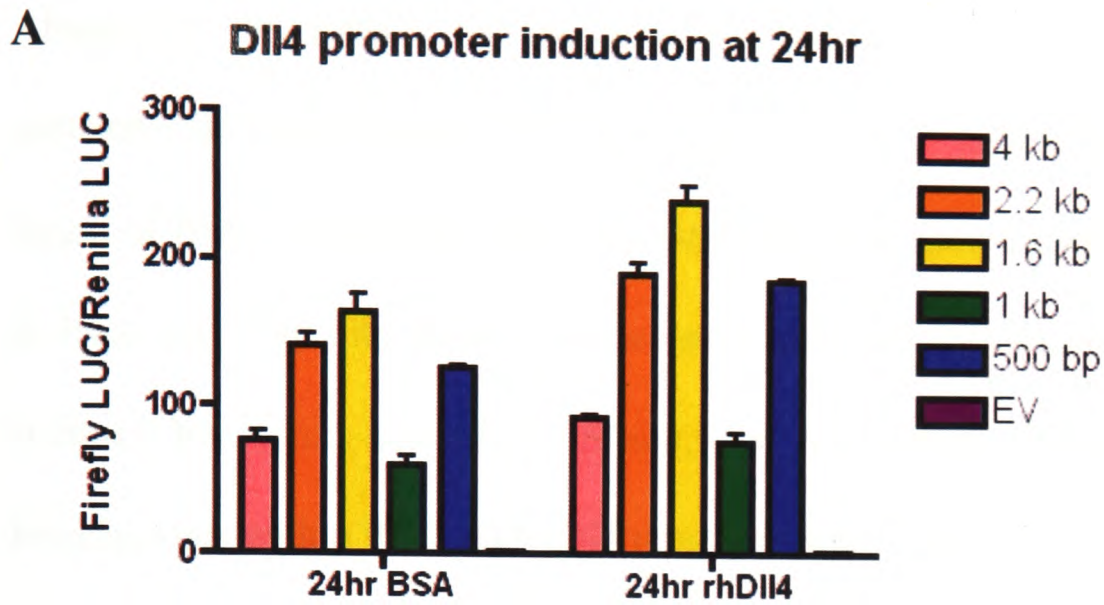


Figure 4.4. Time course of Dll4 induction by exogenous Dll4 ligands.
HUVECs were cultured on plates coated with rhDll4 (1 μg/ml) and harvested at different time points. Real-time PCR was used to measure the time course of Dll4 (A) and Hey1 (B) induction (n=3; figures courtesy of Dr Richard Sainson).



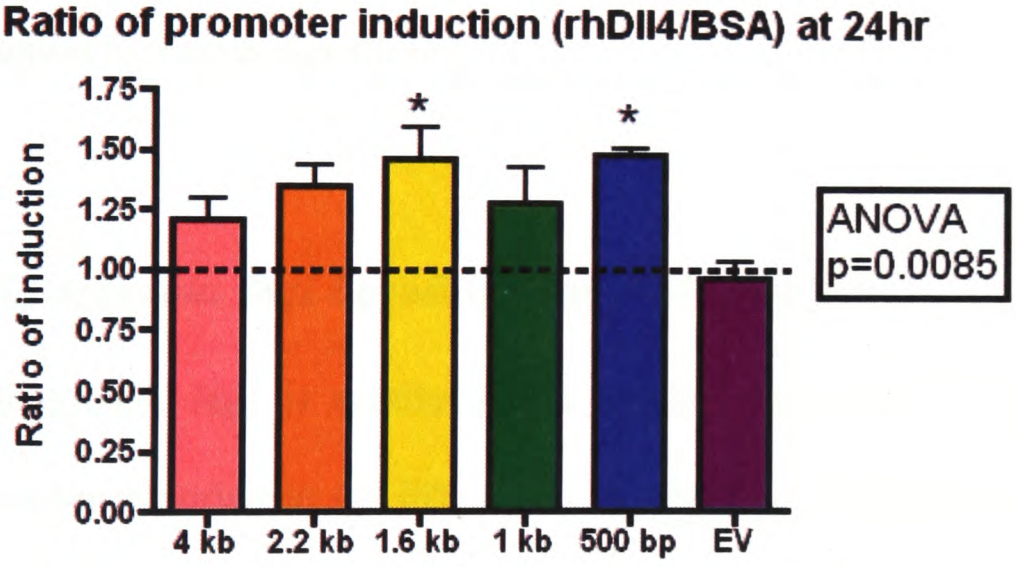


Figure 4.5. Exogenous Dll4 ligands induced Dll4 promoters.
PAE cells were transfected with pGL3e plasmids encoding Dll4 promoter fragments (4 kb, 2.2 kb, 1.6 kb, 1 kb, 500 bp) and empty vector (EV) control together with the pRL plasmid, and cultured on rhDll4- or BSA-coated plates for 24 hours. Luciferase assay was used to measure Dll4 promoter induction, and Firefly-to-Renilla luciferase ratios are presented in (A). Ratios of induction by rhDll4 relative to BSA for the promoters are shown in (B). Stars indicate significant inductions compared with EV control (*$p<0.05$, ANOVA with Bonferroni's post-test, n=6).

rhDll4 ($p<0.05$, ANOVA with Bonferroni's post-test) while the activation of the other promoter fragments was not significant ($p\geq0.05$).

Altogether, the mRNA and promoter studies demonstrated that exogenous Dll4 ligands induced Dll4 transcription via Notch signalling. These results also suggest that Dll4 is a direct target of Notch signalling. Thus, the Dll4 promoter should contain RBP-jκ binding sites, and at least one such site should be located within the 500 bp proximal promoter since it was induced by Notch signalling. Indeed, one recent study identified three putative RBP-jκ binding sites within the 2.6 kb Dll4 promoter, including one within 573 bp (Diez et al., 2007). Mutating these binding sites in future experiments would be expected to prevent Dll4 induction by Notch signalling.

4.2.3 Exogenous Jag1 ligands induced Dll4 expression

Besides Dll4, Jag1 is another Notch ligand implicated in angiogenesis. Mutations in Jag1 have been reported in 60-70% cases of Alagille syndrome, a genetic disorder with notable vascular defects (Shawber and Kitajewski, 2004). A recent study demonstrated that Jag1 expressed in squamous cell carcinoma cells could induce Notch signalling in neighbouring endothelial cells and promote angiogenesis *in vitro* and *in vivo* (Zeng et al., 2005). Here, I examined the effect of recombinant Jag1 protein, and cells stably expressing Jag1, on Dll4 mRNA expression in HUVECs.

Recombinant rat Jag1 (rrJag1) protein, consisting of the extracellular domain, was the only commercially available Jag1 protein. Fortunately, the Jag1 gene is highly conserved through

evolution, and the rat and human proteins share 96% sequence identity, allowing a comparison between rhDll4 and rrJag1.

To ensure the same molar amount of protein was used to coat cell culture plates, the weight/volume concentration used for rhDll4 (1 μg/ml) was converted to molar concentration (18 nM), and the same molar concentration of rrJag1 was used. A dose-response curve was then established for the two proteins: 0 (BSA), 3.6, 7.2, 10.8, 14.4 and 18 nM. After 24 hours, rhDll4 induced endogenous Dll4 expression dose-dependently ($p<0.0001$, ANOVA; Figure 4.6A) as shown in Figure 4.3B. In comparison, rrJag1 also induced Dll4 expression dose-dependently ($p=0.018$, ANOVA). However, the fold induction by rrJag1 was smaller at all concentrations. At the highest concentration, 18 nM, rhDll4 induced Dll4 by 16.1-fold, while rrJag1 induced Dll4 by 4.3-fold. Similarly, both proteins induced Hey2 expression dose-dependently (rhDll4, $p<0.0001$; rrJag1, $p=0.011$, ANOVA; Figure 4.6B). At 18 nM, rhDll4 induced Hey2 by 8.9-fold, while rrJag1 induced Hey2 by 3.2-fold. This suggests that rhDll4 may be a better inducer of Dll4 expression and Notch signalling than rrJag1.

Two reasons could have accounted for the smaller induction by rrJag1 compared with rhDll4. The first reason could be the incompatibility between the rat Jag1 ligand and the human Notch signalling pathway in HUVECs. However, due to the high level of sequence identity (96%) between rat and human Jag1 proteins, this is unlikely. The second reason could be ligand specificity in inducing Notch signalling. Since Dll4 is predominantly expressed in endothelial cells (Shutter et al., 2000), it may be the preferred ligand to induce Notch signalling and Dll4 expression in these cells. In one study, Dll4 but not Jag1 stimulation

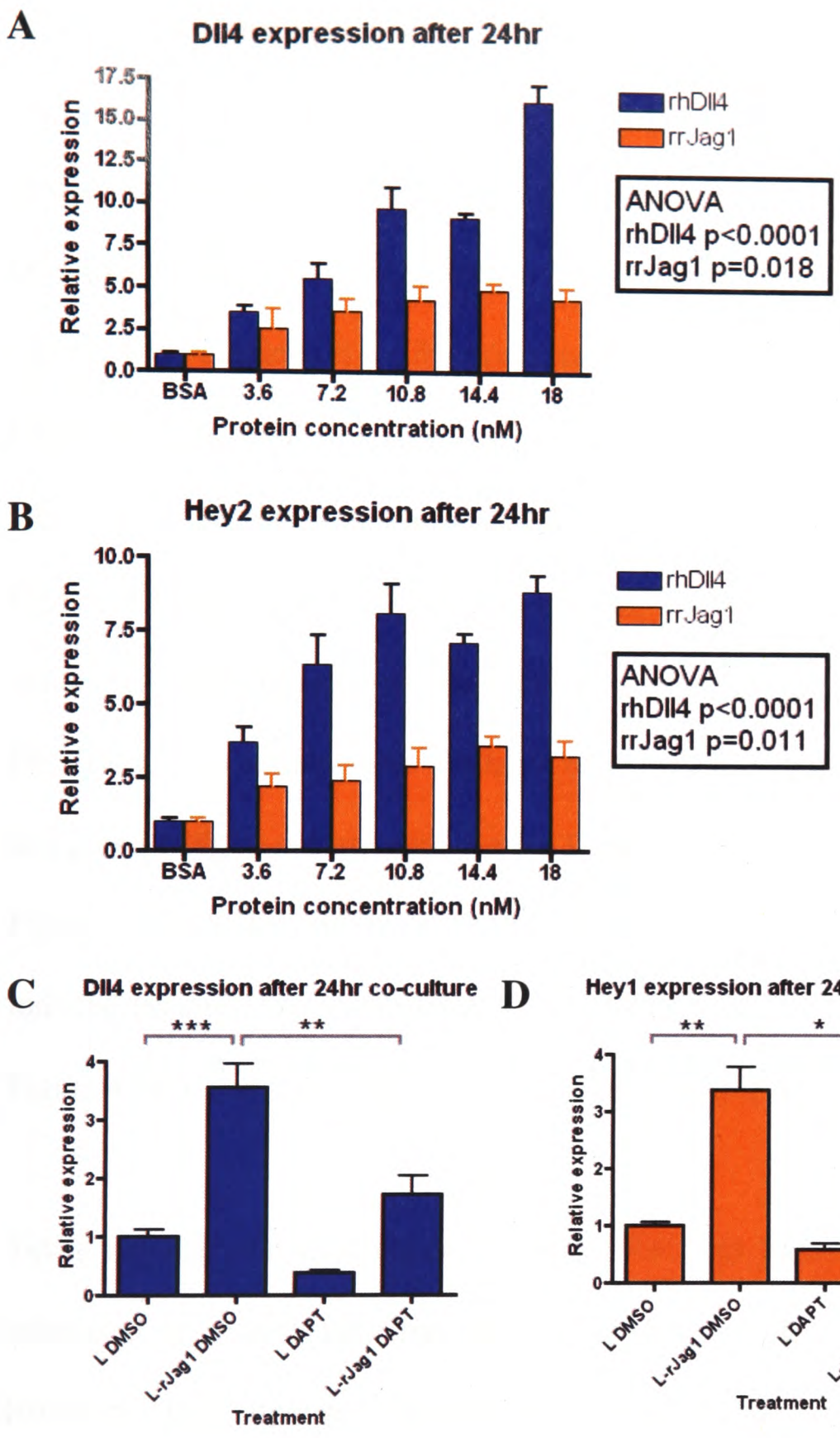


Figure 4.6. Exogenous Jag1 ligands induced Dll4 expression.
(A-B) HUVECs were cultured on plates coated with different concentrations of rhDll4 or rrJag1 for 24 hours, and real-time PCR was used to quantify the expression of Dll4 (A) and Hey2 (B). The data were analysed with ANOVA (n=3). (C-D) HUVECs were co-cultured for 24 hours with L-cells stably expressing rat Jag1 or control L-cells, with 2 μM DAPT or DMSO. Real-time PCR results for Dll4 are shown in (C), and those for Hey1 are shown in (D) (*$p<0.05$, **$p<0.01$, ***$p<0.001$, ANOVA with Bonferroni's post-test, n=3).

induced the expression of Notch target gene ephrin B2 in HUVECs (Iso et al., 2006), offering evidence for Notch ligand specificity in endothelial cells.

In addition to rrJag1-coated plates, cells overexpressing full-length Jag1 were used to induce Dll4 expression in HUVECs. Murine L cells (a fibroblast cell line) stably expressing rat Jag1 (rJag1) were obtained from the Weinmaster laboratory (Lindsell et al., 1995). One million L-rJag1 cells or control L cells were plated per well of a six-well plate. After 24 hours, HUVECs were plated on top of the L cells with HUVEC medium containing either 2 μM DAPT or DMSO. After 24 hours co-culture, total RNA was isolated, and real-time PCR was conducted with human-specific primers to detect human Dll4 and Hey1 expression in HUVECs. Co-culture with L-rJag1 cells induced human Dll4 expression by 3.6-fold, compared with co-culture with control L cells ($p<0.001$, ANOVA with Bonferroni's post-test; Figure 4.6C). The induction was inhibited by DAPT ($p<0.01$). Likewise, L-rJag1 cells induced human Hey1 expression by 3.4-fold ($p<0.01$, ANOVA with Bonferroni's post-test; Figure 4.6D), and the induction was inhibited by DAPT ($p<0.05$).

Taken together, these results demonstrated that Jag1 ligands, either immobilised on a plate or expressed in another cell line, induced Dll4 expression in HUVECs via Notch signalling. However, Jag1 ligands induced Dll4 expression to a smaller extent than Dll4 ligands, suggesting ligand specificity in inducing Notch signalling.

4.2.4 Higher cell density induced Dll4 expression

Since Notch signalling depends on the interaction between ligands and receptors on neighbouring cells, it is hypothesized that cell-cell contact would activate Notch signalling and Dll4 expression. To test this hypothesis, HUVECs were plated at five different densities: $0.5x10^5$, $1x10^5$, $1.5x10^5$, $2x10^5$ and $2.5x10^5$ cells per well in a six-well plate. After 40 hours, cells plated at the lowest density were not in contact, while cells plated at the highest density were fully confluent. RNA was isolated to measure Dll4, Hey1 and Hes1 expression by real-time PCR. As shown in Figure 4.7A, higher cell density increased Dll4 expression dose-dependently ($p<0.0001$, ANOVA). Cells in the highest density, $2.5x10^5$ cells per well, displayed 4.0-fold higher Dll4 expression than cells in the lowest density, $0.5\ x10^5$ cells per well. Similarly, the two Notch target genes Hey1 and Hes1 were also induced dose-dependently (for both genes, $p<0.0001$, ANOVA; Figure 4.7B-C). At the highest cell density, Hey1 was induced by 3.5-fold, and Hes1 was induced by 2.8-fold, respectively. This is consistent with a published report that HUVECs cultured at higher density expressed higher levels of Hey1 (Noseda et al., 2004).

The activation of Notch signalling by higher cell density was also demonstrated at the protein level by Western blotting. HUVECs were plated at the same five densities and cultured for 40 hours before protein isolation. Protein samples were separated by SDS-PAGE and immunoblotted with antibodies recognising Hes1, N1ICD and β-Actin (loading control). As shown in Figure 4.7D, HUVECs plated at the lowest density, $0.5x10^5$ cells per well, accumulated little N1ICD. As plating density increased, so did the accumulation of N1ICD, suggesting that higher cell density led to increased Notch activation. Hes1 protein was also

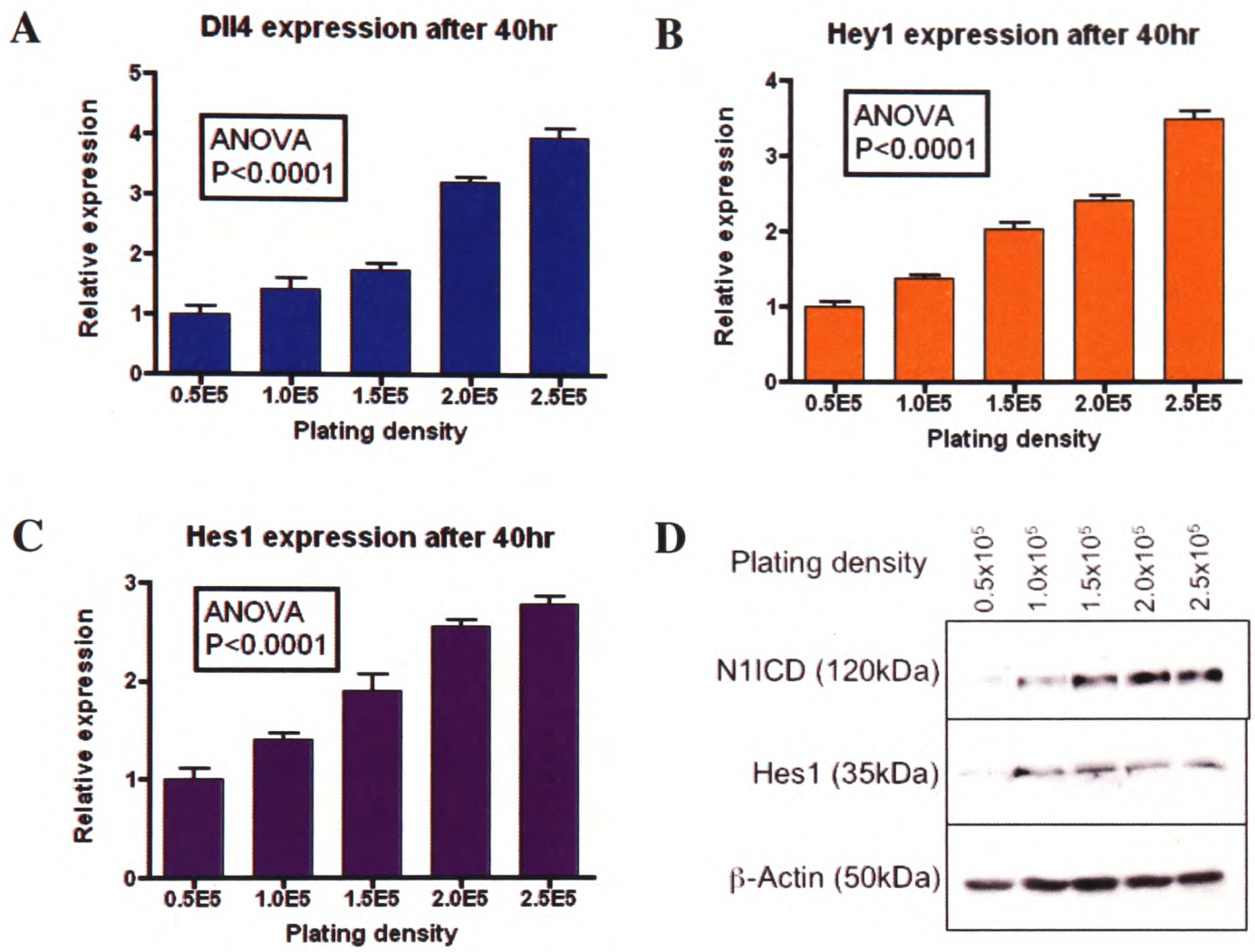
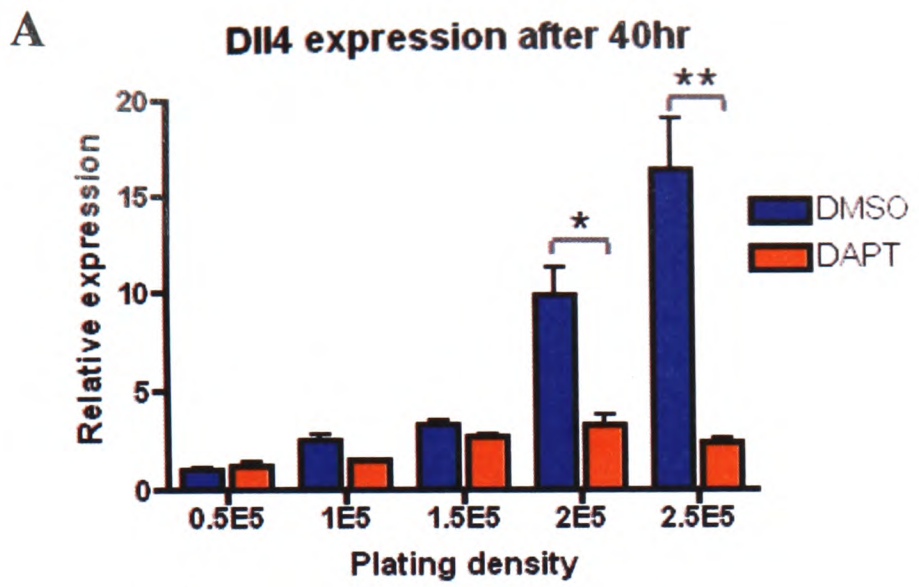
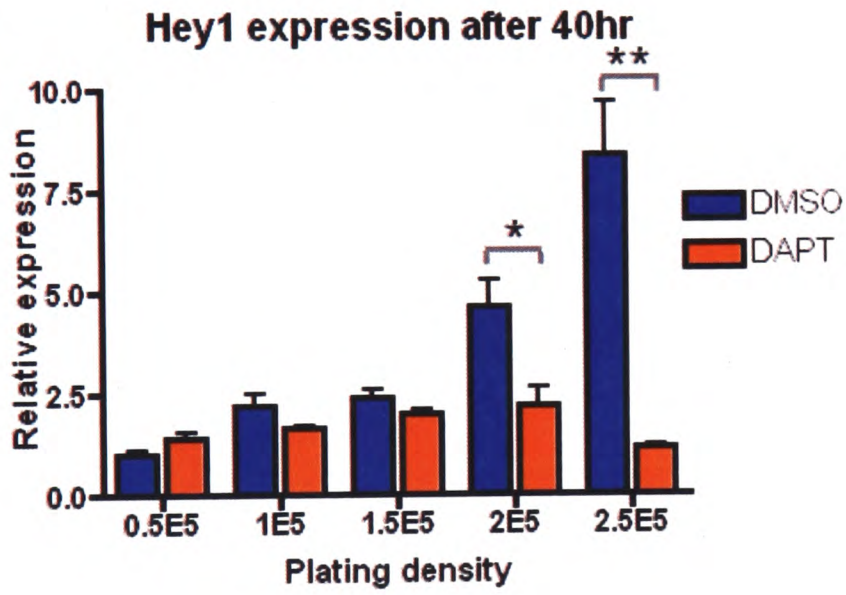


Figure 4.7. Higher cell density induced Dll4 expression.
HUVECs were plated at five different densities, as indicated on the x-axis, for 40 hours before RNA and protein isolation. (A-C) The mRNA levels of Dll4 (A), Hey1 (B) and Hes1 (C) were assessed by real-time PCR. The data were analysed with ANOVA (n=3). (D) Protein samples were separated by SDS-PAGE and blotted with antibodies against cleaved N1ICD, Hes1 and β-actin (n=2; figure courtesy of Dr Laura Harrington).





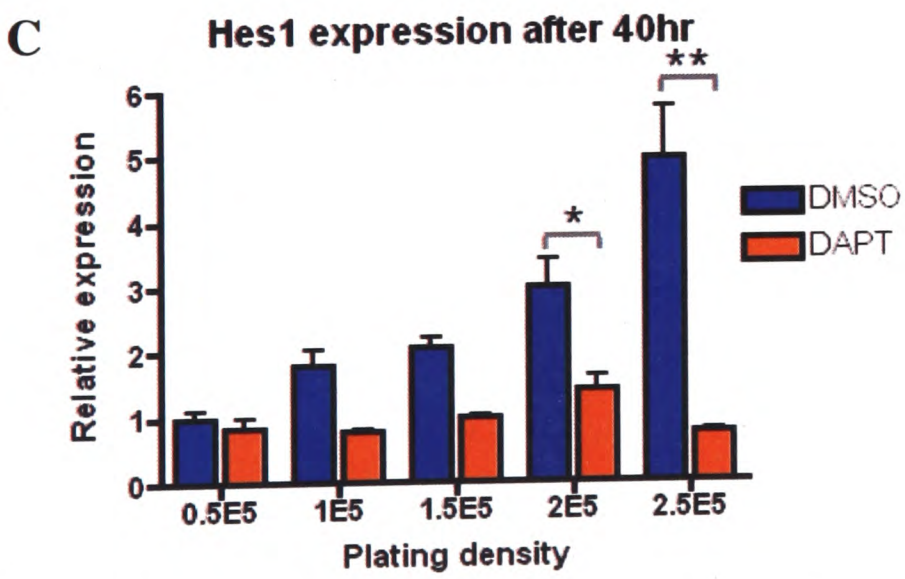


Figure 4.8. Cell density effect on Dll4 expression was Notch-dependent.
HUVECs were plated at five different densities, with 2 μM DAPT or DMSO. The expression levels of Dll4 (A), Hey1 (B) and Hes1 (C) were assessed by real-time PCR after 40 hours (*$p<0.05$, **$p<0.01$, ANOVA with Bonferroni's post-test, n=3).

induced at the higher cell densities compared with the lowest density. The combined mRNA and protein results demonstrated that cell-cell contact promoted Notch signalling and Dll4 mRNA expression.

To confirm that the density-dependent increase of Dll4 expression was mediated by Notch activation, cells plated at each density were treated with 2 μM DAPT or DMSO control for 40 hours. As shown in Figure 4.8A, DAPT treatment abolished the induction of Dll4 at the two highest densities (for $2x10^5$ cells per well, p=0.011; for $2.5x10^5$ cells per well, p=0.0055, unpaired t-test). Likewise, DAPT treatment also inhibited the induction of Hey1 and Hes1 at the two highest densities (Figure 4.8B-C).

Taken together, endothelial cell-cell contact promoted Notch signalling, which in turn induced Dll4 expression in a γ-secretase-dependent manner.

4.3 VEGF induced Dll4 expression

Like Notch signalling, VEGF signalling is a key regulator of physiological and tumour angiogenesis (see Sections 1.4.1 and 1.4.2). VEGF was the first gene shown to be haploinsufficient for mouse development (Carmeliet et al., 1996, Ferrara et al., 1996); the only other such gene was Dll4. VEGF regulates tumour angiogenesis as well, and drugs inhibiting VEGF signalling have been developed to treat several types of solid tumours (Ferrara and Kerbel, 2005).

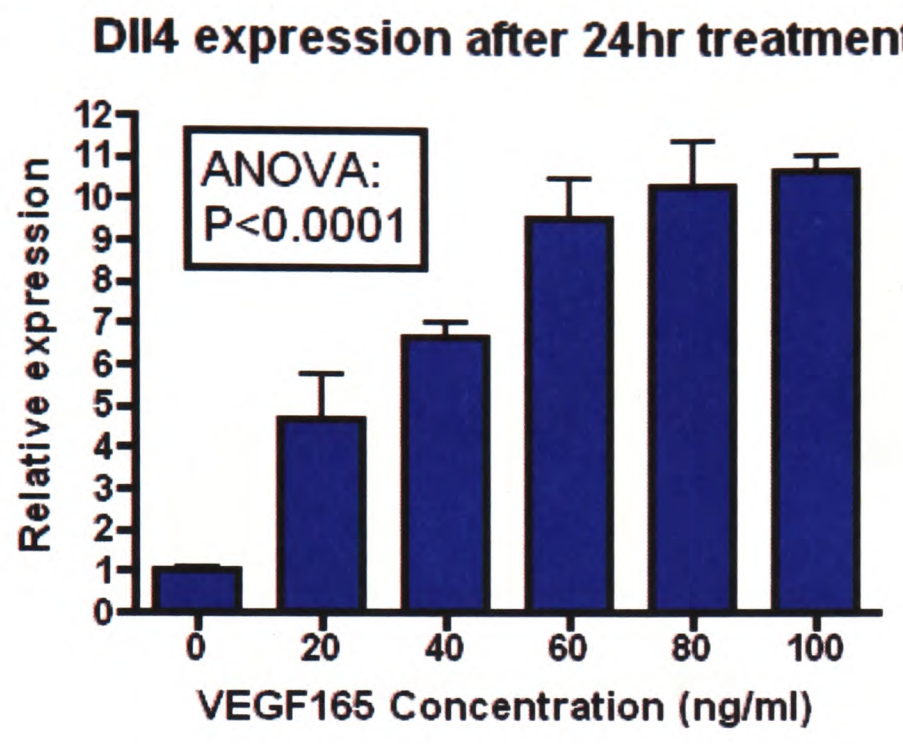
Recently, a number of *in vitro* and *in vivo* studies have shed light on the crosstalk between the VEGF and Dll4-Notch signalling pathways. In particular, VEGF induces Dll4 expression in several endothelial cell types (Liu et al., 2003, Patel et al., 2005). Here I sought to elucidate the mechanism of VEGF induction of Dll4. Notably, the *Vegf* gene has three main splice variants, resulting in protein isoforms containing 121, 165 and 189 amino acids in humans, respectively (Ferrara et al., 2003). $VEGF_{165}$, the predominant isoform, has properties that closely resemble those of native VEGF. Therefore, $VEGF_{165}$ was the isoform used in the *in vitro* experiments.

4.3.1 $VEGF_{165}$ induced Dll4 expression

To confirm previous results that $VEGF_{165}$ induced Dll4 in HUVECs (Patel et al., 2005), a dose-response experiment was conducted to measure Dll4 mRNA expression. First, $2x10^5$ cells were cultured in M199 medium containing 2% FCS without ECGS for 16 hours to remove any effect of residual growth factors in the medium. Next, $VEGF_{165}$ was added to the medium at different concentrations: 0, 20, 40, 60, 80, 100 ng/ml. After 24 hours, total RNA was isolated and analysed by real-time PCR. As shown in Figure 4.9A, $VEGF_{165}$ induced Dll4 expression dose-dependently ($p<0.0001$, ANOVA). $VEGF_{165}$ also induced Hey1 expression dose-dependently ($p<0.0001$, ANOVA; Figure 4.9B), consistent with recent reports that VEGF induced Notch signalling (Hainaud et al., 2006, Takeshita et al., 2007).

The effect of $VEGF_{165}$ on Dll4 promoters was also examined. First, 1 μg of pGL3e plasmids encoding Dll4 promoters of different lengths, and empty vector control, were co-transfected

A



B

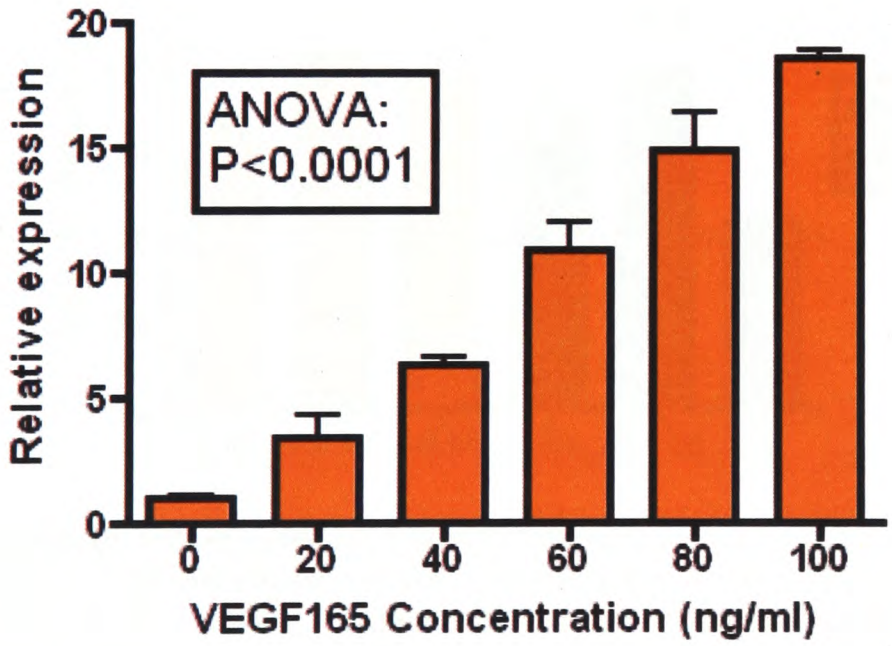


Figure 4.9. $VEGF_{165}$ induced Dll4 expression dose-dependently.
HUVECs were cultured in medium containing 2% serum without ECGS for 16 hours before being treated with different concentrations of $VEGF_{165}$ for 24 hours. Dll4 (A) and Hey1 (B) expressions were measured by real-time PCR, and the data were analysed with ANOVA (n=3).

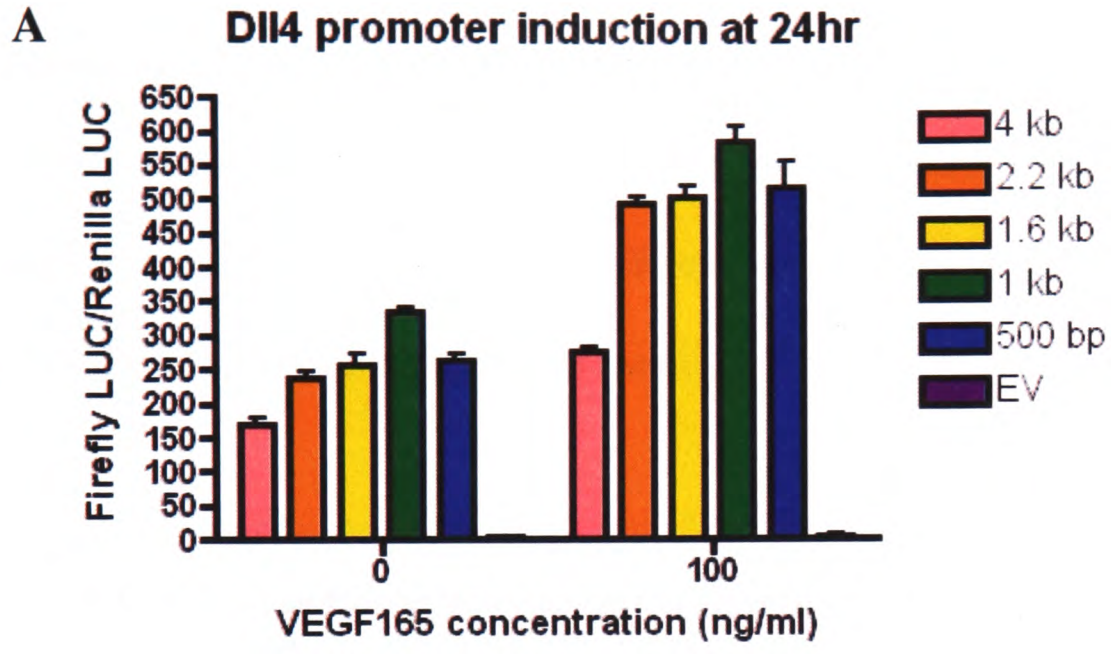


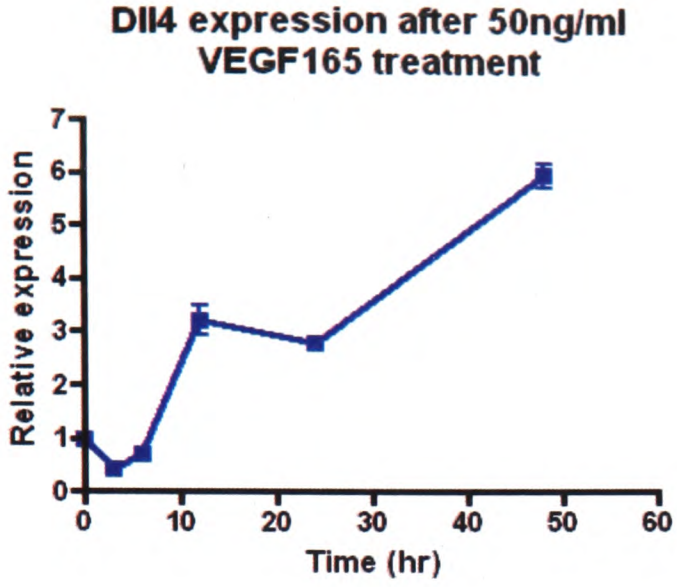
Figure 4.10. $VEGF_{165}$ induced Dll4 promoters.
PAE cells were transfected with pGL3e plasmids encoding Dll4 promoter fragments (4 kb, 2.2 kb, 1.6 kb, 1 kb, 500 bp) and EV control together with the pRL plasmid, and treated with 0 or 100 ng/ml of $VEGF_{165}$ for 24 hours. Luciferase assay was used to measure Dll4 promoter induction, and Firefly-to-Renilla luciferase ratios are presented in (A). Ratios of induction by $VEGF_{165}$ treatment are shown in (B). Stars indicate significant inductions compared with EV control (*$p<0.05$, ***$p<0.001$, ANOVA with Bonferroni's post-test, n=6).

into PAE cells with 50 ng of pRL plasmid. After 16 hours, PAE cells were treated with 0 or 100 ng/ml of $VEGF_{165}$ for 24 hours before being lysed for luciferase assays. The normalised luciferase activities are shown in Figure 4.10A, and the ratios of induction by $VEGF_{165}$ are shown in Figure 4.10B. All five Dll4 promoters were significantly induced by 100 ng/ml $VEGF_{165}$ treatment ($p<0.05$, ANOVA with Bonferroni's post-test), although the ratios of induction were not significantly different among the promoters. Dll4 promoter activation by $VEGF_{165}$ confirmed mRNA-level results.

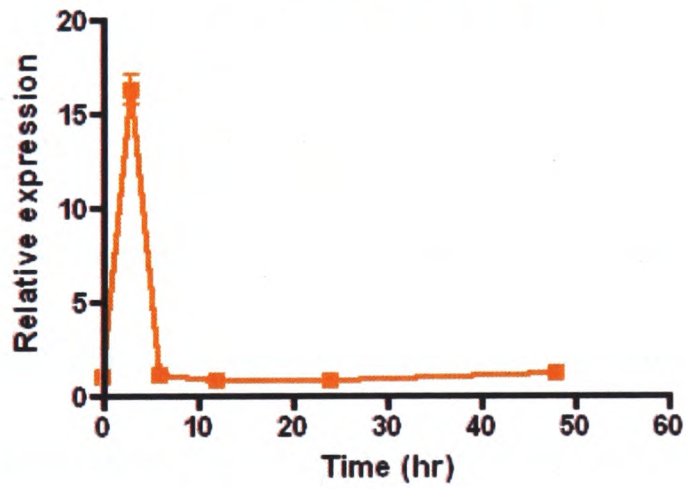
4.3.2 $VEGF_{165}$ induced Dll4 via Notch signalling

To further elucidate the mechanism of Dll4 induction by VEGF, a time course experiment was performed with $VEGF_{165}$ treatment. HUVECs were starved in M199 medium containing 2% FCS without ECGS for 16 hours and then treated with 50 ng/ml of $VEGF_{165}$. RNA was isolated from cells after 0, 3, 6, 12, 24 and 48 hours of treatment. As shown in Figure 4.11A, $VEGF_{165}$ induced Dll4 mRNA expression gradually and almost linearly, with a larger increase between 6 and 12 hours. Interestingly, $VEGF_{165}$ increased the expression of Hey1 and Hey2 sharply (Figure 4.11B-C). Following 3 hours of treatment, Hey1 was induced by 16.4-fold, and Hey2 was induced by 54.2-fold. The expression of both genes quickly decreased to near-basal levels. The rapid activation of Notch signalling may be due to VEGF induction of γ-secretase activity, which occurred within 30 minutes of $VEGF_{165}$ treatment in a recent study (Takeshita et al., 2007). Notch signalling activation may in turn induce Dll4 expression, initiating a positive feedback loop, thus explaining why the time course of Dll4 induction was more gradual.

A



B



C

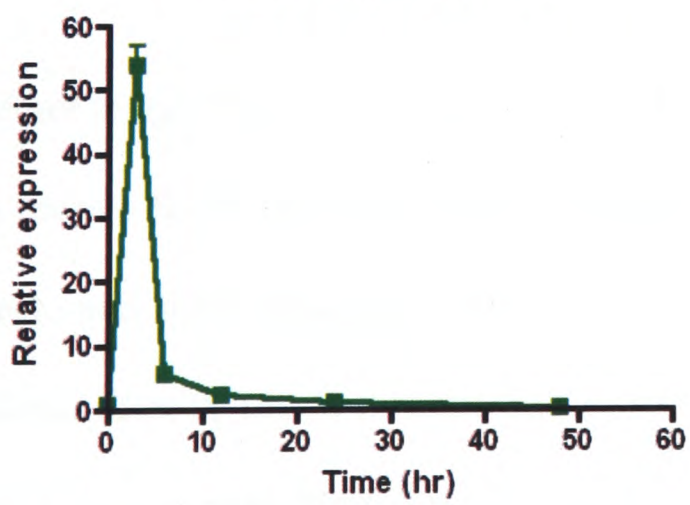


Figure 4.11. Time course of Dll4 induction by $VEGF_{165}$.
HUVECs were cultured in medium containing 2% serum without ECGS for 16 hours before being treated with 50 ng/ml of $VEGF_{165}$, and the cells were harvested at different time points after the start of treatment. Real-time PCR was used to measure the time course of Dll4 (A), Hey1 (B) and Hey2 (C) induction (n=3).

To test the hypothesis that VEGF induction of Dll4 was dependent on Notch signalling, HUVECs were cultured in medium containing 2% FCS with 2 μM DAPT or DMSO for 16 hours, followed by the addition of 0, 20 or 100 ng/ml of $VEGF_{165}$ for 24 hours. As shown in Figure 4.12A, $VEGF_{165}$ at 20 ng/ml induced Dll4 expression ($p<0.01$, ANOVA with Bonferroni's post-test), and the induction was blocked by DAPT ($p<0.05$). Similarly, $VEGF_{165}$ at 100 ng/ml further induced Dll4 ($p<0.001$), and the induction was also blocked by DAPT ($p<0.001$). $VEGF_{165}$ at 100 ng/ml also induced Hey1 expression after 24 hours ($p<0.001$, ANOVA with Bonferroni's post-test; Figure 4.12B), although the induction level would be much lower than the peak level after 3 hours of treatment (see Figure 4.11B). As expected, DAPT treatment significantly reduced Hey1 induction by $VEGF_{165}$ ($p<0.001$). Taken together, $VEGF_{165}$ induced Dll4 expression in a γ-secretase-dependent manner. These results are consistent with recently published findings in which a γ-secretase inhibitor blocked VEGF induction of Notch receptor activation and downstream gene ephrin B2 expression (Hainaud et al., 2006).

Further insight into VEGF-induced Notch signalling was gleaned from a time course study at the protein level. HUVECs were cultured in 2% medium with 2 μM DAPT or DMSO for 16 hours, and then stimulated with 100 ng/ml of $VEGF_{165}$. Cells were harvested and protein isolated after 0, 10, 30 minutes and 4, 16, 24 hours. Protein samples were separated by SDS-PAGE and immunoblotted with an antibody against cleaved N1ICD and an antibody against Hes1, with β-actin as a loading control. As shown in Figure 4.12C, N1ICD accumulated rapidly, as soon as 10 minutes after $VEGF_{165}$ treatment; the level was even higher at 30

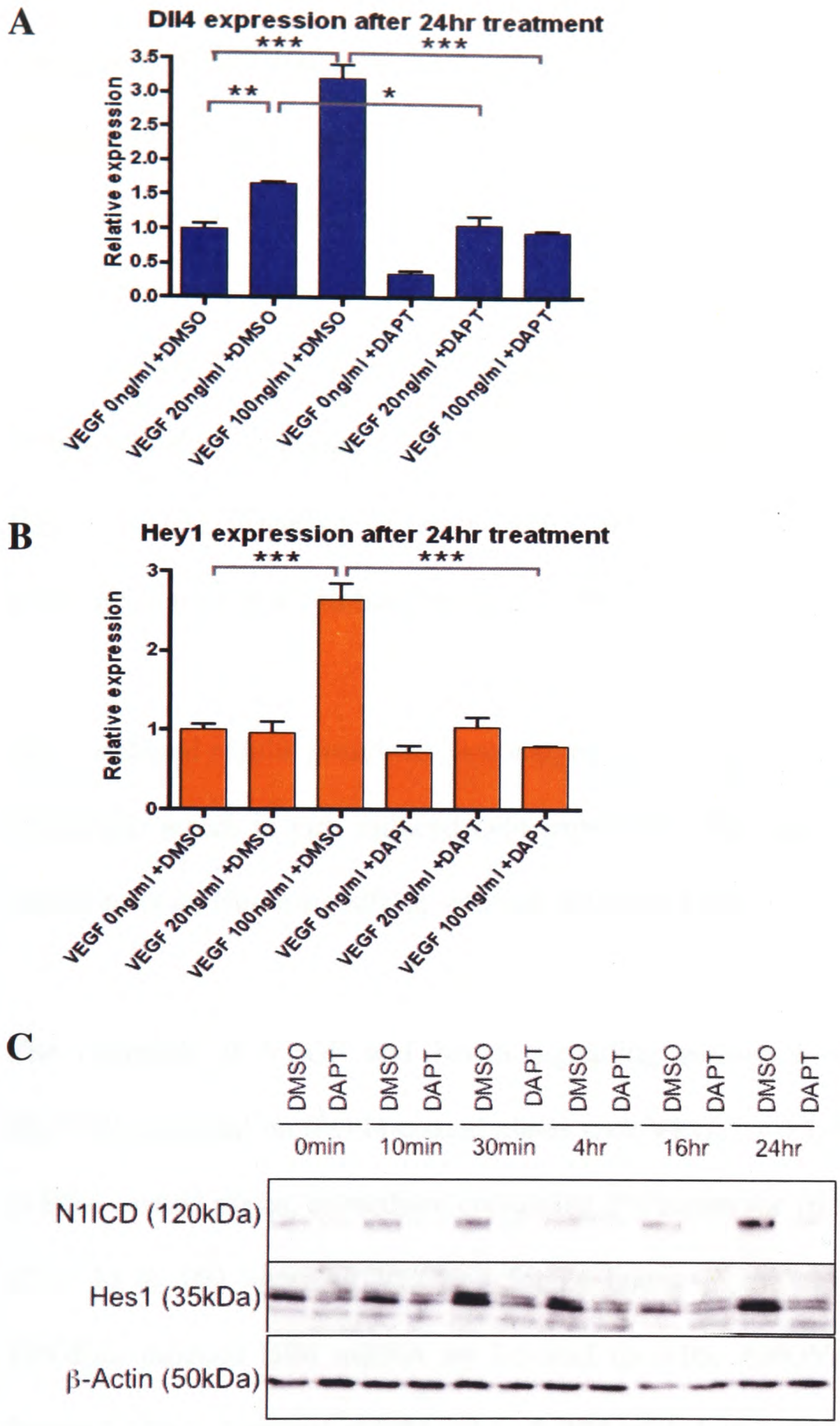


Figure 4.12. $VEGF_{165}$ induction of Dll4 was Notch-dependent.
(A-B) HUVECs were cultured in medium containing 2% serum with 2 μM DAPT or DMSO for 16 hours before being treated for 24 hours with 0, 20 or 100 ng/ml of $VEGF_{165}$. Real-time PCR was used to measure the expression of Dll4 (A) and Hey1 (B) (*$p<0.05$, **$p<0.01$, ***$p<0.001$, ANOVA with Bonferroni's post-test, n=3). (C) HUVECs were cultured in 2% serum with 2 μM DAPT or DMSO for 16 hours before being treated with 100 ng/ml of $VEGF_{165}$. Cells were harvested at the time points indicated for protein isolation. Protein samples were separated by SDS-PAGE and blotted with antibodies against cleaved N1ICD, Hes1 and β-actin (n=2; figure courtesy of Dr Laura Harrington).

minutes. The accumulation returned to basal level at 4 hours before increasing again at later time points. DAPT treatment inhibited N1ICD accumulation at all time points. Hes1, a Notch target gene, showed a similar expression pattern to that of N1ICD. These results suggest that $VEGF_{165}$ activated Notch signalling within the first 30 minutes. This is in agreement with a recent report, in which $VEGF_{165}$ treatment led to Notch1 cleavage and Hes1 expression in HUVECs within 15 to 30 minutes (Takeshita et al., 2007). Furthermore, the second phase of Notch activation in Figure 4.12C may be due to Dll4 expression stimulated by $VEGF_{165}$ (see Figure 4.11A). Finally, VEGF-induced Notch signalling was dependent on γ-secretase cleavage, since it was inhibited by DAPT treatment.

The combined results presented here suggest that $VEGF_{165}$ treatment rapidly activated Notch signalling, which in turn induced Dll4 expression. The hypothesis is that Dll4 upregulation would activate Notch signalling, causing the second phase of N1ICD accumulation.

The crosstalk of VEGF and Notch signalling pathways was further tested by treating HUVECs cultured on rhDll4-coated plates with $VEGF_{165}$. HUVECs were cultured on rhDll4- or BSA-coated plates, in medium containing 2% serum for 16 hours, followed by the addition of 0, 20 or 100 ng/ml of $VEGF_{165}$ for 24 hours. In the absence of rhDll4, 100 ng/ml of $VEGF_{165}$ induced Dll4 mRNA by 3.5-fold ($p<0.05$, ANOVA with Bonferroni's post-test; Figure 4.13A). However, rhDll4 induced Dll4 mRNA to a similar level – on average 12.5-fold – regardless of $VEGF_{165}$ concentration ($p<0.001$ for rhDll4 with all three concentrations of $VEGF_{165}$). Similarly, rhDll4 induced Hey1 to a similar level in the absence or presence of

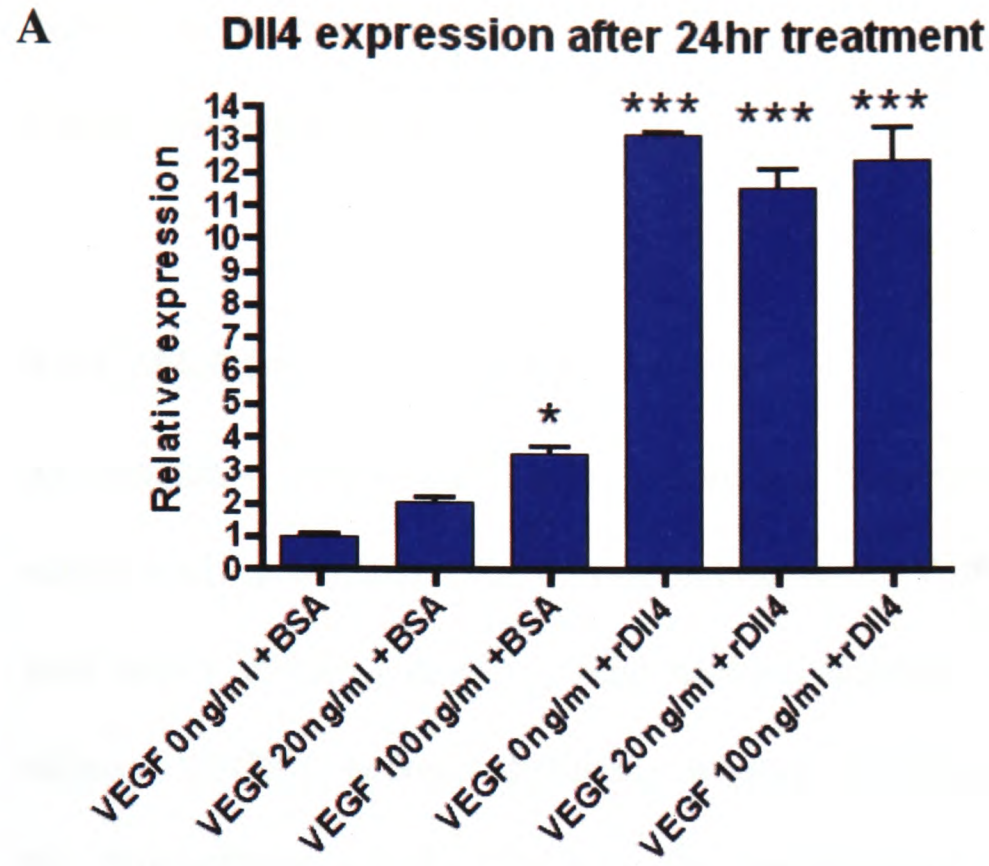


Figure 4.13. $VEGF_{165}$ did not synergise with rhDll4 in inducing Dll4 expression.
HUVECs were cultured on rhDll4- or BSA-coated plates, first in medium containing 2% serum without ECGS for 16 hours, and then in the presence of 0, 20 or 100 ng/ml of $VEGF_{165}$ for 24 hours. Real-time PCR was used to measure the expression of Dll4 (A) and Hey1 (B) (*$p<0.05$, ***$p<0.001$, ANOVA with Bonferroni's post-test, n=3). Stars indicate significant differences with the VEGF 0 ng/ml + BSA sample.

$VEGF_{165}$. Since rhDll4 could directly stimulate Notch signalling and endogenous Dll4 expression, it may saturate the induction system as $VEGF_{165}$ treatment could not further induce Dll4 expression.

4.3.3 VEGF isoforms induced Dll4 in vivo

As mentioned before, the VEGF protein has three main isoforms, with 121, 165 and 189 amino acids in humans. (The corresponding mouse VEGF isoforms are shorter by one amino acid each.) $VEGF_{121}$ does not bind heparin, whereas $VEGF_{189}$ binds to heparin with high affinity. $VEGF_{121}$ is freely diffusible, whereas $VEGF_{189}$ is almost completely sequestered in the extracellular matrix. $VEGF_{165}$, the predominant isoform, has intermediary properties (Ferrara et al., 2003). Mouse allograft tumours expressing only single isoforms of VEGF, a gift of Prof. Gillian Tozer, provided the opportunity to study the effect of each isoform on Dll4 expression *in vivo*.

The allograft tumours were established as described in Section 2.1.12. I processed frozen tumours using the FastPrep machine and TRI reagent to isolate RNA. Real-time PCR was then performed to analyse the expression of murine Notch genes, and the results are shown in Figure 4.14. For each gene, the ANOVA p-value indicates whether gene expression was different among the four types of tumours, while the star(s) indicate whether tumours expressing a VEGF isoform had different gene expression compared with wild-type (WT) tumours.

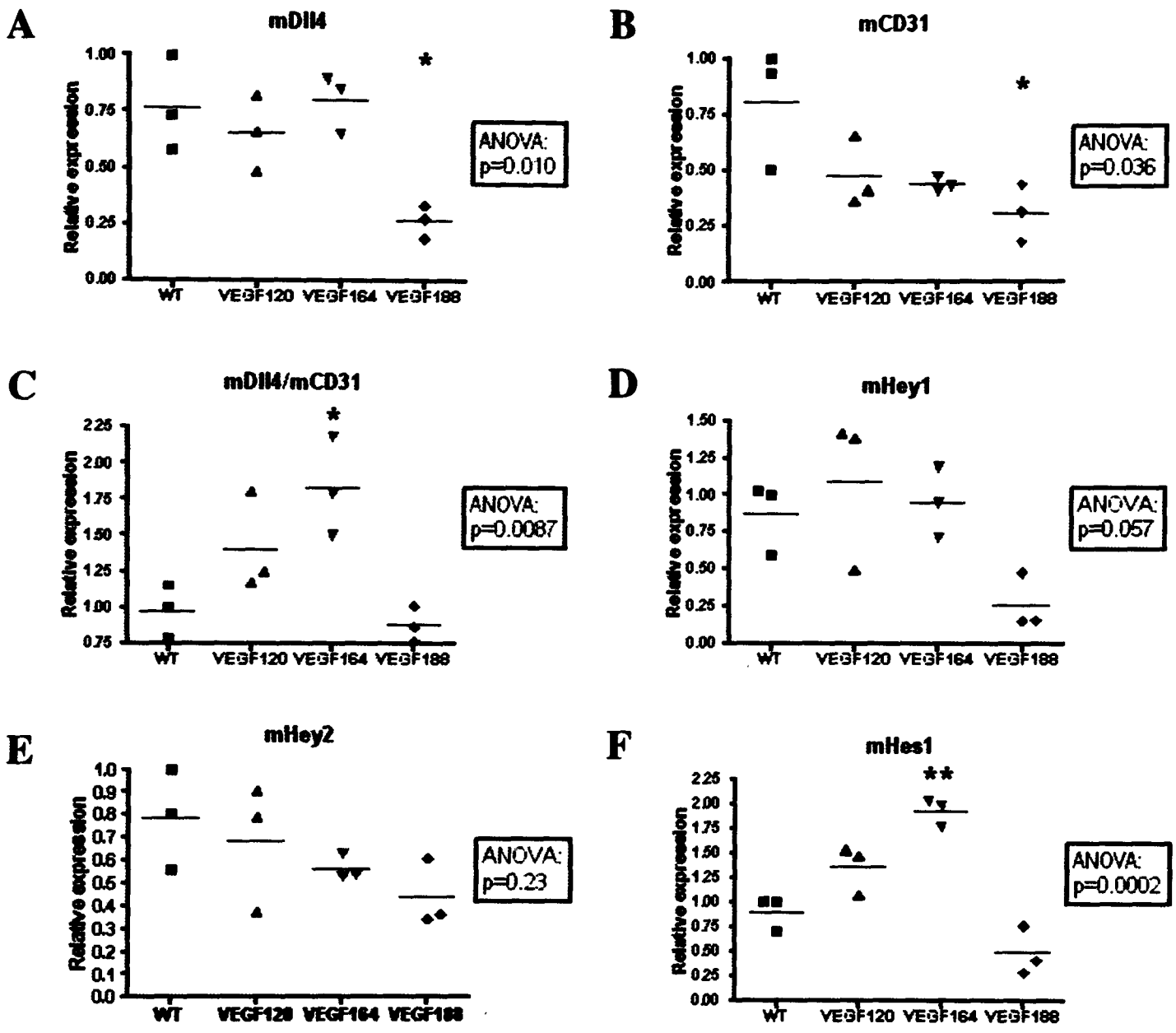


Figure 4.14. Gene expression in mouse tumours expressing single VEGF isoforms.
RNA was isolated from mouse fibrosarcoma tumours expressing single VEGF isoforms (120, 164 or 188) or wild-type VEGF (WT). Real-time PCR was performed to measure the expression levels of mouse Dll4 (A), CD31 (B), Hey1 (D), Hey2 (E), Hes1 (F) and the ratio of Dll4/CD31 (C). For each gene, ANOVA was used to determine whether expression was different among the four types of tumours, and Bonferroni's post-test was used to compare tumours expressing a VEGF isoform with wild-type tumours (*$p<0.05$, **$p<0.01$, $n=3$).

As shown in Figure 4.14A, $VEGF_{120}$ tumours and $VEGF_{164}$ tumours did not show different mDll4 expression compared with WT tumours; however, $VEGF_{188}$ tumours showed lower expression ($p<0.05$, ANOVA with Bonferroni's post-test). Mouse CD31, a marker for endothelial cells (ECs), showed a similar expression pattern, highest in WT tumours and lowest in the $VEGF_{188}$ tumours ($p<0.05$ compared with WT tumours; Figure 4.14B). Since Dll4 is predominantly expressed on ECs (Shutter et al., 2000), the ratio of mDll4 to mCD31 was obtained to normalise Dll4 expression by the vascularity of the tumours (Patel et al., 2005). Notably, $VEGF_{164}$ tumours showed significantly higher mDll4/mCD31 ratio compared with WT tumours ($p<0.05$; Figure 4.14C). $VEGF_{120}$ tumours may express higher mDll4/mCD31 ratio as well but the difference was not significant due to the small sample size. $VEGF_{188}$ tumours showed similar mDll4/mCD31 ratio as WT tumours.

Among the three Notch target genes tested, mHey1 and mHey2 did not show any significant differences among the four types of tumours (mHey1, $p=0.057$; mHey2, $p=0.23$, ANOVA; Figure 4.14D-E). Mouse Hes1, in contrast, showed highly significant differences among the four types ($p=0.0002$, ANOVA; Figure 4.14F). This result is consistent with our own xenograft studies of tumours overexpressing human Dll4, in which mHes1, but not other Notch target genes, was consistently induced (see Section 6.3). Thus, mHes1 may be the key target downstream of VEGF and Notch signalling in tumours.

The expression pattern of mHes1 was similar to that of mDll4/mCD31, with $VEGF_{164}$ tumours showing the highest expression ($p<0.01$, ANOVA with Bonferroni's post-test; Figure 4.14F). Taken together, these data indicate that $VEGF_{164}$ was the only isoform that induced

mouse Dll4 expression (normalised by vascularity) and Notch signalling in tumours, compared with wild-type VEGF.

$VEGF_{164}$ is the predominant mouse VEGF isoform. In this experiment, it was the most effective isoform in inducing Dll4 expression in tumour vessels. $VEGF_{120}$ also appeared to induce Dll4 expression, but the result was not significant due to the small sample size. In contrast, $VEGF_{188}$, due to its low bioavailability, may be the least effective isoform in promoting tumour angiogenesis, as demonstrated by the decreased mCD31 expression compared with WT tumours. However, the mDll4/mCD31 ratio was not significantly changed in $VEGF_{188}$ tumours, suggesting that the isoform did not affect Dll4 expression in the tumour vasculature.

To date, few published studies have examined the effect of VEGF isoforms on Dll4 expression and Notch signalling, either in *vitro* or *in vivo*. In one study, both $VEGF_{121}$ and $VEGF_{165}$ induced Dll4 and Notch1 expression in human iliac artery endothelial cells (HIAECs) (Liu et al., 2003). However, $VEGF_{121}$ was expressed in adenoviruses ($VEGF_{121}$/Ad.5), which were then used to transduce HIAECs; in contrast, recombinant $VEGF_{165}$ protein was added directly to the cell culture medium. Thus, a comparison of the effects of these two isoforms was not possible. Further experiments are needed to elucidate the mechanism of Dll4 induction by VEGF isoforms both *in vitro* and *in vivo*.

4.4 Hypoxia induced Dll4 expression

Hypoxia is another key regulator of angiogenesis (see Sections 1.4.1 and 1.4.2). Hypoxia up-regulates the expression of VEGF, VEGFR1, VEGFR2 and other pro-angiogenic molecules

(Pugh and Ratcliffe, 2003). During tumourigenesis, the lack of blood supply to the tumours causes hypoxia, leading to VEGF secretion, increased angiogenesis and improved blood supply. The cellular hypoxia-sensing pathway is mainly regulated by the transcription factors HIF1 and HIF2 (Harris, 2002).

Previous work in our laboratory has shown that hypoxia induced Dll4 expression in several endothelial cell types including HUVECs (Mailhos et al., 2001, Patel et al., 2005). The induction was dependent on HIF1α but not HIF2α (Patel et al., 2005). Results described in this section aim to further elucidate the mechanism of Dll4 induction by hypoxia. In all experiments, hypoxia treatment was carried out under 0.1% oxygen tension in hypoxic incubators.

4.4.1 Hypoxia induced Dll4 expression

Hypoxic induction of Dll4 expression was confirmed by a time-course experiment. HUVECs were cultured under 0.1% hypoxia or normoxia for 8, 16 or 24 hours; afterwards, RNA was immediately isolated for real-time PCR. As shown in Figure 4.15A, after 16 hours of hypoxia treatment Dll4 was induced by 2.5-fold compared with the normoxic level ($p=0.0001$, unpaired t-test), in agreement with previous reports (Patel et al., 2005). However, Dll4 mRNA levels were not elevated after 8 or 24 hours of hypoxia treatment. Thus, 16 hours of hypoxia treatment was used in all hypoxia experiments in this thesis unless otherwise noted.

Interestingly, hypoxia repressed both Hey1 and Hey2 mRNA levels. After 8 hours of hypoxia, Hey1 expression was 0.52 compared with the normoxic level ($p=0.011$, unpaired t-test; Figure

4.15B). After 16 hours of hypoxia, Hey1 expression was 0.54 compared with the normoxic level ($p=0.0029$, unpaired t-test). Hey2 expression was reduced even further by hypoxia (Figure 4.15C). After 8, 16 and 24 hours of hypoxia, Hey2 expression was 0.24 ($p=0.046$, unpaired t-test), 0.16 ($p=0.0003$) and 0.15 ($p=0.048$), respectively, compared with the corresponding normoxic levels. Together, these data suggest that hypoxic regulation of Dll4 is independent of its regulation of Hey1 and Hey2.

In addition to real-time PCR analysis, luciferase assays were carried out to determine the effect of hypoxia on Dll4 promoter activation. As described previously, 1 μg of pGL3e plasmids encoding Dll4 promoters of different lengths, and empty vector control, were co-transfected into PAE cells with 50 ng of pRL plasmid. After 16 hours, PAE cells were exposed to 0.1% hypoxia or normoxia for 24 or 48 hours. The normalised luciferase activities are shown in Figure 4.16A for 24 hours and Figure 4.16C for 48 hours. The ratios of induction by hypoxia are shown in Figure 4.16B for 24 hours and Figure 4.16D for 48 hours. Among the five promoter fragments, the 1.6 kb fragment showed the highest activation level under both normoxia and hypoxia, at both 24 and 48 hours (Figure 4.16A-C). Interestingly, hypoxia did not activate any of the promoters at 24 hours, as all promoters had a hypoxia-to-normoxia ratio close to 1 (Figure 4.16B). At 48 hours, hypoxia induced all promoters except the 4 kb promoter ($p<0.05$, ANOVA with Bonferroni's post-test; Figure 4.16D). The 4 kb promoter, which encompasses all the sequences of the smaller promoters, was not activated as much as the others. This suggests that the Dll4 promoter may harbour a negative regulatory sequence between 4 kb and 2.2 kb upstream of the ATG site.

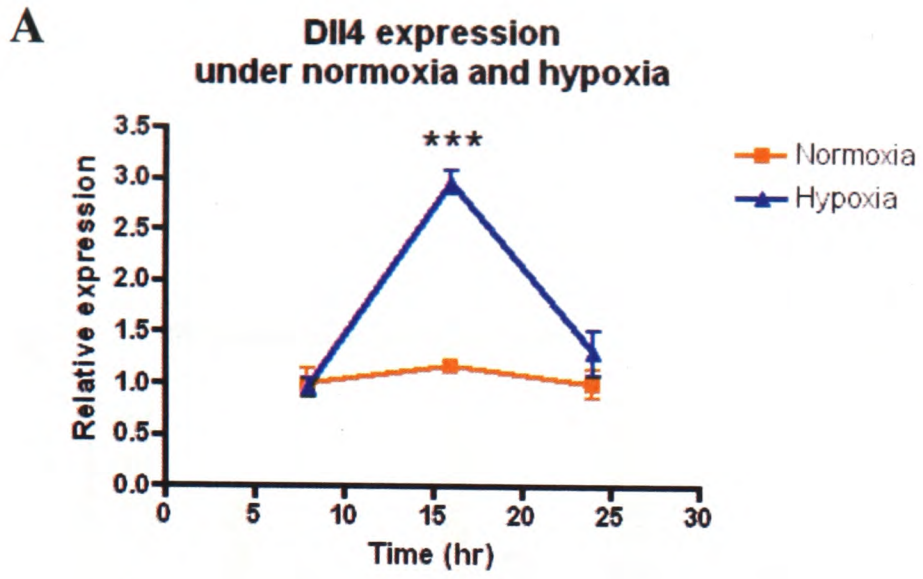


Figure 4.15. Time course of Dll4 induction by hypoxia.
HUVECs were cultured under 0.1% hypoxia or normoxia and harvested at different time points. Real-time PCR was used to measure the time course of Dll4 (A), Hey1 (B) and Hey2 (C) expression. Stars indicate significant induction or repression by hypoxia (*$p<0.05$, ***$p<0.001$, unpaired t-test, n=3).

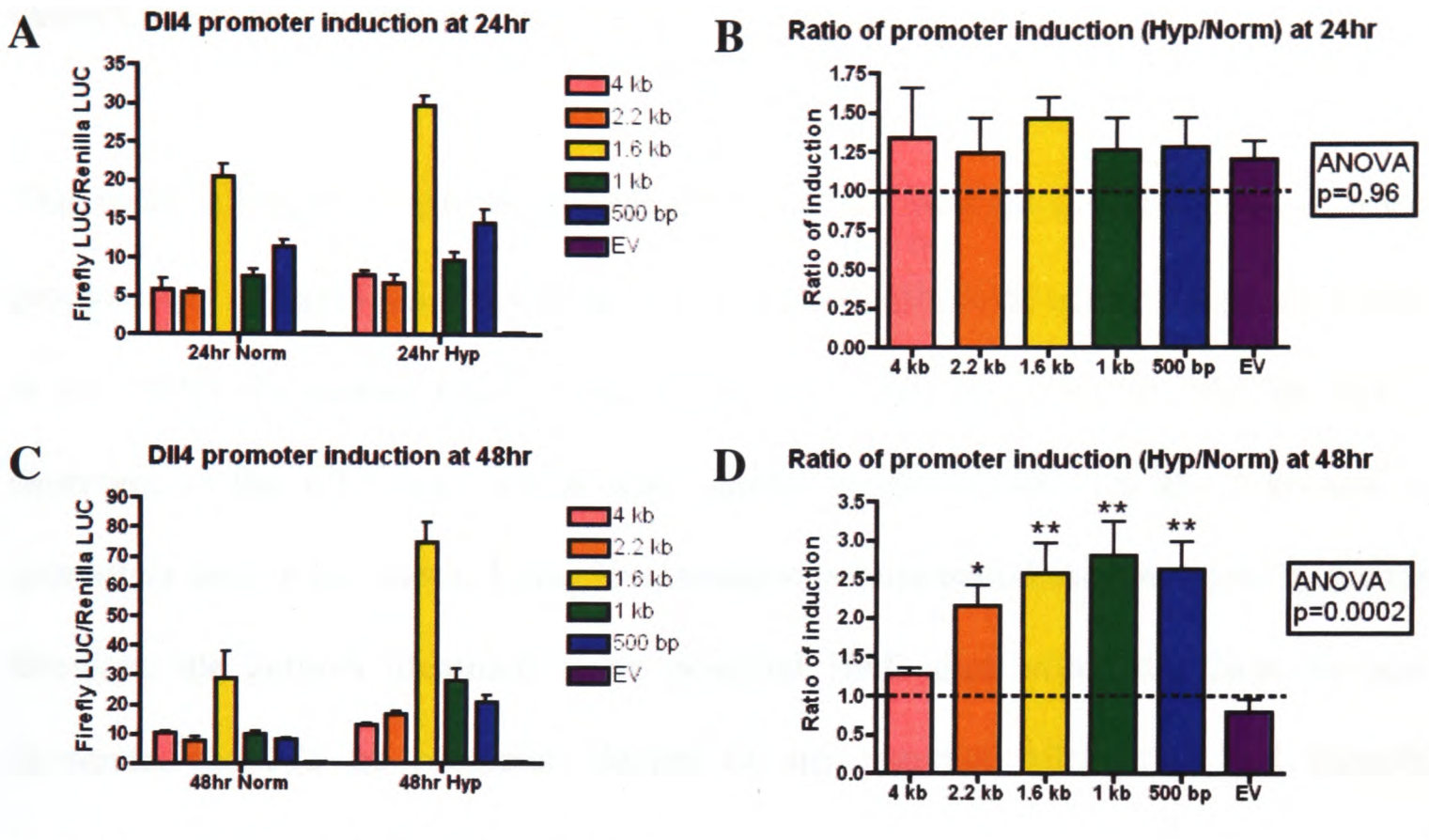


Figure 4.16. Hypoxia activated Dll4 promoters.
PAE cells were transfected with pGL3e plasmids encoding Dll4 promoter fragments (4 kb, 2.2 kb, 1.6 kb, 1 kb, 500 bp) and EV control together with the pRL plasmid, and treated with 0.1% hypoxia or normoxia for 24 or 48 hours. Luciferase assay was used to measure Dll4 promoter induction, and Firefly-to-Renilla luciferase ratios are presented in for 24 hours (A) and for 48 hours (C). Ratios of induction by hypoxia are shown in for 24 hours (B) and for 48 hours (D). Stars indicate significant inductions compared with EV control (*p<0.05, **p<0.01, ANOVA with Bonferroni's post-test, n=6).

On the other hand, truncation of the 2.2 kb promoter to 500 bp did not lead to any diminished activation by hypoxia. Notably, the only putative HRE within the promoter is located 1930 bp upstream of ATG (see Figure 4.1); thus, the 1.6 kb, 1 kb and 500 bp promoters did not contain any putative HRE but was still activated by hypoxia.

This result is largely in agreement with a recent study from the Gessler group, in which Dll4 promoters of different lengths were activated by a constitutively active HIF1α construct (Diez et al., 2007). Promoters used in that study were 2616 bp, 1587 bp, 931 bp and 573 bp upstream of the ATG site, which were similar to the 2.2 kb, 1.6 kb, 1 kb and 500 bp promoters used in this thesis. Using less stringent criteria than those employed by the Genome Browser, the authors identified seven potential HRE sites within the 2616 bp promoter. However, the 573 bp promoter, devoid of any potential HRE, was still inducible by HIF1α (Diez et al., 2007) . It is possible that the Dll4 promoter could be activated without direct binding of HIF1α to an HRE; rather, the hypoxia pathway may interact with other pathways such as Notch to induce Dll4 transcription. Further mutation of the 500 bp promoter would shed light on the mechanism of Dll4 promoter activation.

4.4.2 Hypoxia induced Dll4 via Notch signalling

Previous data showed that Dll4 expression was induced by hypoxia; however, Hey1 and Hey2 expression was repressed by hypoxia. To investigate whether the hypoxic induction of Dll4 was dependent on Notch signalling, the γ-secretase inhibitor DAPT was used. HUVECs were cultured with 2 μM DAPT or DMSO for 40 hours, the last 16 of which under 0.1% hypoxia

or normoxia. RNA and protein samples were isolated for real-time PCR and Western blotting, respectively. As shown in Figure 4.17A, hypoxia treatment induced Dll4 expression by 2.0-fold ($p<0.01$, ANOVA with Bonferroni's post-test), and the induction was blocked by DAPT treatment ($p<0.001$). This is consistent with protein-level results. Protein samples were separated by SDS-PAGE and immunoblotted with antibodies recognising activated N1ICD and β-actin (loading control). As shown in Figure 4.17D, hypoxia induced N1ICD accumulation, and DAPT treatment inhibited the accumulation under hypoxia. Taken together, these data suggest that hypoxia induced Dll4 expression via Notch signalling.

The expression of Notch target genes Hey1 and Hey2 was also measured by real-time PCR. Hey1 expression was repressed by hypoxia ($p<0.01$, ANOVA with Bonferroni's post-test; Figure 4.17B). The addition of DAPT did not affect Hey1 expression under normoxia or hypoxia. Hey2 expression was repressed by either hypoxia ($p<0.01$, ANOVA with Bonferroni's post-test; Figure 4.17C) or DAPT treatment under normoxia ($p<0.01$). There was no evidence of a synergistic effect on Hey2 expression when HUVECs were treated with both hypoxia and DAPT. Thus, hypoxia paradoxically repressed Hey1 and Hey2 while inducing Notch signalling. It is possible that hypoxia interacts with other pathways to repress Hey1 and Hey2 expression, overcoming its induction of Notch signalling.

The crosstalk of hypoxia and Notch signalling pathways was further explored by culturing HUVECs on rhDll4-coated plates under hypoxia. HUVECs were cultured on rhDll4- or BSA-coated plates for 24 hours under normoxia, and then for 16 hours under 0.1% hypoxia or normoxia. In cells cultured on BSA, hypoxia induced Dll4 expression by 2.0-fold ($p<0.05$,

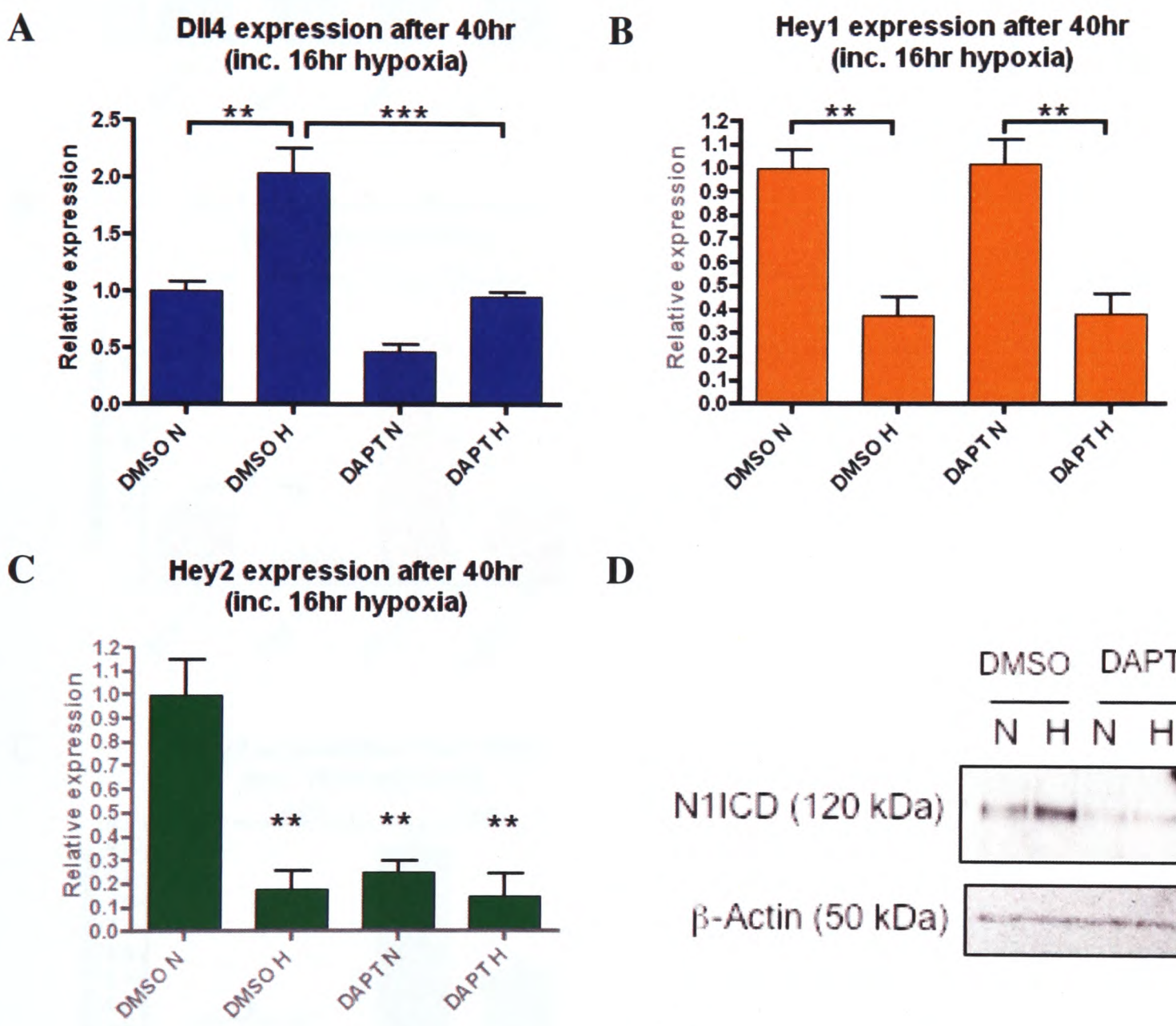
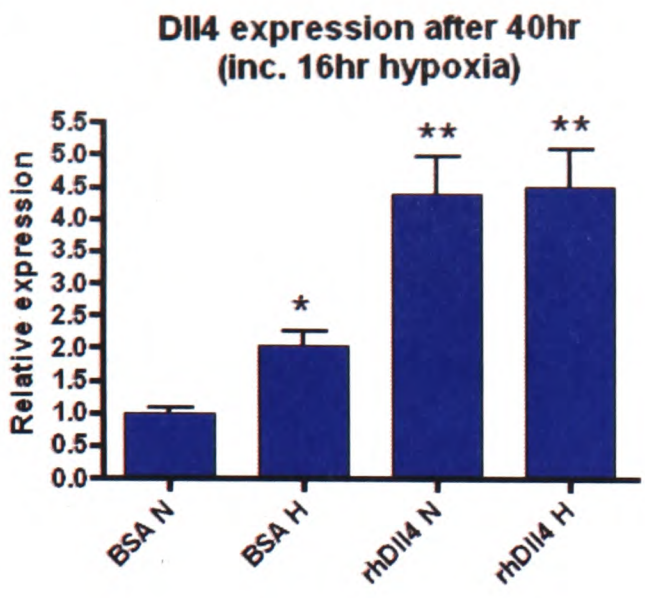
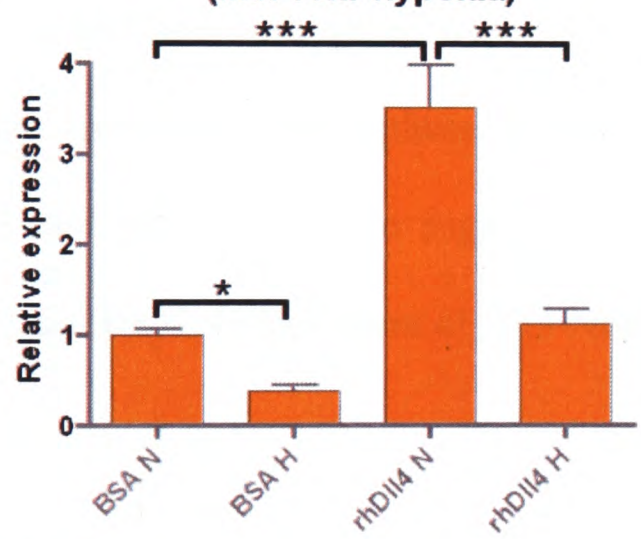


Figure 4.17. Hypoxia induction of Dll4 was Notch-dependent.
(A-C) HUVECs were cultured in medium containing 2 μM DAPT or DMSO for 24 hours under normoxia, and then 16 hours under 0.1% hypoxia or normoxia. Real-time PCR was used to measure the expression of Dll4 (A), Hey1 (B) and Hey2 (C) (**$p<0.01$, ***$p<0.001$, ANOVA with Bonferroni's post-test, n=3). In (C), stars indicate significant differences with the DMSO N sample. (D) Protein samples from the same experiment were separated by SDS-PAGE and blotted with antibodies against cleaved N1ICD and β-actin (n=2).

A



B



C

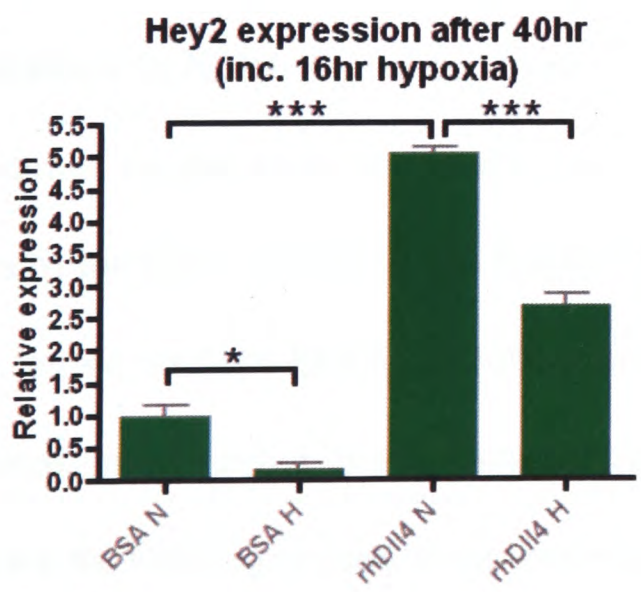


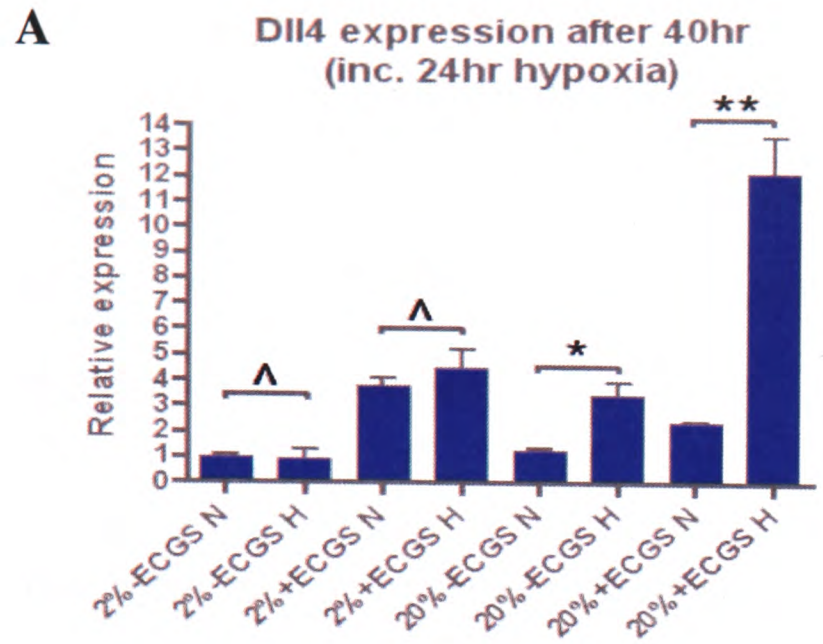
Figure 4.18. Hypoxia did not synergise with rhDll4 in inducing Dll4 expression.
HUVECs were cultured on rhDll4- or BSA-coated plates for 24 hours under normoxia, followed by 16 hours under 0.1% hypoxia or normoxia. Real-time PCR was used to measure the expression of Dll4 (A), Hey1 (B) and Hey2 (C) (*$p<0.05$, **$p<0.01$, ***$p<0.001$, ANOVA with Bonferroni's post-test, n=3). In (A), stars indicate significant differences with the BSA N sample.

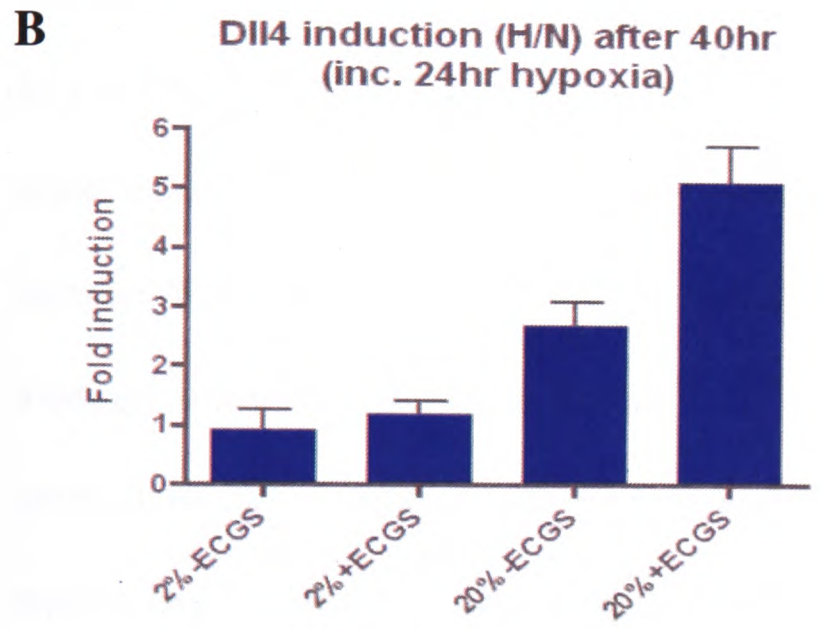
ANOVA with Bonferroni's post-test; Figure 4.18A). However, rhDll4 induced Dll4 expression to a higher level under either normoxia (4.4-fold, $p<0.01$) or hypoxia (4.5-fold, $p<0.01$). Hypoxia did not further induce Dll4 expression beyond the induction by rhDll4 alone. This result is similar to the predominance of rhDll4 over $VEGF_{165}$ in inducing endogenous Dll4 expression (see Figure 4.13A).

Hey1 and Hey2 expression followed a different pattern in this experiment (Figure 4.18B-C). Both Hey1 and Hey2 were induced by rhDll4 ($p<0.001$, ANOVA with Bonferroni's post-test). In addition, both genes were repressed by hypoxia when cultured on BSA- ($p<0.05$) or rhDll4- ($p<0.001$) coated plates. Hence, rhDll4 did not overcome the hypoxic repression of Hey1 and Hey2. This also suggests that hypoxia interacts with other pathways to repress Hey1 and Hey2, independent of Dll4-Notch signalling.

4.4.3 Hypoxic induction of Dll4 is serum-dependent

In addition to Notch signalling, hypoxic induction of Dll4 expression also depended on the amount of serum present in the culture medium. HUVECs were cultured for 40 hours in four types of medium containing the following: 2% serum without ECGS, 2% serum with ECGS, 20% serum without ECGS or 20% serum with ECGS. During the last 16 hours, cells were cultured under either 0.1% hypoxia or normoxia, and RNA was isolated immediately afterwards. Dll4 expression under normoxia and hypoxia for each type of medium is shown in Figure 4.19A, and Dll4 induction by hypoxia for each type of medium is shown in Figure 4.19B.





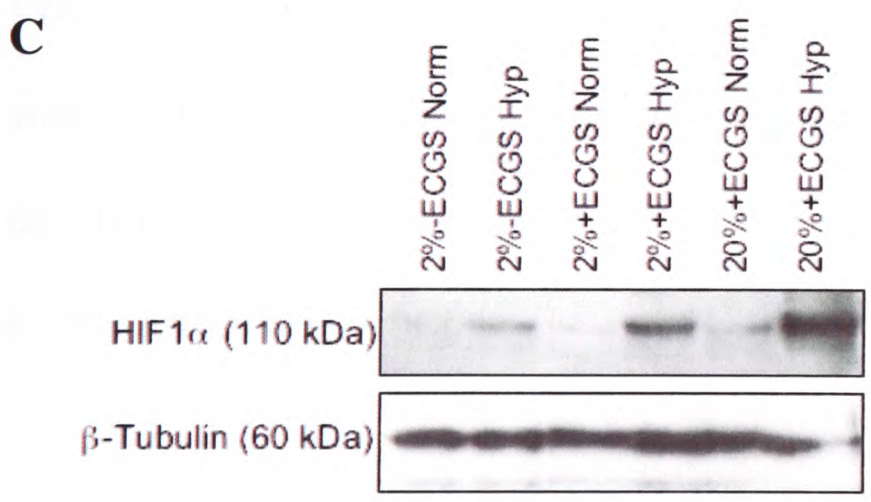


Figure 4.19. Hypoxia induction of Dll4 was serum-dependent.
(A-B) HUVECs were cultured in medium containing 2% or 20% serum with or without ECGS for 24 hours under normoxia, and then 16 hours under 0.1% hypoxia or normoxia. Real-time PCR was used to measure Dll4 expression under each condition (A). The stars indicate significant induction by hypoxia (^$p \geq 0.05$, *$p < 0.05$, ** $p < 0.01$, unpaired t-test, n=3). The fold induction of Dll4 by hypoxia is shown in (B). (C) HUVECs were similarly cultured in three of the four types of medium for protein isolation. Protein samples were separated by SDS-PAGE and blotted with antibodies against HIF1α and β-tubulin (n=2).

Hypoxia did not induce Dll4 expression in the low serum (2%) medium, either without ECGS ($p \geq 0.05$, unpaired t-test) or with ECGS ($p \geq 0.05$). Hypoxia did induce Dll4 by 2.7-fold in 20% serum without ECGS ($p < 0.05$). Hypoxia also induced Dll4 by 5.1-fold in 20% serum with ECGS ($p < 0.01$). Thus, a determining factor for Dll4 induction by hypoxia is high serum concentration in the culture medium.

This result may be explained by differential expressions of HIF1α protein under different serum conditions. HUVECs were cultured for 40 hours in three types of medium: 2% without ECGS, 2% with ECGS and 20% with ECGS. During the last 16 hours, cells were cultured under either hypoxia or normoxia, and protein was isolated immediately afterwards. Protein samples were separated by SDS-PAGE and immunoblotted for HIF1α, with β-tubulin as a loading control. As shown in Figure 4.19C, the hypoxic expression of HIF1α protein was greatest in 20% medium with ECGS, and lowest in 2% serum without ECGS. Previous reports had demonstrated that growth factors could activate HIF1α translation via PI3K and MAPK signalling pathways (Semenza, 2003). High-serum medium, rich in growth factors, would induce HIF1α protein expression. Furthermore, since Dll4 upregulation is dependent on HIF1α (Patel et al., 2005), the greatest HIF1α induction in high-serum medium would lead to the greatest Dll4 induction.

4.5 Summary

Experiments presented in this chapter examined the regulation of Dll4 expression by other signalling pathways. Two approaches were used. First, RNA was isolated from HUVECs for

real-time PCR analysis to measure Dll4 and Notch target gene expression. Second, pGL3e plasmids encoding Dll4 promoter fragments were transfected into PAE cells, and luciferase assays were performed to measure Dll4 promoter activation.

The first approach showed Dll4 expression in HUVECs was induced by Notch, VEGF and hypoxia signalling pathways, all important regulators of angiogenesis (Figure 4.20). Activation of Notch signalling by N1ICD overexpression or Dll4 or Jag1 stimulation increased the mRNA levels of Dll4 and Notch target genes such as Hey1 and Hey2. In particular, culturing HUVECs on rhDll4-coated plates activated Notch signalling and induced Dll4 expression in a γ-secretase-dependent manner. The higher Dll4 expression could in turn lead to more Notch signalling, suggesting a positive feedback loop. Additionally, since Notch signalling is dependent on cell-cell contact, cells cultured at higher densities expressed higher levels of Dll4 and other Notch target genes, an effect that was blocked by γ-secretase inhibition.

VEGF signalling also induced Dll4 expression. Treating HUVECs with $VEGF_{165}$ up-regulated the expression of Dll4 and Notch target genes dose-dependently. Interestingly, $VEGF_{165}$ induced Notch cleavage and Hey1 and Hey2 expression rapidly, but it induced Dll4 expression more gradually. In addition, the induction of all three genes was γ-secretase-dependent. These results support the hypothesis that $VEGF_{165}$ treatment activated Notch signalling, which induced Dll4 expression. The upregulation of Dll4 would further activate Notch signalling, launching the Dll4-Notch feedback loop, thus explaining the more gradual induction of Dll4 by $VEGF_{165}$. Additionally, the effect of VEGF isoforms on Notch signalling

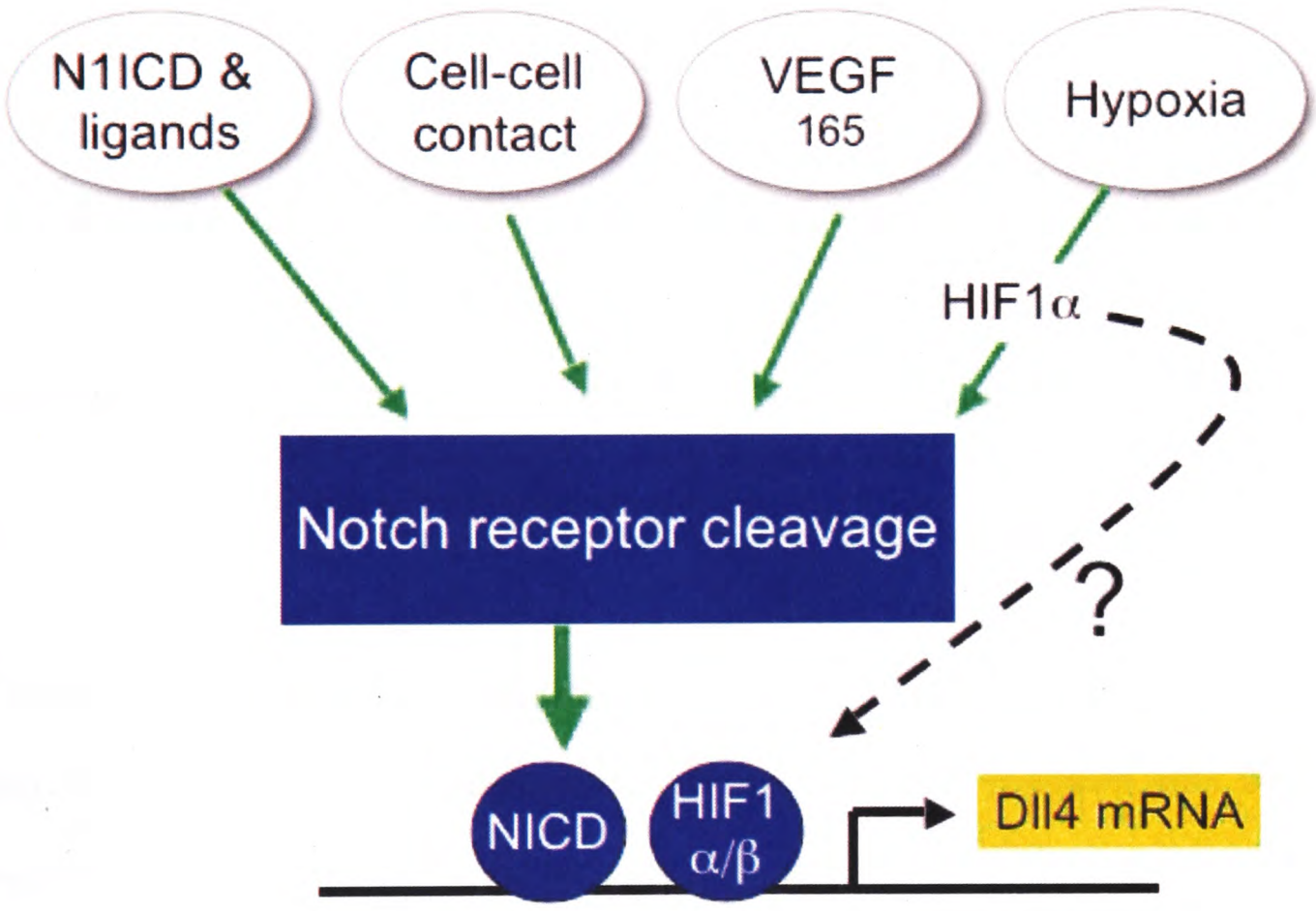


Figure 4.20. Schematic diagram of signalling pathways that regulate Dll4 expression *in vitro*.

in tumours was examined. Murine $VEGF_{164}$ was the most effective isoform in inducing Dll4 expression and Notch signalling *in vivo*.

Another inducer of Dll4 expression was hypoxia. Dll4 was up-regulated after 16 hours under 0.1% hypoxia, and the upregulation was γ-secretase-dependent. Similarly, N1ICD accumulation increased under hypoxia, and the increase was also γ-secretase-dependent. These results suggest that hypoxia induced Dll4 expression via Notch signalling. Unexpectedly, hypoxia repressed the expression of Notch target genes Hey1 and Hey2, possibly due to Notch-independent mechanisms. Additionally, the hypoxic induction of Dll4 depended on high serum concentration in the culture medium. This may be due to the lack of HIF1α induction in the low-serum medium.

Promoter studies largely confirmed mRNA-level results. In PAE cells, Dll4 promoters were activated by rhDll4-coated plates after 24 hours, $VEGF_{165}$ treatment after 24 hours or 0.1% hypoxia treatment after 48 hours. Interestingly, the 4 kb promoter was not induced by hypoxia as much as the others, suggesting a possible negative regulatory element located between 4 kb and 2.2 kb upstream of ATG. In addition, truncation of the promoter to 500 bp did not lead to decreased hypoxic induction. The 500 bp fragment does not include any known HRE sites for HIF binding. It is possible that the HRE is located outside the 4 kb proximal promoter; alternatively, hypoxia may activate Dll4 expression through Notch signalling only, without HIF binding to HRE. More promoter studies are needed to distinguish between these two possibilities. Finally, since Dll4 was shown to be a direct target of Notch signalling, future experiments will identify and mutate potential RBP-jκ binding sites in the Dll4 promoter.

CHAPTER FIVE

Regulation of Dll4 Expression by Co-culturing with Cancer Cells

5.1 Introduction

The previous chapter focused on the regulation of Dll4 expression in endothelial cells (ECs) by the Notch, VEGF and hypoxia signalling pathways. Indeed, a number of recent publications have used a similar approach and studied ECs in isolation; however, few have investigated how tumour cells may signal to ECs via Notch signalling.

One such study on tumour-endothelial crosstalk involves the Notch ligand Jag1 (Zeng et al., 2005). The authors used growth factors to induce Jag1 expression in head and neck squamous cell carcinoma cells, and showed that the ligand could activate Notch signalling in ECs in a co-culture study. Further, tumour Jag1-induced Notch signalling promoted EC network formation *in vitro* and tumour angiogenesis *in vivo*. These results described a novel mechanism of juxtacrine signalling from tumours to the surrounding vasculature (Li and Harris, 2005).

Co-culture studies in this chapter seek to study Dll4 regulation in endothelial cells by cancer cell lines. Inducing Dll4 expression may be important in tumour angiogenesis as recent studies, and experiments presented in Chapter 6, showed that blocking Dll4-Notch signalling disrupted tumour vascular networks and inhibited tumour growth (Ridgway et al., 2006, Noguera-Troise et al., 2006, Scehnet et al., 2007).

In experiments presented in Section 5.2 of this chapter, HUVECs were co-cultured with the mouse melanoma cell line B16. The major advantage of using a mouse cell line was that

human-specific PCR primers could be used to detect changes in human Dll4 mRNA expression in ECs. Preliminary co-culture studies were also conducted with human breast cancer cell lines, and these results are described in Section 5.3.

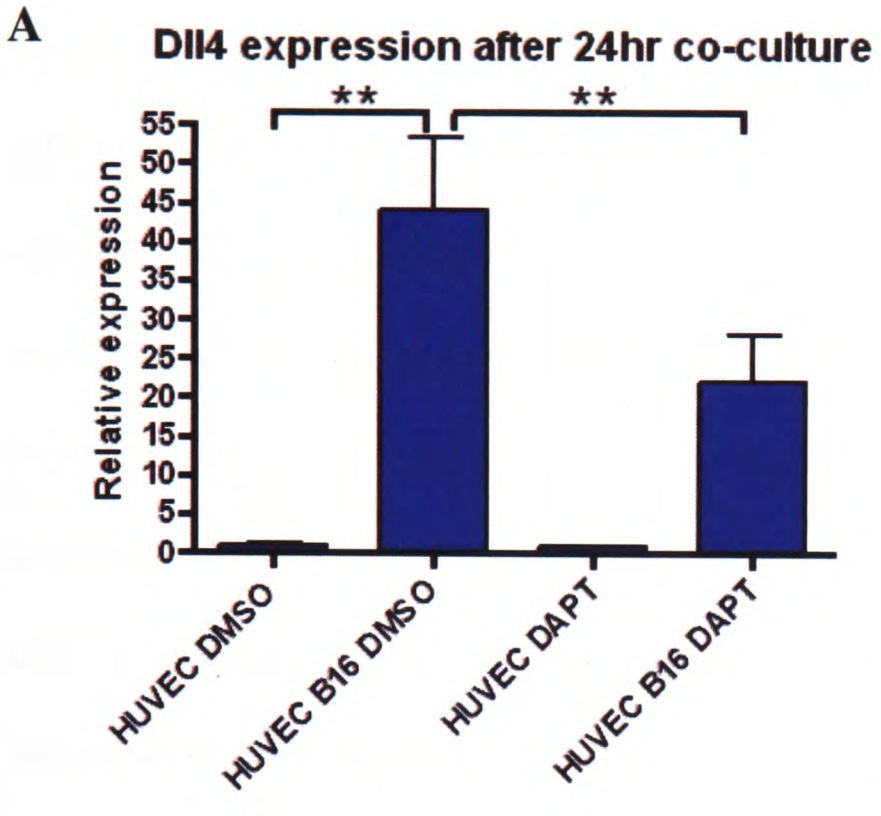
5.2 HUVECs co-culture with B16 mouse melanoma cells

5.2.1 B16 cells induced Dll4 expression in HUVECs

Notch signalling is required for melanoma growth both *in vitro* and *in vivo* (Balint et al., 2005). Thus, it is reasonable to hypothesize that Notch signalling is also involved in tumour angiogenesis of melanomas. To test this hypothesis, the B16 cell line was used. B16, also known as B16F10, is an aggressive melanoma cell line originating from mice of the C57BL/6 strain (Fidler, 1975).

In the first experiment, $1x10^6$ B16 cells were plated per well of a six-well plate. After 24 hours, $2.5x10^5$ HUVECs were plated either in empty wells or on top of the B16 cells, with HUVEC medium containing 2 μM DAPT or DMSO. After 24 hours co-culture, total RNA was isolated, and real-time PCR was conducted with human-specific primers to detect human Dll4 and Hey1 expression.

As shown in Figure 5.1A, co-culture with B16 cells markedly induced human Dll4 expression, by 44.0-fold ($p<0.01$, ANOVA with Bonferroni's post-test). The induction was significantly reduced by DAPT treatment ($p<0.01$). However, B16 cells still induced Dll4 by



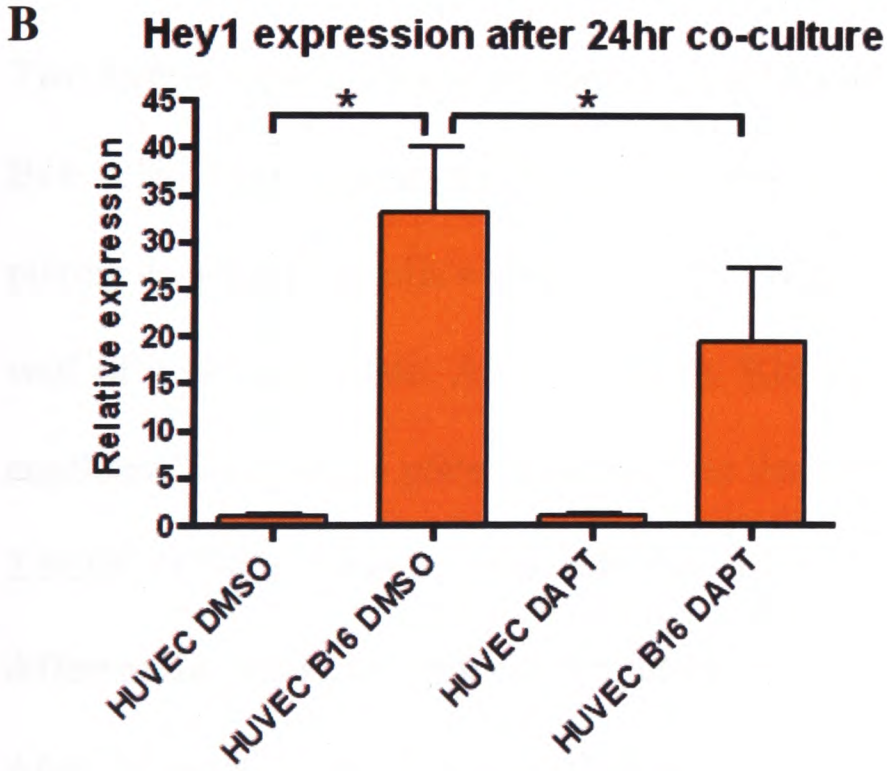


Figure 5.1. Co-culture with B16 cells induced Dll4 expression in HUVECs.
HUVECs were co-cultured with B16 melanoma cells for 24 hours, with 2 μM DAPT or DMSO. Real-time PCR results for human Dll4 are shown in (A), and those for human Hey1 are shown in (B) (*$p<0.05$, **$p<0.01$, ANOVA with Bonferroni's post-test, n=3).

22.0-fold in the presence of DAPT. The Notch target gene Hey1 showed a similar expression pattern (Figure 5.1B). B16 cells induced Hey1 by 33.1-fold ($p<0.05$, ANOVA with Bonferroni's post-test), and the induction was reduced to 19.4-fold by DAPT ($p<0.05$). Thus, B16 cells induced Dll4 expression in HUVECs in at least a partially γ-secretase-dependent manner, indicating that Notch signalling plays a key role in this induction. These results are reminiscent of the co-culture studies cited earlier (Zeng et al., 2005), in which cancer cells expressing Jag1 activated a Notch reporter construct in endothelial cells. In that study, a γ-secretase inhibitor completed blocked Notch activation; however, in this case the high levels of Dll4 and Hey1 expression in the presence of DAPT suggest that there may be a Notch-independent mechanism, which is explored in Section 5.2.3.

Two further experiments were conducted to characterise the induction of Dll4 in HUVECs by B16 cells. First, a dose-response curve was set up by varying the ratios of B16: HUVEC plating density. B16 cells were plated at $6.25x10^4$, $1.25x10^5$, $2.5x10^5$, $5x10^5$ or $1x10^6$ cells per well of a six-well plate. After 24 hours, B16 cells plated at the highest density were fully confluent, while those plated at the lowest density were not in contact with each other. Then, $2.5x10^5$ HUVECs were plated either in empty wells or on top of the B16 cells at the five different densities. The cell culture medium contained either 2 μM DAPT or DMSO control. After 24 hours of co-culture, total RNA was isolated and human Dll4 mRNA expression was detected using real-time PCR.

As shown in Figure 5.2, the ratios of B16: HUVEC plating density were 0 (HUVEC alone),

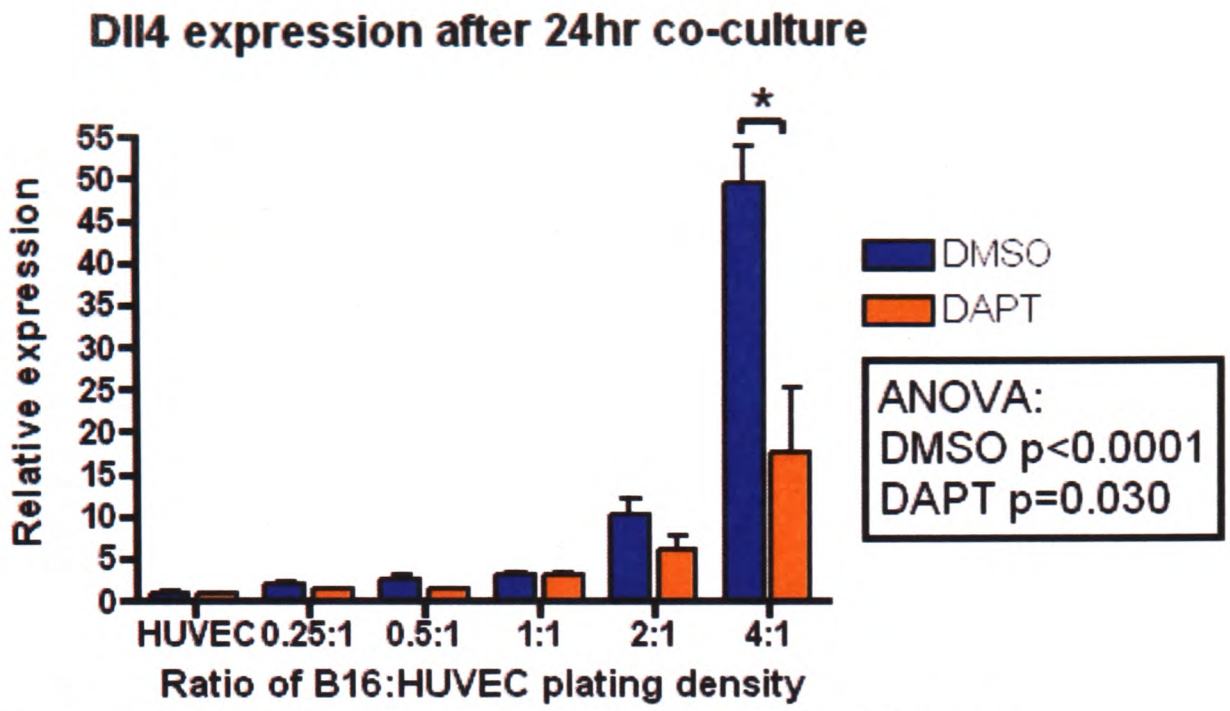


Figure 5.2. Dll4 induction by B16 cells depended on B16: HUVEC ratio.
Different numbers of B16 cells were plated to achieve the ratios indicated on the x-axis. The cells were co-cultured for 24 hours in medium containing 2 μM DAPT or DMSO. Dll4 expression was measured by real-time PCR using human-specific primers, and the data were analysed with ANOVA. The star indicates significant repression of Dll4 by DAPT (*p<0.05, unpaired t-test, n=3).

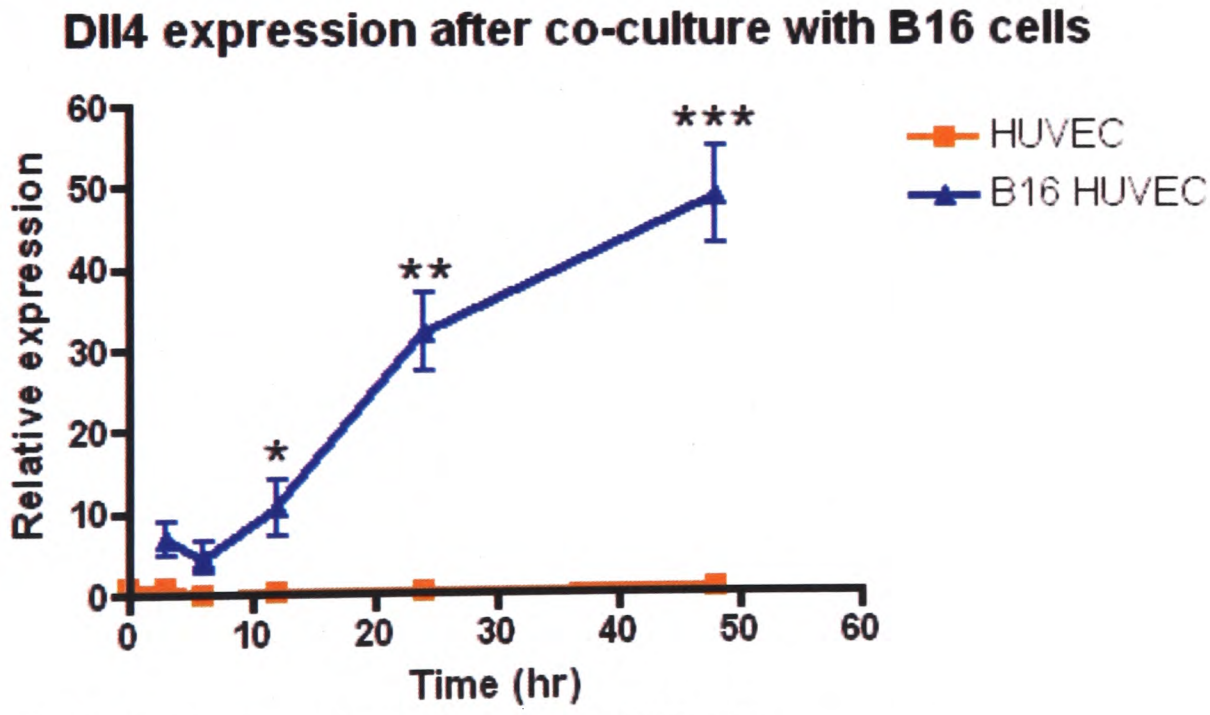


Figure 5.3. Time course of Dll4 induction by B16 cells.
HUVECs were cultured either alone or together with B16 cells, and total RNA was isolated at different time points as indicated. Dll4 expression was measured by real-time PCR using human-specific primers. Stars indicate significant induction of Dll4 by B16 cells at each time point (*p<0.05, **p<0.01, ***p<0.001, unpaired t-test, n=3).

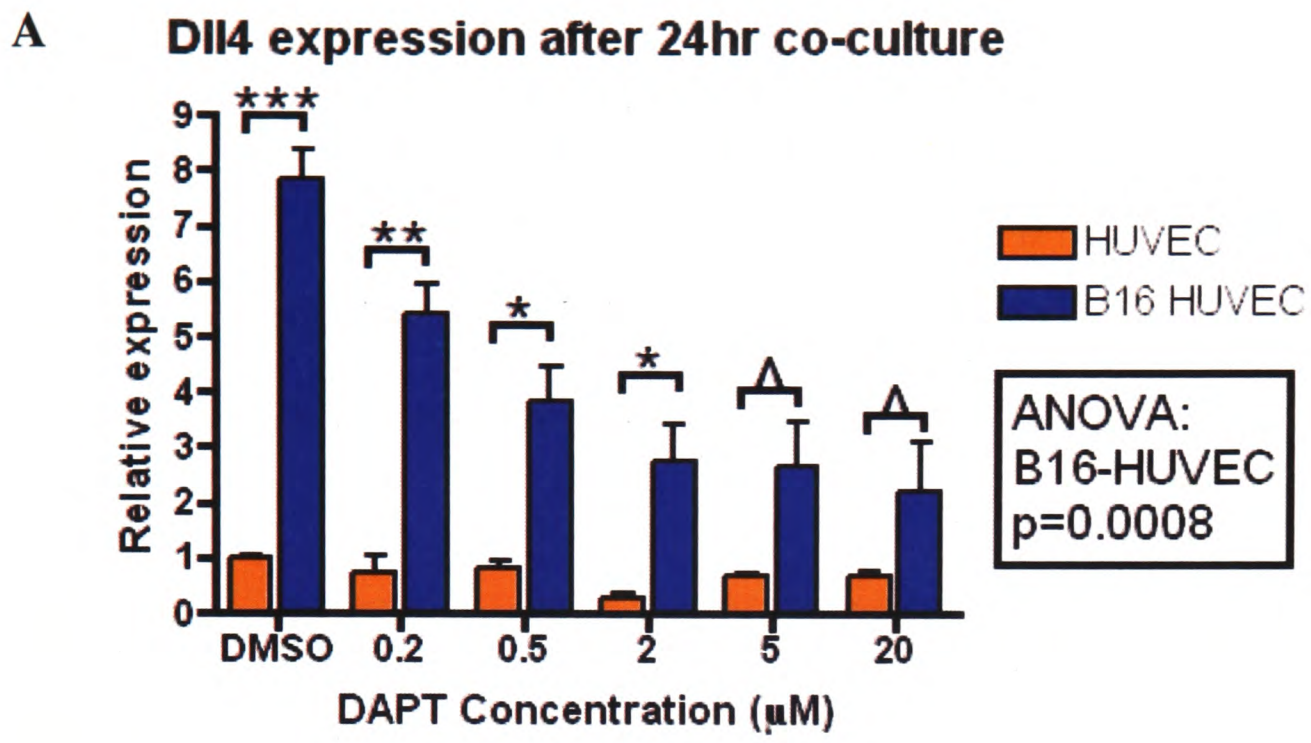
0.25:1, 0.5:1, 1:1, 2:1 and 4:1. Increasing densities of B16 induced human Dll4 expression in HUVECs dose-dependently, without DAPT ($p<0.0001$, ANOVA) or with DAPT ($p=0.030$). Only at the highest B16: HUVEC ratio did DAPT significantly inhibit Dll4 induction by B16 cells ($p=0.024$, unpaired t-test). This suggests that Notch signalling plays a major role in Dll4 induction at the highest density. The result can be explained by a previous finding that Notch signalling was dependent on cell-cell contact and induced by higher cell densities (see Section 4.2.4).

In addition, the time course of Dll4 induction in HUVECs by B16 cells was established. One million B16 cells were plated per well of a six-well plate. After 24 hours, $2.5x10^5$ HUVECs were plated either in empty wells or on top of the B16 cells. A sample of HUVECs was harvested at time 0 to measure Dll4 expression just after trypsinization. After 3, 6, 12, 24 and 48 hours, one sample of HUVEC alone and one sample of B16-HUVEC co-culture were harvested. Real-time PCR results of human Dll4 expression are presented in Figure 5.3. For HUVEC alone, Dll4 expression was low overall but higher between 0 and 3 hours than after 3 hours. The early induction of Dll4 in HUVEC alone samples was likely due to the presence of the calcium chelator EDTA, used together with trypsin to remove cells from plates. The Notch receptor is a heterodimer linked non-covalently by calcium binding. EDTA treatment has been shown to dissociate the heterodimer, promoting γ-secretase cleavage at S3 and activating Notch signalling (Rand et al., 2000). Dll4 may be activated downstream of Notch signalling after EDTA treatment. In the same experiment, Dll4 expression in HUVECs co-cultured with B16 cells was strongly induced. Although it decreased slightly at 6 hours (likely due to initial Notch activation by EDTA), it then increased up to 48 hours, when the last

sample was harvested. B16 cells significantly induced Dll4 expression in HUVECs at 12 hours ($p=0.042$, unpaired t-test), 24 hours ($p=0.0027$) and 48 hours ($p=0.001$). Thus, co-culture with B16 cells steadily induced Dll4 expression in HUVECs up to 48 hours.

5.2.2 B16 cells induced Dll4 in HUVECs partially via Notch signalling

To elucidate the role of Notch signalling in Dll4 induction by B16 cells, several inhibitors of Notch signalling were used in the co-culture experiments. First, a dose-response curve of the γ-secretase inhibitor DAPT was established to determine whether higher doses of the drug would completely block Dll4 induction. As in previous experiments, $1x10^6$ B16 cells were plated per well of a six-well plate and cultured for 24 hours. Next, $2.5x10^5$ HUVECs were plated either in empty wells or on top of the B16 cells. The culture medium contained DMSO or various concentrations of DAPT: 0.2 μM, 0.5 μM, 2 μM, 5 μM, 20 μM. Total RNA was isolated after 24 hours of co-culture for real-time PCR. As shown in Figure 5.4A, DAPT reduced human Dll4 induction by B16 cells dose-dependently ($p=0.0008$, ANOVA). B16 induced Dll4 expression significantly, in the absence of DAPT ($p=0.0003$, unpaired t-test), or with DAPT at lower concentrations 0.2 μM ($p=0.0019$), 0.5 μM ($p=0.010$) and 2 μM ($p=0.022$). B16 failed to induce Dll4 expression significantly at the two highest DAPT concentrations 5 μM ($p=0.070$) and 20 μM ($p=0.16$), although the fold inductions were 3.9 and 3.2, respectively. Human Hey1 showed a similar expression pattern (Figure 5.4B). DAPT reduced Hey1 induction by B16 cells dose-dependently ($p=0.0006$, ANOVA). Hey1 was significantly induced by B16 cells in the absence of DAPT or with DAPT at lower concentrations. The induction was not significant at the highest concentration of DAPT, 20 μM ($p=0.42$, unpaired t-test).



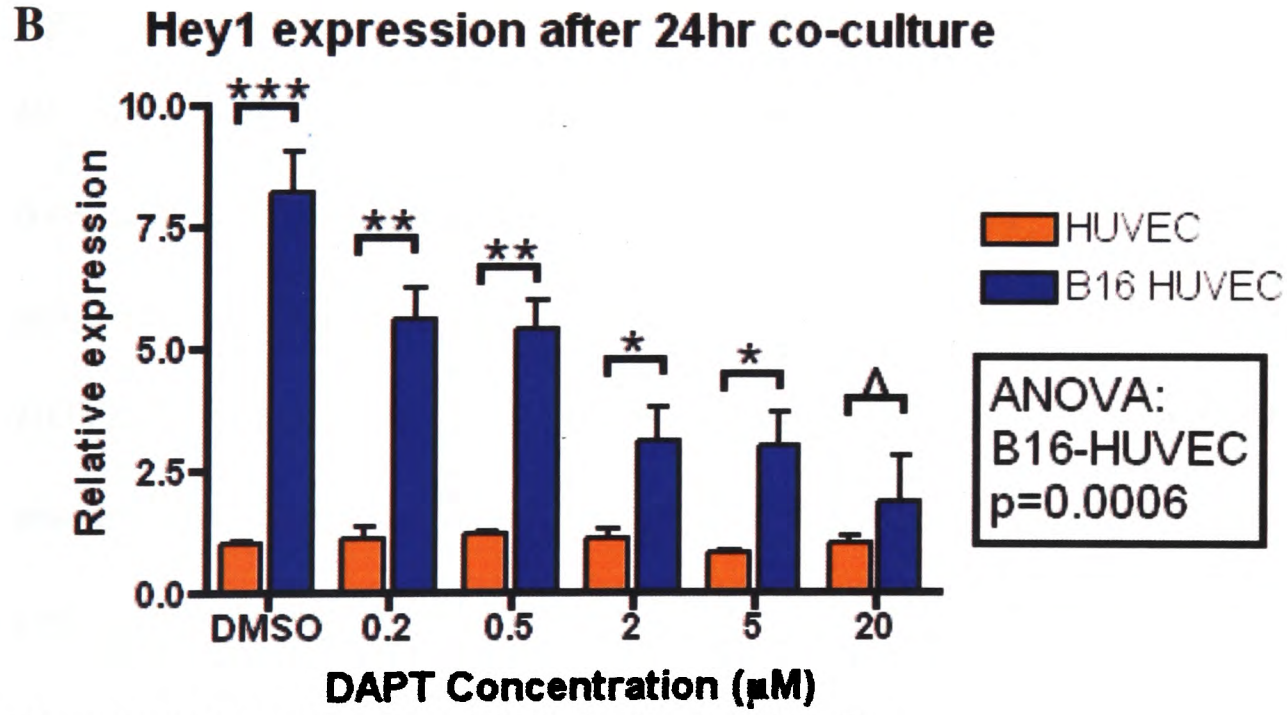


Figure 5.4. Effect of DAPT on Dll4 induction by B16 cells.
HUVECs were cultured either alone or together with B16 cells in medium containing increasing concentrations of DAPT, as indicated on the x-axis. After 24 hours co-culture, total RNA was isolated and real-time PCR using human specific primers was performed. Results for Dll4 (A) and Hey1 (B) were analysed with ANOVA. Stars indicate significant induction by B16 cells at each concentration (^$p \geq 0.05$, *$p < 0.05$, **$p < 0.01$, ***$p < 0.001$, unpaired t-test, n=3).

There are two possible explanations for these results. First, higher concentrations of DAPT completely blocked Dll4 and Hey1 induction in HUVECs by B16 cells, suggesting that Notch signalling was solely responsible for the induction. Second, DAPT did not completely block Dll4 induction; however, high concentrations of the drug led to cellular toxicity (data not shown), poor RNA quality and more variable real-time PCR results. These in turn could lead to large error bars that might obscure otherwise significant results.

To test these possibilities, another γ-secretase inhibitor, DBZ, was used. DBZ is a more potent inhibitor of γ-secretase cleavage and can be used at lower concentrations to block Notch signalling (Ridgway et al., 2006). In a repeat of the previous experiment, B16 cells and HUVECs were co-cultured in medium containing DMSO or various concentrations of DBZ: 0.05 μM, 0.2 μM, 0.5 μM, 2 μM, 5 μM. Like DAPT, DBZ also reduced human Dll4 induction by B16 cells dose-dependently ($p<0.0001$, ANOVA; Figure 5.5A). Notably, HUVECs treated with DBZ yielded better-quality RNA and real-time PCR results with smaller error bars. As a result, B16 significantly induced Dll4 expression at all DBZ concentrations tested: 0 μM ($p<0.0001$, unpaired t-test), 0.05 μM ($p<0.0001$), 0.2 μM ($p<0.0001$), 0.5 μM ($p<0.0001$), 2 μM ($p=0.0004$) and 5 μM ($p=0.0046$). The residual fold-induction at the highest DBZ concentration, 4.2-fold, was comparable with the residual fold-induction at the highest DAPT concentration, 3.2-fold (see Figure 5.4A). DBZ also dose-dependently reduced human Hey1 induction by B16 cells ($p<0.0001$, ANOVA; Figure 5.5B). The induction was significant at all concentrations except the highest, suggesting that 5 μM of

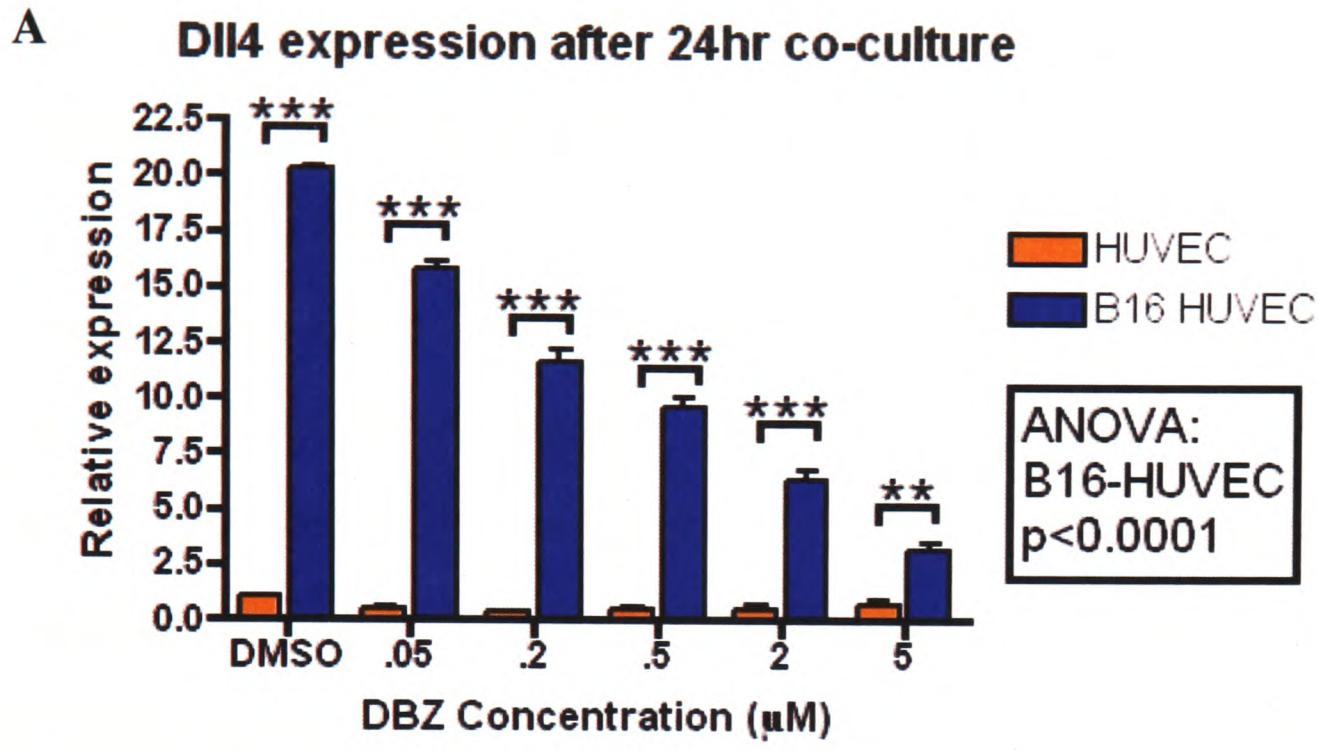
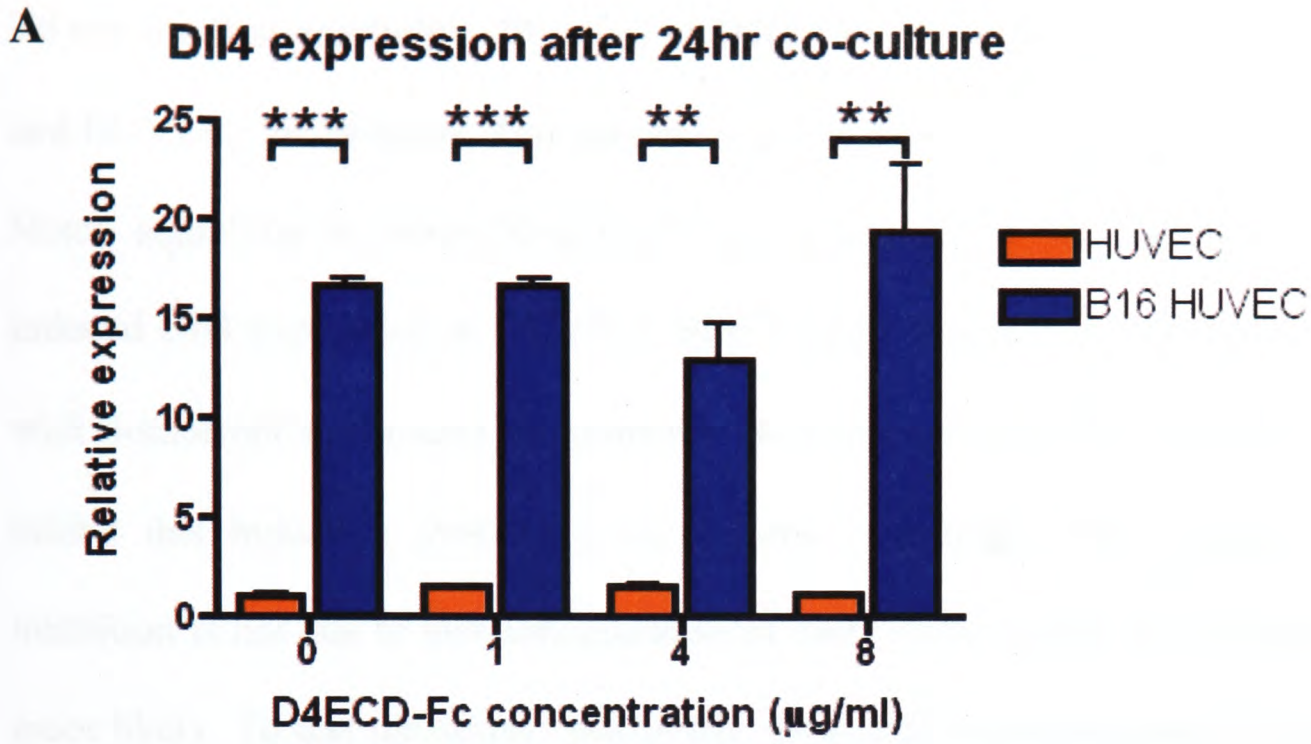


Figure 5.5. Effect of DBZ on Dll4 induction by B16 cells.
HUVECs were cultured either alone or together with B16 cells in medium containing increasing concentrations of DBZ, as indicated on the x-axis. After 24 hours co-culture, total RNA was isolated and real-time PCR using human specific primers was performed. Results for Dll4 (A) and Hey1 (B) were analysed with ANOVA. Stars indicate significant induction by B16 cells at each concentration (^$p \geq 0.05$, **$p < 0.01$, ***$p < 0.001$, unpaired t-test, n=3).

DBZ completely blocked Notch signalling from B16 cells to HUVECs. The fact that co-culture with B16 cells still significantly induced Dll4 expression in the presence of 5 μM DBZ, which totally prevented the induction of Notch target gene Hey1, suggests that Dll4 induction by B16 is composed of Notch-dependent and -independent mechanisms.

The third Notch inhibitor tested was the human Dll4 extracellular domain fused to the human IgG1 Fc region (D4ECD-Fc), produced by Dr Richard Sainson in our laboratory. In contrast to Dll4 ECD immobilised on a plate, Dll4 ECD added to the culture medium inhibits Notch signalling (Hicks et al., 2002, Noguera-Troise et al., 2006, Scehnet et al., 2007). It has been hypothesized that ligand binding exerts a mechanical pulling force on the Notch ECD, enabling receptor cleavage and activation (Gordon et al., 2007). Dll4 ECD suspended in the culture medium does not provide this pulling force but rather competes with functional ligands in binding to Notch receptors.

A dose-response curve of D4ECD-Fc was established for the B16-HUVEC co-culture experiment. B16 cells and HUVECs were co-cultured in medium containing 0 μg/ml, 1 μg/ml, 4 μg/ml or 8 μg/ml of D4ECD-Fc. As expected, B16 induced human Dll4 expression by 16.7-fold ($p<0.0001$, unpaired t-test; Figure 5.6A). However, D4ECD-Fc did not inhibit this induction at all. Several reasons for this result were considered. It is possible that the concentration of D4ECD-Fc, 8 μg/ml, was not high enough. Alternatively, D4ECD-Fc may only block Notch signalling induced by Dll4 but not signalling induced by other ligands.



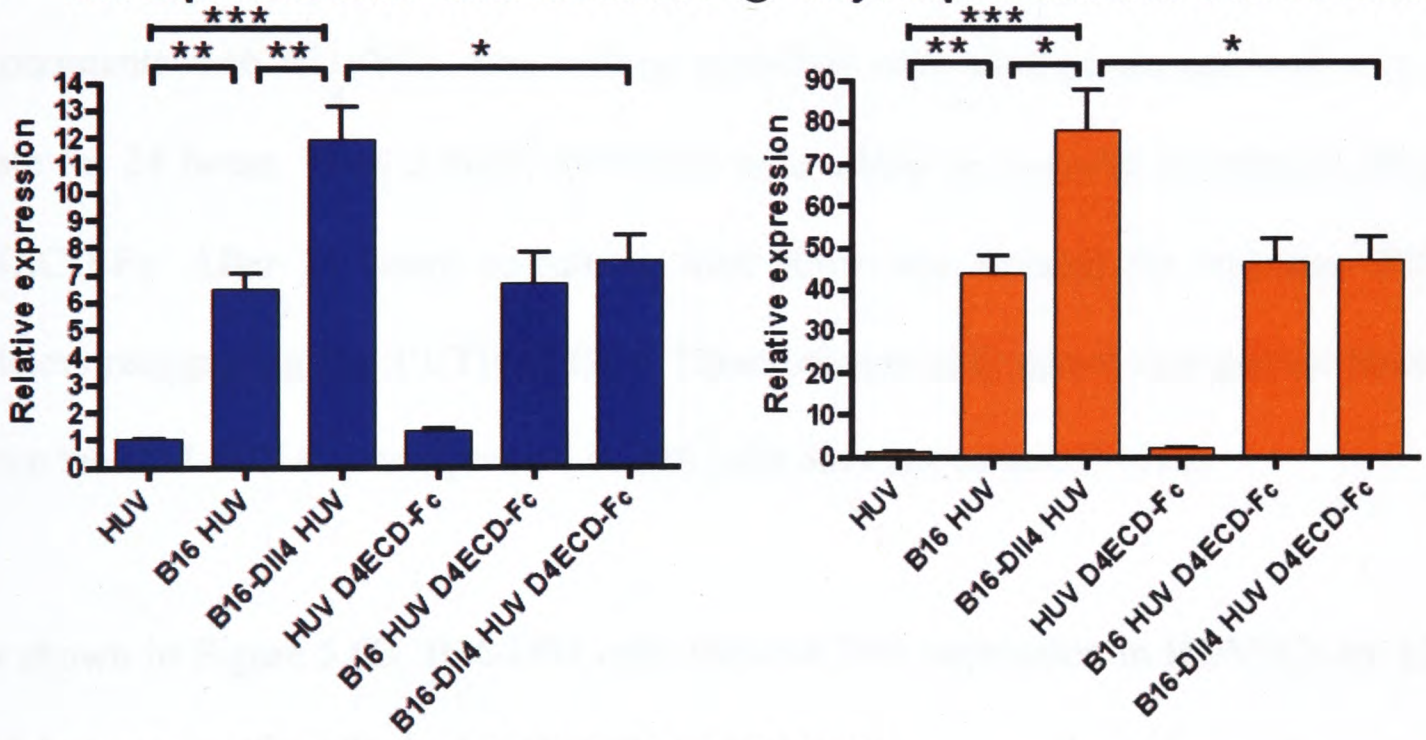


Figure 5.6. Effect of D4ECD-Fc on Dll4 induction by B16 cells.
(A) HUVECs were cultured either alone or together with B16 cells in medium containing increasing concentrations of D4ECD-Fc, as indicated on the x-axis. After 24 hours, RNA was isolated, and human Dll4 expression was measured by real-time PCR. Stars indicate significant induction by B16 cells at each concentration (**p<0.01, ***p<0.001, unpaired t-test, n=3). (B-C) HUVECs were co-cultured with either B16 cells or B16 cells overexpressing full-length human Dll4 (B16-Dll4 cells) in medium containing 20 µg/ml of D4ECD-Fc. After 24 hours, RNA was isolated, and human Dll4 (B) and Hey1 (C) expression was measured by real-time PCR (*p<0.05, **p<0.01, ***p<0.001, ANOVA with Bonferroni's post-test, n=3).

To test the first possibility, st p
and HUVECs for 24 hours. for
Notch signalling *in vitro* ing
induced Dll4 expression in exp
with Bonferroni's post-test) ni's
inhibit this induction (col duc
inhibition is not due to low ot d
more likely. To test the sec o te
cDNA by retroviral trans rov
experiments with HUVECs. ith
plate for 24 hours. Then 2.5 urs
D4ECD-Fc. After 24 hours fter
primers recognising the 3'U isin
since the Dll4 cDNA overexp DN

As shown in Figure 5.6B, B gur
which was significantly highific
$p<0.01$). Notably, D4ECD-Fc y, I
3 vs. column 6, $p<0.05$), to , p<
words, D4ECD-Fc abrogated Fc a

Figure 5.6C shows that Hey1 expression in HUVECs followed a similar pattern to Dll4 expression. B16 cells induced Hey1 expression by 44.0-fold (column 1 vs. column 2, $p<0.01$, ANOVA with Bonferroni's post-test). B16-Dll4 cells further induced Hey1 expression to 78.2-fold (column 2 vs. column 3, $p<0.05$). D4ECD-Fc treatment did not reduce the induction by B16 cells (column 2 vs. column 5, $p\geq0.05$). However, it did reduce the induction by B16-Dll4 cells (column 3 vs. column 6, $p<0.05$) to a level comparable with the induction by B16 cells. Taken together, these results suggest that D4ECD-Fc specifically inhibited Dll4-induced Notch signalling but not signalling induced by other ligands or by soluble factors (see next section).

5.2.3 B16 cells induced Dll4 in HUVECs via soluble factors

Based on the experiments in Section 5.2.2, B16 cells could also induce Dll4 expression in HUVECs via a Notch-independent mechanism. Preliminary experiments have been carried out to investigate what factors and pathways may play a role in the Notch-independent induction. First, to determine whether soluble factors are involved, B16-conditioned medium was used to culture HUVECs. Since Notch signalling depends on cell-cell contact, conditioned medium prevents Notch signalling to HUVECs from B16 cells. In the experiment, $1x10^6$ B16 cells per well of a six-well plate were cultured in HUVEC medium for 24 hours. The medium was then used to culture $2.5x10^5$ HUVECs for 24 hours, with 2 μM DAPT or DMSO. B16-conditioned medium did not induce Dll4 expression in HUVECs, as shown in Figure 5.7 (column 1 vs. column 2, $p\geq0.05$, ANOVA with Bonferroni's post-test).

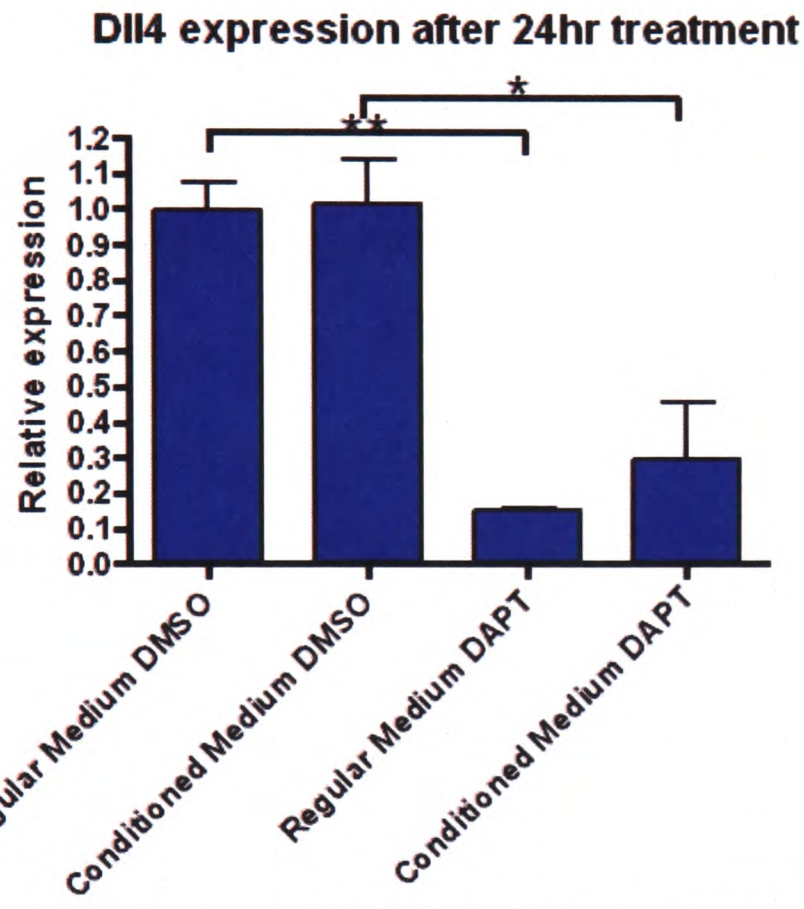


Figure 5.7. B16-conditioned medium did not induce Dll4 expression in HUVECs.
B16 cells were cultured in HUVEC medium for 24 hours. The conditioned medium or regular medium was then used to culture HUVECs for 24 hours, with 2 μM DAPT or DMSO. Dll4 expression was measured by real-time PCR (*$p<0.05$, **$p<0.01$, ANOVA with Bonferroni's post-test, n=3).

This would imply that the Notch-independent component of Dll4 induction by B16 cells was not due to soluble factors. However, this experiment did not preclude the involvement of labile soluble factors, which may be rapidly degraded in the conditioned medium.

To determine whether there are indeed such soluble factors, an alternative approach was used. B16 cells and HUVECs were co-cultured in two compartments separated by a Transwell insert. As illustrated in Figure 5.8A, the bottom of the insert is a porous membrane with 0.4 μm-diameter pores, allowing the exchange of small molecules but not cells between the two compartments. One million B16 cells were plated per well in the lower compartment. After 24 hours, $2.5x10^5$ HUVECs were plated on the membrane in the upper compartment. Both B16 cells and HUVECs were submerged in HUVEC culture medium containing either 2 μM DAPT or DMSO. After 24 hours, HUVECs were trypsinized from the membrane for RNA isolation and real-time PCR.

As shown in Figure 5.8B, B16 cells, through the Transwell membrane, strongly induced Dll4 expression by 8.0-fold (column 1 vs. column 2, $p<0.0001$, ANOVA with Bonferroni's post-test), suggesting that Dll4 induction did not require cell-cell contact. In addition, this induction was not inhibited by DAPT treatment. More interestingly, Hey1 expression showed a similar pattern (Figure 5.8C). Hey1 was induced by B16 through the membrane, and the induction was not inhibited by DAPT. These results, together with the conditioned medium results, indicate that B16 cells secrete soluble factors that can induce Dll4 and Hey1

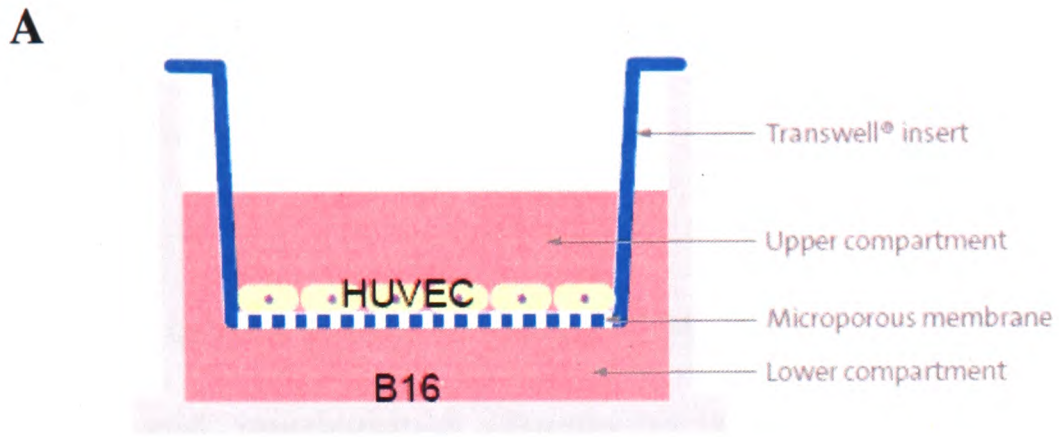


Figure 5.8. B16 induced Dll4 expression in HUVECs through Transwell insert.
(A) Schematic diagram of a Transwell (adapted from product manual). (B-C) B16 cells were cultured in the lower compartment and HUVECs were cultured in the upper compartment in medium containing 2 μM DAPT or DMSO. After 24 hours, HUVECs were trypsinized from the membrane for RNA isolation. Real-time PCR results for Dll4 (B) and Hey1 (C) are presented (**p<0.01, ***p<0.001, ANOVA with Bonferroni's post-test, n=3).

expression in HUVECs in a γ-secretase-independent manner, suggesting that Notch signalling is not involved. Thus, the induction of Dll4 that could not be inhibited by DAPT (see Figure 5.4A) or DBZ (see Figure 5.5A) was mediated by labile soluble factors produced by the B16 cells.

Soluble factors known to induce Dll4 expression include VEGF, basic FGF (Patel et al., 2005) and interleukin-6 (Suzuki et al., 2006). Future experiments will measure the concentration and stability of these molecules in the medium of co-culture experiments. Specific inhibitors will also be used to block their function to see if the Notch-independent induction of Dll4 by B16 cells is reduced.

5.2.4 Hypoxia reduced B16 induction of Dll4 in HUVECs

Results presented in Section 3.3 showed that hypoxia induced Jag1 expression in the cancer cell line MCF7. Hypoxia treatment may also induce Notch ligand expression in B16 cells, thus increasing its ability to induce Notch signalling and Dll4 expression in HUVECs. To test this hypothesis, $1x10^6$ B16 cells per well were cultured under 0.1% hypoxia or normoxia for 16 hours before co-culturing with $2.5x10^5$ HUVECs for 24 hours under normoxia. As shown in Figure 5.9A, B16 cells cultured under normoxia induced Dll4 expression by 18.0-fold ($p<0.01$, ANOVA with Bonferroni's post-test). However, hypoxia pre-treatment of B16 cells slightly reduced Dll4 induction ($p<0.05$). Hey1 expression was also induced by B16 cells, and the induction was reduced if the B16 cells had been cultured under hypoxia (Figure 5.9B). Interestingly, hypoxia pre-treatment reduced mouse Dll4 expression in B16 cells ($p=0.031$,

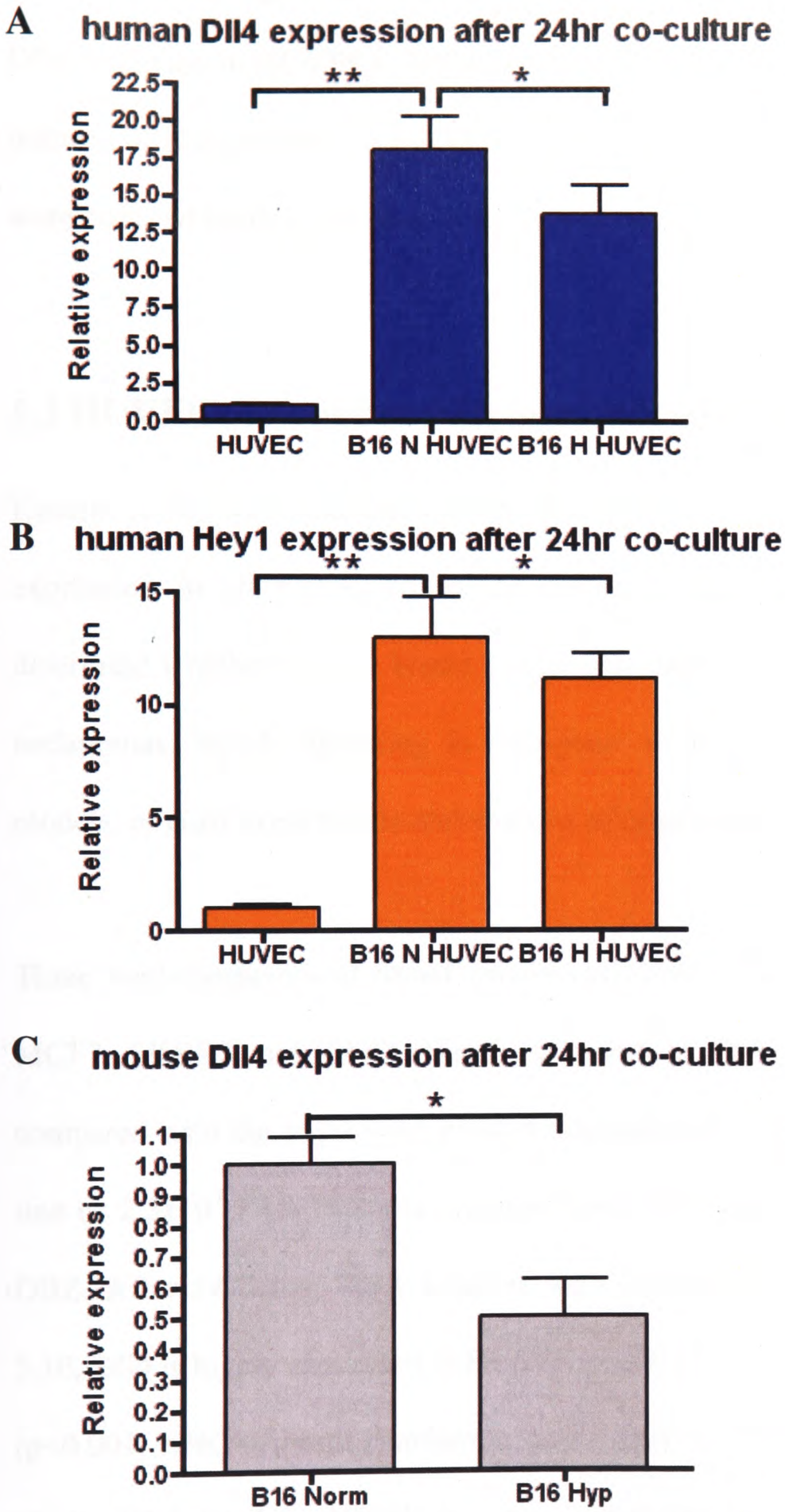


Figure 5.9. Hypoxia pre-treatment of B16 cells did not further induce Dll4 in HUVECs.
B16 cells were pre-treated under 0.1% hypoxia or normoxia for 16 hours before co-culturing with HUVECs for 24 hours. Human Dll4 (A) and Hey1 (B) expression was measured by real-time PCR with human-specific primers (*$p<0.05$, **$p<0.01$, ANOVA with Bonferroni's post-test, n=3). Mouse Dll4 (C) expression was measured with mouse-specific primers (*$p<0.05$, unpaired t-test, n=3).

unpaired t-test; Figure 5.9C). This could lead to reduced Notch signalling and thus human Dll4 induction in HUVECs. These results are not in conflict with the conclusion that hypoxia induced Dll4 expression in HUVECs (Section 4.4), because only B16 cells and not HUVECs were cultured under hypoxia in this experiment.

5.3 HUVECs co-culture with human breast cancer cell lines

Results in the previous section showed that a mouse melanoma cell line induced Dll4 expression in HUVECs. To extend these results, experiments in this section sought to determine whether human breast cancer cell lines could do the same. Similar to its role in melanomas, Notch signalling is oncogenic in breast cancer, as demonstrated by animal models, *in vitro* experiments and analysis of human tumour samples (Shi and Harris, 2006).

Three well-characterised breast cancer cell lines were used in the co-culture experiments: MCF7, SKBR3 and T47D. First, the levels of Dll4 expression in these cell lines were compared with the basal level of Dll4 expression in HUVECs. One million cells of each cell line or $2.5x10^5$ HUVECs were cultured per well of a 6-well plate, with or without 500 nM DBZ. After 24 hours, RNA samples were isolated for real-time PCR. As shown in Figure 5.10, Dll4 is highly expressed in HUVECs, and the expression was reduced by DBZ treatment ($p<0.001$, ANOVA with Bonferroni's post-test). In comparison, MCF7 cells expressed 2.5% of the Dll4 level in HUVECs. This is expected as Dll4 is predominantly expressed in endothelial cells (Shutter et al., 2000). In the co-culture experiment, it would not be possible

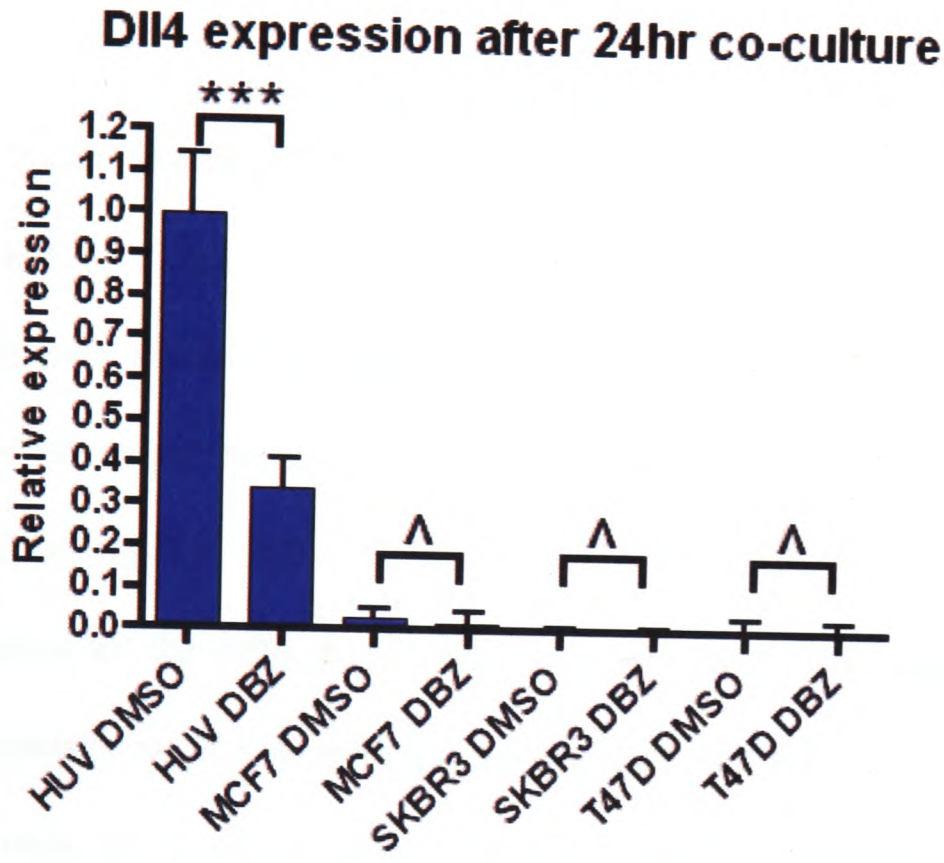


Figure 5.10. Dll4 expression in HUVECS and three breast cancer cell lines.
HUVECs and MCF7, SKBR3, T47D breast cancer cells were cultured separately for 24 hours, with 500 nM DBZ or DMSO. Dll4 expression in each cell line was measured by real-time PCR (^$p \geq 0.05$, ***$p < 0.001$, ANOVA with Bonferroni's post-test, n=3).

to distinguish between Dll4 expression in HUVECs versus that in MCF7 cells. However, even at the highest MCF7: HUVEC ratio (4:1), more than 90% of the Dll4 expression would be derived from HUVECs. As for the other two cell lines, SKBR3 expressed 0.47% of the Dll4 level in HUVECs, and T47D expressed 0.23%. These two cell lines would contribute even less Dll4 expression in co-culture samples.

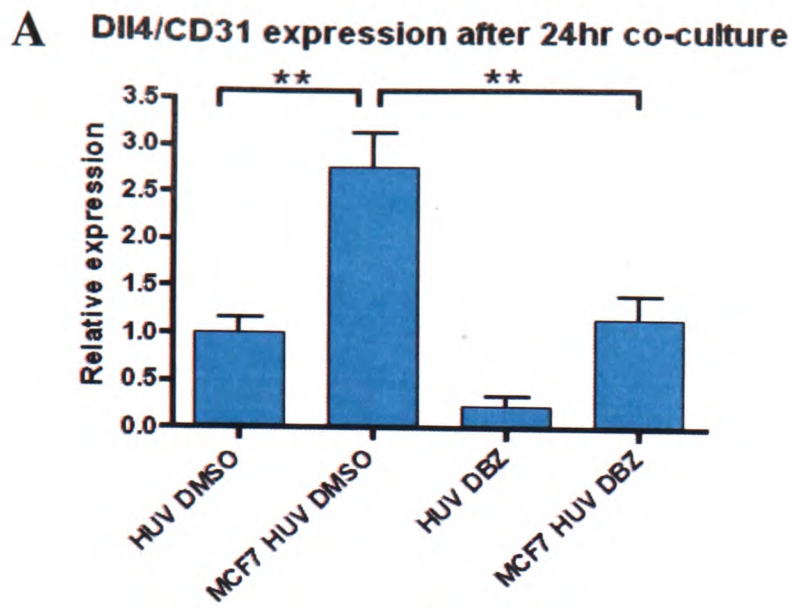
The three breast cancer cell lines were co-cultured with HUVECs, and DBZ was used to determine if any Dll4 induction was Notch-dependent. Using this approach, $1x10^6$ MCF7 cells were plated per well of a six-well plate. After 24 hours, $2.5x10^5$ HUVECs were plated either in empty wells or on top of the MCF7 cells, with HUVEC medium containing 500 nM DBZ or DMSO. After 24 hours co-culture, total RNA was isolated for real-time PCR. To account for the different HUVEC numbers in HUVEC alone versus co-culture samples, Dll4 expression in each sample was normalised by CD31 expression. CD31, a vessel marker, was not detected in breast cancer cell lines (data not shown). Since Dll4 expression was largely restricted to HUVECs and CD31 expression was HUVEC-specific, the Dll4/CD31 ratio would measure Dll4 expression in HUVECs more accurately. This method could not be used to measure HUVEC-specific expression of other Notch genes such as Hey1, since they were expressed in both HUVECs and breast cancer cells (data not shown).

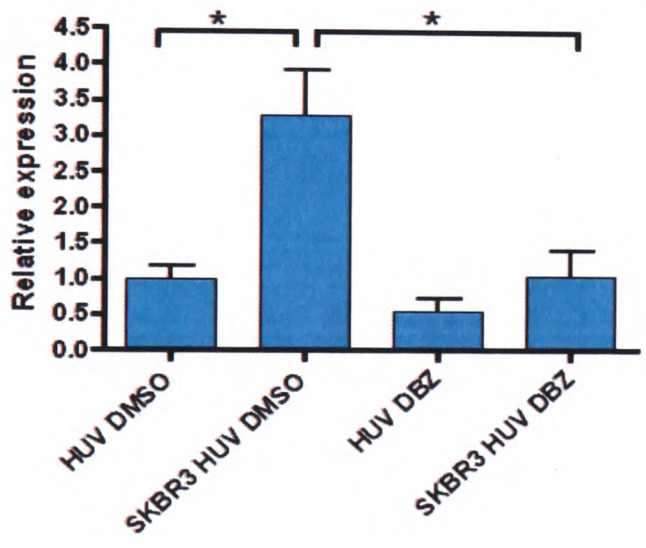
The real-time PCR results are shown in Figure 5.11A. Co-culture with MCF7 cells induced Dll4/CD31 ratio by 2.8-fold. This induction is modest compared with the induction of Dll4 by B16 cells, 44.0-fold, but it was still significant ($p<0.01$, ANOVA with Bonferroni's post-test). More interestingly, DBZ treatment completely blocked the induction of Dll4/CD31 by MCF7

cells ($p<0.01$). This suggests that the induction was entirely Notch-dependent, unlike the induction by B16 cells, which was partially Notch-dependent.

The co-culture experiments of SKBR3 or T47D cells with HUVECs were conducted similarly. As shown in Figure 5.11B, co-culture with SKBR3 cells induced Dll4/CD31 ratio by 3.3-fold ($p<0.05$, ANOVA with Bonferroni's post-test), and the induction was completely blocked by DBZ treatment ($p<0.05$). In contrast, co-culture with T47D cells did not affect Dll4/CD31 ratio, and DBZ treatment reduced Dll4/CD31 ratio to similar levels in HUVEC alone and co-culture samples (Figure 5.11C). Taken together, both MCF7 and SKBR3 cells induced Dll4 expression in HUVECs in a Notch-dependent manner. T47D cells did not induce Dll4 expression at all, or they did not induce Dll4 at the T47D: HUVEC ratio used in this experiment. To distinguish between these two possibilities, various ratios of breast cancer: HUVECs were used in a subsequent experiment.

The three breast cancer cell lines, MCF7, T47D and SKBR3, were co-cultured with HUVECs at different ratios. Breast cancer cells were plated at $6.25x10^4$, $1.25x10^5$, $2.5x10^5$, $5x10^5$ or $1x10^6$ cells per well of a six-well plate. After 24 hours, cancer cells plated at the highest density were fully confluent, while those plated at the lowest density were not in contact with each other. Then, $2.5x10^5$ HUVECs were plated either in an empty well or on top of the cancer cells. The cells were cultured for 24 hours before RNA isolation and real-time PCR analysis.





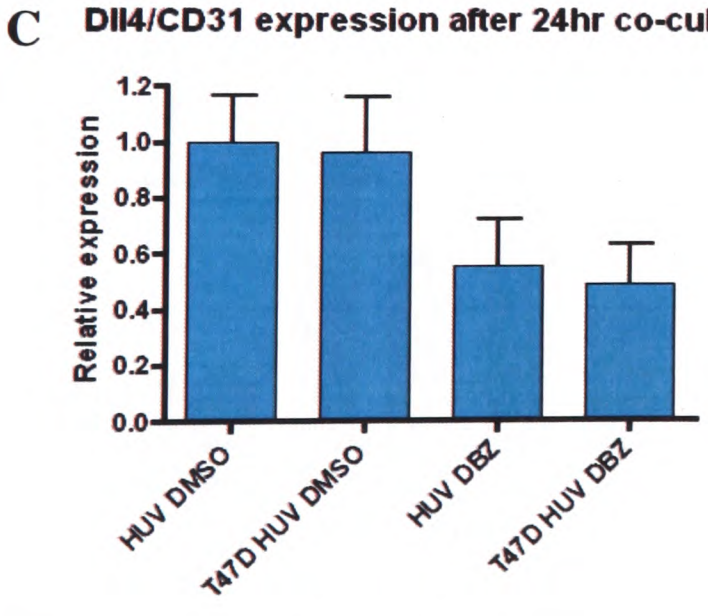
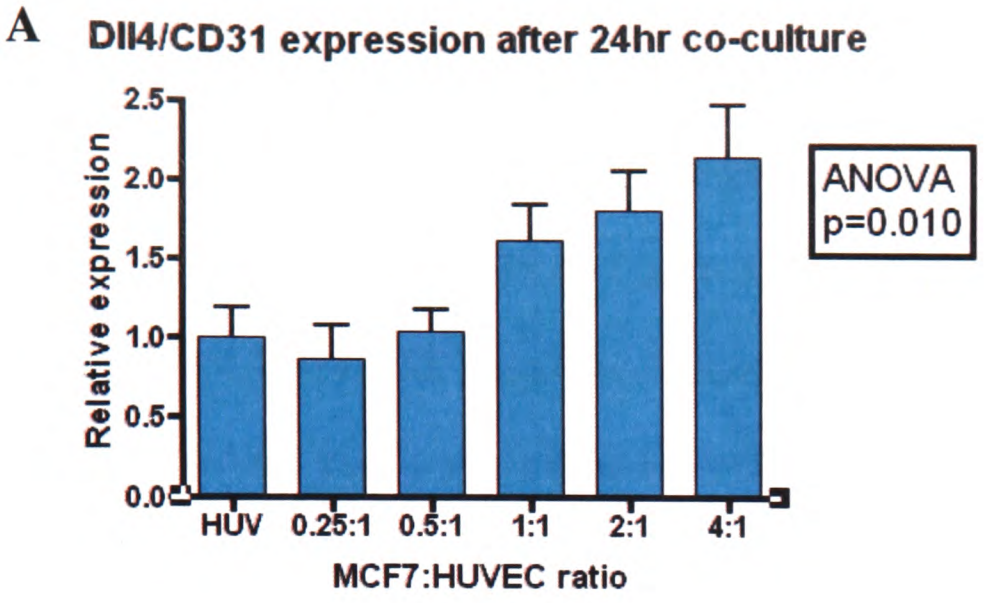
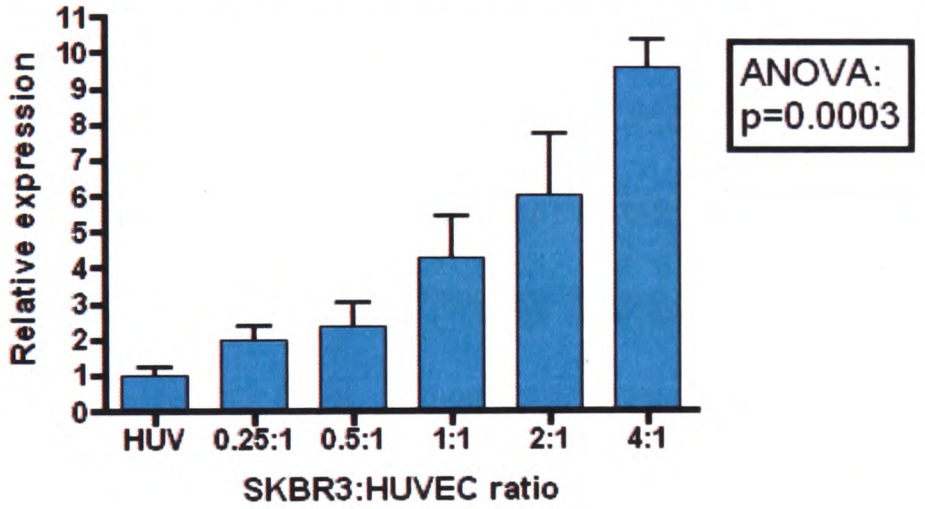


Figure 5.11. Co-culture with breast cancer cells induced Dll4 expression in HUVECs
MCF7 (A), SKBR3 (B) and T47D (C) cells were co-cultured with HUVECs for 24 hours, with 500 nM DBZ or DMSO. Dll4 and CD31 expression was measured by real-time PCR (*$p<0.05$, **$p<0.01$, ANOVA with Bonferroni's post-test, n=3).





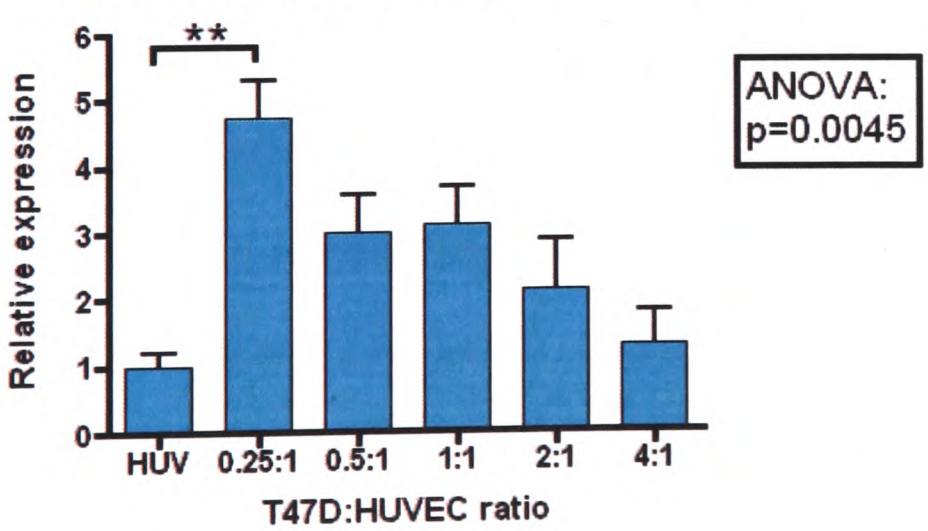


Figure 5.12. Dll4 induction by breast cancer cells depended on cancer: HUVEC ratio.
Different numbers of MCF7 (A), SKBR3 (B) and T47D (C) cells were plated to achieve the cancer: HUVEC ratios indicated on the x-axis. Dll4 and CD31 expression was measured by real-time PCR and the results were analysed with ANOVA (**$p<0.01$, ANOVA with Bonferroni's post-test, n=3).

As shown in Figure 5.12, six cancer: HUVEC ratios were used: 0 (HUVEC alone), 0.25:1, 0.5:1, 1:1, 2:1 and 4:1. Increasing densities of MCF7 cells induced Dll4/CD31 ratio dose-dependently ($p=0.010$, ANOVA; Figure 5.12A). Similarly, increasing densities of SKBR3 cells induced Dll4/CD31 ratio dose-dependently ($p=0.0003$, ANOVA; Figure 5.12B). These are similar to the results of the B16-HUVEC ratio experiment (see Figure 5.2). In both cases, cancer cells induced Dll4 expression in HUVECs via Notch signalling, which is activated by higher cell densities (see Section 4.2.4).

The T47D-HUVEC co-culture results were more paradoxical. In the previous experiment, T47D cells did not induce Dll4 expression in HUVECs at the 4:1 plating ratio. However, this experiment showed that T47D cells induced Dll4/CD31 by 4.8-fold at the lowest ratio, 0.25:1 ($p<0.01$, ANOVA with Bonferroni's post-test; Figure 5.12C). Moreover, as the T47D: HUVEC ratio increased, the induction of Dll4/CD31 decreased. At the 4:1 ratio, Dll4/CD31 was induced by 1.3-fold, which was not significant ($p\geq0.05$) and thus comparable with the result of the previous experiment (see Figure 5.11C). One possible explanation for these results is that T47D cells express higher levels of Notch ligands compared with the other two cell lines and can activate Notch signalling in HUVECs at the low 0.25:1 ratio. At higher ratios, T47D cells may over-activate Notch signalling, leading to decreased Dll4 induction in HUVECs. Additionally, Notch-independent mechanisms of Dll4 induction by T47D cells cannot be ruled out. In the future, Notch ligand expression in these breast cancer cell lines should be examined, and the T47D: HUVEC ratio experiment should be repeated in the presence of DBZ to determine if Notch signalling is involved.

Altogether, these studies provided evidence for Dll4 induction in HUVECs by co-culturing with three breast cancer cell lines. Induction by MCF7 and SKBR3 cells, at least, appeared Notch-dependent. Measuring the expression of Notch target genes such as Hey1 would further clarify the role of Notch signalling; however, that would require the separation of HUVECs from the cancer cells since Hey1 is expressed in both cell types. One possibility would be to sort out HUVECs by fluorescence-activated cell sorting (FACS), using a primary antibody against CD31 and a fluorescently labelled secondary antibody. Alternatively, HUVECs and cancer cells could be injected with vital dyes of different colours, and separated by FACS after co-culture.

5.4 Summary

Experiments in this chapter expanded upon those in the previous chapter and explored the regulation of Dll4 expression in HUVECs by co-culturing with cancer cell lines.

The chapter focused on co-culturing HUVECs with the mouse melanoma cell line B16. B16 cells strongly induced Dll4 and Hey1 expression in HUVECs, and higher B16: HUVEC ratios led to higher inductions. Interestingly, the γ-secretase inhibitor DBZ only partially reduced Dll4 induction, even though it completely blocked Hey1 induction. This suggests that B16 could induce Dll4 expression in HUVECs via Notch-dependent and -independent mechanisms. Another inhibitor of Notch signalling, D4ECD-Fc, specifically blocked Dll4-induced Notch signalling between B16 cells and HUVECs.

The Notch-dependent induction of Dll4 by B16 cells probably resulted from Notch ligands expressed in B16 cells. An incomplete analysis showed that B16 cells expressed mouse Dll4 (Figure 5.9C), Dll1 and Jag1 (data not shown), and further characterisation is needed.

The Notch-independent mechanism of Dll4 induction by B16 cells was also examined. Interestingly, B16-conditioned medium did not induce Dll4 or Hey1 expression in HUVECs. However, co-culturing B16 cells and HUVECs using a Transwell apparatus did lead to Dll4 and Hey1 upregulation in HUVECs in a γ-secretase-independent manner. This suggests that the Notch-independent induction of Dll4 by B16 cells was mediated by labile soluble factors. Further experiments are needed to identify such factors.

Preliminary studies of co-culturing HUVECs with human breast cancer cell lines were also conducted. MCF7 and SKBR3 cells induced Dll4 expression in HUVECs via Notch signalling. T47D cells also induced Dll4 expression, although the mechanism awaits clarification. Notably, Dll4 induction in HUVECs by breast cancer cells was much smaller than Dll4 induction by B16 cells. Breast cancer cells lack the Notch-independent mechanism of inducing Dll4 expression. In addition, the Notch-dependent induction may differ due to the different expression profiles of Notch ligands in the cell lines. Future studies will examine Notch ligand expression in cancer cell lines and Notch signalling activation in HUVECs.

Altogether, results in this chapter demonstrate that Notch signalling is important in the crosstalk between cancer cells and endothelial cells. Manipulating Notch signalling could

have a dramatic effect on tumour angiogenesis and growth *in vivo*. This is the topic of the next chapter.

CHAPTER SIX

Effect of Dll4 Overexpression on Tumour Growth in Vivo

6.1 Introduction

The previous chapter explored how Dll4 expression in HUVECs was induced by co-culturing with cancer cell lines, suggesting that Dll4-Notch signalling plays a role in tumour angiogenesis. This is consistent with the conclusions of several *in vivo* studies.

In a xenograft study involving MCF7 cells, tumours were shown to express high levels of mouse Dll4 within their vasculature (Mailhos et al., 2001). Similarly, Lewis lung carcinoma allograft tumours specifically induced Dll4 expression in tumour vessels (Noguera-Troise et al., 2006). These results suggest that Dll4 may be crucial for tumour angiogenesis.

Several recent studies have manipulated Dll4-Notch signalling in xenograft tumours. In two studies that produced similar results, cancer cells expressing either full-length Dll4 (Fl-Dll4) or soluble Dll4 (sDll4) were implanted into mice (Noguera-Troise et al., 2006, Scehnet et al., 2007). Fl-Dll4 cells induced Notch signalling, whereas sDll4 repressed Notch signalling in the xenograft tumours. With the cancer cell lines tested, Fl-Dll4 cells did not affect tumour growth; however, sDll4 cells led to smaller tumours resulting from harbouring a poorly functional vasculature. In addition, treatment with a VEGF-trap decreased Dll4 mRNA expression in tumour vessels (Noguera-Troise et al., 2006). The hypothesis is that the Dll4-Notch pathway normally acts downstream of VEGF as a negative regulator that restrains excessive vascular sprouting and branching. Disruption of this pathway leads to unrestrained and unproductive angiogenesis and decreased tumour growth (Thurston et al., 2007).

Several agents, including sDll4 protein fused with an Fc tag and a blocking antibody against Dll4, have been shown to reduce tumour growth in xenograft models (Noguera-Troise et al., 2006, Ridgway et al., 2006). In addition, anti-Dll4 treatment was effective against several

tumour types resistant to VEGF blockade, and co-treatment with anti-Dll4 and anti-VEGF antibodies synergistically reduced tumour growth (Ridgway et al., 2006). These studies suggest that the Dll4-Notch pathway could be a viable target for cancer therapy.

Independent of these published studies, our laboratory has conducted xenograft experiments to study the role of Dll4 in tumour angiogenesis. We overexpressed human Dll4 in five cancer cell lines, implanted them into mice and measured the effect of Dll4 overexpression on tumour growth, the tumour vasculature and Notch activation in the host. We also treated mice with inhibitors against VEGF and Notch signalling and compared their effects on Dll4-overexpressing versus control tumours. All experiments were designed by the Notch group in the laboratory, including Prof Adrian Harris, Dr Ji-Liang Li, several post-doctoral fellows and me. Animal experiments were then conducted by trained technicians. I isolated RNA from xenograft tumours and conducted real-time PCR analysis to measure Notch signalling activation in host stromal cells.

This chapter describes the tumour growth and real-time PCR data from these experiments. (Others in the Notch group have performed immunohistochemistry on tumour sections, and these results can be found in a manuscript under review.) Section 6.2 describes the generation of cell lines overexpressing Dll4. Section 6.3 describes the effect of Dll4 overexpression on xenograft tumour growth. Section 6.4 describes the effect of anti-VEGF treatment on these tumours. Section 6.5 describes the effect of combined anti-VEGF and anti-Notch treatments on these tumours.

6.2 Dll4 overexpression induced Notch signalling *in vitro*

Cancer cell lines overexpressing human Dll4 were generated using retrovirus-mediated transduction as previously described (Williams et al., 2006). Briefly, the phoenix packaging cell line was transfected with an IRES-GFP retroviral vector encoding full-length human Dll4 (Dll4) or with an empty vector (EV) as control. The culture medium of transfected phoenix cells was then used to infect a range of human (U87 glioblastoma, PC3 prostate cancer, HT1080 fibrosarcoma, MDA-MB-231 breast cancer) and mouse (B16 melanoma) cell lines.

After three infections with the viruses, Dll4 overexpression in each cell line was validated by Western blotting (Figure 6.1). For each cell line, the expression of GFP encoded by the retroviral vector was similar between Dll4- and EV-transduced cells, indicating comparable levels of viral transduction. As expected, cells infected with Dll4 viruses showed increased Dll4 expression compared with cells infected with EV viruses. However, Dll4 upregulation was much higher in U87, HT1080 and B16 cells than in PC3 and MDA-MB-231 cells. This difference may be due to lower translational efficiencies in the latter two cell lines; alternatively, post-translational modifications of the Dll4 protein in those cell lines may cause it to be degraded more rapidly.

To determine if the overexpressed Dll4 ligands were functional, we assessed Notch signalling activation in the cancer cell lines by Western blotting and real-time PCR. Protein samples were immunoblotted for cleaved N1ICD and the Notch target gene Hes1, with β-tubulin as a loading control. As shown in Figure 6.2A, in Dll4-overexpressing cells, N1ICD accumulation was increased in HT1080, MDA-MB-231 and B16 cells, and to a smaller extent in U87 cells.

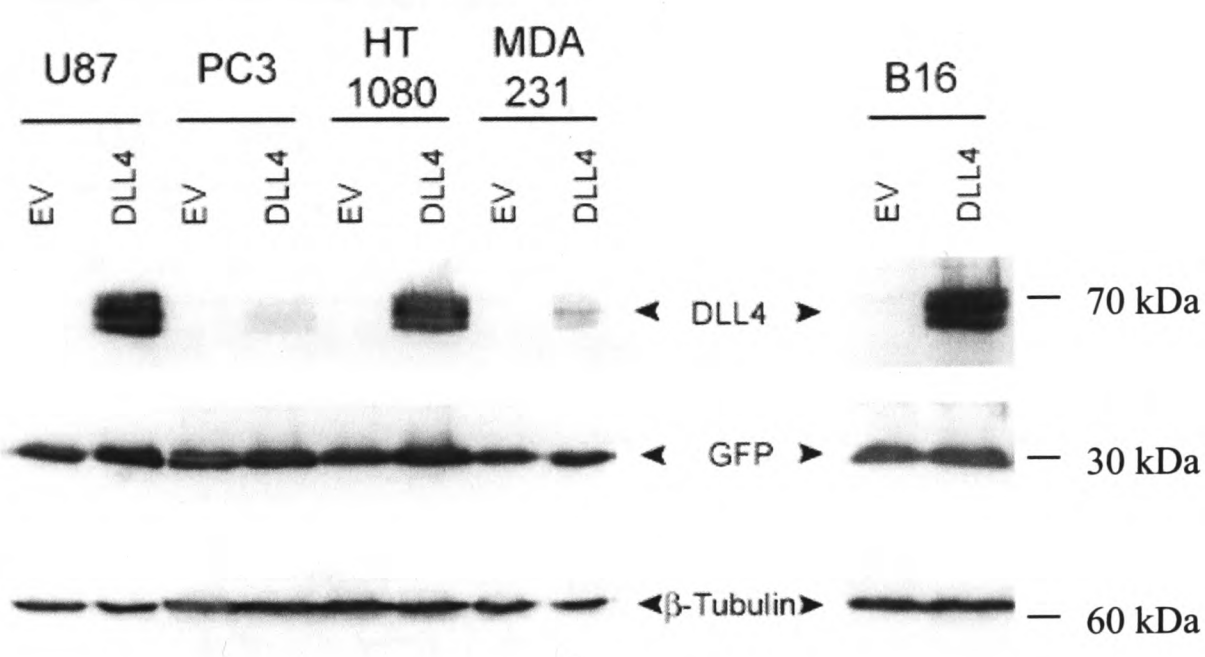


Figure 6.1. Dll4 overexpression in five cancer cell lines.
U87, PC3, HT1080, MDA-MB-231 and B16 cell lines were infected with EV control retroviruses or Dll4 retroviruses. Protein samples were isolated from each cell type, separated by SDS-PAGE and blotted with antibodies against Dll4, GFP and β-tubulin (n=2; figure courtesy of Dr Ji-Liang Li).

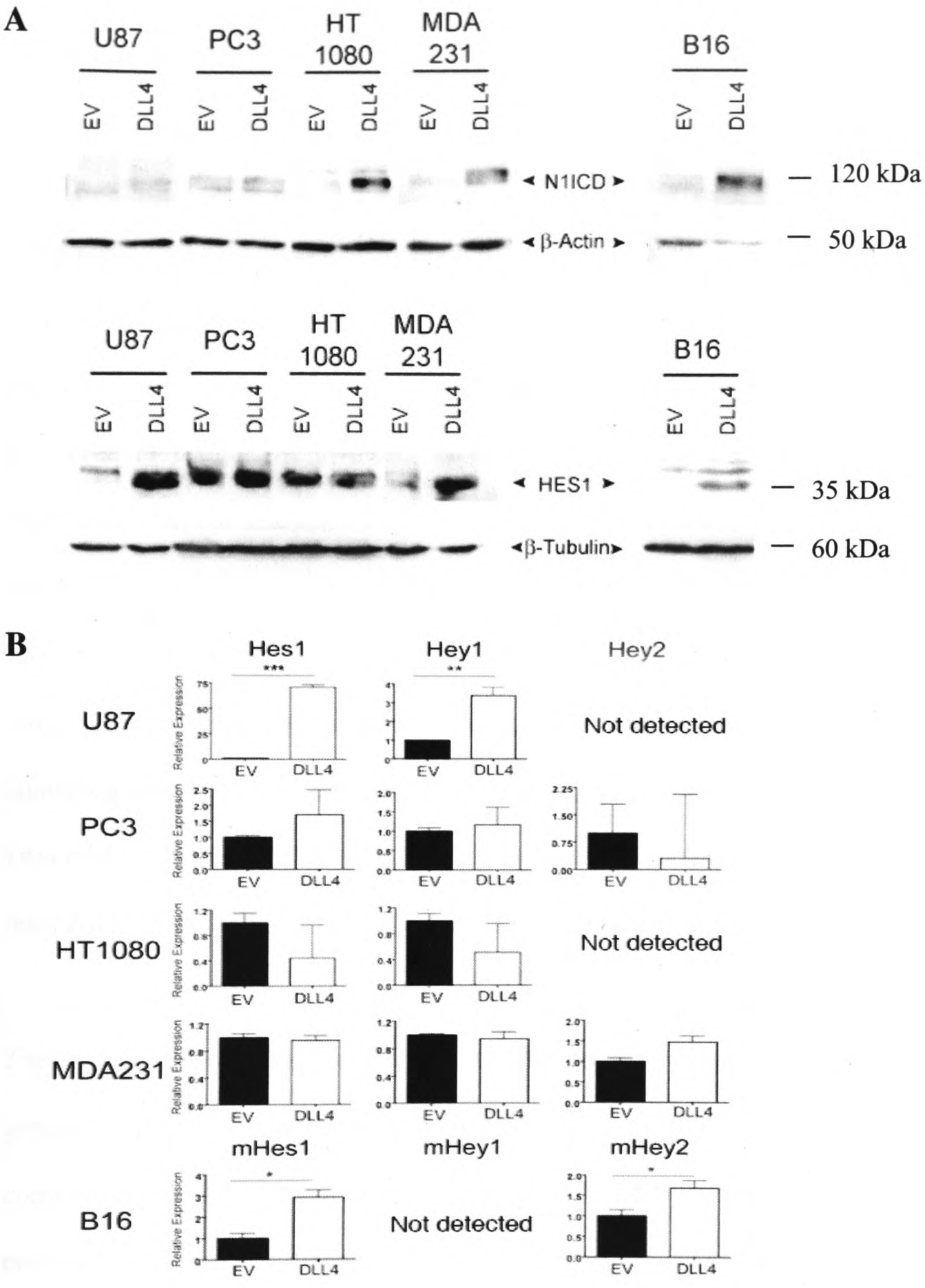


Figure 6.2. Dll4 overexpression activated Notch signalling in cancer cell lines.
(A) Protein samples were isolated from the five cell lines infected with EV or Dll4 retroviruses, and blotted with antibodies against N1ICD, Hes1 and β-tubulin (n=2; figure courtesy of Dr Ji-Liang Li). (B) RNA samples were isolated from the same cells, and real-time PCR was used to measure the expression of Hes1, Hey1 and Hey2 (*p<0.05, **p<0.01, ***p<0.001, unpaired t-test, n=3).

In addition, Hes1 expression was increased in U87, MDA-MB-231 and B16 cells overexpressing Dll4 compared with the corresponding EV control cells. Hes1 induction was not observed in PC3 or HT1080 cells overexpressing Dll4.

In parallel, total RNA was also isolated from the five cell lines and analysed by real-time PCR to measure the mRNA levels of Hes1, Hey1 and Hey2. As shown in Figure 6.2B, in U87 cells overexpressing Dll4, Hes1 was induced by 71.0-fold ($p<0.0001$, unpaired t-test), confirming protein-level results. In addition, Hey1 was induced by 3.4-fold ($p=0.0058$), but Hey2 expression was not detected in U87 cells. Similarly, in B16 cells overexpressing human Dll4, mouse Hes1 (mHes1) was induced by 2.9-fold ($p=0.010$, unpaired t-test), confirming protein-level results. In addition, mouse Hey2 (mHey2) was induced by 1.7-fold ($p=0.046$), but mouse Hey1 (mHey1) expression was not detected in B16 cells. These results indicate Notch signalling activation in these two cells lines through endogenous Notch receptors. In contrast, Dll4 overexpression did not significantly change the mRNA levels of any Notch target genes tested in PC3, HT1080 or MDA-MB-231 cells (Figure 6.2B).

The five cell lines differed in the level of Dll4 protein overexpressed, and in the downstream genes activated. These differences may reflect variable expression of Notch pathway components in different cell lines. Altogether, the combined protein- and mRNA-level results provided evidence for Notch signalling activated by Dll4 overexpression in all cell lines except PC3.

6.3 Dll4 overexpression promoted U87 and PC3 tumour growth

To assess the effect of Dll4 overexpression on tumour growth *in vivo*, the five cell lines, transduced with Dll4 or EV viruses, were subcutaneously implanted into SCID mice, five

mice per treatment group. Tumour sizes were monitored two to three times a week. After they reached the maximum permitted, the mice were sacrificed and tumours excised.

The tumour growth curves are shown in Figure 6.3. Dll4 overexpression increased the rate of tumour growth in U87 and PC3 xenografts (Figure 6.3A-B). U87 tumours overexpressing Dll4 grew more rapidly and the tumour volumes were significantly larger than EV control tumours after 10 days ($p<0.01$, unpaired t-test; Figure 6.3A). A similar but smaller effect was observed for PC3 tumours overexpressing Dll4, which were significantly larger than EV control tumours after 20 days ($p<0.01$, unpaired t-test; Figure 6.3B). To explain this effect, immunostaining showed that U87 and PC3 tumours overexpressing Dll4 had fewer vessels but larger vessel diameters. Further, these vessels were better perfused, and the tumours were less hypoxic and less necrotic, explaining their faster growth (manuscript under review). These vascular morphology results were consistent with a recently published xenograft study (Noguera-Troise et al., 2006). In that study, rat C6 gliomas overexpressing full-length Dll4 displayed fewer branches and sprouts compared with control tumours, leading to better vessel perfusion. However, no difference in tumour size was observed. This may be due to the different cancer cell lines (human U87 and PC3 vs. rat C6) used in the two studies.

In contrast to U87 and PC3 tumours but like the C6 tumours (Noguera-Troise et al., 2006), HT1080, MDA-MB-231 and B16 tumours overexpressing Dll4 did not show any change in growth rates compared with EV control tumours (Figure 6.3C-E). This is despite the observation that all three cell lines showed Notch signalling activation *in vitro* (see Figure 6.2). The lack of effect on tumour growth by Dll4 overexpression may be due to the specific gene expression and vascular morphology of these tumours.

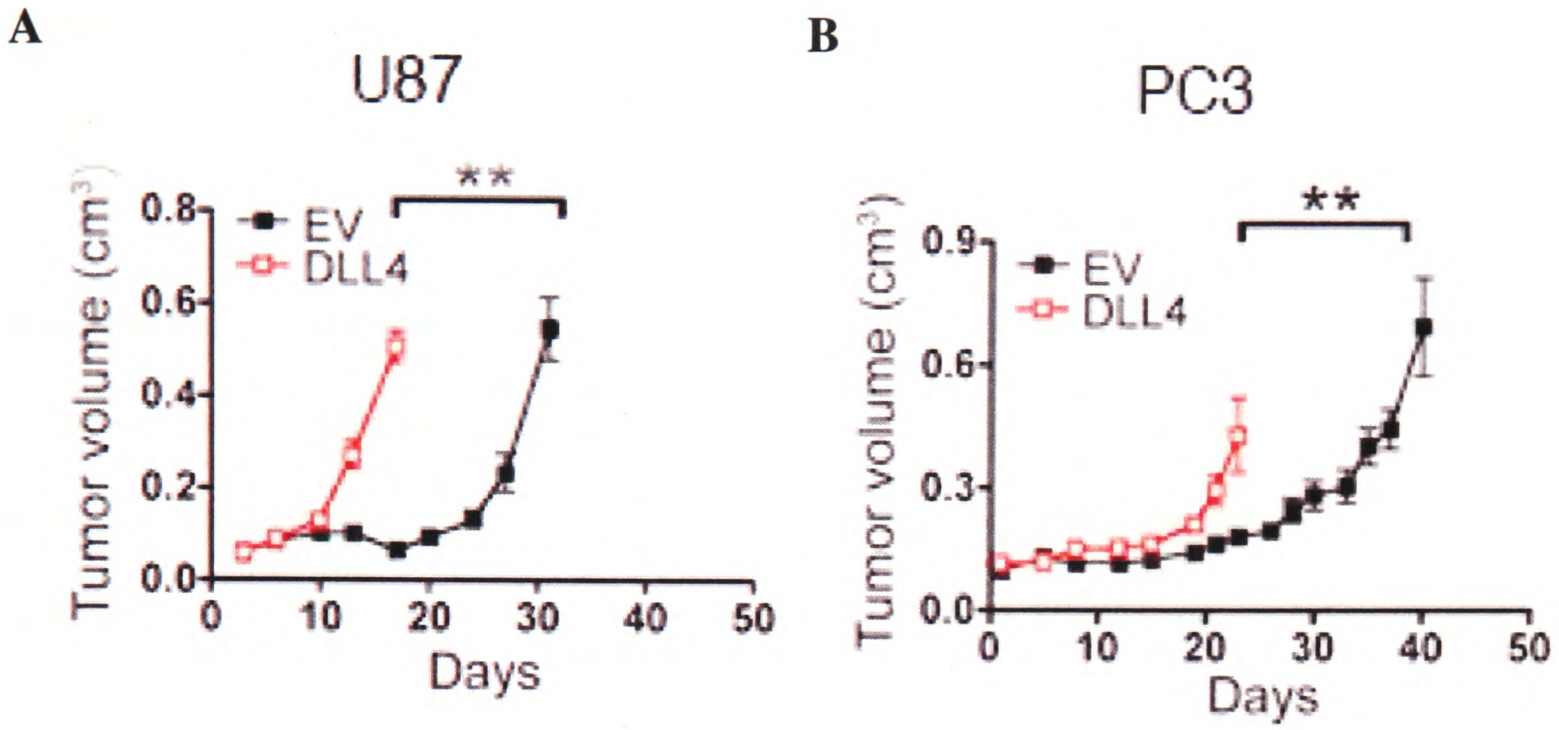


Figure 6.3. Dll4 overexpression promoted the xenograft growth of two cell lines.
Cancer cells infected with Dll4 or EV retroviruses were implanted into SCID mice on Day 0. Tumour sizes were then measured twice a week until they reached the maximum permitted. Results are the mean ± SEM from five mice per treatment group (**$p<0.01$, unpaired t-test).

To measure Notch signalling activation in the host stromal cells, RNA was isolated from U87, PC3 and B16 tumours using the FastPrep machine and TRI reagent. Real-time PCR was conducted with mouse-specific primers to measure the effect of Dll4 overexpression on Notch target genes in the host cells of these tumours.

As shown in Figure 6.4A, mHes1 expression was significantly upregulated in U87 tumours overexpressing Dll4 compared with EV control tumours ($p=0.011$, unpaired t-test), providing evidence that Dll4 expressed in cancer cells activated Notch signalling in host cells. The expression of mHey1 and mHey2 was not affected. Ephrin B2 (Efnb2) is another Notch target gene (Iso et al., 2006), and VEGFR2 is repressed by Notch activation *in vitro* (Taylor et al., 2002). However, the expression of mEfnb2 and mVEGFR2 was not significantly different with the sample size available (Figure 6.4A). Previous studies have shown that Notch signalling could activate Dll4 expression *in vitro* (see Section 4.2), suggesting that Dll4 is another Notch target gene. In U87 tumours overexpressing human Dll4, mouse Dll4 expression was not significantly changed. However, since Dll4 is predominantly expressed in the tumour vasculature (Shutter et al., 2000), the ratio of mDll4 to the vessel marker mCD31 was used to normalise Dll4 expression by the vascularity of the tumours (Patel et al., 2005). The mDll4/mCD31 ratio was significantly higher in U87 tumours overexpressing Dll4 than in control tumours ($p=0.025$, unpaired t-test; Figure 6.4A). Altogether, human Dll4 in cancer cells induced Notch signalling and Dll4 expression in the vasculature of U87 tumours, which may have accounted for the vascular morphology and faster growth rate of these tumours.

Unlike U87 tumours, PC3 tumours overexpressing Dll4 showed no change in expression of any of the Notch target genes tested, including mHes1, mHey1, mHey2, mEfnb2, mVEGFR2,

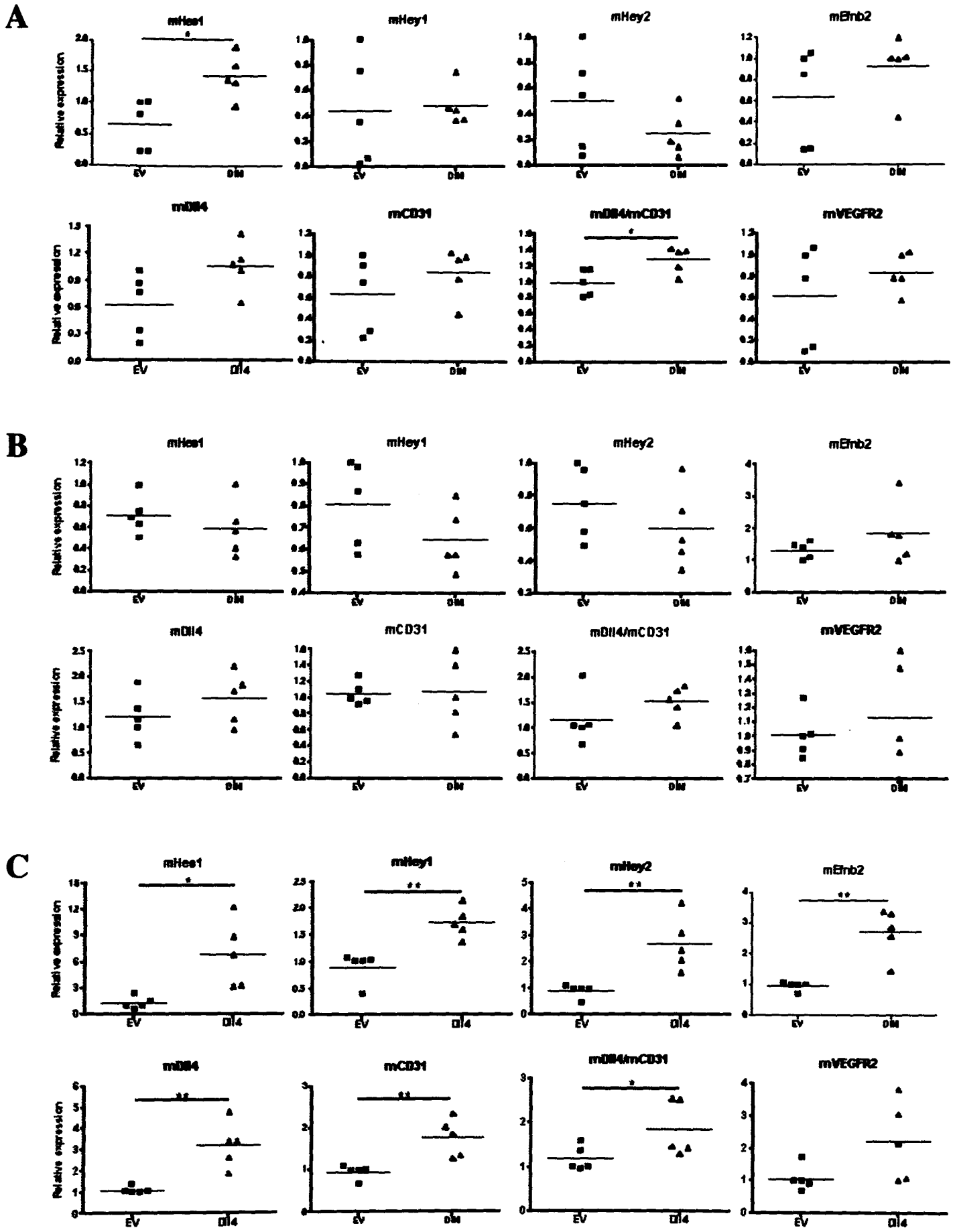


Figure 6.4. Dll4 overexpression activated Notch signalling in xenograft tumours.
Total RNA was isolated from U87 (A) and PC3 (B) xenograft tumours as well as B16 (C) allograft tumours, and real-time PCR with mouse-specific primers was used to measure Notch target gene expression in the host stromal cells (*$p<0.05$, **$p<0.01$, unpaired t-test, n=5).

mDll4 and mDll4/CD31 (Figure 6.4B). As mentioned before, Dll4 overexpression also did not induce any human Notch genes in PC3 cells *in vitro* (see Figure 6.2). Surprisingly, PC3 tumours overexpressing Dll4 grew faster *in vivo* (see Figure 6.3B). The lack of significant target gene induction may be due to the low level of Dll4 overexpression in PC3 cells (see Figure 6.1). It is also possible that Dll4 overexpression activated other Notch targets (e.g. Hes5, Hes7, HeyL) that were not measured in this experiment.

As shown in Figure 6.4C, B16 tumours overexpressing human Dll4 significantly induced almost all Notch target genes tested. These include mHes1 ($p=0.013$, unpaired t-test), mHey1 ($p=0.0019$), mHey2 ($p=0.0053$), mEfnb2 ($p=0.0012$), mDll4 ($p=0.0026$) and mDll4/mCD31 ($p=0.029$). For most of these genes, it was not possible to distinguish between expression in the implanted murine B16 cells and that in the host cells. However, mHey1 was not detected in B16 cells *in vitro* (see Figure 6.2B); therefore, its induction in the tumours probably reflected gene expression in the host stromal cells. Since B16 tumours overexpressing Dll4 did not grow faster than B16 EV control tumours *in vivo* (see Figure 6.3E), these results suggest that Notch signalling activation in the host cells was not sufficient to promote tumour growth. The cell type-specific effect of Dll4 overexpression on tumour growth needs to be further investigated.

The RNA results of U87 and B16 tumours are consistent with a recent study (Noguera-Troise et al., 2006), in which C6 tumours overexpressing human Dll4 showed increased expression of Notch target genes mouse Hey1, Hey2 and Nrarp, indicating that Dll4 overexpression activated Notch signalling in the stroma of xenograft tumours.

6.4 VEGF inhibition retarded the growth of Dll4-overexpressing tumours

U87 and PC3 xenograft tumours were studied further to determine the effect of VEGF inhibition on Dll4-overexpressing tumours. VEGF plays a key role in tumour angiogenesis, and blocking the VEGF pathway has been shown to inhibit tumour growth in a number of preclinical models (Ferrara and Kerbel, 2005). In addition, bevacizumab, a monoclonal anti-human VEGF antibody, has been successfully used in the clinic in combination with standard chemotherapy to treat several types of cancers (Jain et al., 2006).

Since the level of VEGF secretion by tumour cells affects their response to anti-VEGF treatment (Ferrara and Kerbel, 2005), I first measured the amount of VEGF protein secreted by U87 and PC3 cells under normoxia and hypoxia. VEGF secretion is up-regulated by hypoxia in numerous cell types (Ferrara et al., 2003). In the experiment, U87 and PC3 cells transduced with Dll4 or EV viruses were cultured under normoxia or 0.1% hypoxia for 16 hours, and the conditioned medium was isolated to assess the level of VEGF secretion by enzyme-linked immunosorbent assay (ELISA). Both $VEGF_{165}$ and $VEGF_{121}$, the two secreted isoforms, were detected by the assay. The amount of VEGF protein was normalised by cell number, since the two cell lines had different proliferation rates.

As shown in Figure 6.5, under normoxia, U87 cells secreted approximately 0.3 ng of VEGF per 10^6 cells (Figure 6.5A), and PC3 cells secreted approximately 0.01 ng of VEGF per 10^6 cells (Figure 6.5B). Thus, the endogenous VEGF secretion was 30-fold higher in U87 cells than in PC3 cells.

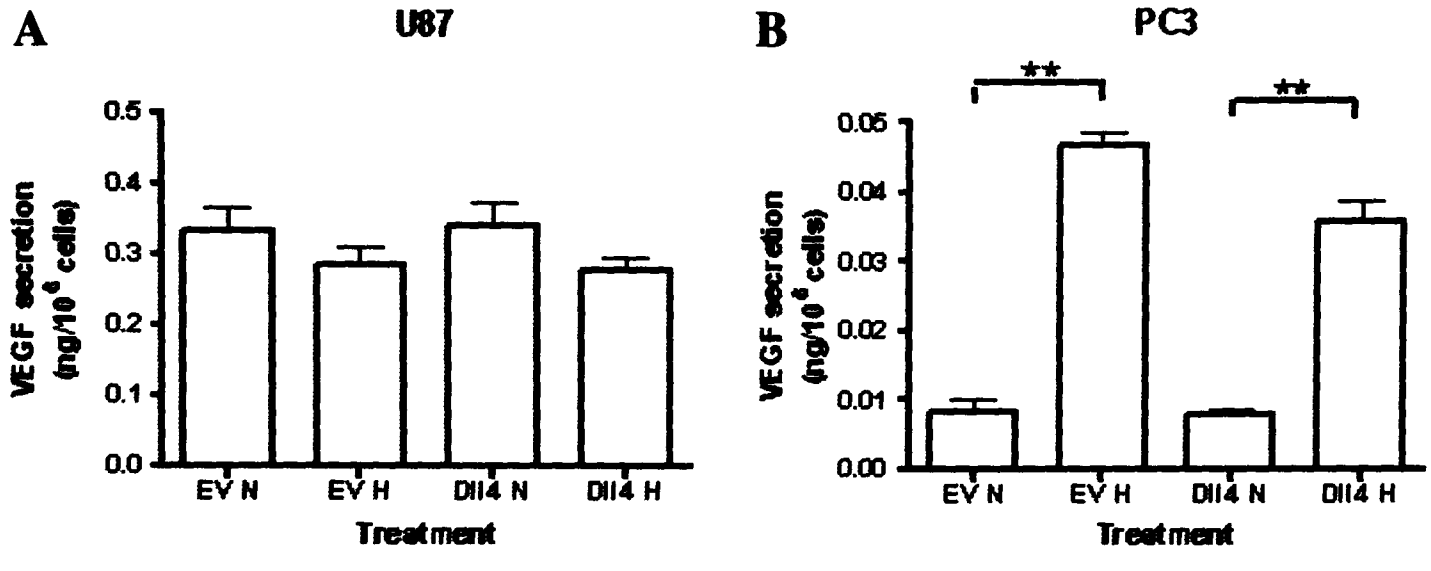


Figure 6.5. U87 cells secreted higher levels of VEGF than PC3 cells *in vitro*.
U87 (A) and PC3 (B) cells infected with Dll4 or EV retroviruses were cultured under normoxia or 0.1% hypoxia for 16 hours, and the VEGF concentration in the culture medium was measured by ELISA. VEGF concentration was then normalised by cell number (**$p<0.01$, ANOVA with Bonferroni's post-test, n=3).

Interestingly, hypoxia did not induce VEGF secretion in U87 cells, but it did induce it in PC3 cells by 5.6-fold ($p<0.01$, ANOVA with Bonferroni's post-test; Figure 6.5B). Nevertheless, the hypoxic level of VEGF secretion was still higher in U87 cells than in PC3 cells.

Dll4 overexpression did not affect VEGF secretion by either cell line, under normoxia or hypoxia. This result was expected since Dll4 is a downstream target of VEGF (see Section 4.3). No evidence has been reported that Dll4 expression regulates VEGF secretion.

Because U87 and PC3 cells secrete different levels of VEGF *in vitro*, their xenograft tumours should respond differently to anti-VEGF treatment *in vivo*. U87 and PC3 cells, transduced with Dll4 or EV viruses, were subcutaneously implanted into SCID mice. Starting from day 0 (the day of tumour implantation), bevacizumab (mAb for monoclonal antibody) or PBS was injected intraperitoneally every three days, for a total of five injections (for U87 tumours) or seven injections (for PC3 tumours). Tumours were excised after they reached the maximum size permitted.

The growth curves of U87 and PC3 tumours treated with bevacizumab are shown in Figure 6.6. Bevacizumab treatment inhibited the growth of U87 EV tumours ($p<0.01$, ANOVA with Bonferroni's post-test). In contrast, bevacizumab did not significantly affect the growth of PC3 EV tumours ($p\geq0.05$, ANOVA with Bonferroni's post-test; Figure 6.6B), even though the mice received two more injections of bevacizumab. A possible explanation is that U87 cells secreted 30 times more VEGF than PC3 cells *in vitro* (see Figure 6.5) and thus would be more sensitive to anti-VEGF treatment *in vivo*.

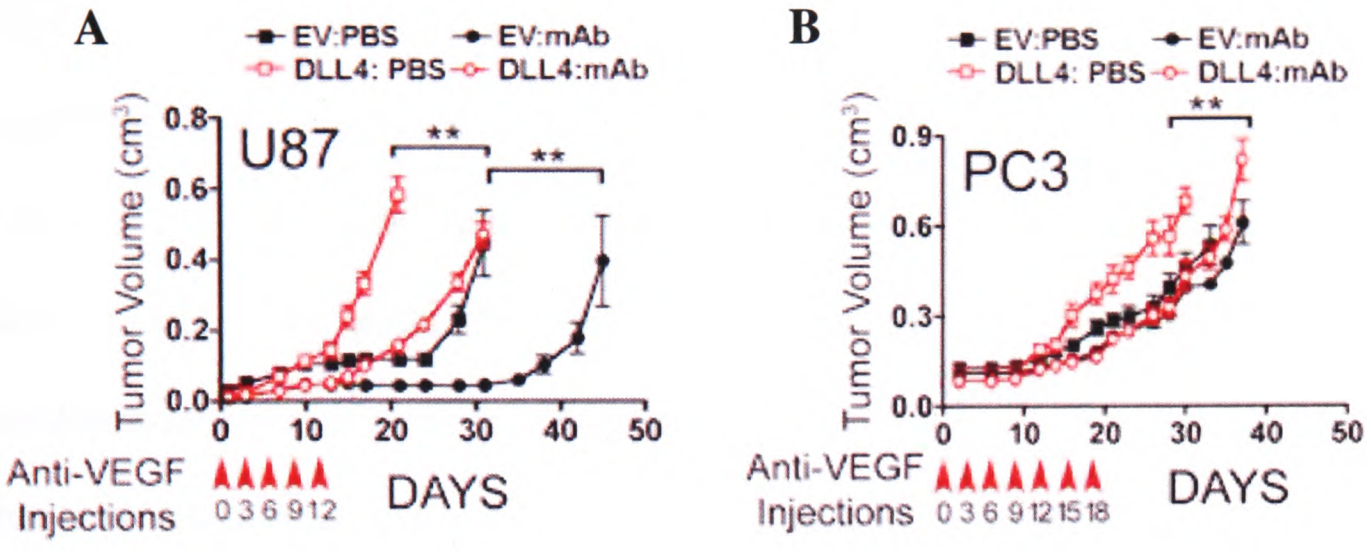


Figure 6.6. Dll4 overexpression affected tumour response to VEGF inhibition.
U87 (A) and PC3 (B) cells infected with Dll4 or EV retroviruses were implanted into SCID mice on Day 0. The mice then received intraperitoneal injections of bevacizumab (mAb) on the days indicated by red arrows. Tumour sizes were measured twice a week until they reached the maximum permitted. Results are the mean ± SEM from five mice per treatment group (**$p<0.01$, ANOVA with Bonferroni's post-test).

Compared with U87 and PC3 EV tumours, the corresponding Dll4 tumours grew faster in the absence of bevacizumab treatment, as in the previous experiment (see Figure 6.3A-B). As shown in Figure 6.6A, bevacizumab inhibited the growth of U87 tumours overexpressing Dll4 ($p<0.01$) just as it inhibited the growth of U87 EV tumours. However, after cessation of treatment, Dll4 overexpression was associated with rapid tumour regrowth. Thus, in U87 tumours the effect of anti-VEGF treatment, given during early stages of vascular development, was predominant over the effect of Dll4 overexpression. However, the predominance was reversible after cessation of treatment. Similar results were found in PC3 tumours, which were less sensitive to VEGF inhibition (Figure 6.6B).

To measure Notch activation in the host stromal cells, RNA samples from U87 tumours were analysed by real-time PCR with mouse-specific primers. As shown in Figure 6.7, mHes1, mHey1 and mDll4 expression showed significant differences among the four treatment groups ($p<0.05$, ANOVA), suggesting that anti-VEGF treatment inhibited Notch signalling in the host cells. However, Bonferroni's post-test comparing any two groups did not show statistical significance. This is probably because the tumours were harvested at the end of the experiment, up to 20 days after the end of bevacizumab treatment (see Figure 6.6A). An alternative regimen of injecting bevacizumab until the end of the experiment may produce a larger effect on Notch target genes in xenograft tumours.

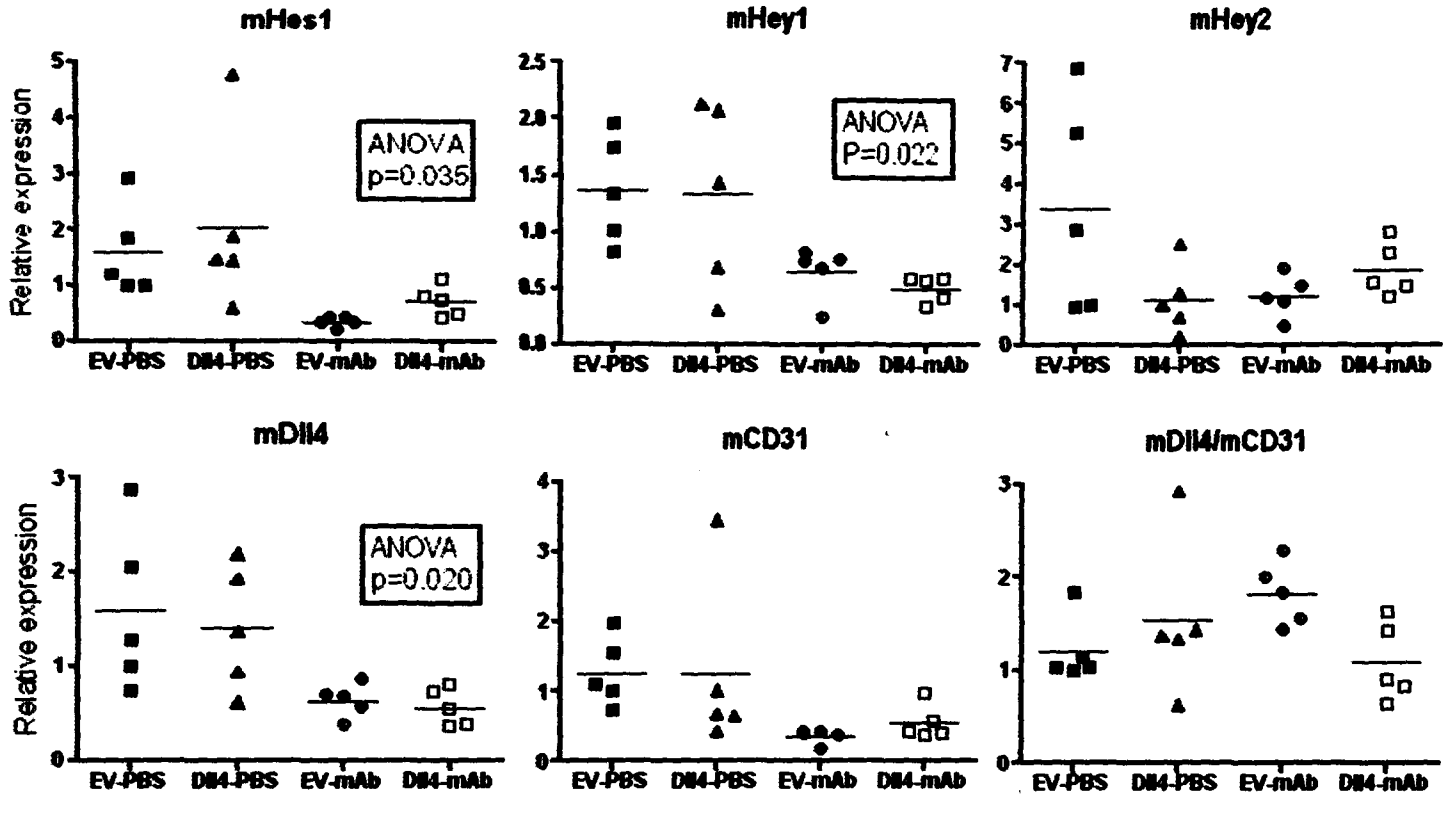


Figure 6.7. VEGF inhibition reduced Notch signalling in xenograft tumours.
Total RNA was isolated from U87 xenograft tumours in mice treated with bevacizumab (mAb), and real-time PCR with mouse-specific primers was used to measure Notch target gene expression in the host stromal cells. The data were analysed with ANOVA (n=5).

6.5 VEGF inhibition and Notch inhibition synergistically retarded the growth of Dll4-overexpressing tumours

Experiments in Section 6.3 showed that Dll4 overexpression activated Notch signalling and promoted tumour growth in U87 xenografts; therefore, blocking Notch signalling may reduce tumour growth in this model. Further, anti-Notch treatment may have a synergistic effect with anti-VEGF treatment on tumour growth. To determine the effect of these two treatments, another xenograft experiment was conducted. U87 cells transduced with Dll4 or EV viruses were subcutaneously implanted into SCID mice. Mice were injected every three days with PBS, bevacizumab, the γ-secretase inhibitor DBZ or both drugs. The dosing regimen was different from the bevacizumab-only experiment, however. Instead of starting from day 0, in this experiment drug treatment started on day 11, when the first two tumours in any treatment group reached 150 mm^3 in size. The treatment continued until the mice were sacrificed. This modified regimen was more relevant to the clinical setting and designed to suppress tumour growth with continued treatment.

The growth curves of U87 tumours treated with bevacizumab and DBZ are shown in Figure 6.8. In the absence of treatments, Dll4 tumours grew faster than EV tumours, consistent with previous experiments.

Bevacizumab treatment strongly retarded the growth of EV tumours ($p<0.01$, ANOVA with Bonferroni's post-test). This agrees with the previous experiment (see Figure 6.6A). In contrast, bevacizumab did not affect the growth rate of Dll4 tumours. This is contrary to the previous experiment, in which bevacizumab did inhibit the growth of Dll4 tumours. The

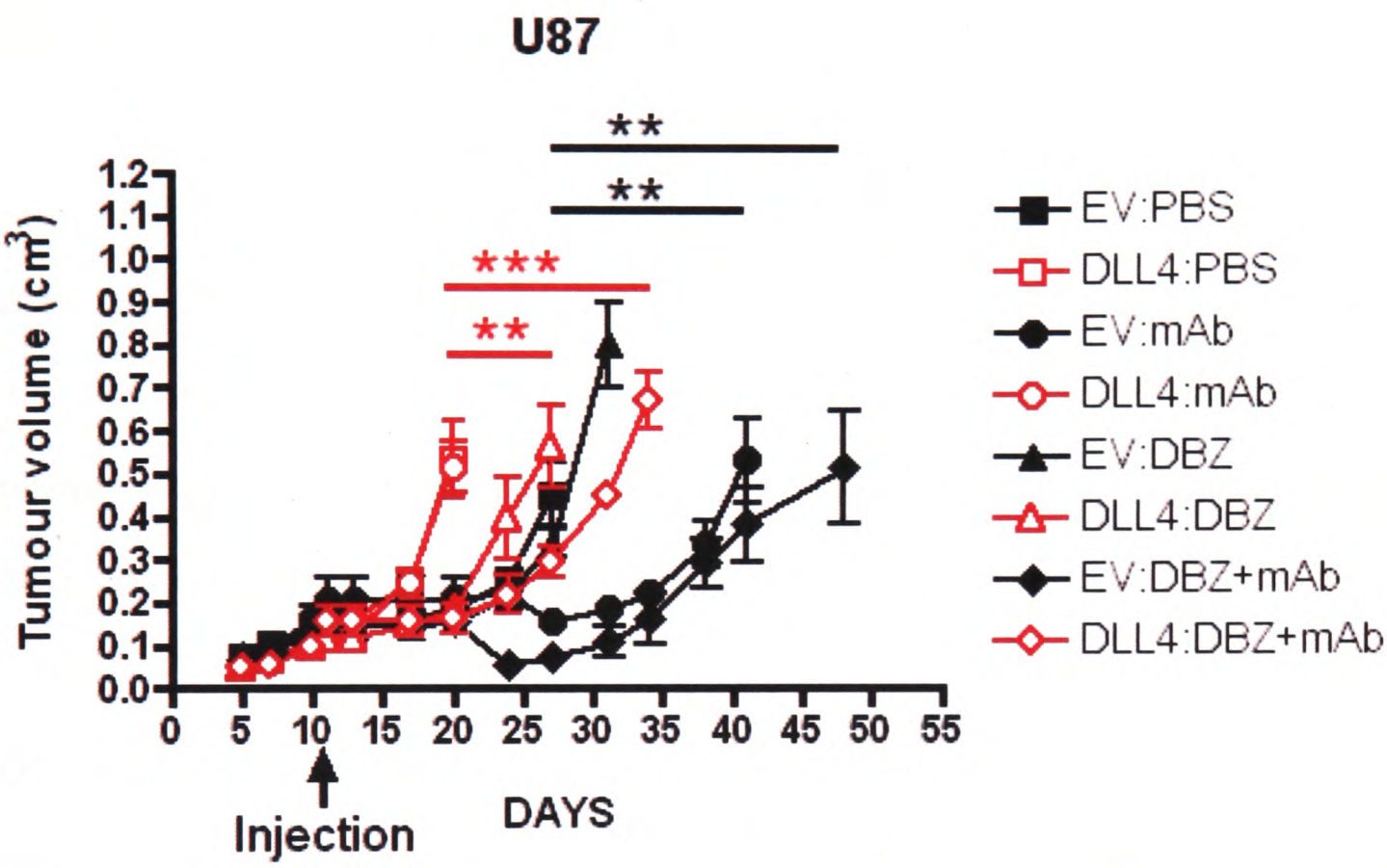


Figure 6.8. VEGF and Notch inhibition synergistically reduced the growth of Dll4-overexpressing tumours.

U87 cells infected with Dll4 or EV retroviruses were implanted into SCID mice on Day 0. Starting from Day 11 (indicated by the black arrow) until they were sacrificed, the mice received injections of bevacizumab (mAb), DBZ or both every three days. Tumour sizes were measured twice a week until they reached the maximum permitted. Results are the mean ± SEM from five mice per treatment group (**$p<0.01$, ***$p<0.001$, ANOVA with Bonferroni's post-test).

discrepancy is most likely the result of starting treatment early versus late. Dll4 tumours were responsive to anti-VEGF treatment delivered during early stages; however, after they became established (reaching 150 mm^3 in this experiment), anti-VEGF treatment lost its effectiveness. This observation is relevant to the clinical setting, as cancers expressing high levels of Dll4 may become unresponsive to VEGF inhibition during later stages.

Compared with bevacizumab treatment, DBZ treatment had different effects on tumour growth. DBZ did not affect the growth rate of EV tumours. In contrast, it significantly inhibited the growth of Dll4 tumours ($p<0.01$), which were resistant to bevacizumab treatment. The Dll4 tumours expressed higher levels of Dll4-induced Notch signalling; thus, DBZ may have a larger effect on the growth of such tumours.

Our results indicated that DBZ did not affect the growth of control U87 tumours. In comparison, several recent studies have reported that Notch inhibitors retarded tumour growth in a variety of xenograft models. Two studies used sDll4 fused with Fc (Noguera-Troise et al., 2006, Scehnet et al., 2007), and a third study used a blocking antibody against Dll4 (Ridgway et al., 2006). However, none of these studies used DBZ to block Notch signalling in xenografts, precluding direct comparison of the results. It is possible that all tumour types in the published studies expressed high levels of Notch signalling and were therefore responsive to Notch inhibition. More likely, the differences result from the different cell lines and Notch inhibitors used in our study versus published studies. Experiments are currently underway in the laboratory to test other Notch inhibitors against U87 EV tumours.

Notably, two of the published studies reported that Notch inhibitors were effective against tumours resistant to VEGF inhibition. The human HT1080 fibrosarcoma (Noguera-Troise et

al., 2006) and mouse WEHI3 leukaemia (Ridgway et al., 2006) were unresponsive to anti-VEGF treatments; however, anti-Notch treatments significantly inhibited tumour growth. These tumours behaved similarly to the U87 tumours overexpressing Dll4 in our study, which were unresponsive to bevacizumab but responsive to Notch inhibition by DBZ.

The effect of the combined bevacizumab and DBZ treatment was also assessed in our xenograft experiment (Figure 6.8). For EV tumours, the combined treatment retarded tumour growth ($p<0.01$) to a similar extent as bevacizumab alone did, confirming that DBZ did not affect the growth of EV tumours. For Dll4 tumours, the combined treatment further inhibited tumour growth ($p<0.001$) compared with DBZ alone, suggesting a synergy between anti-VEGF and anti-Notch treatments against Dll4-overexpressing tumours.

The synergy between VEGF inhibition and Notch inhibition has recently been reported. The human MV-522 lung cancer xenografts responded modestly to either anti-VEGF or anti-Dll4 antibody alone. In contrast, combined treatment with both antibodies resulted in significant inhibition of tumour growth (Ridgway et al., 2006).

According to published studies and unpublished observations from our laboratory, the synergy between anti-VEGF and anti-Notch treatments may be explained by their different effects on the tumour vasculature. Anti-VEGF treatment reduced EC density and vessel numbers, resulting in decreased tumour perfusion and growth. Anti-Notch treatment had the opposite effect on the vasculature, increasing EC density and vessel numbers. However, these vessels had smaller lumens and were poorly functional, also resulting in decreased tumour perfusion and growth (Ridgway et al., 2006, Thurston et al., 2007). The non-overlapping mechanisms of these two treatments suggest that anti-Notch therapy may be used to treat

cancers resistant to anti-VEGF therapy. Based on the results of our experiment (Figure 6.8), anti-Notch therapy may significantly increase the efficacy of anti-VEGF treatment against tumours expressing high levels of Dll4.

In addition to their effects on the vasculature, bevacizumab and DBZ also had different effects on Notch activation in the host stromal cells. Total RNA was isolated from the tumours and analysed by real-time PCR as before. As shown in Figure 6.9, mHes1, mHey1, mDll4, mCD31 and the mDll4/mCD31 ratio all showed significant differences among the eight treatment groups ($p<0.001$, ANOVA). The effect of each drug treatment on EV and Dll4 tumours is examined in detail below.

Bevacizumab treatment alone significantly reduced the expression of mHes1 in EV tumours (Figure 6.9A), and the expression of mHey1, mDll4 and mCD31 in both EV and Dll4 tumours (Figure 6.9B, D-E). All comparisons were made using ANOVA with Bonferroni's post-test. Notably, none of these comparisons was statistically significant in the previous experiment, in which U87 tumours were treated with bevacizumab (see Figure 6.7). This discrepancy is likely due to the modified dosing regimen in this experiment. Mice were treated until sacrifice, and received more doses overall, prompting a larger effect on Notch target genes in the tumours. These results suggest that anti-VEGF treatment decreased Notch signalling and Dll4 expression in xenograft tumours. The conclusion is consistent with earlier results that VEGF promoted Notch signalling and Dll4 expression *in vitro* and *in vivo* (see Section 4.3). In addition, a published study reported that treatment with a VEGF trap decreased Dll4 expression in tumour vessels (Noguera-Troise et al., 2006).

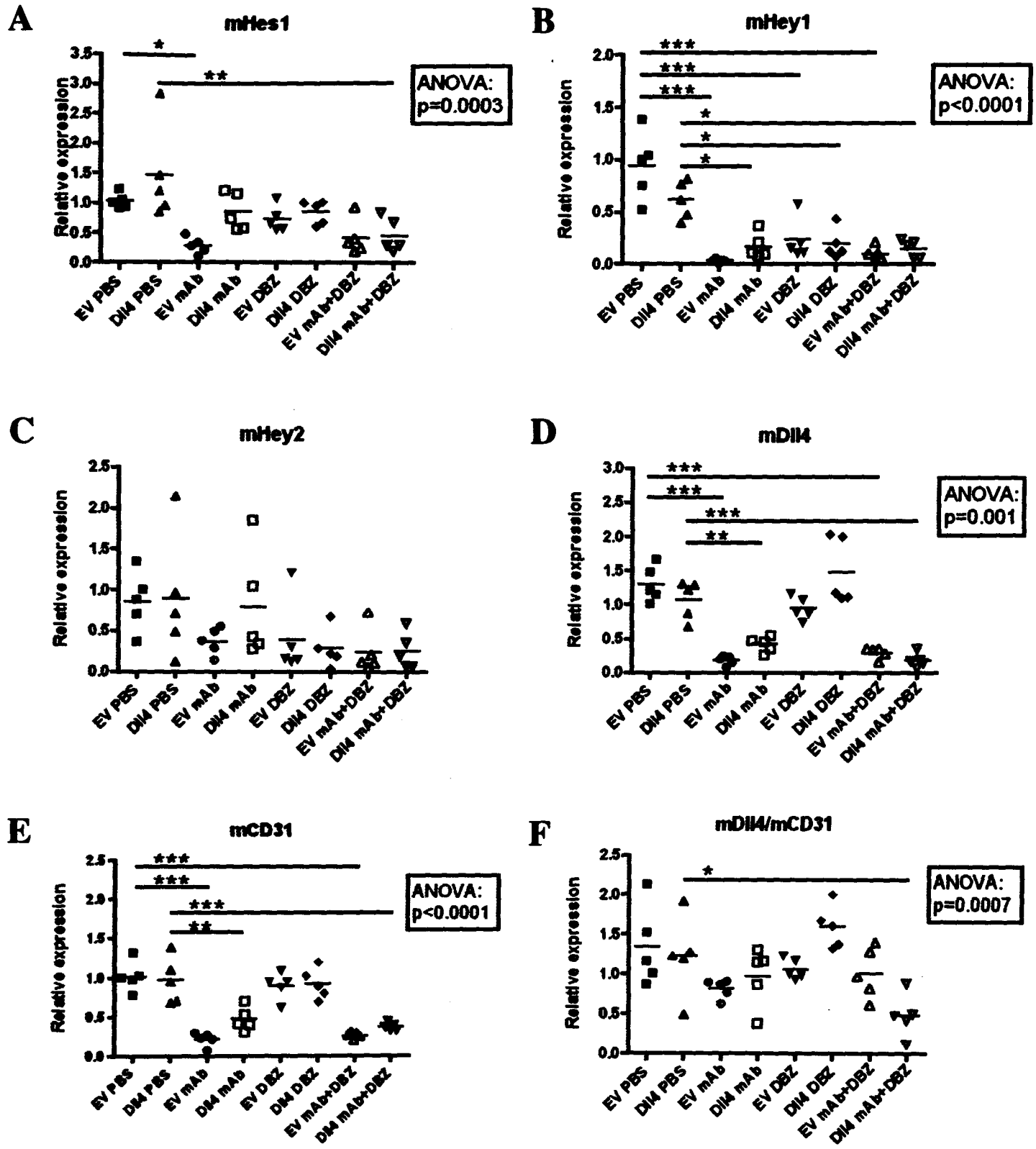


Figure 6.9. VEGF and Notch inhibition reduced Notch signalling in xenograft tumours.
Total RNA was isolated from U87 xenograft tumours in mice treated with bevacizumab (mAb), DBZ or both, and real-time PCR with mouse-specific primers was used to measure Notch target gene expression in the host stromal cells (*p<0.05, **p<0.01, ***p<0.001, ANOVA with Bonferroni's post-test, n=5).

DBZ, an inhibitor of γ-secretase cleavage, would be expected to reduce Notch target gene expression *in vivo*. Real-time PCR showed that DBZ treatment significantly reduced the expression of mHey1 in EV and Dll4 tumours (Figure 6.9B) but did not affect the expression of other genes.

The combined bevacizumab and DBZ treatment, compared with PBS, reduced the expression of mHey1, mDll4 and mCD31 in EV and Dll4 tumours (Figure 6.9B, D-E). However, the level of expression for each gene was similar to that in bevacizumab alone samples. Notably, the combined treatment significantly reduced mHes1 expression and the mDll4/mCD31 ratio in Dll4 tumours, while bevacizumab alone did not (Figure 6.9A, F). This result suggests that anti-VEGF and anti-Notch treatments may synergistically repress mHes1 and mDll4 expression in the vasculature of Dll4-overexpressing tumours.

Altogether, the real-time PCR analysis showed that bevacizumab alone reduced the expression of multiple Notch target genes in the host stromal cells, while DBZ alone reduced the expression of mHey1. The combined treatment synergistically reduced host Notch signalling and Dll4 expression in Dll4-overexpressing tumours. This result may help explain how bevacizumab and DBZ synergistically retarded the growth of Dll4-overexpressing tumours (see Figure 6.8).

6.6 Summary

Experiments presented in this chapter examined the effect of Dll4 overexpression on tumour growth, and the effect of anti-VEGF and anti-Notch treatments on EV control and Dll4-overexpressing tumours.

Human full-length Dll4 was overexpressed by retroviral transduction in five cell lines: U87, PC3, HT1080, MDA-MB-231 and B16. Western blotting and real-time PCR showed evidence of Notch signalling activation in all cell lines except PC3. The five cell lines, transduced with Dll4 or EV viruses, were then implanted into mice. Among the xenografts, U87 and PC3 tumours overexpressing Dll4 showed significantly faster growth than the corresponding EV control tumours. Real-time PCR analysis also showed that Dll4 overexpression induced host Notch signalling in U87 but not PC3 tumours. It is possible that Dll4 also induced Notch signalling in PC3 tumours, but the effect was not detected in this experiment.

The effect of VEGF inhibition on Dll4-overexpressing tumours was then examined. U87 cells secreted 30 times more VEGF than PC3 cells *in vitro*. This may explain why bevacizumab was more effective against U87 EV tumours than it was against PC3 EV tumours. Bevacizumab treatment, delivered from day 0 for five doses, also inhibited the growth of U87 tumours overexpressing Dll4. However, after cessation of treatment, Dll4 tumours regrew rapidly. In addition, bevacizumab seemed to reduce the expression of Notch target genes in U87 tumours. These results suggest that VEGF inhibition was predominant over the effect of Dll4 overexpression on tumour growth, but the predominance was reversible after cessation of treatment.

The effect of combined anti-VEGF and anti-Notch treatment was then studied in U87 xenografts. In EV tumours, bevacizumab significantly inhibited tumour growth but DBZ had no effect. In contrast, bevacizumab did not inhibit the growth of Dll4 tumours after they became established, but DBZ did inhibit the growth of these tumours. The combined treatment synergistically inhibited the growth of Dll4-overexpressing tumours. The combined treatment also synergistically inhibited mHes1 and mDll4/mCD31 levels in the stroma of

these tumours. The synergy may be due to the different effects of these two treatments on the tumour vasculature. A detailed analysis of the vessels of these tumours still needs to be conducted. Altogether, anti-Notch treatment may prove effective against tumours resistant to anti-VEGF treatment, especially if these tumours express high levels of Dll4.

CHAPTER SEVEN

Discussions and Conclusions

7.1 Summary

Notch signalling is an evolutionarily conserved pathway that plays an important role in numerous cancer types (Radtke and Raj, 2003, Leong and Karsan, 2006). Recently, the discovery and investigation of Dll4, a Notch ligand with predominantly endothelial expression, have shed light on the role of Notch signalling in both physiological and tumour angiogenesis. The expression level of Dll4 is crucial for angiogenesis *in vitro* and *in vivo*. Normally Dll4-Notch signalling functions downstream of VEGF to limit excessive branching and sprouting; disrupting this pathway could lead to unproductive angiogenesis and reduced tumour growth (Rehman and Wang, 2006, Thurston et al., 2007).

Experiments presented in this thesis have explored the regulation and function of Dll4-Notch signalling in angiogenesis and tumourigenesis. Chapter 3 focused on the functional crosstalk between Dll4-Notch signalling and hypoxia signalling. Chapter 4 investigated the regulation of Dll4 expression in endothelial cells, by Notch, VEGF and hypoxia pathways. Chapter 5 built upon the results of Chapter 4 and examined Dll4 regulation in endothelial cells by co-culturing with cancer cells, a setting relevant to tumour angiogenesis. Finally, Chapter 6 extended the findings of Chapter 5 *in vivo* and studied how cancer cells overexpressing Dll4 could signal to endothelial cells and affect tumour growth. This chapter discusses the overall themes of the thesis and lays out plans for future work.

7.2 Functional crosstalk between Notch and hypoxia pathways

The interaction of Notch and hypoxia pathways is a key theme of this thesis. Like Notch signalling, hypoxia signalling is a key regulator of tumour growth (Harris, 2002). A number of studies have demonstrated that hypoxia up-regulates Notch ligand Dll4 in endothelial cells (Mailhos et al., 2001, Patel et al., 2005) and promotes Notch signalling in stem cells (Gustafsson et al., 2005) and cancer cells (Jogi et al., 2002), providing the impetus for this research. The Notch-hypoxia crosstalk was explored in both HUVECs (Section 3.2 and 4.4) and the MCF7 breast cancer cell line (Section 3.3).

In HUVECs, the level of Dll4-induced Notch signalling was modulated to determine its effect on hypoxia-regulated genes. Dll4 knockdown did not have any effect on hypoxic induction. In contrast, Dll4 overexpression repressed the induction of four hypoxia-regulated genes, and the repression was blocked by DAPT treatment, suggesting that it was Notch-dependent.

The different effects of Dll4 knockdown versus Dll4 overexpression on hypoxic induction may be due to the differential regulation of Notch target gene Hey2. Dll4 knockdown did not affect Hey2 expression, whereas Dll4 overexpression induced Hey2 expression. Results presented in Section 3.2 suggest that Hey2 acted downstream of Dll4 overexpression to repress hypoxic induction, since the repression was blocked by Hey2 siRNA just as it was blocked by DAPT treatment.

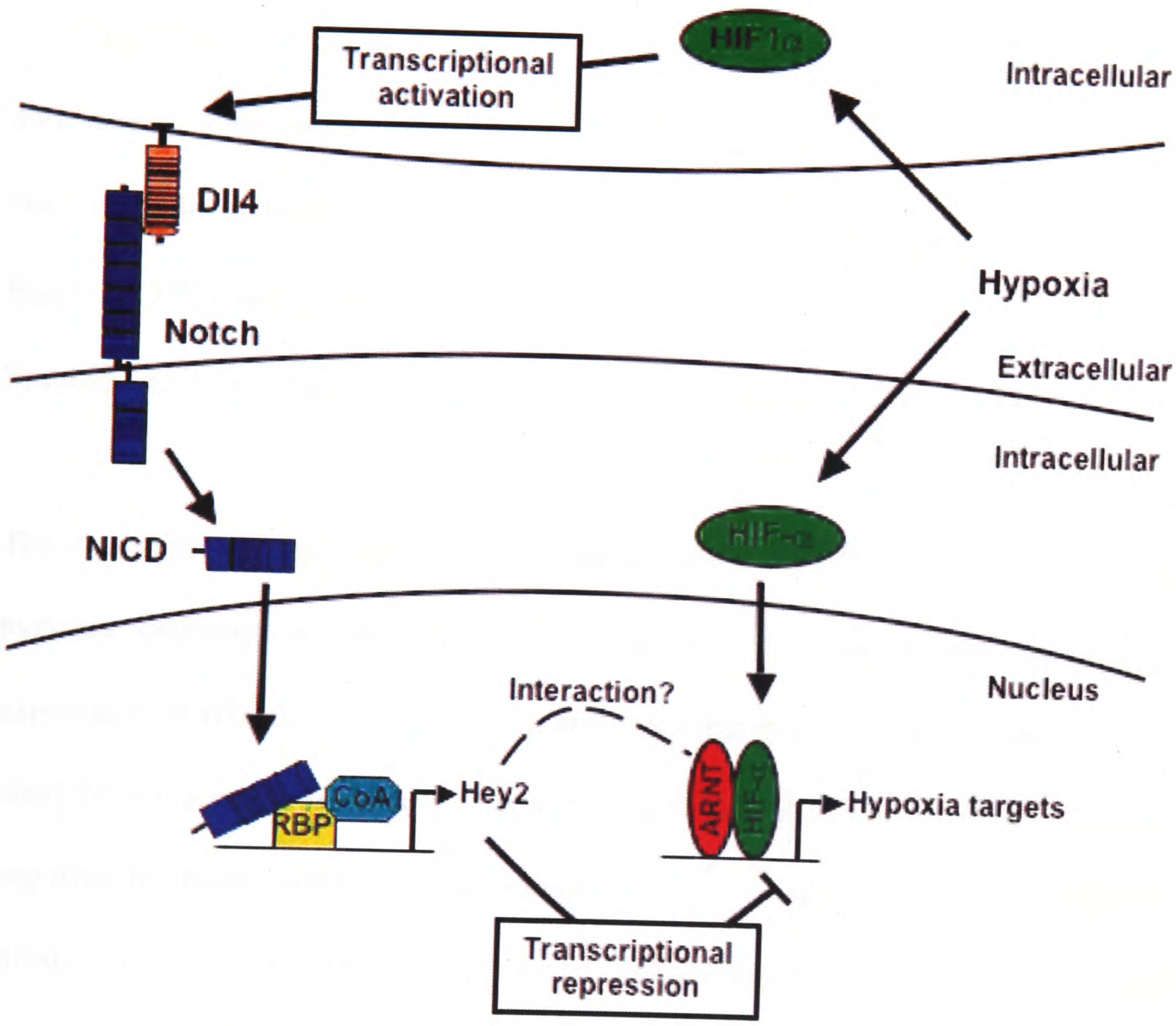


Figure 7.1. Notch-hypoxia signalling crosstalk in HUVECs.

For future experiments, it will be interesting to explore the mechanism of interaction between Hey2 and the HIF pathway (Figure 7.1). Previous research suggested that Hey2 interacted with ARNT, preventing the binding of HIF2α-ARNT complex to the HRE and impairing HIF2-dependent induction (Chin et al., 2000). Since both HIF1α and HIF2α require ARNT for signalling, it is likely that Hey2 affects HIF1-dependent induction via a similar mechanism. Chromatin immunoprecipitation (ChIP) will be used to measure the effect of Hey2 on HIF1α binding to HREs. Luciferase assays will be used to measure the effect of Hey2 on HIF1-dependent transcription. The hypothesis is that Hey2 would inhibit HIF1α binding and thus reduce HIF1-dependent transcription.

The function of this negative crosstalk between the Dll4-Notch-Hey2 pathway and the hypoxia pathway should also be investigated. Considering that hypoxia induced Dll4 expression in HUVECs (Section 4.4), and that Dll4 overexpression repressed the induction of other hypoxia-regulated genes, it is tempting to hypothesize that Dll4-Notch-Hey2 acts as a negative feedback mechanism to prevent excessive hypoxic induction (Figure 7.1). This is similar to the model proposed by a recent publication (Diez et al., 2007). To further test this model, Hey2 will be overexpressed in HUVECs to see whether it represses hypoxic induction as Dll4 does. This negative feedback model also has implications for tumourigenesis. Since Dll4-Notch signalling is involved in tumour angiogenesis and therefore re-oxygenation of hypoxic tissues, it may also modulate gene activation in tumours in response to hypoxia.

In the breast cancer cell line MCF7, hypoxia treatment induced the expression of Hey1 and Jag2 via HIF1. The hypoxic induction of Hey1 was blocked by DAPT, suggesting that it was

Notch-dependent. Moreover, rhDll4-induced Notch activation further induced Hey1 expression under hypoxia. In contrast, the hypoxic induction of Jag2 was not affected by DAPT or rhDll4. The likely explanation is that Jag2 is not a Notch target gene like Hey1.

The Notch-hypoxia synergy in inducing Hey1 expression may have several possible mechanisms (Figure 7.2). First, hypoxia may promote Notch cleavage, either by inducing Jag2 expression or by activating γ-secretase activity directly (Wang et al., 2006). Western blotting showed that hypoxia did not promote Notch1 cleavage, but other Notch receptors may be involved. Alternatively, hypoxia may increase the stability of NICD. This can be tested by a pulse-chase experiment that radioactively labels NICD. In addition, HIF1α may also interact with NICD at RBP-jκ binding sites to enhance Hey1 transcription. The interaction can be tested by co-immunoprecipitation and ChIP assays, and the effect of HIF1α on Hey1 transcription can be tested by luciferase assays. Indeed, one study reported that hypoxia promoted Notch signalling in neural stem cells and muscle precursors via the latter two mechanisms (Gustafsson et al., 2005).

The function of the hypoxic induction of Hey1 and Jag2 also warrants further investigation. Since Hey1 is a transcriptional repressor, it may function to limit the transcription of hypoxia-regulated genes in MCF7 cells, just as Hey2 does in HUVECs. To test this hypothesis, Hey1 expression will be knocked down by siRNA to measure its effect on hypoxic induction. Alternatively, Hey1 may help maintain an undifferentiated state under hypoxia. This can be tested in a mammosphere model with MCF7 cells (Dontu et al., 2004).

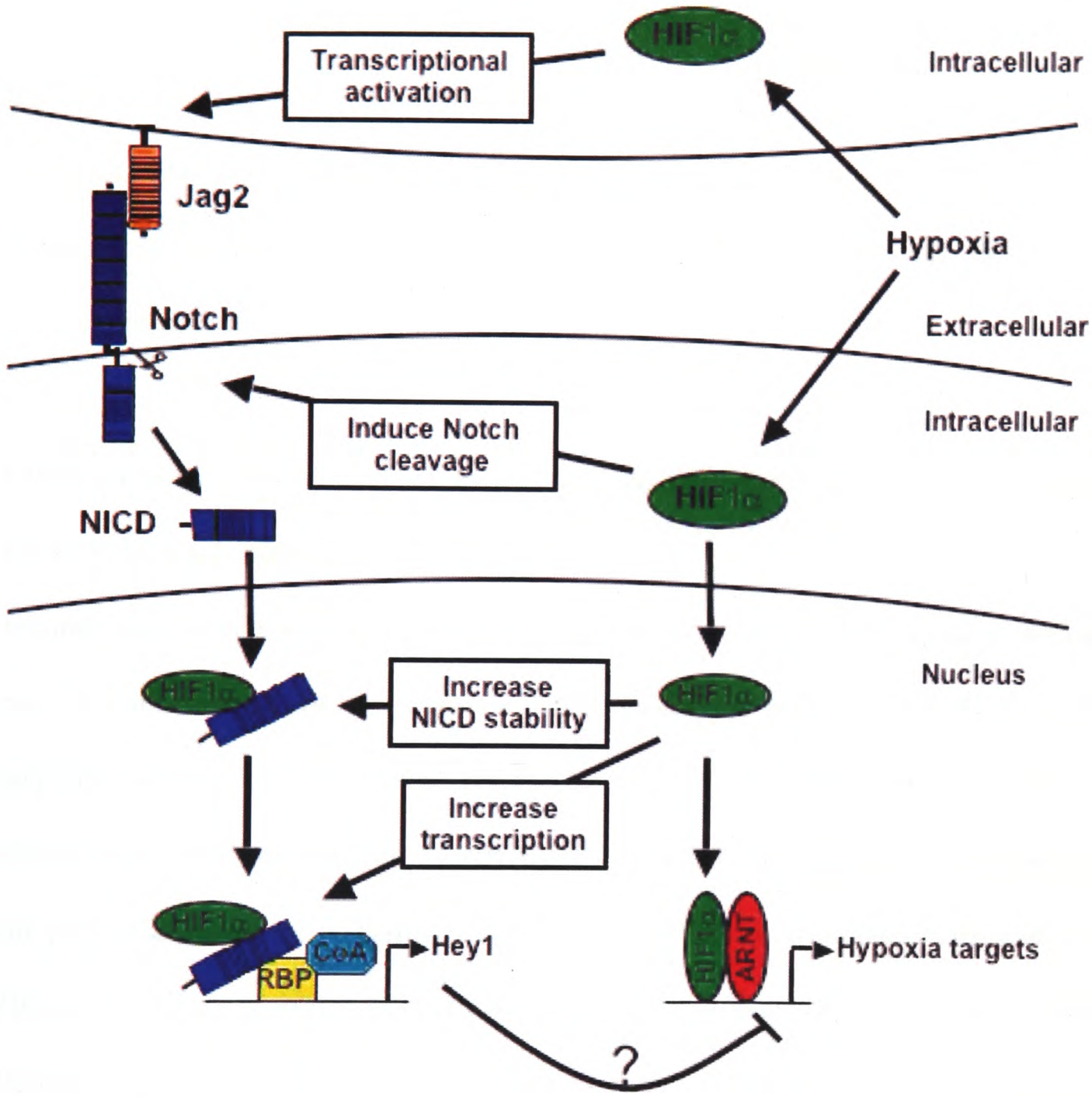


Figure 7.2. Notch-hypoxia signalling crosstalk in MCF7 cells.

7.3 Regulation of Dll4 expression by Notch, VEGF and hypoxia signalling

Dll4 is predominantly expressed in endothelial cells (Shutter et al., 2000) and plays a key role in both physiological and tumour angiogenesis (Sainson and Harris, 2007). Dll4 expression is tightly regulated *in vitro* (Patel et al., 2005, Williams et al., 2006), and is haploinsufficient for developmental angiogenesis *in vivo* (Krebs et al., 2004, Duarte et al., 2004, Gale et al., 2004). Experiments in Chapter 4 investigated the regulation of Dll4 expression in HUVECs by several pathways important in angiogenesis.

Dll4 expression was induced by Notch signalling activated by N1ICD overexpression, human Dll4 or rat Jag1 stimulation or higher cell densities. Interestingly, rat Jag1, in the form of recombinant protein or overexpressed in the mouse L cells, could activate the human Notch receptor and induce Dll4 expression in HUVECs. This is likely due to the high degree of sequence identity (96%) between rat and human Jag1 proteins. However, rrJag1 was not as effective as rhDll4 in inducing Notch signalling and Dll4 expression, suggesting that Dll4 is the preferred ligand for activating Notch in HUVECs. This is in agreement with a recent study (Iso et al., 2006), in which Dll4 but not Jag1 induced ephrin B2 expression in HUVECs. The ligand specificity may be due to the different Notch receptors activated. Dll4 activates Notch1 and Notch4 in endothelial cells (Shutter et al., 2000), and future experiments will identify the Notch receptors activated by Jag1 and other ligands. The differential activation of downstream targets will also be examined.

Another intriguing observation was that exogenous rhDll4 induced more endogenous Dll4 expression. The Dll4 ligands could then activate Notch signalling even further, creating a positive feedback loop. It will be interesting to investigate how this loop is limited to prevent excessive Notch signalling. The time-course expression of Notch antagonists such as Numb (Pece et al., 2004) and Nrarp (Pirot et al., 2004) in cells cultured on rhDll4-coated plats will be measured and compared with the time-course expression of Dll4. Notably, Nrarp is another Notch target gene and may serve as a negative feedback to limit Notch signalling (Pirot et al., 2004).

The mechanism of Notch-dependent activation of Dll4 expression should also be explored. The time-course of Dll4 induction suggests that Dll4 is a direct target of Notch signalling. To confirm the hypothesis, HUVECs will be cultured on rhDll4-coated plates in the presence of cycloheximide, an inhibitor of *de novo* protein synthesis. Dll4 mRNA should still be induced by Notch signalling. In addition, the Dll4 promoter would be expected to contain RBP-jκ binding sites. Promoter studies conducted so far suggest that the 500 bp proximal promoter was still inducible by rhDll4, indicating that an RBP-jκ site could be located within this short fragment. Future experiments will identify and mutate potential RBP-jκ binding sites to confirm direct Notch regulation of Dll4 transcription.

In addition to Notch signalling, Dll4 expression was also induced by VEGF signalling. $VEGF_{165}$ treatment induced Notch1 cleavage after 10 minutes, and also induced Hey1, Hey2 and Dll4 expression; further, the inductions were γ-secretase-dependent. These results suggest that $VEGF_{165}$ induced Notch signalling rapidly, possibly by promoting γ-secretase cleavage,

in agreement with a recent study (Takeshita et al., 2007). Both Hey1 and Hey2 were rapidly induced by $VEGF_{165}$; however, the induction of Dll4 was more gradual. This could be explained by the Dll4-Notch loop. Dll4 induction would activate Notch signalling further, which would induce more Dll4 expression. In support of this hypothesis, after 16 hours of $VEGF_{165}$ treatment there was a second wave of Notch1 cleavage. This was probably activated by Dll4 induction.

The effect of various VEGF isoforms on Notch signalling and Dll4 expression was also examined. Mouse $VEGF_{120}$ does not bind heparin and is freely diffusible, while $VEGF_{188}$ binds heparin with high affinity and is sequestered in the ECM. $VEGF_{164}$ has intermediary properties (Ferrara et al., 2003). Using mouse fibrosarcoma tumours expressing single isoforms, I showed that murine $VEGF_{164}$ was the most effective isoform in inducing Notch signalling and Dll4 expression in the tumour vasculature.

To date, few published studies have measured the effect of VEGF isoforms on Notch signalling and Dll4 expression. One study infected endothelial cells with an adenovirus expressing human $VEGF_{121}$, and treated other cells with $VEGF_{165}$ protein. Dll4 expression was induced in both cases, but the results were incomparable (Liu et al., 2003). Additional studies are needed to address this question. For example, $VEGF_{121}$ and $VEGF_{165}$ proteins can be added to the culture medium ($VEGF_{189}$ protein is not commercially available since it is sequestered in the ECM). The three isoforms can also be expressed in adenoviruses used to infect endothelial cells. Alternatively, fibrosarcoma cell lines expressing single VEGF isoforms, available from the Tozer laboratory, can be used to co-culture with endothelial cells.

The *in vivo* studies should be repeated with larger sample sizes to achieve higher statistical power. Additionally, the effects of VEGF isoforms on tumour growth and vasculature should be assessed.

Yet another inducer of Dll4 expression was hypoxia. Hypoxia induced N1ICD cleavage and Dll4 expression in a γ-secretase-dependent manner. This suggests that hypoxia induced Dll4 expression via Notch signalling. However, hypoxia also repressed Hey1 and Hey2 expression, and the mechanism for the repression remains to be elucidated. Future experiments will involve cloning the Hey1 and Hey2 promoter and analysing their response to hypoxia in various cell types.

The mechanism of Dll4 induction by hypoxia should also be investigated. Hypoxia may induce Dll4 by directly activating Notch signalling, or by activating Notch signalling via the VEGF pathway; however, direct binding of the HIF proteins to HRE within the Dll4 promoter cannot be ruled out. Promoter studies in this thesis demonstrated that a 500 bp promoter fragment devoid of any known HRE sequence was still induced by hypoxia, in agreement with a recent publication (Diez et al., 2007). Future studies will involve mutating RBP-jκ binding sites within the 500 bp promoter. The hypothesis is that Dll4 induction by hypoxia will be impaired since it depends on Notch signalling.

7.4 Regulation of Dll4 expression by co-culturing with cancer cells

Maintaining Dll4-Notch signalling is important not only for physiological angiogenesis but also for tumour angiogenesis. We have previously shown that Dll4 expression is up-regulated in the tumour vasculature (Mailhos et al., 2001, Patel et al., 2005, Patel et al., 2006). Blocking this upregulation may be crucial to reducing tumour growth, as recent studies have demonstrated (Ridgway et al., 2006, Noguera-Troise et al., 2006, Scehnet et al., 2007). However, it is not clear how tumour cells affect Dll4 expression in the neighbouring endothelial cells. To help answer this question, experiments in Chapter 5 investigated the regulation of Dll4 expression in HUVECs by co-culturing with cancer cells *in vitro*.

Co-culturing with the mouse melanoma cell line B16 strongly induced Dll4 and Hey1 expression in HUVECs, and the induction was higher at higher B16: HUVEC ratios. Notably, the γ-secretase inhibitor DBZ partially inhibited Dll4 induction at high concentrations, while it completed blocked Hey1 induction. This suggests that B16 cells induced Dll4 expression in HUVECs via Notch-dependent and Notch-independent mechanisms.

Co-culturing with human breast cancer cell lines also induced Dll4 expression in HUVECs. Since Dll4 was predominantly expressed in HUVECs, its expression was normalised by CD31 expression to account for the different HUVEC numbers in the samples. Co-culturing with MCF7 and SKBR3 cell lines induced Dll4/CD31 significantly, and the induction was completely blocked by DBZ treatment. This suggests that the cell lines induced Dll4 expression in HUVECs via Notch signalling. Another cell line, T47D, induced Dll4/CD31 at lower T47D: HUVEC ratios only. It is possible that T47D cells express higher levels of Notch

ligands than the other two cell lines; thus, the optimal Notch ligand: receptor ratio occurs with fewer T47D cells relative to HUVECs.

Notably, the Dll4 fold induction was much larger when co-culturing with B16 cells than with breast cancer cell lines. Partly this was due to the Notch-independent mechanism of Dll4 induction by B16 cells. In addition, the cell lines may have different patterns of Notch ligand expression. The next step will be to profile Notch ligand expression in these cell lines. In addition, it will be interesting to study Notch signalling activation in HUVECs co-cultured with human cancer cell lines. This experiment will require separating HUVECs from cancer cells after co-culture, since the Notch receptors and target genes are expressed in both cell types.

Previously, cancer-endothelial cell crosstalk via Notch signalling has been reported in the literature (Zeng et al., 2005). Jag1 ligand expressed in head and neck cancer cells induced Notch signalling in neighbouring ECs, and promoted angiogenesis *in vitro* and *in vivo*. The studies in this chapter can be extended by investigating how the increased Dll4 expression in HUVECs affects angiogenesis. For example, HUVECs can be co-cultured with cancer cells on Matrigel to measure tube formation, as used in the study cited (Zeng et al., 2005).

In addition to Notch-dependent induction, the Notch-independent induction of Dll4 by B16 cells also awaits further investigation. Preliminary studies showed that B16-conditioned medium did not induce Dll4 in HUVECs; however, B16 cells did induce Dll4 in HUVECs through a Transwell insert. This suggests that labile soluble factors were responsible for the

induction. Future studies will determine the concentration and stability of candidate molecules such as VEGF, bFGF and interleukin-6 in the co-culture medium. In addition, the soluble factors may be isolated using gel filtration chromatography and analysed using mass spectrometry.

7.5 Effect of Dll4 overexpression on tumour growth *in vivo*

Experiments in Chapter 5 showed that cancer cells induced Dll4 expression in endothelial cells *in vitro*. The increased Dll4 levels may in turn affect tumour angiogenesis and growth *in vivo*. Experiments in Chapter 6 investigated this hypothesis by overexpressing Dll4 in xenograft models.

Human full-length Dll4 was overexpressed in five cancer cell lines, U87, PC3, HT1080, MDA-MB-231 and B16, which were then implanted into mice. U87 tumours overexpressing Dll4 grew faster and activated Notch signalling in the host stromal cells. In PC3 tumours, Dll4 overexpression also promoted tumour growth, despite no evidence of Notch signalling activation *in vitro* or *in vivo*. In both tumour types, Dll4 overexpression resulted in larger vessels that were better perfused, leading to faster tumour growth. On the other hand, the growth of the other cell lines was not affected. It is important to understand why Dll4 overexpression promoted tumour growth in some but not all tumour types. The reason may be the different gene expression and vascular morphology of the xenograft tumours, which need to be characterised by real-time PCR and immunohistochemistry, respectively.

Two recent studies have overexpressed Dll4 in xenograft models. One study used mouse C6 cells (Noguera-Troise et al., 2006), and the other used human HT29 and KS-SLK cells (Scehnet et al., 2007). The first study reported similar Notch signalling activation and vascular phenotypes as we found in our study; however, neither study reported increased tumour growth. Thus, we are the first to describe that Dll4 overexpression promoted tumour growth.

Next, we investigated whether Dll4 overexpression in U87 and PC3 xenografts affected tumour response to anti-VEGF treatment. VEGF inhibitors are the most promising therapy that blocks tumour angiogenesis; however, many tumour types are resistant to this therapy (Kerbel et al., 2001, Casanovas et al., 2005).

In the experiment, bevacizumab was injected during early stages of tumour angiogenesis. U87 control tumours were more sensitive to bevacizumab than PC3 control tumours. One possible explanation is that U87 cells may secrete more VEGF *in vivo* (just as they did *in vitro*). To investigate this possibility, xenograft tumours will be homogenised to measure VEGF protein levels by Western blotting.

In the same experiment, the growth of U87 tumours overexpressing Dll4 was also inhibited by bevacizumab; however, these tumours regrew rapidly after cessation of treatment. Bevacizumab also inhibited the growth of PC3 tumours overexpressing Dll4.

Finally, we examined the effect of combined anti-VEGF and anti-Notch treatment on U87 xenografts. Bevacizumab, DBZ or both drugs was injected after tumours were established until the end of the experiment. Under the new regimen, control tumours still responded to bevacizumab; in contrast, Dll4-overexpressing tumours did not respond. This result suggests that tumours with high Dll4 expression may become resistant to VEGF inhibition after they are established.

DBZ treatment had different effects on U87 tumours. Control tumours did not respond to DBZ; in contrast, Dll4-overexpressing tumours did. DBZ was more effective against tumours expressing higher levels of Dll4-Notch signalling. Several recent studies have reported that inhibiting Notch signalling reduced tumour growth in xenograft models (Noguera-Troise et al., 2006, Ridgway et al., 2006, Scehnet et al., 2007).

Notably, the combined bevacizumab and DBZ treatment synergistically retarded the growth of Dll4-overexpresssing tumours, suggesting that anti-Notch treatment may be used in the clinic against tumours resistant to VEGF inhibition. A recent study reported similar results with the human MV-522 xenograft tumours (Ridgway et al., 2006).

Real-time PCR analysis helped explain the tumour growth results. Either bevacizumab or DBZ reduced the expression of Notch target genes in the host stromal cells, and the combined treatment synergistically reduced the expression of mouse Hes1 and Dll4/CD31 in Dll4-overexpressing tumours only. Immunohistochemical analysis of the tumour vasculature still needs to be carried out. The hypothesis is that bevacizumab would reduce vessel numbers,

while DBZ would lead to smaller and non-functional vessels. Thus, both treatments would result in reduced tumour perfusion and growth.

The next step would be to test the combined treatment in animal models of human cancers resistant to VEGF inhibition. In addition, anti-Notch treatment would be tested in combination with commonly used chemotherapeutic agents such as doxorubicin and taxol in animal models. These experiments are currently underway in our laboratory, with the eventual goal of developing Notch inhibitors into viable cancer therapy.

All in all, research presented in this thesis has made a significant and original contribution to the field by elucidating the mechanisms of the Notch-hypoxia signalling crosstalk, the regulation of Dll4 expression in endothelial cells and the effect of Dll4 overexpression on tumour growth. Future work will build upon these results to further unravel the role of Dll4-Notch signalling in angiogenesis and develop therapeutic agents inhibiting this pathway for the benefit of cancer patients.

References

AMERI, K., BURKE, B., LEWIS, C. E. & HARRIS, A. L. (2002) Regulation of a rat VL30 element in human breast cancer cells in hypoxia and anoxia: role of HIF-1. *Br J Cancer,* 87, 1173-81.

ANDERSEN, C. L., JENSEN, J. L. & ORNTOFT, T. F. (2004) Normalization of real-time quantitative reverse transcription-PCR data: a model-based variance estimation approach to identify genes suited for normalization, applied to bladder and colon cancer data sets. *Cancer Res,* 64, 5245-50.

ANDROUTSELLIS-THEOTOKIS, A., LEKER, R. R., SOLDNER, F., HOEPPNER, D. J., RAVIN, R., POSER, S. W., RUEGER, M. A., BAE, S. K., KITTAPPA, R. & MCKAY, R. D. (2006) Notch signalling regulates stem cell numbers in vitro and in vivo. *Nature,* 442, 823-6.

ARTAVANIS-TSAKONAS, S., RAND, M. D. & LAKE, R. J. (1999) Notch signaling: cell fate control and signal integration in development. *Science,* 284, 770-6.

AYYANAN, A., CIVENNI, G., CIARLONI, L., MOREL, C., MUELLER, N., LEFORT, K., MANDINOVA, A., RAFFOUL, W., FICHE, M., DOTTO, G. P. & BRISKEN, C. (2006) Increased Wnt signaling triggers oncogenic conversion of human breast epithelial cells by a Notch-dependent mechanism. *Proc Natl Acad Sci U S A,* 103, 3799-804.

BACON, A. L., FOX, S., TURLEY, H. & HARRIS, A. L. (2007) Selective silencing of the hypoxia-inducible factor 1 target gene BNIP3 by histone deacetylation and methylation in colorectal cancer. *Oncogene,* 26, 132-41.

BALINT, K., XIAO, M., PINNIX, C. C., SOMA, A., VERES, I., JUHASZ, I., BROWN, E. J., CAPOBIANCO, A. J., HERLYN, M. & LIU, Z. J. (2005) Activation of Notch1 signaling is required for beta-catenin-mediated human primary melanoma progression. *J Clin Invest,* 115, 3166-76.

BENEDITO, R. & DUARTE, A. (2005) Expression of Dll4 during mouse embryogenesis suggests multiple developmental roles. *Gene Expr Patterns,* 5, 750-5.

BERGERS, G. & BENJAMIN, L. E. (2003) Tumorigenesis and the angiogenic switch. *Nat Rev Cancer,* 3, 401-10.

BLAUMUELLER, C. M., QI, H., ZAGOURAS, P. & ARTAVANIS-TSAKONAS, S. (1997) Intracellular cleavage of Notch leads to a heterodimeric receptor on the plasma membrane. *Cell,* 90, 281-91.

BURNETTE, W. N. (1981) "Western blotting": electrophoretic transfer of proteins from sodium dodecyl sulfate--polyacrylamide gels to unmodified

nitrocellulose and radiographic detection with antibody and radioiodinated protein A. *Anal Biochem,* 112, 195-203.

CALLAHAN, R. & EGAN, S. E. (2004) Notch signaling in mammary development and oncogenesis. *J Mammary Gland Biol Neoplasia,* 9, 145-63.

CARLSON, T. R., YAN, Y., WU, X., LAM, M. T., TANG, G. L., BEVERLY, L. J., MESSINA, L. M., CAPOBIANCO, A. J., WERB, Z. & WANG, R. (2005) Endothelial expression of constitutively active Notch4 elicits reversible arteriovenous malformations in adult mice. *Proc Natl Acad Sci U S A,* 102, 9884-9.

CARMELIET, P. (2000) Mechanisms of angiogenesis and arteriogenesis. *Nat Med,* 6, 389-95.

CARMELIET, P., FERREIRA, V., BREIER, G., POLLEFEYT, S., KIECKENS, L., GERTSENSTEIN, M., FAHRIG, M., VANDENHOECK, A., HARPAL, K., EBERHARDT, C., DECLERCQ, C., PAWLING, J., MOONS, L., COLLEN, D., RISAU, W. & NAGY, A. (1996) Abnormal blood vessel development and lethality in embryos lacking a single VEGF allele. *Nature,* 380, 435-9.

CASANOVAS, O., HICKLIN, D. J., BERGERS, G. & HANAHAN, D. (2005) Drug resistance by evasion of antiangiogenic targeting of VEGF signaling in late-stage pancreatic islet tumors. *Cancer Cell,* 8, 299-309.

CASTELLO, R., ESTELLES, A., VAZQUEZ, C., FALCO, C., ESPANA, F., ALMENAR, S. M., FUSTER, C. & AZNAR, J. (2002) Quantitative real-time reverse transcription-PCR assay for urokinase plasminogen activator, plasminogen activator inhibitor type 1, and tissue metalloproteinase inhibitor type 1 gene expressions in primary breast cancer. *Clin Chem,* 48, 1288-95.

CHEN, C., PORE, N., BEHROOZ, A., ISMAIL-BEIGI, F. & MAITY, A. (2001) Regulation of glut1 mRNA by hypoxia-inducible factor-1. Interaction between H-ras and hypoxia. *J Biol Chem,* 276, 9519-25.

CHEN, Y., FISCHER, W. H. & GILL, G. N. (1997) Regulation of the ERBB-2 promoter by RBPJkappa and NOTCH. *J Biol Chem,* 272, 14110-4.

CHIN, M. T., MAEMURA, K., FUKUMOTO, S., JAIN, M. K., LAYNE, M. D., WATANABE, M., HSIEH, C. M. & LEE, M. E. (2000) Cardiovascular basic helix loop helix factor 1, a novel transcriptional repressor expressed preferentially in the developing and adult cardiovascular system. *J Biol Chem,* 275, 6381-7.

CLARKE, R. B., SPENCE, K., ANDERSON, E., HOWELL, A., OKANO, H. & POTTEN, C. S. (2005) A putative human breast stem cell population is enriched for steroid receptor-positive cells. *Dev Biol,* 277, 443-56.

CLAXTON, S. & FRUTTIGER, M. (2004) Periodic Delta-like 4 expression in developing retinal arteries. *Gene Expr Patterns,* 5, 123-7.

CURRY, C. L., REED, L. L., GOLDE, T. E., MIELE, L., NICKOLOFF, B. J. & FOREMAN, K. E. (2005) Gamma secretase inhibitor blocks Notch activation and induces apoptosis in Kaposi's sarcoma tumor cells. *Oncogene.*

DICKSON, B. C., MULLIGAN, A. M., ZHANG, H., LOCKWOOD, G., O'MALLEY F, P., EGAN, S. E. & REEDIJK, M. (2007) High-level JAG1 mRNA and protein predict poor outcome in breast cancer. *Mod Pathol,* 20, 685-93.

DIEVART, A., BEAULIEU, N. & JOLICOEUR, P. (1999) Involvement of Notch1 in the development of mouse mammary tumors. *Oncogene,* 18, 5973-81.

DIEZ, H., FISCHER, A., WINKLER, A., HU, C. J., HATZOPOULOS, A. K., BREIER, G. & GESSLER, M. (2007) Hypoxia-mediated activation of Dll4-Notch-Hey2 signaling in endothelial progenitor cells and adoption of arterial cell fate. *Exp Cell Res,* 313, 1-9.

DONTU, G., AL-HAJJ, M., ABDALLAH, W. M., CLARKE, M. F. & WICHA, M. S. (2003) Stem cells in normal breast development and breast cancer. *Cell Prolif,* 36 Suppl 1, 59-72.

DUARTE, A., HIRASHIMA, M., BENEDITO, R., TRINDADE, A., DINIZ, P., BEKMAN, E., COSTA, L., HENRIQUE, D. & ROSSANT, J. (2004) Dosage-sensitive requirement for mouse Dll4 in artery development. *Genes Dev,* 18, 2474-8.

ELLISEN, L. W., BIRD, J., WEST, D. C., SORENG, A. L., REYNOLDS, T. C., SMITH, S. D. & SKLAR, J. (1991) TAN-1, the human homolog of the Drosophila notch gene, is broken by chromosomal translocations in T lymphoblastic neoplasms. *Cell,* 66, 649-61.

FAN, X., MATSUI, W., KHAKI, L., STEARNS, D., CHUN, J., LI, Y. M. & EBERHART, C. G. (2006) Notch pathway inhibition depletes stem-like cells and blocks engraftment in embryonal brain tumors. *Cancer Res,* 66, 7445-52.

FARNIE, G., CLARKE, R. B., SPENCE, K., PINNOCK, N., BRENNAN, K., ANDERSON, N. G. & BUNDRED, N. J. (2007) Novel cell culture technique for primary ductal carcinoma in situ: role of Notch and epidermal growth factor receptor signaling pathways. *J Natl Cancer Inst,* 99, 616-27.

FERRARA, N., CARVER-MOORE, K., CHEN, H., DOWD, M., LU, L., O'SHEA, K. S., POWELL-BRAXTON, L., HILLAN, K. J. & MOORE, M. W. (1996) Heterozygous embryonic lethality induced by targeted inactivation of the VEGF gene. *Nature,* 380, 439-42.

FERRARA, N., GERBER, H. P. & LECOUTER, J. (2003) The biology of VEGF and its receptors. *Nat Med,* 9, 669-76.

FERRARA, N. & KERBEL, R. S. (2005) Angiogenesis as a therapeutic target. *Nature,* 438, 967-74.

FIDLER, I. J. (1975) Biological behavior of malignant melanoma cells correlated to their survival in vivo. *Cancer Res,* 35, 218-24.

FIELD, J. K. & SPANDIDOS, D. A. (1990) The role of ras and myc oncogenes in human solid tumours and their relevance in diagnosis and prognosis (review). *Anticancer Res,* 10, 1-22.

FISCHER, A., SCHUMACHER, N., MAIER, M., SENDTNER, M. & GESSLER, M. (2004) The Notch target genes Hey1 and Hey2 are required for embryonic vascular development. *Genes Dev,* 18, 901-11.

FITZGERALD, K., HARRINGTON, A. & LEDER, P. (2000) Ras pathway signals are required for notch-mediated oncogenesis. *Oncogene,* 19, 4191-8.

FORSYTHE, J. A., JIANG, B. H., IYER, N. V., AGANI, F., LEUNG, S. W., KOOS, R. D. & SEMENZA, G. L. (1996) Activation of vascular endothelial growth factor gene transcription by hypoxia-inducible factor 1. *Mol Cell Biol,* 16, 4604-13.

FRE, S., HUYGHE, M., MOURIKIS, P., ROBINE, S., LOUVARD, D. & ARTAVANIS-TSAKONAS, S. (2005) Notch signals control the fate of immature progenitor cells in the intestine. *Nature,* 435, 964-8.

FYNAN, T. M. & REISS, M. (1993) Resistance to inhibition of cell growth by transforming growth factor-beta and its role in oncogenesis. *Crit Rev Oncog,* 4, 493-540.

GALE, N. W., DOMINGUEZ, M. G., NOGUERA, I., PAN, L., HUGHES, V., VALENZUELA, D. M., MURPHY, A. J., ADAMS, N. C., LIN, H. C., HOLASH, J., THURSTON, G. & YANCOPOULOS, G. D. (2004) Haploinsufficiency of delta-like 4 ligand results in embryonic lethality due to major defects in arterial and vascular development. *Proc Natl Acad Sci U S A,* 101, 15949-54.

GALLAHAN, D. & CALLAHAN, R. (1987) Mammary tumorigenesis in feral mice: identification of a new int locus in mouse mammary tumor virus (Czech II)-induced mammary tumors. *J Virol,* 61, 66-74.

GALLAHAN, D. & CALLAHAN, R. (1997) The mouse mammary tumor associated gene INT3 is a unique member of the NOTCH gene family (NOTCH4). *Oncogene,* 14, 1883-90.

GARAYOA, M., MARTINEZ, A., LEE, S., PIO, R., AN, W. G., NECKERS, L., TREPEL, J., MONTUENGA, L. M., RYAN, H., JOHNSON, R., GASSMANN, M. & CUTTITTA, F. (2000) Hypoxia-inducible factor-1 (HIF-1) up-regulates adrenomedullin expression in human tumor cell lines during oxygen deprivation: a possible promotion mechanism of carcinogenesis. *Mol Endocrinol,* 14, 848-62.

GERHARDT, H., GOLDING, M., FRUTTIGER, M., RUHRBERG, C., LUNDKVIST, A., ABRAMSSON, A., JELTSCH, M., MITCHELL, C., ALITALO, K., SHIMA, D. & BETSHOLTZ, C. (2003) VEGF guides angiogenic sprouting utilizing endothelial tip cell filopodia. *J Cell Biol,* 161, 1163-77.

GORDON, W. R., VARDAR-ULU, D., HISTEN, G., SANCHEZ-IRIZARRY, C., ASTER, J. C. & BLACKLOW, S. C. (2007) Structural basis for autoinhibition of Notch. *Nat Struct Mol Biol,* 14, 295-300.

GUSTAFSSON, M. V., ZHENG, X., PEREIRA, T., GRADIN, K., JIN, S., LUNDKVIST, J., RUAS, J. L., POELLINGER, L., LENDAHL, U. & BONDESSON, M. (2005) Hypoxia requires notch signaling to maintain the undifferentiated cell state. *Dev Cell,* 9, 617-28.

HAINAUD, P., CONTRERES, J. O., VILLEMAIN, A., LIU, L. X., PLOUET, J., TOBELEM, G. & DUPUY, E. (2006) The Role of the Vascular Endothelial Growth Factor-Delta-like 4 Ligand/Notch4-Ephrin B2 Cascade in Tumor Vessel Remodeling and Endothelial Cell Functions. *Cancer Res,* 66, 8501-10.

HALLAHAN, A. R., PRITCHARD, J. I., HANSEN, S., BENSON, M., STOECK, J., HATTON, B. A., RUSSELL, T. L., ELLENBOGEN, R. G., BERNSTEIN, I. D., BEACHY, P. A. & OLSON, J. M. (2004) The SmoA1 mouse model reveals that notch signaling is critical for the growth and survival of sonic hedgehog-induced medulloblastomas. *Cancer Res,* 64, 7794-800.

HALTIWANGER, R. S. & STANLEY, P. (2002) Modulation of receptor signaling by glycosylation: fringe is an O-fucose-beta1,3-N-acetylglucosaminyltransferase. *Biochim Biophys Acta,* 1573, 328-35.

HANAHAN, D. & WEINBERG, R. A. (2000) The hallmarks of cancer. *Cell,* 100, 57-70.

HARRINGTON, L. S., SAINSON, R. C., WILLIAMS, C. K., TAYLOR, J. M., SHI, W., LI, J. L. & HARRIS, A. L. (2007) Regulation of multiple angiogenic pathways by Dll4 and Notch in human umbilical vein endothelial cells. *Microvasc Res,* 74, (accepted).

HARRIS, A. L. (2002) Hypoxia--a key regulatory factor in tumour growth. *Nat Rev Cancer,* 2, 38-47.

HARRIS, C. C. (1996) p53 tumor suppressor gene: from the basic research laboratory to the clinic--an abridged historical perspective. *Carcinogenesis,* 17, 1187-98.

HELLSTROM, M., PHNG, L. K., HOFMANN, J. J., WALLGARD, E., COULTAS, L., LINDBLOM, P., ALVA, J., NILSSON, A. K., KARLSSON, L., GAIANO, N., YOON, K., ROSSANT, J., IRUELA-ARISPE, M. L., KALEN, M., GERHARDT, H. & BETSHOLTZ, C. (2007) Dll4 signalling through Notch1 regulates formation of tip cells during angiogenesis. *Nature,* 445, 776-80.

HENDERSON, A. M., WANG, S. J., TAYLOR, A. C., AITKENHEAD, M. & HUGHES, C. C. (2001) The basic helix-loop-helix transcription factor HESR1 regulates endothelial cell tube formation. *J Biol Chem,* 276, 6169-76.

HICKS, C., LADI, E., LINDSELL, C., HSIEH, J. J., HAYWARD, S. D., COLLAZO, A. & WEINMASTER, G. (2002) A secreted Delta1-Fc fusion protein functions both as an activator and inhibitor of Notch1 signaling. *J Neurosci Res,* 68, 655-67.

HUBER, M. A., KRAUT, N. & BEUG, H. (2005) Molecular requirements for epithelial-mesenchymal transition during tumor progression. *Curr Opin Cell Biol,* 17, 548-58.

IMATANI, A. & CALLAHAN, R. (2000) Identification of a novel NOTCH-4/INT-3 RNA species encoding an activated gene product in certain human tumor cell lines. *Oncogene,* 19, 223-31.

ISO, T., HAMAMORI, Y. & KEDES, L. (2003a) Notch signaling in vascular development. *Arterioscler Thromb Vasc Biol,* 23, 543-53.

ISO, T., KEDES, L. & HAMAMORI, Y. (2003b) HES and HERP families: multiple effectors of the Notch signaling pathway. *J Cell Physiol,* 194, 237-55.

ISO, T., MAENO, T., OIKE, Y., YAMAZAKI, M., DOI, H., ARAI, M. & KURABAYASHI, M. (2006) Dll4-selective Notch signaling induces ephrinB2 gene expression in endothelial cells. *Biochem Biophys Res Commun,* 341, 708-14.

JAIN, R. K., DUDA, D. G., CLARK, J. W. & LOEFFLER, J. S. (2006) Lessons from phase III clinical trials on anti-VEGF therapy for cancer. *Nat Clin Pract Oncol,* 3, 24-40.

JHAPPAN, C., GALLAHAN, D., STAHLE, C., CHU, E., SMITH, G. H., MERLINO, G. & CALLAHAN, R. (1992) Expression of an activated Notch-related int-3 transgene interferes with cell differentiation and induces neoplastic transformation in mammary and salivary glands. *Genes Dev,* 6, 345-55.

JOGI, A., ORA, I., NILSSON, H., LINDEHEIM, A., MAKINO, Y., POELLINGER, L., AXELSON, H. & PAHLMAN, S. (2002) Hypoxia alters gene expression in human neuroblastoma cells toward an immature and neural crest-like phenotype. *Proc Natl Acad Sci U S A,* 99, 7021-6.

KAGEYAMA, R. & OHTSUKA, T. (1999) The Notch-Hes pathway in mammalian neural development. *Cell Res,* 9, 179-88.

KENDALL, R. L. & THOMAS, K. A. (1993) Inhibition of vascular endothelial cell growth factor activity by an endogenously encoded soluble receptor. *Proc Natl Acad Sci U S A,* 90, 10705-9.

KERBEL, R. S., YU, J., TRAN, J., MAN, S., VILORIA-PETIT, A., KLEMENT, G., COOMBER, B. L. & RAK, J. (2001) Possible mechanisms of acquired resistance to anti-angiogenic drugs: implications for the use of combination therapy approaches. *Cancer Metastasis Rev,* 20, 79-86.

KIARIS, H., POLITI, K., GRIMM, L. M., SZABOLCS, M., FISHER, P., EFSTRATIADIS, A. & ARTAVANIS-TSAKONAS, S. (2004) Modulation of notch signaling elicits signature tumors and inhibits hras1-induced oncogenesis in the mouse mammary epithelium. *Am J Pathol,* 165, 695-705.

KLINAKIS, A., SZABOLCS, M., POLITI, K., KIARIS, H., ARTAVANIS-TSAKONAS, S. & EFSTRATIADIS, A. (2006) Myc is a Notch1 transcriptional target and a requisite for Notch1-induced mammary tumorigenesis in mice. *Proc Natl Acad Sci U S A,* 103, 9262-7.

KOPAN, R. & GOATE, A. (2000) A common enzyme connects notch signaling and Alzheimer's disease. *Genes Dev,* 14, 2799-806.

KREBS, L. T., SHUTTER, J. R., TANIGAKI, K., HONJO, T., STARK, K. L. & GRIDLEY, T. (2004) Haploinsufficient lethality and formation of arteriovenous malformations in Notch pathway mutants. *Genes Dev,* 18, 2469-73.

KREBS, L. T., XUE, Y., NORTON, C. R., SHUTTER, J. R., MAGUIRE, M., SUNDBERG, J. P., GALLAHAN, D., CLOSSON, V., KITAJEWSKI, J., CALLAHAN, R., SMITH, G. H., STARK, K. L. & GRIDLEY, T. (2000) Notch signaling is essential for vascular morphogenesis in mice. *Genes Dev,* 14, 1343-52.

LAI, E. C. (2002) Protein degradation: four E3s for the notch pathway. *Curr Biol,* 12, R74-8.

LANDGREN, E., SCHILLER, P., CAO, Y. & CLAESSON-WELSH, L. (1998) Placenta growth factor stimulates MAP kinase and mitogenicity but not phospholipase C-gamma and migration of endothelial cells expressing Flt 1. *Oncogene,* 16, 359-67.

LANFORD, P. J., LAN, Y., JIANG, R., LINDSELL, C., WEINMASTER, G., GRIDLEY, T. & KELLEY, M. W. (1999) Notch signalling pathway mediates hair cell development in mammalian cochlea. *Nat Genet,* 21, 289-92.

LEONG, K. G., HU, X., LI, L., NOSEDA, M., LARRIVEE, B., HULL, C., HOOD, L., WONG, F. & KARSAN, A. (2002) Activated Notch4 inhibits angiogenesis: role of beta 1-integrin activation. *Mol Cell Biol,* 22, 2830-41.

LEONG, K. G. & KARSAN, A. (2006) Recent insights into the role of Notch signaling in tumorigenesis. *Blood,* 107, 2223-33.

LI, J. L. & HARRIS, A. L. (2005) Notch signaling from tumor cells: a new mechanism of angiogenesis. *Cancer Cell,* 8, 1-3.

LIMBOURG, F. P., TAKESHITA, K., RADTKE, F., BRONSON, R. T., CHIN, M. T. & LIAO, J. K. (2005) Essential role of endothelial Notch1 in angiogenesis. *Circulation,* 111, 1826-32.

LINDSELL, C. E., SHAWBER, C. J., BOULTER, J. & WEINMASTER, G. (1995) Jagged: a mammalian ligand that activates Notch1. *Cell,* 80, 909-17.

LIU, Z. J., SHIRAKAWA, T., LI, Y., SOMA, A., OKA, M., DOTTO, G. P., FAIRMAN, R. M., VELAZQUEZ, O. C. & HERLYN, M. (2003) Regulation of Notch1 and Dll4 by vascular endothelial growth factor in arterial endothelial cells: implications for modulating arteriogenesis and angiogenesis. *Mol Cell Biol,* 23, 14-25.

LIU, Z. J., XIAO, M., BALINT, K., SOMA, A., PINNIX, C. C., CAPOBIANCO, A. J., VELAZQUEZ, O. C. & HERLYN, M. (2006) Inhibition of endothelial cell proliferation by Notch1 signaling is mediated by repressing MAPK and PI3K/Akt pathways and requires MAML1. *Faseb J,* 20, 1009-11.

LIVAK, K. J. & SCHMITTGEN, T. D. (2001) Analysis of relative gene expression data using real-time quantitative PCR and the 2(-Delta Delta C(T)) Method. *Methods,* 25, 402-8.

LOBOV, I. B., RENARD, R. A., PAPADOPOULOS, N., GALE, N. W., THURSTON, G., YANCOPOULOS, G. D. & WIEGAND, S. J. (2007) Delta-like ligand 4 (Dll4) is induced by VEGF as a negative regulator of angiogenic sprouting. *Proc Natl Acad Sci U S A,* 104, 3219-24.

LOFSTEDT, T., FREDLUND, E., HOLMQUIST-MENGELBIER, L., PIETRAS, A., OVENBERGER, M., POELLINGER, L. & PAHLMAN, S. (2007) Hypoxia inducible factor-2alpha in cancer. *Cell Cycle,* 6, 919-26.

MAEMURA, K., HSIEH, C. M., JAIN, M. K., FUKUMOTO, S., LAYNE, M. D., LIU, Y., KOUREMBANAS, S., YET, S. F., PERRELLA, M. A. & LEE, M. E. (1999) Generation of a dominant-negative mutant of endothelial PAS domain protein 1 by deletion of a potent C-terminal transactivation domain. *J Biol Chem,* 274, 31565-70.

MAILHOS, C., MODLICH, U., LEWIS, J., HARRIS, A., BICKNELL, R. & ISH-HOROWICZ, D. (2001) Delta4, an endothelial specific notch ligand expressed at sites of physiological and tumor angiogenesis. *Differentiation,* 69, 135-44.

MARTINEZ ARIAS, A., ZECCHINI, V. & BRENNAN, K. (2002) CSL-independent Notch signalling: a checkpoint in cell fate decisions during development? *Curr Opin Genet Dev,* 12, 524-33.

MASUDA, S., KUMANO, K., SHIMIZU, K., IMAI, Y., KUROKAWA, M., OGAWA, S., MIYAGISHI, M., TAIRA, K., HIRAI, H. & CHIBA, S. (2005) Notch1 oncoprotein antagonizes TGF-beta/Smad-mediated cell growth suppression via sequestration of coactivator p300. *Cancer Sci,* 96, 274-82.

MINCHENKO, O. H., OPENTANOVA, I. L., OGURA, T., MINCHENKO, D. O., KOMISARENKO, S. V., CARO, J. & ESUMI, H. (2005) Expression and hypoxia-responsiveness of 6-phosphofructo-2-kinase/fructose-2,6-bisphosphatase 4 in mammary gland malignant cell lines. *Acta Biochim Pol,* 52, 881-8.

MOURITZEN, P., NIELSEN, A. T., PFUNDHELLER, H. M., CHOLEVA, KONGSBAK, L. & MOLLER, S. (2003) Single nucleotide polymorph genotyping using locked nucleic acid (LNA). *Expert Rev Mol Diagn,* 3, 38.

MUNGAMURI, S. K., YANG, X., THOR, A. D. & SOMASUNDARAM, K. (20 Survival signaling by Notch1: mammalian target of rapamycin (mTO dependent inhibition of p53. *Cancer Res,* 66, 4715-24.

NGUYEN, B. C., LEFORT, K., MANDINOVA, A., ANTONINI, D., DEVGAN, DELLA GATTA, G., KOSTER, M. I., ZHANG, Z., WANG, J., TOMM DI VIGNANO, A., KITAJEWSKI, J., CHIORINO, G., ROOP, D. MISSERO, C. & DOTTO, G. P. (2006) Cross-regulation between Notch p63 in keratinocyte commitment to differentiation. *Genes Dev,* 20, 1028-4

NICKOLOFF, B. J., OSBORNE, B. A. & MIELE, L. (2003) Notch signaling a therapeutic target in cancer: a new approach to the development of cell modifying agents. *Oncogene,* 22, 6598-608.

NICOLAS, M., WOLFER, A., RAJ, K., KUMMER, J. A., MILL, P., VAN NOOI M., HUI, C. C., CLEVERS, H., DOTTO, G. P. & RADTKE, F. (20 Notch1 functions as a tumor suppressor in mouse skin. *Nat Genet,* 33, 4 21.

NOGUERA-TROISE, I., DALY, C., PAPADOPOULOS, N. J., COETZEE, BOLAND, P., GALE, N. W., LIN, H. C., YANCOPOULOS, G. D. THURSTON, G. (2006) Blockade of Dll4 inhibits tumour growth promoting non-productive angiogenesis. *Nature,* 444, 1032-7.

NOSEDA, M., CHANG, L., MCLEAN, G., GRIM, J. E., CLURMAN, B. SMITH, L. L. & KARSAN, A. (2004) Notch activation induces endothel cell cycle arrest and participates in contact inhibition: role of p21Cip repression. *Mol Cell Biol,* 24, 8813-22.

NOSEDA, M., FU, Y., NIESSEN, K., WONG, F., CHANG, L., MCLEAN, G. KARSAN, A. (2006) Smooth Muscle alpha-actin is a direct target Notch/CSL. *Circ Res,* 98, 1468-70.

OKANO, H., IMAI, T. & OKABE, M. (2002) Musashi: a translational regulator cell fate. *J Cell Sci,* 115, 1355-9.

PARIS, D., QUADROS, A., PATEL, N., DELLEDONNE, A., HUMPHREY, J. MULLAN, M. (2005) Inhibition of angiogenesis and tumor growth by be and gamma-secretase inhibitors. *Eur J Pharmacol,* 514, 1-15.

PARK, J. T., LI, M., NAKAYAMA, K., MAO, T. L., DAVIDSON, B., ZHANG, Z., KURMAN, R. J., EBERHART, C. G., SHIH IE, M. & WANG, T. L. (2006) Notch3 gene amplification in ovarian cancer. *Cancer Res,* 66, 6312-8.

PARR, C., WATKINS, G. & JIANG, W. G. (2004) The possible correlation of Notch-1 and Notch-2 with clinical outcome and tumour clinicopathological parameters in human breast cancer. *Int J Mol Med,* 14, 779-86.

PATEL, N. S., DOBBIE, M. S., ROCHESTER, M., STEERS, G., POULSOM, R., LE MONNIER, K., CRANSTON, D. W., LI, J. L. & HARRIS, A. L. (2006) Up-regulation of endothelial delta-like 4 expression correlates with vessel maturation in bladder cancer. *Clin Cancer Res,* 12, 4836-44.

PATEL, N. S., LI, J. L., GENERALI, D., POULSOM, R., CRANSTON, D. W. & HARRIS, A. L. (2005) Up-regulation of delta-like 4 ligand in human tumor vasculature and the role of basal expression in endothelial cell function. *Cancer Res,* 65, 8690-7.

PEAR, W. S. & RADTKE, F. (2003) Notch signaling in lymphopoiesis. *Semin Immunol,* 15, 69-79.

PECE, S., SERRESI, M., SANTOLINI, E., CAPRA, M., HULLEMAN, E., GALIMBERTI, V., ZURRIDA, S., MAISONNEUVE, P., VIALE, G. & DI FIORE, P. P. (2004) Loss of negative regulation by Numb over Notch is relevant to human breast carcinogenesis. *J Cell Biol,* 167, 215-21.

PIROT, P., VAN GRUNSVEN, L. A., MARINE, J. C., HUYLEBROECK, D. & BELLEFROID, E. J. (2004) Direct regulation of the Nrarp gene promoter by the Notch signaling pathway. *Biochem Biophys Res Commun,* 322, 526-34.

POLITI, K., FEIRT, N. & KITAJEWSKI, J. (2004) Notch in mammary gland development and breast cancer. *Semin Cancer Biol,* 14, 341-7.

PROWELLER, A., TU, L., LEPORE, J. J., CHENG, L., LU, M. M., SEYKORA, J., MILLAR, S. E., PEAR, W. S. & PARMACEK, M. S. (2006) Impaired notch signaling promotes de novo squamous cell carcinoma formation. *Cancer Res,* 66, 7438-44.

PUGH, C. W. & RATCLIFFE, P. J. (2003) Regulation of angiogenesis by hypoxia: role of the HIF system. *Nat Med,* 9, 677-84.

RAAFAT, A., BARGO, S., ANVER, M. R. & CALLAHAN, R. (2004) Mammary development and tumorigenesis in mice expressing a truncated human Notch4/Int3 intracellular domain (h-Int3sh). *Oncogene,* 23, 9401-7.

RADTKE, F. & RAJ, K. (2003) The role of Notch in tumorigenesis: oncogene or tumour suppressor? *Nat Rev Cancer,* 3, 756-67.

RAND, M. D., GRIMM, L. M., ARTAVANIS-TSAKONAS, S., PATRIUB, V., BLACKLOW, S. C., SKLAR, J. & ASTER, J. C. (2000) Calcium depletion dissociates and activates heterodimeric notch receptors. *Mol Cell Biol,* 20, 1825-35.

RANGARAJAN, A., TALORA, C., OKUYAMA, R., NICOLAS, M., MAMMUCARI, C., OH, H., ASTER, J. C., KRISHNA, S., METZGER, D., CHAMBON, P., MIELE, L., AGUET, M., RADTKE, F. & DOTTO, G. P. (2001) Notch signaling is a direct determinant of keratinocyte growth arrest and entry into differentiation. *Embo J,* 20, 3427-36.

RAVAL, R. R., LAU, K. W., TRAN, M. G., SOWTER, H. M., MANDRIOTA, S. J., LI, J. L., PUGH, C. W., MAXWELL, P. H., HARRIS, A. L. & RATCLIFFE, P. J. (2005) Contrasting properties of hypoxia-inducible factor 1 (HIF-1) and HIF-2 in von Hippel-Lindau-associated renal cell carcinoma. *Mol Cell Biol,* 25, 5675-86.

REEDIJK, M., ODORCIC, S., CHANG, L., ZHANG, H., MILLER, N., MCCREADY, D. R., LOCKWOOD, G. & EGAN, S. E. (2005) High-level coexpression of JAG1 and NOTCH1 is observed in human breast cancer and is associated with poor overall survival. *Cancer Res,* 65, 8530-7.

REHMAN, A. O. & WANG, C. Y. (2006) Notch signaling in the regulation of tumor angiogenesis. *Trends Cell Biol,* 16, 293-300.

REYA, T., MORRISON, S. J., CLARKE, M. F. & WEISSMAN, I. L. (2001) Stem cells, cancer, and cancer stem cells. *Nature,* 414, 105-11.

RIDGWAY, J., ZHANG, G., WU, Y., STAWICKI, S., LIANG, W. C., CHANTHERY, Y., KOWALSKI, J., WATTS, R. J., CALLAHAN, C., KASMAN, I., SINGH, M., CHIEN, M., TAN, C., HONGO, J. A., DE SAUVAGE, F., PLOWMAN, G. & YAN, M. (2006) Inhibition of Dll4 signalling inhibits tumour growth by deregulating angiogenesis. *Nature,* 444, 1083-7.

RONCHINI, C. & CAPOBIANCO, A. J. (2001) Induction of cyclin D1 transcription and CDK2 activity by Notch(ic): implication for cell cycle disruption in transformation by Notch(ic). *Mol Cell Biol,* 21, 5925-34.

ROY, M., PEAR, W. S. & ASTER, J. C. (2007) The multifaceted role of Notch in cancer. *Curr Opin Genet Dev,* 17, 52-9.

SAINSON, R. C., AOTO, J., NAKATSU, M. N., HOLDERFIELD, M., CONN, E., KOLLER, E. & HUGHES, C. C. (2005) Cell-autonomous notch signaling regulates endothelial cell branching and proliferation during vascular tubulogenesis. *Faseb J,* 19, 1027-9.

SAINSON, R. C. & HARRIS, A. L. (2007) Anti-Dll4 therapy: can we block tumor growth by increasing angiogenesis? *Trends Mol Med,* 13, (accepted).

SAKAMAKI, T., LIU, M., KATIYAR, S., RAO, M., LI, S., YIN, Y., DETTIN, L., PESTELL, R. G. & GLAZER, R. I. (2005) ErbB2 activation of Notch1 signaling in breast cancer. *Proc Am Assoc Cancer Res.*

SANTAGATA, S., DEMICHELIS, F., RIVA, A., VARAMBALLY, S., HOFER, M. D., KUTOK, J. L., KIM, R., TANG, J., MONTIE, J. E., CHINNAIYAN, A. M., RUBIN, M. A. & ASTER, J. C. (2004) JAGGED1 expression is associated with prostate cancer metastasis and recurrence. *Cancer Res,* 64, 6854-7.

SCEHNET, J. S., JIANG, W., KUMAR, S. R., KRASNOPEROV, V., TRINDADE, A., BENEDITO, R., DJOKOVIC, D., BORGES, C., LEY, E. J., DUARTE, A. & GILL, P. S. (2007) Inhibition of Dll4-mediated signaling induces proliferation of immature vessels and results in poor tissue perfusion. *Blood,* 109, 4753-60.

SEMENZA, G. L. (2003) Targeting HIF-1 for cancer therapy. *Nat Rev Cancer,* 3, 721-32.

SEO, S., FUJITA, H., NAKANO, A., KANG, M., DUARTE, A. & KUME, T. (2006) The forkhead transcription factors, Foxc1 and Foxc2, are required for arterial specification and lymphatic sprouting during vascular development. *Dev Biol,* 294, 458-70.

SHAWBER, C. J., DAS, I., FRANCISCO, E. & KITAJEWSKI, J. (2003) Notch signaling in primary endothelial cells. *Ann N Y Acad Sci,* 995, 162-70.

SHAWBER, C. J. & KITAJEWSKI, J. (2004) Notch function in the vasculature: insights from zebrafish, mouse and man. *Bioessays,* 26, 225-34.

SHI, S. & STANLEY, P. (2003) Protein O-fucosyltransferase 1 is an essential component of Notch signaling pathways. *Proc Natl Acad Sci U S A,* 100, 5234-9.

SHI, W. & HARRIS, A. L. (2006) Notch signaling in breast cancer and tumor angiogenesis: cross-talk and therapeutic potentials. *J Mammary Gland Biol Neoplasia,* 11, 41-52.

SHUTTER, J. R., SCULLY, S., FAN, W., RICHARDS, W. G., KITAJEWSKI, J., DEBLANDRE, G. A., KINTNER, C. R. & STARK, K. L. (2000) Dll4, a novel Notch ligand expressed in arterial endothelium. *Genes Dev,* 14, 1313-8.

SOARES, R., BALOGH, G., GUO, S., GARTNER, F., RUSSO, J. & SCHMITT, F. (2004) Evidence for the notch signaling pathway on the role of estrogen in angiogenesis. *Mol Endocrinol,* 18, 2333-43.

SRIURANPONG, V., BORGES, M. W., RAVI, R. K., ARNOLD, D. R., NELKIN, B. D., BAYLIN, S. B. & BALL, D. W. (2001) Notch signaling induces cell cycle arrest in small cell lung cancer cells. *Cancer Res,* 61, 3200-5.

STEWART, M., TURLEY, H., COOK, N., PEZZELLA, F., PILLAI, G., OGILVIE, D., CARTLIDGE, S., PATERSON, D., COPLEY, C., KENDREW, J., BARNES, C., HARRIS, A. L. & GATTER, K. C. (2003) The angiogenic receptor KDR is widely distributed in human tissues and tumours and relocates intracellularly on phosphorylation. An immunohistochemical study. *Histopathology,* 43, 33-9.

STYLIANOU, S., CLARKE, R. B. & BRENNAN, K. (2006) Aberrant activation of notch signaling in human breast cancer. *Cancer Res,* 66, 1517-25.

SUCHTING, S., FREITAS, C., LE NOBLE, F., BENEDITO, R., BREANT, C., DUARTE, A. & EICHMANN, A. (2007) The Notch ligand Delta-like 4 negatively regulates endothelial tip cell formation and vessel branching. *Proc Natl Acad Sci U S A,* 104, 3225-30.

SUN, Y., LOWTHER, W., KATO, K., BIANCO, C., KENNEY, N., STRIZZI, L., RAAFAT, D., HIROTA, M., KHAN, N. I., BARGO, S., JONES, B., SALOMON, D. & CALLAHAN, R. (2005) Notch4 intracellular domain binding to Smad3 and inhibition of the TGF-beta signaling. *Oncogene,* 24, 5365-74.

SUZUKI, M., YAMAMOTO, M., SUGIMOTO, A., NAKAMURA, S., MOTODA, R. & ORITA, K. (2006) Delta-4 expression on a stromal cell line is augmented by interleukin-6 via STAT3 activation. *Exp Hematol,* 34, 1143-50.

TAKESHITA, K., SATOH, M., II, M., SILVER, M., LIMBOURG, F. P., MUKAI, Y., RIKITAKE, Y., RADTKE, F., GRIDLEY, T., LOSORDO, D. W. & LIAO, J. K. (2007) Critical role of endothelial Notch1 signaling in postnatal angiogenesis. *Circ Res,* 100, 70-8.

TALORA, C., SGROI, D. C., CRUM, C. P. & DOTTO, G. P. (2002) Specific down-modulation of Notch1 signaling in cervical cancer cells is required for

sustained HPV-E6/E7 expression and late steps of malignant transformation. *Genes Dev,* 16, 2252-63.

TAYLOR, K. L., HENDERSON, A. M. & HUGHES, C. C. (2002) Notch activation during endothelial cell network formation in vitro targets the basic HLH transcription factor HESR-1 and downregulates VEGFR-2/KDR expression. *Microvasc Res,* 64, 372-83.

THURSTON, G., NOGUERA-TROISE, I. & YANCOPOULOS, G. D. (2007) The Delta paradox: DLL4 blockade leads to more tumour vessels but less tumour growth. *Nat Rev Cancer,* 7, 327-31.

UYTTENDAELE, H., HO, J., ROSSANT, J. & KITAJEWSKI, J. (2001) Vascular patterning defects associated with expression of activated Notch4 in embryonic endothelium. *Proc Natl Acad Sci U S A,* 98, 5643-8.

UYTTENDAELE, H., MARAZZI, G., WU, G., YAN, Q., SASSOON, D. & KITAJEWSKI, J. (1996) Notch4/int-3, a mammary proto-oncogene, is an endothelial cell-specific mammalian Notch gene. *Development,* 122, 2251-9.

UYTTENDAELE, H., SORIANO, J. V., MONTESANO, R. & KITAJEWSKI, J. (1998) Notch4 and Wnt-1 proteins function to regulate branching morphogenesis of mammary epithelial cells in an opposing fashion. *Dev Biol,* 196, 204-17.

VAN ES, J. H., VAN GIJN, M. E., RICCIO, O., VAN DEN BORN, M., VOOIJS, M., BEGTHEL, H., COZIJNSEN, M., ROBINE, S., WINTON, D. J., RADTKE, F. & CLEVERS, H. (2005) Notch/gamma-secretase inhibition turns proliferative cells in intestinal crypts and adenomas into goblet cells. *Nature,* 435, 959-63.

WANG, R., ZHANG, Y. W., ZHANG, X., LIU, R., ZHANG, X., HONG, S., XIA, K., XIA, J., ZHANG, Z. & XU, H. (2006) Transcriptional regulation of APH-1A and increased gamma-secretase cleavage of APP and Notch by HIF-1 and hypoxia. *Faseb J,* 20, 1275-7.

WEIJZEN, S., RIZZO, P., BRAID, M., VAISHNAV, R., JONKHEER, S. M., ZLOBIN, A., OSBORNE, B. A., GOTTIPATI, S., ASTER, J. C., HAHN, W. C., RUDOLF, M., SIZIOPIKOU, K., KAST, W. M. & MIELE, L. (2002) Activation of Notch-1 signaling maintains the neoplastic phenotype in human Ras-transformed cells. *Nat Med,* 8, 979-86.

WENG, A. P., FERRANDO, A. A., LEE, W., MORRIS, J. P. T., SILVERMAN, L. B., SANCHEZ-IRIZARRY, C., BLACKLOW, S. C., LOOK, A. T. & ASTER, J. C. (2004) Activating mutations of NOTCH1 in human T cell acute lymphoblastic leukemia. *Science,* 306, 269-71.

WENG, A. P., MILLHOLLAND, J. M., YASHIRO-OHTANI, Y., ARCANGELI, M. L., LAU, A., WAI, C., DEL BIANCO, C., RODRIGUEZ, C. G., SAI, H., TOBIAS, J., LI, Y., WOLFE, M. S., SHACHAF, C., FELSHER, D., BLACKLOW, S. C., PEAR, W. S. & ASTER, J. C. (2006) c-Myc is an important direct target of Notch1 in T-cell acute lymphoblastic leukemia/lymphoma. *Genes Dev,* 20, 2096-109.

WHELAN, J. T., FORBES, S. L. & BERTRAND, F. E. (2007) CBF-1 (RBP-J kappa) binds to the PTEN promoter and regulates PTEN gene expression. *Cell Cycle,* 6, 80-4.

WILLIAMS, C. K., LI, J. L., MURGA, M., HARRIS, A. L. & TOSATO, G. (2006) Up-regulation of the Notch ligand Delta-like 4 inhibits VEGF-induced endothelial cell function. *Blood,* 107, 931-9.

WU, L. & GRIFFIN, J. D. (2004) Modulation of Notch signaling by mastermind-like (MAML) transcriptional co-activators and their involvement in tumorigenesis. *Semin Cancer Biol,* 14, 348-56.

YURUGI-KOBAYASHI, T., ITOH, H., SCHROEDER, T., NAKANO, A., NARAZAKI, G., KITA, F., YANAGI, K., HIRAOKA-KANIE, M., INOUE, E., ARA, T., NAGASAWA, T., JUST, U., NAKAO, K., NISHIKAWA, S. & YAMASHITA, J. K. (2006) Adrenomedullin/cyclic AMP pathway induces Notch activation and differentiation of arterial endothelial cells from vascular progenitors. *Arterioscler Thromb Vasc Biol,* 26, 1977-84.

ZAVADIL, J., CERMAK, L., SOTO-NIEVES, N. & BOTTINGER, E. P. (2004) Integration of TGF-beta/Smad and Jagged1/Notch signalling in epithelial-to-mesenchymal transition. *Embo J,* 23, 1155-65.

ZENG, Q., LI, S., CHEPEHA, D. B., GIORDANO, T. J., LI, J., ZHANG, H., POLVERINI, P. J., NOR, J., KITAJEWSKI, J. & WANG, C. Y. (2005) Crosstalk between tumor and endothelial cells promotes tumor angiogenesis by MAPK activation of Notch signaling. *Cancer Cell,* 8, 13-23.

Appendices

Two manuscripts related to my thesis work are attached.

The first is a review article written by me under the guidance of Professor Adrian Harris. It was published last year.

SHI, W. & HARRIS, A. L. (2006) Notch signaling in breast cancer and tumor angiogenesis: cross-talk and therapeutic potentials. *J Mammary Gland Biol Neoplasia,* 11, 41-52.

The second is a paper written by the Notch group in our laboratory. I contributed to Figure 2. The manuscript has been accepted for publication in September 2007.

HARRINGTON, L. S., SAINSON, R. C., WILLIAMS, C. K., TAYLOR, J. M., SHI, W., LI, J. L. & HARRIS, A. L. (2007) Regulation of multiple angiogenic pathways by Dll4 and Notch in human umbilical vein endothelial cells. *Microvasc Res,* 74, (accepted).

J Mammary Gland Biol Neoplasia (2006) 11: 41–52
DOI 10.1007/s10911-006-9011-7

Notch Signaling in Breast Cancer and Tumor Angiogenesis: Cross-Talk and Therapeutic Potentials

Wen Shi · Adrian L. Harris

Published online: 9 August 2006
© Springer Science + Business Media, Inc. 2006

Abstract Notch signaling is an evolutionarily conserved pathway that regulates numerous physiological processes. Disruption of Notch has been implicated in multiple tumor types. Evidence from *in vitro* experiments, mouse models and human tumor samples indicates that Notch plays a predominantly oncogenic role in breast cancer and interacts with other pathways involved in tumorigenesis. In addition, Notch signaling is required for physiological angiogenesis and may promote tumor angiogenesis. A variety of strategies for blocking Notch signaling, in particular γ-secretase inhibition, are discussed as potential therapies for breast cancer and tumor angiogenesis.

Keywords Notch signaling · Breast cancer · Angiogenesis · γ-Secretase inhibitors · Anti-Notch therapy

Abbreviations

Dll4	Delta-like 4
Jag1	Jagged1
RAM	RBP-jκ associated module
N-ICD	Notch intracellular domain
TACE	TNFα converting enzyme
RBP	re-combination-signal binding protein
CSL	CBF1, Suppressor of Hairless or Lag-1
Hes	hairy/enhancer of split
Hey	hairy/enhancer of split related with YRPW motif
GSI	γ-secretase inhibitor
HIF	hypoxia inducible factor
VEGF	vascular endothelial growth factor
MMTV	mouse mammary tumor virus
APC	adenomatous polyposis coli

W. Shi · A. L. Harris (✉)
Molecular Oncology Laboratories, Cancer Research UK,
Weatherall Institute of Molecular Medicine,
John Radcliffe Hospital, University of Oxford,
Headington, Oxford OX3 9DS, UK
e-mail: aharris.lab@cancer.org.uk

Introduction

The Notch gene was originally discovered in *Drosophila* because flies heterozygous for this gene displayed notches at their wing margins. Further analyses in flies indicated that loss-of-function mutations of Notch produced a lethal "neurogenic" phenotype, in which cells destined to become epidermis switch fate and give rise to neural tissue [1]. Notch signaling has also been studied in a variety of other organisms, including *Caenorhabditis elegans*, zebrafish and mammals, and the pathway is conserved from flies to humans. Notch signaling is involved in a wide range of physiological and pathological processes. This review provides an overview of Notch signaling in the context of breast cancer tumorigenesis and angiogenesis, highlighting the therapeutic potential of anti-Notch strategies.

Overview of Notch Signaling

There is a single Notch receptor and two ligands (Delta and Serrate) in *Drosophila*. In mammals, there are four receptors and five ligands, which are the focus of this review. Notch1–4 are homologues of *Drosophila* Notch; Delta-like-1, -3 and -4 (Dll1, Dll3, Dll4) are homologues of Delta; Jagged1 and Jagged2 (Jag1 and Jag2) are homologues of Serrate.

Each Notch receptor is synthesized as a full-length precursor protein consisting of extracellular, transmembrane

and intracellular domains. Within the Golgi apparatus, the precursor protein is cleaved by a furin-like convertase at a site called S1 and subsequently presented on the cell surface as a heterodimer, as shown in Fig. 1. One subunit of the heterodimer contains the majority of the extracellular domain; the other contains the remainder of the extracellular domain, the transmembrane domain and the intracellular domain. The two subunits are linked non-covalently forming a complete Type I receptor [2].

All four Notch receptors contain conserved sequences. Within the extracellular domain are a number of epidermal-growth-factor (EGF)-like repeats, followed by three cysteine-rich Notch/Lin12 (LN) repeats. EGF-like repeats 11 and 12 are involved in ligand binding. The intracellular domain contains a RAM domain, six Ankyrin (also known as CDC10) repeats flanked by nuclear localization signals, and a transactivation domain containing amino acid sequence PEST near the C-terminal. The intracellular domain is responsible for transducing Notch signaling to the nucleus [3].

Similar to the receptors, Notch ligands are also Type I transmembrane proteins. All five ligands possess the conserved N-terminal structure named DSL (Delta, Serrate or LAG-2 from *C. elegans*), followed by EGF-like repeats. Jagged ligands also contain a cysteine-rich domain that is not present in Delta-like ligands [3].

Notch signaling is normally activated by ligand-receptor binding between two neighboring cells. This interaction induces a conformational change in the receptor, exposing a cleavage site, S2, in its extracellular domain. After cleavage by the metalloprotease TACE and/or Kuzbanian, Notch receptor undergoes intramembrane proteolysis at cleavage site S3. This cleavage, mediated by the γ-secretase complex, liberates the Notch intracellular domain (N-ICD), which then translocates into the nucleus to activate Notch target genes (Fig. 2). Inhibiting γ-secretase function prevents the final cleavage of the Notch receptor, blocking Notch signal transduction.

In the absence of N-ICD cleavage, transcription of Notch target genes is inhibited by a repressor complex mediated by the protein RBP-jκ (also known as CBF1, CSL or Suppressor of Hairless in *Drosophila*, see Table 1). When N-ICD enters the nucleus, it disrupts the repressor complex, binds to RBP-jκ, switching it into a transcriptional activator. N-ICD then recruits co-activators such as Mastermind-like (MAML) and the histone acetyltransferase p300/CBP that activate Notch target gene transcription [4].

Notch Target Genes

The best-characterized Notch targets are transcriptional repressors of the Hes and Hey (also known as Herp, Hesr, Hrt or Chf) families (Table 1). Both Hes and Hey proteins contain a basic domain, which determines DNA binding specificity, and a helix-loop-helix domain, which allows the proteins to form homo- or hetero-dimers. Dimers of Hes and/or Hey proteins repress the transcription of a variety of genes by interacting with other co-repressors or sequestering transcriptional activators [5].

Several lines of evidence suggest that Hes-1, -5, -7 and Hey-1, -2, -L are primary targets of Notch signaling. Activation of Notch signaling upregulated Hes and Hey mRNA levels in the presence of cycloheximide, an inhibitor of de novo protein synthesis. This upregulation is

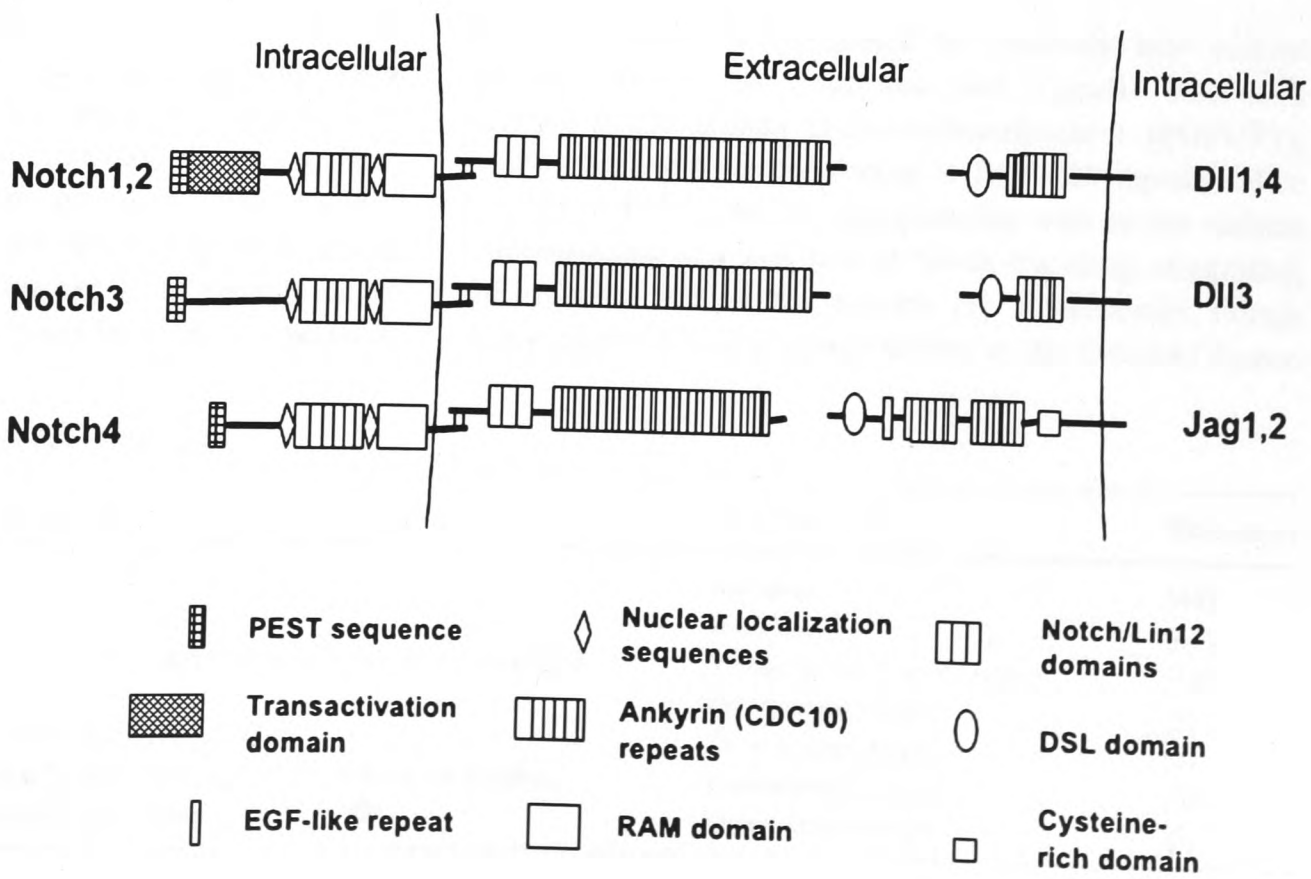


Figure 1 Mammalian Notch receptors and ligands. The extracellular domains of Notch receptors contain a number of EGF-like repeats followed by three Notch/Lin12 domains. The extracellular domains are connected to the transmembrane domains non-covalently. Within the intracellular domains, there is a RAM domain, six Ankyrin repeats flanked by nuclear localization signals and transactivation domains (in Notch1 and 2 only). Finally, the receptors contain a conserved PEST sequence near the C-terminus. Both the Delta-like and Jagged receptors contain a DSL domain followed by EGF-like repeats. Jagged ligands also contain a cysteine-rich domain.

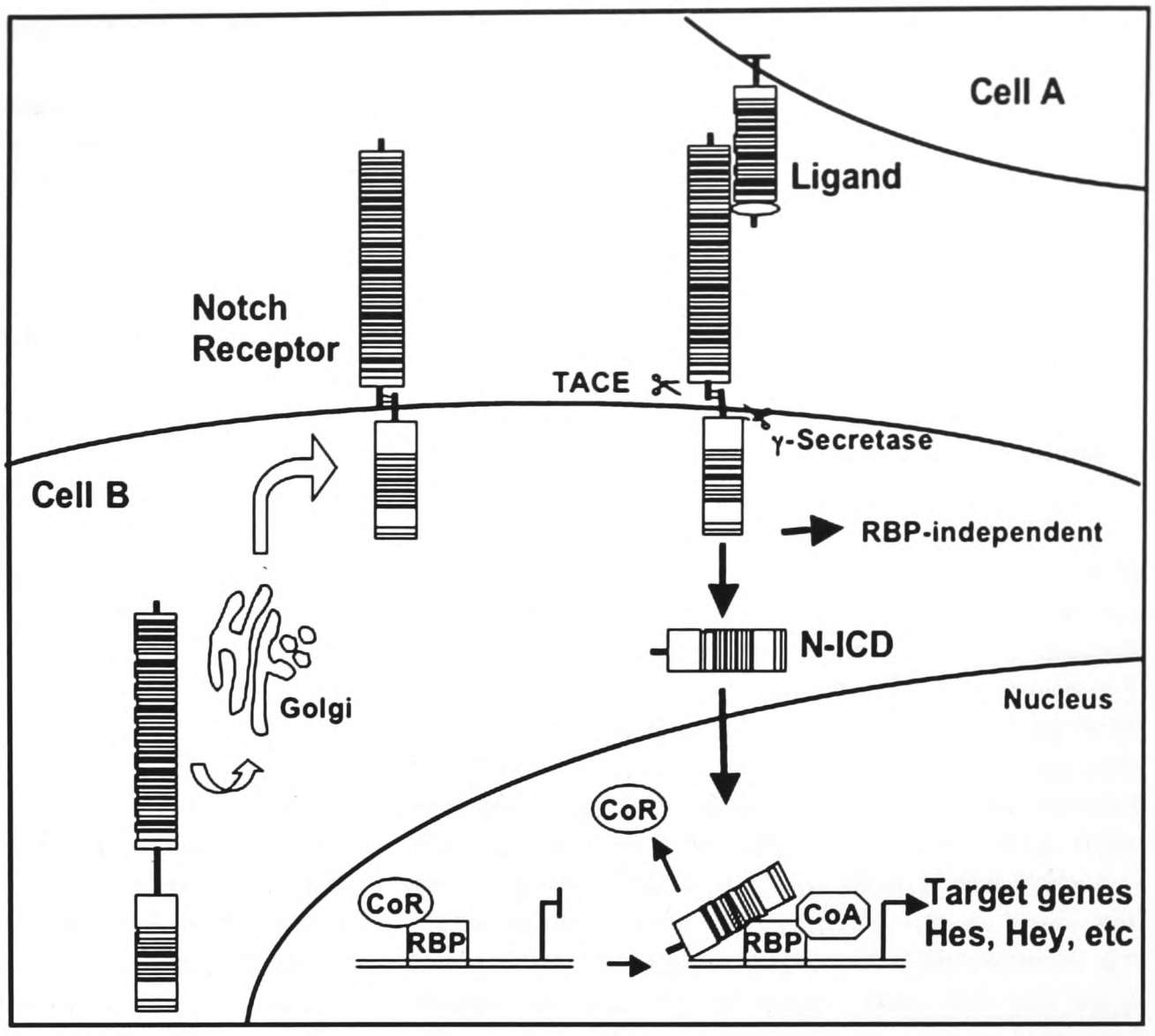


Figure 2 Ligand-mediated Notch signaling. Each Notch receptor is synthesized as a single precursor protein and then cleaved into a heterodimer within the Golgi apparatus. Upon ligand binding, the receptor undergoes a conformational change that allows cleavage by TACE/Kuzbanian. Next, the Notch receptor undergoes an intramembrane cleavage, mediated by γ-secretase, that liberates the Notch intercellular domain (N-ICD). N-ICD translocates into the nucleus, interacts with the transcription factor RBP-jκ and co-activators such as Mastermind-like and p300, and activates target genes of the Hes and Hey families.

dependent on RBP-jκ; further, promoters of Hes and Hey contain RBP-jκ binding sites [5]. Moreover, Hes and Hey are physiological effectors of Notch. Mice doubly deficient for Hes1 and Hes5 replicated the neurogenic phenotype of Notch1 knockout mice [6], while mice doubly deficient for Hey1 and Hey2 displayed an angiogenic phenotype similar to that of Notch1 knockout mice [7].

Recent studies in *Drosophila* have suggested that Notch can signal independently of the canonical Suppressor of Hairless (RBP-jκ homologue) pathway. However, it is unclear if this is the case in vertebrates. Some early evidence from myogenic cell lines and the developing avian neural crest suggests that Notch signaling can occur in the presence of dominant negative RBP-jκ, but additional characterization is needed to establish alternative downstream pathways in vertebrates [8].

Modulation of Notch Signaling

Notch signaling is modulated by enzymes that control glycosylation of the receptors and ligands. One such enzyme is the protein O-fucosyltransferase 1 (POFUT1), which transfers O-linked fucose to EGF-like repeats. Mice lacking POFUT1 died at mid-gestation with severe defects corresponding to a total loss of Notch signaling, suggesting the essential role of this enzyme [9]. Additionally, Fringe enzymes add N-acetyl-glucosamines to the O-linked fucose

Table 1 Nomenclature for Notch pathway components.

Name used in this review	Other names	Function	References
Notch1	TAN1	Receptor	[44]
Notch4	INT3	Receptor	[41]
RBP-jκ	CBF1, CSL, Suppressor of Hairless (*Drosophila*)	Transcriptional co-activator	[13]
Hes-1, -5, -7		Downstream target	[5]
Hey1	Hesr1, Hrt1, Herp2, Chf2	Downstream target	[5]
Hey2	Hesr2, Hrt2, Herp1, Chf1, Gridlock (Zebrafish)	Downstream target	[5]
HeyL	Hesr3, Hrt3, Herp3	Downstream target	[5]

and thus affect the binding affinity of Notch receptors and ligands [10].

Notch signaling is also regulated by ubiquitination and proteolysis. Several E3 ubiquitin ligases transfer ubiquitin to Notch pathway components, targeting them for degradation [11, 12]. Su(dx)/Itch and Cbl both target membrane-bound Notch receptors for endocytosis and degradation in the lysosome. In contrast, Sel-10 ubiquitinates N-ICD in the nucleus, thereby limiting Notch signaling following receptor activation. Mindbomb and Neuralized interact with the intracellular domain of Delta-like ligands to promote their ubiquitination and internalization. Without ligand internalization, Notch activation in adjacent cells may be suppressed. Finally, LNX (ligand of Numb-protein X) regulates the Notch antagonist Numb. It has been proposed that LNX promotes Notch signaling by targeting Numb for proteasomal degradation [12].

Physiological Notch Signaling

Notch signaling regulates a variety of cellular processes, including stem cell maintenance, cellular differentiation, proliferation and apoptosis. Notch inhibits differentiation in the developing nervous system, muscles, intestines and T-cells, but promotes differentiation in the skin. In addition, Notch signaling participates in cell-fate decisions. For example, during mouse lymphopoiesis, thymic epithelial cells expressing Notch ligands induce lymphocyte precursors to adopt the T-cell fate; in the absence of such signals, the precursors adopt the B-cell fate as the default pathway [3, 13].

Due to its role in regulating cellular differentiation and specifying cell fate, Notch signaling is critical in the development of multicellular organisms. In mammals, loss of Notch signaling leads to embryonic lethality due to severe defects in somitogenesis, angiogenesis, cardiogenesis and neurogenesis. Notch signaling also regulates the development of postnatal and adult tissues [1].

Notch Signaling in Cancer

Just as Notch signaling is important in regulating numerous physiological processes, disruption of Notch has been implicated in a variety of hematological and solid cancers. The best-studied example is the link between mutations of Notch1 and T-cell acute lymphoblastic leukemia and lymphoma (T-ALL). In a subset of T-ALL tumor cells, a t(7;9) chromosomal translocation fuses the 3′ portion of Notch1 to the T-cell receptor Jβ locus. This results in a truncated Notch1 protein, which is constitutively active and aberrantly expressed (Fig. 3) [14]. In addition, activating mutations in Notch1 independent of the t(7;9) translocation have been found in more than 50% of human T-ALL cases [15].

Abnormal Notch signaling has also been reported in solid tumors, including cancers of the breast, kidney, pancreas, prostate, cervix, endometrium, brain, intestine, lung and skin, although without evidence of genetic lesions [3, 13]. Notch may play either an oncogenic or a tumor-suppressive role, depending on the cancer type, other signaling pathways present and the identity of Notch receptor activated. However, in a large majority of cases including breast cancer, Notch signaling promotes tumor growth [16].

One mechanism for the oncogenic role of Notch may derive from its ability to prevent differentiation and maintain the stem cell phenotype. Stem cells and tumor cells share common characteristics, such as unlimited proliferation and undifferentiation. Further, self-renewal in stem cells and tumor cells are regulated by similar pathways, including sonic hedgehog, Wnt and Notch. It is possible that tumor cells may derive from normal stem cells or that cancers may harbor "cancer stem cells" that are resistant to treatment [17].

The role of Notch signaling in stem cells versus cancer cells has been elucidated in the intestine. The intestinal epithelium consists of differentiated villi and proliferative crypts. The maintenance of stem cells, located in the crypts, depends on both Wnt and Notch signals [18]. Intestine-specific deletion of RBP-jκ in mice turned on genes normally repressed by Notch

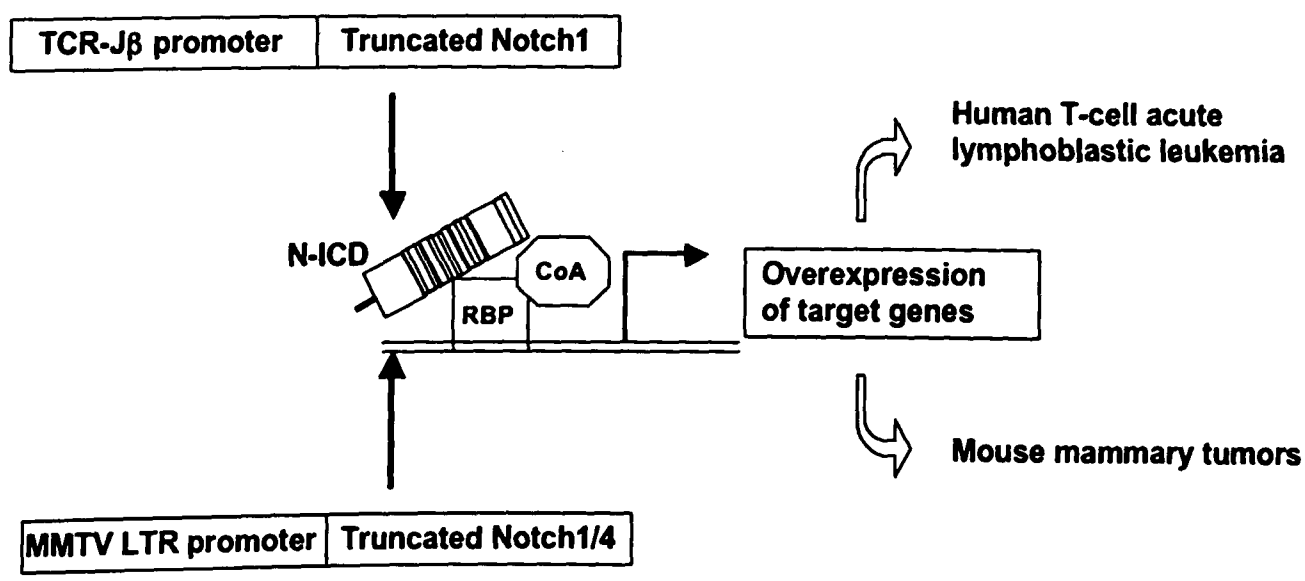


Figure 3 Constitutive activation of Notch signaling. Chromosomal translocation t(7;9) in humans juxtaposes the 3′ portion of Notch1 with the T-cell receptor Jβ promoter. This results in constitutive activation of the Notch1 intracellular domain and human T-ALL cases. The mouse mammary tumor virus may insert into the *Notch1* or *Notch4* locus and lead to truncated Notch1 and Notch4 proteins. The constitutively active Notch proteins cause mouse mammary tumors. This figure is adapted from [83].

downstream genes, and converted proliferative crypt cells into differentiated goblet cells [19]. In contrast, overexpression of Notch1-ICD in murine intestinal epithelium prevented differentiation of crypt cells [20].

Notch signaling may play similar roles in stem cells of the breast. In an *in vitro* model, Notch induced mammary stem cells to self-renew and early progenitor cells to proliferate. This effect was inhibited by Notch4 neutralizing antibody or γ-secretase inhibitor (GSI) treatment. Notch signaling had no effect on differentiated mammary epithelial cells [21]. Notch regulation of mammary stem cells may involve the protein Musashi1 (Msi1). Msi1 activates Notch signaling by translationally repressing the Notch antagonist Numb, and plays essential roles in maintaining neural stem cells [22]. Recently, Msi1 has been proposed as a marker for mammary stem cells. In putative stem cells positive for Msi1, Notch1 was undetectable at the cell surface by antibodies against the intracellular domain, suggestive of Notch receptor activation and cleavage. Interestingly, both Msi1 and Notch1 proteins were absent in human breast cancer samples [23].

Notch signaling may interact with the hypoxia-sensing pathway to synergistically promote the stem cell phenotype. The transcription factor HIF-1, which regulates most hypoxia responses, consists of α and β subunits. Under normoxia, HIF-1α is hydroxylated at two proline residues and ubiquitinated by the von Hippel-Lindau (VHL) complex, targeting it for proteasomal degradation. Under hypoxia, hydroxylation does not occur and HIF-1α is not degraded. Instead, it translocates to the nucleus, binds to the HIF-1β subunit and activates transcription. A related protein, HIF-2α, also binds HIF-1β and upregulates a different set of hypoxia genes [24]. Recent data point to the interaction of the Notch and hypoxia pathways. In neuronal stem cells and muscle precursors, hypoxia activated Notch downstream genes and promoted the undifferentiated state in a Notch-dependent manner, as shown in Fig. 4. In addition, HIF-1α interacted with Notch1-ICD, enhancing its stability. Moreover, upon Notch activation under hypoxia, HIF-1α was recruited to the promoter of the Notch target gene Hey2 [25]. This interaction may have implications for tumor growth. The hypoxia response upregulates a number of pathways conducive for tumor survival, such as angiogenesis, cell survival, glucose metabolism and invasion. Inhibiting HIF-1 has been explored as a cancer therapy [26].

Evidence already suggests that Notch–hypoxia cross-talk is not limited to stem and precursor cells. In neuroblastomas, hypoxia upregulated Notch1 and Hes1, normally expressed in the neural crest during development. This altered gene expression resulted in de-differentiation and a more aggressive tumor [27]. Notch signaling impinges on the hypoxia pathway as well. In the breast cancer cell line MCF7, overexpression of full-length Notch1 or Notch1-ICD upregulated HIF-1α protein levels [28]. Additionally, Hey2 is known to interact with HIF-1β and block induction of the hypoxia-regulated gene VEGF by HIF-2α [29], suggesting the relationship between Notch and hypoxia signaling may be synergistic or antagonistic, depending on the HIF protein involved and cellular context.

The Notch pathway interacts with not only hypoxia but also other signaling pathways involved in tumorigenesis. For example, Notch and Ras signaling synergize for oncogenic activity. In Ras-transformed fibroblasts, Notch1, Notch4 and Dll4 were upregulated. Inhibiting Notch signaling by antisense RNA or GSI reduced proliferation of Ras-transformed cells and their tumor-formation ability *in vivo* [30]. In another study, among mice transgenic for human Ras, 80% developed mammary tumors within 10 months. In comparison, among mice transgenic for both Ras and the Notch antagonist Deltex, only 20% developed mammary tumors in the same period [31]. On the other hand, Ras signaling is required for Notch4-induced transformation. Treatment with Ras pathway inhibitors decreased the colony-formation ability of mammary tumor cells overexpressing Notch4-ICD. Dominant negative Ras also reduced the growth of Notch4-ICD-expressing tumor cells in xenograft models [32].

Notch signaling also interacts with the TGFβ pathway, which plays a dual role in tumor development. During early stages, TGFβ acts as a tumor suppressor by inhibiting proliferation; during later stages, it functions as an oncogene by promoting invasion and metastasis through an epithelial–mesenchymal transition (EMT) [13]. Notch signaling is involved in both these roles. The cervical cancer cell line CaSki, which spontaneously activates Notch1, did not show growth inhibition in response to TGFβ [33]. Similarly, the MCF7 cell line expresses Notch4 and was resistant to the growth-inhibitory effects of TGFβ; blocking Notch receptor processing by GSI restored growth inhibition [34]. However, Notch and TGFβ signaling may act synergistically. Activation of TGFβ pathway led to upregulation of Notch target genes via interactions between the TGFβ effector Smad3 and Notch1-ICD [35]. At the onset of EMT, TGFβ induced Hey1 in mammary epithelial cells. Treatment with Hey1 antisense RNA or GSI blocked TGFβ-induced EMT [36]. Taken together, Notch signaling antagonizes or synergizes with TGFβ, but promotes tumor growth in either case.

Complex cross-talk also occurs between Notch and Wnt pathways. As mentioned before, Notch and Wnt signals cooperate to promote the stem cell phenotype. One possible link between these two pathways is the kinase GSK-3β. In the absence of Wnt agonists, GSK-3β phosphorylates β-catenin, leading to its degradation and preventing Wnt signal transduction. GSK-3β also phosphorylated Notch2 and inhibited downstream gene Hes1. Wnt1 overexpression, which represses GSK-3β, led to the activation of the

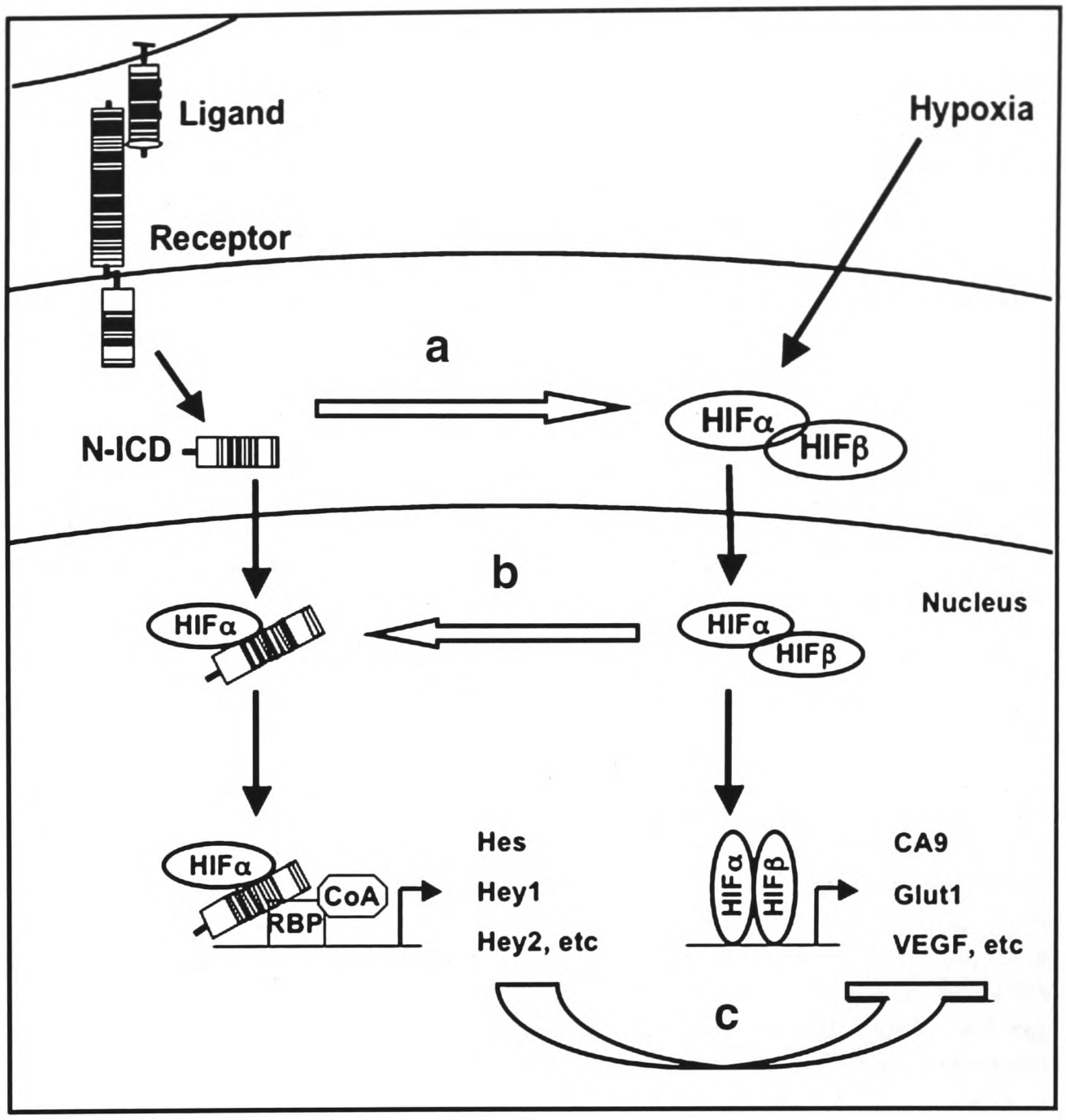


Figure 4 Cross-talk of Notch and hypoxia-sensing pathways. Notch signaling (*depicted on the left*) and hypoxia signaling (*depicted on the right*) may interact both synergistically and antagonistically. (a) In MCF7 cells, overexpression of N-ICD increased HIF-1α protein levels by an unknown mechanism. (b) In stem cells, HIF-1α was recruited to the promoter of Notch target genes, and promoted Notch signaling and stem cell phenotype. Hypoxia also upregulated Notch pathway components in neuroblastomas. (c) Notch target gene Hey2 may interact with HIF-1β and block the hypoxia induction of VEGF by HIF-2α.

Hes1 promoter [37]. Other evidence suggests an antagonistic relationship between Notch and Wnt pathways. Wnt1 promoted branching morphogenesis of the murine mammary epithelial cell line TAC-2 while Notch4-ICD inhibited branching. Co-expression of Wnt1 overcame Notch4-mediated inhibition [38].

For a list of major signaling pathways known to interact with Notch, see Table 2.

Notch Signaling in Breast Cancer

The causal link between Notch signaling and breast cancer has been established by a series of experiments in mouse models, which have been reviewed previously [12, 39]. The first indication came from a study of the mouse mammary tumor virus (MMTV) in Czech II mice. MMTV itself does not have transformation ability; however, its insertion into the mouse genome may activate flanking proto-oncogenes and cause malignant transformation of the mammary gland. According to one study, in 20% (9 out of 45) of the mammary tumors thus developed, MMTV was inserted into the *Notch4* locus, originally referred to as *int3* [40]. These insertions resulted in truncated Notch4/Int3 proteins, which contain the trans-

Table 2 Signaling pathways that interact with Notch.

Pathway	Synergistic (S) with or Antagonistic (A) to Notch	References
HIF1α	S	[25, 27, 28]
HIF2α	A	[29]
Ras	S	[30–32]
EGFR	S	[74, 79]
TGFβ//BMP	A	[33, 34, 80]
	S	[35, 36, 80]
Wnt	A	[38]
	S	[18, 37]
ErbB2/Neu	S	[44, 51, 52]
Estrogen	S	[28]
PTEN	S	[81]
JAK-STAT	S	[82]

membrane and intracellular domains and are constitutively active (Fig. 3). The gain-of-function mutation profoundly altered mammary growth and differentiation, resulting in spontaneous mammary tumors [41].

Additional confirmation for the oncogenic activity of Notch4 in the murine mammary gland came from transgenic studies. Truncated Notch4/Int3 genes were expressed in mice under the control of either the MMTV long terminal repeat or the whey acidic protein promoter [42, 43]. In both studies, murine mammary glands did not develop normally, and mammary carcinomas were formed with subsequent metastasis to the lungs.

Besides Notch4, Notch1 is also involved in mammary tumorigenesis. Mice overexpressing the oncogene erbB2/neu were infected with MMTV, and among the tumors developed, 2 out of 24 had MMTV insertion into the *Notch1* locus. Similar to Notch4/Int3, the resulting Notch1 proteins also lacked the extracellular domain and were constitutively active [44]. This result suggests that Notch1 may cooperate with erbB2/neu in tumorigenesis.

The evidence has been less robust for the involvement of Notch signaling in human breast cancer. Callahan and colleagues identified a novel truncated form of Notch4 in several human breast, lung and colon cancer cell lines [45]. The short form, which they named h-Int3sh, consists of only partial Ankyrin repeats and residues C-terminal to them, but lacks the transmembrane domain and the RAM domain. H-Int3sh transformed "normal" human mammary epithelial cell line MCF10A *in vitro*. In a follow-up study, mice transgenic for h-Int3sh developed mammary tumors, but with a long latency (average 18 months). In contrast, mice transgenic for murine Notch4/Int3 developed tumors earlier (average 4.5 months) and with higher frequency [46]. Recently, Artavanis-Tsakonas and colleagues developed a transgenic mouse model with human Notch1-ICD under the control of the MMTV long terminal repeat. These mice developed lactation-dependent tumors that evolved into adenocarcinomas [31].

Other studies have investigated the expression of Notch pathway components in human breast cancer samples. In most studies, mRNA of various genes was detected using *in situ* hybridization or quantitative real-time PCR (qPCR) [47, 48]. These methods do not require antibodies; however, they cannot detect Notch proteins. A more informative method of assessing Notch expression in tumor samples is measuring protein levels by immunohistochemistry [30, 48, 49]. Activated Notch receptors can only be detected at the protein level by determining its cellular localization [23].

Notch pathway components may be differentially expressed in normal breast tissues versus breast cancers of different grades. In one study, all seven tumors expressed Notch1 protein, while normal samples expressed little or no Notch1 protein [30]. According to another study, Notch1 and Notch4 were undetectable in normal samples; only Notch1 was expressed in ductal hyperplasias. Both Notch1 and Notch4 were expressed in a portion of ductal carcinomas *in situ* [50]. In a third study examining 97 samples, Notch1 mRNA level was higher in more aggressive tumors while Notch2 mRNA level was higher in less aggressive tumors [47]. This is the only evidence to date suggesting that a Notch receptor might play a tumor-suppressive role in breast cancer.

A recent study demonstrated that the Notch antagonist Numb plays a role in breast tumorigenesis [49]. Normal breast tissues expressed Numb; however, 50% of human breast tumors exhibited reduced levels of Numb. Numb protein expression negatively correlated with the grade of the tumors. In primary cultures of breast cancer cells expressing low levels of Numb, reintroduction of Numb protein decreased Notch signaling and colony-formation ability. Conversely, in breast cancer cells expressing high levels of Numb, RNAi-mediated knockdown of Numb increased Notch signaling and colony-formation ability. These results provide interesting therapeutic possibilities for breast cancer by inhibiting Notch signaling or restoring Numb levels.

The expression levels of certain Notch genes may also be a prognostic marker for breast cancer patient survival. Egan and colleagues studied the expression of multiple Notch receptors and ligands in 184 tumors using *in situ* hybridization [48]. High Notch1 or Jag1 expression (in the top quartile) predicted poor overall survival for the patient. Tumors expressing high levels of both Notch1 and Jag1 indicated even worse survival, suggestive of a synergistic relationship between the two genes.

Overall, evidence suggests that Notch signaling plays an oncogenic role in human breast cancer. This may be facilitated by Notch cooperating with two signaling pathways important in breast tumorigenesis: erbB2/neu and estrogen. In addition to the possible interaction between Notch1 and erbB2 in the mouse model mentioned above [44], RBP-jκ was able to bind to the promoter of the human erbB2 gene and enhance basal transcription by 16-fold. Notch-ICD further increased RBP-jκ-mediated transcription of erbB2 by 82-fold [51]. Several breast cancer cell lines that overexpress erbB2 exhibited marked activation of Notch1, which was abrogated by an erbB2 antagonist [52]. Estrogen is another crucial player in breast cancer. In the estrogen-sensitive cell line MCF7, 17β-estradiol treatment upregulated Notch1 and Jag1, and promoted Jag1-induced Notch signaling [28].

Notch Signaling in Angiogenesis

The role of Notch signaling in both physiological and pathological angiogenesis has long been recognized. Notch

pathway mutations have been linked to several vascular diseases [53]. One is the neurovascular disorder, cerebral autosomal dominant arteriopathy with subcortical infarcts and leukoencephalopathy (CADASIL). Patients suffer from neurological symptoms resulting from the destruction of the vascular smooth muscle cells surrounding the cerebral arteries. The CADASIL phenotype correlates with missense mutations in Notch3 in a majority of patients, suggesting a role for Notch3 in maintaining vascular smooth muscle cells. In addition, the Notch ligand Jag1 has been implicated in Alagille syndrome (AGS). Mutations in Jag1 have been identified in 60–70% cases of AGS, a multi-organ developmental disorder with notable vascular phenotypes.

Direct evidence for Notch signal transduction in angiogenesis has come from a variety of *in vivo* and *in vitro* studies in which Notch pathway components were downregulated or overexpressed. Homozygous deletion of Notch1 in mice, either globally or endothelial-specifically, caused vascular remodeling defects in the yolk sac, placenta and embryo proper, leading to embryonic lethality by day E10.5 [54, 55]. Notch4 is specifically expressed in arterial endothelial cells [56]; however, Notch4-null mice developed normally and were fertile. Interestingly, homozygous deletions of both Notch1 and Notch4 had a synergistic effect, as the double mutant mice exhibited more severe vascular defects than Notch1-null mice [54]. Overexpression of Notch4 also caused vascular abnormalities. Expression of activated Notch4 in the mouse embryonic vasculature led to angiogenic defects similar to that of the Notch1/4 double knockout mice [57]. Taken together, these results indicate that either reduction or constitutive activation of Notch disrupts blood vessel development, suggesting an optimal range of Notch signaling is required for angiogenesis.

The angiogenic role of Notch signaling extends beyond embryonic development. Expression of activated Notch4 in adult mice using a tetracycline-repressible system led to arteriovenous malformations (AVM) in the liver and lethality within weeks. Notch4 overexpression induced hepatic vascular shunting, arterialization and induction of other Notch pathway genes. The AVM was reversible in moribund mice after suppression of Notch4 with doxycycline [58].

The recent discovery of Dll4 as an endothelial-specific Notch ligand [59] has expanded our understanding of the link between Notch and angiogenesis. Dll4 is expressed in the arterial endothelium during mouse embryogenesis; its expression level is reduced in most adult tissues [60]. Notably, mice heterozygous for Dll4 mutation displayed vascular remodeling defects, growth retardation and embryonic lethality, indicating Dll4 haploinsufficiency [61–63]. The dosage-sensitive requirement for Dll4 is reminiscent of that of the angiogenic master switch VEGF [64, 65] but is unique among the Notch ligands and receptors.

In primary endothelial cells, Dll4 mRNA levels were induced by either VEGF or hypoxia [66, 67]. We have also demonstrated that either RNAi-mediated downregulation or retroviral overexpression of Dll4 in endothelial cells inhibited proliferation, migration and network formation, all crucial processes in angiogenesis [67, 68]. In both cases, cell cycle arrest in G0–G1 was observed, indicating that an optimal window of Dll4 expression is essential for angiogenesis.

Further *in vitro* evidence points to the critical role of Notch signaling in angiogenesis. Expression of dominant negative Notch1 or Notch4 disrupted endothelial network formation, as did knockdown or overexpression of the Notch effector Hey1 [69, 70]. Activated Notch signaling also inhibited endothelial sprouting and induced cell cycle arrest [71, 72]. On the other hand, Sainson et al. [73] showed autonomous Notch signaling inhibited proliferation and enhanced vessel diameter in an *in vitro* 3-dimensional angiogenesis model.

Notch Signaling in Tumor Angiogenesis

Tumor angiogenesis involves many of the same pathways as physiological angiogenesis, including Notch. This has been shown in both human tumor samples and mouse xenografts. Measured by *in situ* hybridization and qPCR, Dll4 mRNA was undetectable in normal kidney or breast samples, but highly expressed in the vasculature of human clear-cell renal cell carcinomas and breast cancers. Among the tumor samples, Dll4 expression positively correlated with VEGF expression at the mRNA level [67]. In a xenograft study, the human MCF7 cell line, which does not express Dll4, resulted in tumors expressing high levels of mouse Dll4 within their vasculature [60]. Currently, the study of Dll4 expression in tumors is hampered by the lack of a good monoclonal antibody. Work is underway to develop antibodies that allow measurement of Dll4 protein levels by immunohistochemistry.

The best-characterized example of Notch signaling in tumor angiogenesis involves the ligand Jag1. In a series of elegant experiments, Wang and colleagues demonstrated that Jag1 expressed in head and neck squamous cell carcinoma (HNSCC) cells triggered Notch activation in neighboring endothelial cells and promoted network formation. This effect was abolished by blocking Notch signaling through γ-secretase inhibition, soluble Jag1 treatment or dominant negative RBP-jκ expression in the endothelial cells. In xenograft models, HNSCC cells overexpressing Jag1 formed larger tumors with increased vascularization. Moreover, Jag1 protein levels were significantly higher in human HNSCC samples compared with dysplasias and normal samples. Jag1 protein levels corre-

lated with vascular density in tumors [74]. These results are exciting as they provide the first causal link between Notch signaling and tumor angiogenesis, and describe a novel mechanism of juxtacrine signaling from tumors to the surrounding vasculature.

Preliminary data suggest that Notch signaling may play a role in breast cancer angiogenesis as well. Estrogen upregulated Jag1 and Notch1 expression in both MCF7 cells and endothelial cells and promoted network formation in the latter [28]. Notch3 was highly expressed in neovessels in human breast tumors, suggesting a role for this receptor in blood vessel maintenance [12].

Possibilities for Anti-Notch Therapy in Cancer

Notch signaling plays an oncogenic role in a majority of hematological and solid tumors including breast cancer; furthermore, it is required for angiogenesis during development and possibly in tumor angiogenesis. Therefore, Notch inhibition may represent a viable treatment for cancer. A number of genetic and pharmacological strategies are either available or theoretically possible to block Notch signaling at different points of the pathway [16]. For example, Notch receptors and ligands may be inhibited by monoclonal antibodies or RNAi-mediated silencing. Small molecule inhibitors for individual receptors and ligands are not yet available. Ligand-mediated receptor activation may be blocked by soluble ligands [74], receptor decoys [75], or inhibition of enzymes involved in glycosylation or cleavage of the receptors. Downstream pathway components RBP-jκ, MAML, HES and HEY are further targets for Notch inhibition. Alternatively, Notch antagonists such as Numb and Deltex may be upregulated by therapy.

The best-developed tool for Notch signaling inhibition is the small molecule inhibitor of γ-secretase. A number of such GSIs have been developed, since γ-secretase also cleaves β-amyloid peptides, known to play a key role in plaque formation in Alzheimer's disease [76].

Experiments using GSIs to inhibit tumorigenesis and angiogenesis *in vivo* have shown promising results. One study involved mice carrying a mutation of the APC tumor suppressor gene. These mice spontaneously develop multiple intestinal adenomas overexpressing Notch target genes such as Hes1. Treatment with GSI downregulated Hes1 and turned proliferative adenoma cells into differentiated Goblet cells [19].

Kaposi's sarcoma (KS) is a type of tumor that derives from endothelial cells. Activated forms of Notch-1, -2, -4 as well as Hey1 and Hey2 are markedly overexpressed in KS tumor samples and cell lines compared with endothelial cells. GSI treatment reduced Notch signaling and caused apoptosis of KS cells *in vitro*. In xenograft models of KS tumors, intratumoral injection of GSI inhibited tumor growth by decreasing proliferation and increasing apoptosis [77].

In addition to targeting several types of cancers, GSIs may also be used to inhibit tumor angiogenesis. Several different GSIs reduced endothelial cell proliferation, tube formation and microvessel outgrowths *in vitro*. In mouse models of human glioblastomas and lung adenocarcinomas, both highly vascularized tumors, the γ-secretase inhibitor DAPT potently reduced tumor growth and vascularization [78].

There are several advantages for using GSIs as anti-tumoral and anti-angiogenic agents. They are small molecule inhibitors and have superior pharmacological properties to antibodies or siRNAs. They are relatively easy to produce and cheaper in cost. Several GSIs of different chemical compositions are available from research into drugs for Alzheimer's disease. The major downside of GSIs is their non-specificity, as they target all Notch receptors (and an increasing list of other transmembrane proteins). Since Notch signaling is required for many physiological processes, GSI treatment may cause widespread toxicity. Therefore, specific inhibitors targeting individual Notch pathway components overexpressed in different cancer types may need to be developed. Systemic toxicity may also be ameliorated by localized release of anti-tumoral agents. Notably, both Notch4 and Dll4 are specifically expressed in developing blood vessels, in particular tumor vasculature in adults. Antibodies recognizing Notch4 or Dll4 may be coupled with chemotherapeutic or anti-angiogenic drugs for targeted delivery.

Acknowledgments Research in the lab of A.L.H. is funded by Cancer Research UK and the Sixth Framework Program of the European Union (Angiotargeting). W.S. is a Rhodes Scholar. We would like to thank Drs. Ji-Liang Li, Richard Sainson, Laura Harrington, John Moore and Ms. Cassin Williams for helpful discussions.

References

1. Artavanis-Tsakonas S, Rand MD, Lake RJ. Notch signaling: cell fate control and signal integration in development. Science 1999;284(5415):770–6.
2. Blaumueller CM, Qi H, Zagouras P, Artavanis-Tsakonas S. Intracellular cleavage of Notch leads to a heterodimeric receptor on the plasma membrane. Cell 1997;90(2):281–91.
3. Radtke F, Raj K. The role of Notch in tumorigenesis: oncogene or tumour suppressor? Nat Rev Cancer 2003;3(10):756–67.
4. Wu L, Griffin JD. Modulation of Notch signaling by mastermind-like (MAML) transcriptional co-activators and their involvement in tumorigenesis. Semin Cancer Biol 2004;14(5):348–56.
5. Iso T, Kedes L, Hamamori Y. HES and HERP families: multiple effectors of the Notch signaling pathway. J Cell Physiol 2003;194 (3):237–55.
6. Kageyama R, Ohtsuka T. The Notch–Hes pathway in mammalian neural development. Cell Res 1999;9(3):179–88.

7. Fischer A, Schumacher N, Maier M, Sendtner M, Gessler M. The Notch target genes Hey1 and Hey2 are required for embryonic vascular development. Genes Dev 2004;18(8):901–11.
8. Martinez Arias A, Zecchini V, Brennan K. CSL-independent Notch signalling: a checkpoint in cell fate decisions during development? Curr Opin Genet Dev 2002;12(5):524–33.
9. Shi S, Stanley P. Protein O-fucosyltransferase 1 is an essential component of Notch signaling pathways. Proc Natl Acad Sci USA 2003;100(9):5234–9.
10. Haltiwanger RS, Stanley P. Modulation of receptor signaling by glycosylation: fringe is an O-fucose-beta1,3-N-acetylglucosaminyltransferase. Biochim Biophys Acta 2002;1573(3):328–35.
11. Lai EC. Protein degradation: four E3s for the notch pathway. Curr Biol 2002;12(2):R74–8.
12. Callahan R, Egan SE. Notch signaling in mammary development and oncogenesis. J Mammary Gland Biol Neoplasia 2004;9 (2):145–63.
13. Leong KG, Karsan A. Recent insights into the role of Notch signaling in tumorigenesis. Blood 2005.
14. Ellisen LW, Bird J, West DC, Soreng AL, Reynolds TC, Smith SD, Sklar J. TAN-1, the human homolog of the Drosophila notch gene, is broken by chromosomal translocations in T lymphoblastic neoplasms. Cell 1991;66(4):649–61.
15. Weng AP, Ferrando AA, Lee W, Morris JPt, Silverman LB, Sanchez-Irizarry C, Blacklow SC, Look AT, Aster JC. Activating mutations of NOTCH1 in human T cell acute lymphoblastic leukemia. Science 2004;306(5694):269–71.
16. Nickoloff BJ, Osborne BA, Miele L. Notch signaling as a therapeutic target in cancer: a new approach to the development of cell fate modifying agents. Oncogene 2003;22(42):6598–608.
17. Reya T, Morrison SJ, Clarke MF, Weissman IL. Stem cells, cancer, and cancer stem cells. Nature 2001;414(6859):105–11.
18. van Es JH, Clevers H. Notch and Wnt inhibitors as potential new drugs for intestinal neoplastic disease. Trends Mol Med 2005;11 (11):496–502.
19. van Es JH, van Gijn ME, Riccio O, van den Born M, Vooijs M, Begthel H, Cozijnsen M, Robine S, Winton DJ, Radtke F, Clevers H. Notch/gamma-secretase inhibition turns proliferative cells in intestinal crypts and adenomas into goblet cells. Nature 2005;435 (7044):959–63.
20. Fre S, Huyghe M, Mourikis P, Robine S, Louvard D, Artavanis-Tsakonas S. Notch signals control the fate of immature progenitor cells in the intestine. Nature 2005;435(7044):964–8.
21. Dontu G, Al-Hajj M, Abdallah WM, Clarke MF, Wicha MS. Stem cells in normal breast development and breast cancer. Cell Prolif 2003;36 Suppl 1:59–72.
22. Okano H, Imai T, Okabe M. Musashi: a translational regulator of cell fate. J Cell Sci 2002;115(Pt 7):1355–9.
23. Clarke RB, Spence K, Anderson E, Howell A, Okano H, Potten CS. A putative human breast stem cell population is enriched for steroid receptor-positive cells. Dev Biol 2005;277(2):443–56.
24. Harris AL. Hypoxia—a key regulatory factor in tumour growth. Nat Rev Cancer 2002;2(1):38–47.
25. Gustafsson MV, Zheng X, Pereira T, Gradin K, Jin S, Lundkvist J, Ruas JL, Poellinger L, Lendahl U, Bondesson M. Hypoxia requires notch signaling to maintain the undifferentiated cell state. Dev Cell 2005;9(5):617–28.
26. Semenza GL. Targeting HIF-1 for cancer therapy. Nat Rev Cancer 2003;3(10):721–32.
27. Jogi A, Ora I, Nilsson H, Lindeheim A, Makino Y, Poellinger L, Axelson H, Pahlman S. Hypoxia alters gene expression in human neuroblastoma cells toward an immature and neural crest-like phenotype. Proc Natl Acad Sci USA 2002;99(10):7021–6.
28. Soares R, Balogh G, Guo S, Gartner F, Russo J, Schmitt F. Evidence for the notch signaling pathway on the role of estrogen in angiogenesis. Mol Endocrinol 2004;18(9):2333–43.
29. Chin MT, Maemura K, Fukumoto S, Jain MK, Layne MD, Watanabe M, Hsieh CM, Lee ME. Cardiovascular basic helix loop helix factor 1, a novel transcriptional repressor expressed preferentially in the developing and adult cardiovascular system. J Biol Chem 2000;275(9):6381–7.
30. Weijzen S, Rizzo P, Braid M, Vaishnav R, Jonkheer SM, Zlobin A, Osborne BA, Gottipati S, Aster JC, Hahn WC, Rudolf M, Siziopikou K, Kast WM, Miele L. Activation of Notch-1 signaling maintains the neoplastic phenotype in human Ras-transformed cells. Nat Med 2002;8(9):979–86.
31. Kiaris H, Politi K, Grimm LM, Szabolcs M, Fisher P, Efstratiadis A, Artavanis-Tsakonas S. Modulation of notch signaling elicits signature tumors and inhibits hras1-induced oncogenesis in the mouse mammary epithelium. Am J Pathol 2004;165(2):695–705.
32. Fitzgerald K, Harrington A, Leder P. Ras pathway signals are required for notch-mediated oncogenesis. Oncogene 2000;19 (37):4191–8.
33. Masuda S, Kumano K, Shimizu K, Imai Y, Kurokawa M, Ogawa S, Miyagishi M, Taira K, Hirai H, Chiba S. Notch1 oncoprotein antagonizes TGF-beta/Smad-mediated cell growth suppression via sequestration of coactivator p300. Cancer Sci 2005;96(5):274–82.
34. Sun Y, Lowther W, Kato K, Bianco C, Kenney N, Strizzi L, Raafat D, Hirota M, Khan NI, Bargo S, Jones B, Salomon D, Callahan R. Notch4 intracellular domain binding to Smad3 and inhibition of the TGF-beta signaling. Oncogene 2005;24 (34):5365–74.
35. Blokzijl A, Dahlqvist C, Reissmann E, Falk A, Moliner A, Lendahl U, Ibanez CF. Cross-talk between the Notch and TGF-beta signaling pathways mediated by interaction of the Notch intracellular domain with Smad3. J Cell Biol 2003;163(4):723–8.
36. Zavadil J, Cermak L, Soto-Nieves N, Bottinger EP. Integration of TGF-beta/Smad and Jagged1/Notch signalling in epithelial-to-mesenchymal transition. Embo J 2004;23(5):1155–65.
37. Espinosa L, Ingles-Esteve J, Aguilera C, Bigas A. Phosphorylation by glycogen synthase kinase-3 beta down-regulates Notch activity, a link for Notch and Wnt pathways. J Biol Chem 2003;278(34):32227–35.
38. Uyttendaele H, Soriano JV, Montesano R, Kitajewski J. Notch4 and Wnt-1 proteins function to regulate branching morphogenesis of mammary epithelial cells in an opposing fashion. Dev Biol 1998;196(2):204–17.
39. Politi K, Feirt N, Kitajewski J. Notch in mammary gland development and breast cancer. Semin Cancer Biol 2004;14(5):341–7.
40. Gallahan D, Callahan R. Mammary tumorigenesis in feral mice: identification of a new int locus in mouse mammary tumor virus (Czech II)-induced mammary tumors. J Virol 1987;61(1): 66–74.
41. Gallahan D, Callahan R. The mouse mammary tumor associated gene INT3 is a unique member of the NOTCH gene family (NOTCH4). Oncogene 1997;14(16):1883–90.
42. Jhappan C, Gallahan D, Stahle C, Chu E, Smith GH, Merlino G, Callahan R. Expression of an activated Notch-related int-3 transgene interferes with cell differentiation and induces neoplastic transformation in mammary and salivary glands. Genes Dev 1992;6(3):345–55.
43. Gallahan D, Jhappan C, Robinson G, Hennighausen L, Sharp R, Kordon E, Callahan R, Merlino G, Smith GH. Expression of a truncated Int3 gene in developing secretory mammary epithelium specifically retards lobular differentiation resulting in tumorigenesis. Cancer Res 1996;56(8):1775–85.
44. Dievart A, Beaulieu N, Jolicoeur P. Involvement of Notch1 in the development of mouse mammary tumors. Oncogene 1999;18 (44):5973–81.
45. Imatani A, Callahan R. Identification of a novel NOTCH-4/INT-3 RNA species encoding an activated gene product in certain human tumor cell lines. Oncogene 2000;19(2):223–31.

46. Raafat A, Bargo S, Anver MR, Callahan R. Mammary development and tumorigenesis in mice expressing a truncated human Notch4/Int3 intracellular domain (h-Int3sh). Oncogene 2004;23 (58):9401–7.
47. Parr C, Watkins G, Jiang WG. The possible correlation of Notch-1 and Notch-2 with clinical outcome and tumour clinicopathological parameters in human breast cancer. Int J Mol Med 2004;14 (5):779–86.
48. Reedijk M, Odorcic S, Chang L, Zhang H, Miller N, McCready DR, Lockwood G, Egan SE. High-level coexpression of JAG1 and NOTCH1 is observed in human breast cancer and is associated with poor overall survival. Cancer Res 2005;65 (18):8530–7.
49. Pece S, Serresi M, Santolini E, Capra M, Hulleman E, Galimberti V, Zurrida S, Maisonneuve P, Viale G, Di Fiore PP. Loss of negative regulation by Numb over Notch is relevant to human breast carcinogenesis. J Cell Biol 2004;167(2):215–21.
50. Siziopikou K, Jang MS, Miao H, Miele L. Notch signaling in ductal carcinoma *in situ* of the breast. In: Proc Am Assoc Cancer Res; 2002; 2002.
51. Chen Y, Fischer WH, Gill GN. Regulation of the ERBB-2 promoter by RBPJkappa and NOTCH. J Biol Chem 1997;272 (22):14110–4.
52. Sakamaki T, Liu M, Katiyar S, Rao M, Li S, Yin Y, Dettin L, Pestell RG, Glazer RI. ErbB2 activation of Notch1 signaling in breast cancer. In: Proc Am Assoc Cancer Res; 2005; 2005. p. 869.
53. Shawber CJ, Kitajewski J. Notch function in the vasculature: insights from zebrafish, mouse and man. Bioessays 2004;26 (3):225–34.
54. Krebs LT, Xue Y, Norton CR, Shutter JR, Maguire M, Sundberg JP, Gallahan D, Closson V, Kitajewski J, Callahan R, Smith GH, Stark KL, Gridley T. Notch signaling is essential for vascular morphogenesis in mice. Genes Dev 2000;14(11):1343–52.
55. Limbourg FP, Takeshita K, Radtke F, Bronson RT, Chin MT, Liao JK. Essential role of endothelial Notch1 in angiogenesis. Circulation 2005;111(14):1826–32.
56. Uyttendaele H, Marazzi G, Wu G, Yan Q, Sassoon D, Kitajewski J. Notch4/int-3, a mammary proto-oncogene, is an endothelial cell-specific mammalian Notch gene. Development 1996;122 (7):2251–9.
57. Uyttendaele H, Ho J, Rossant J, Kitajewski J. Vascular patterning defects associated with expression of activated Notch4 in embryonic endothelium. Proc Natl Acad Sci USA 2001;98(10):5643–8.
58. Carlson TR, Yan Y, Wu X, Lam MT, Tang GL, Beverly LJ, Messina LM, Capobianco AJ, Werb Z, Wang R. Endothelial expression of constitutively active Notch4 elicits reversible arteriovenous malformations in adult mice. Proc Natl Acad Sci USA 2005;102(28):9884–9.
59. Shutter JR, Scully S, Fan W, Richards WG, Kitajewski J, Deblandre GA, Kintner CR, Stark KL. Dll4, a novel Notch ligand expressed in arterial endothelium. Genes Dev 2000;14(11):1313–8.
60. Mailhos C, Modlich U, Lewis J, Harris A, Bicknell R, Ish-Horowicz D. Delta4, an endothelial specific notch ligand expressed at sites of physiological and tumor angiogenesis. Differentiation 2001;69(2–3):135–44.
61. Duarte A, Hirashima M, Benedito R, Trindade A, Diniz P, Bekman E, Costa L, Henrique D, Rossant J. Dosage-sensitive requirement for mouse Dll4 in artery development. Genes Dev 2004;18(20):2474–8.
62. Krebs LT, Shutter JR, Tanigaki K, Honjo T, Stark KL, Gridley T. Haploinsufficient lethality and formation of arteriovenous malformations in Notch pathway mutants. Genes Dev 2004;18 (20):2469–73.
63. Gale NW, Dominguez MG, Noguera I, Pan L, Hughes V, Valenzuela DM, Murphy AJ, Adams NC, Lin HC, Holash J, Thurston G, Yancopoulos GD. Haploinsufficiency of delta-like 4 ligand results in embryonic lethality due to major defects in arterial and vascular development. Proc Natl Acad Sci USA 2004;101(45):15949–54.
64. Carmeliet P, Ferreira V, Breier G, Pollefeyt S, Kieckens L, Gertsenstein M, Fahrig M, Vandenhoeck A, Harpal K, Eberhardt C, Declercq C, Pawling J, Moons L, Collen D, Risau W, Nagy A. Abnormal blood vessel development and lethality in embryos lacking a single VEGF allele. Nature 1996;380(6573):435–9.
65. Ferrara N, Carver-Moore K, Chen H, Dowd M, Lu L, O'Shea KS, Powell-Braxton L, Hillan KJ, Moore MW. Heterozygous embryonic lethality induced by targeted inactivation of the VEGF gene. Nature 1996;380(6573):439–42.
66. Liu ZJ, Shirakawa T, Li Y, Soma A, Oka M, Dotto GP, Fairman RM, Velazquez OC, Herlyn M. Regulation of Notch1 and Dll4 by vascular endothelial growth factor in arterial endothelial cells: implications for modulating arteriogenesis and angiogenesis. Mol Cell Biol 2003;23(1):14–25.
67. Patel NS, Li JL, Generali D, Poulsom R, Cranston DW, Harris AL. Up-regulation of delta-like 4 ligand in human tumor vasculature and the role of basal expression in endothelial cell function. Cancer Res 2005;65(19):8690–7.
68. Williams CK, Li JL, Murga M, Harris AL, Tosato G. Upregulation of the Notch ligand Delta-like 4 inhibits VEGF-induced endothelial cell function. Blood 2005.
69. Henderson AM, Wang SJ, Taylor AC, Aitkenhead M, Hughes CC. The basic helix-loop-helix transcription factor HESR1 regulates endothelial cell tube formation. J Biol Chem 2001;276(9):6169–76.
70. Taylor KL, Henderson AM, Hughes CC. Notch activation during endothelial cell network formation *in vitro* targets the basic HLH transcription factor HESR-1 and downregulates VEGFR-2/KDR expression. Microvasc Res 2002;64(3):372–83.
71. Leong KG, Hu X, Li L, Noseda M, Larrivee B, Hull C, Hood L, Wong F, Karsan A. Activated Notch4 inhibits angiogenesis: role of beta 1-integrin activation. Mol Cell Biol 2002;22(8):2830–41.
72. Noseda M, Chang L, McLean G, Grim JE, Clurman BE, Smith LL, Karsan A. Notch activation induces endothelial cell cycle arrest and participates in contact inhibition: role of p21Cip1 repression. Mol Cell Biol 2004;24(20):8813–22.
73. Sainson RC, Aoto J, Nakatsu MN, Holderfield M, Conn E, Koller E, Hughes CC. Cell-autonomous notch signaling regulates endothelial cell branching and proliferation during vascular tubulogenesis. Faseb J 2005;19(8):1027–9.
74. Zeng Q, Li S, Chepeha DB, Giordano TJ, Li J, Zhang H, Polverini PJ, Nor J, Kitajewski J, Wang CY. Crosstalk between tumor and endothelial cells promotes tumor angiogenesis by MAPK activation of Notch signaling. Cancer Cell 2005;8(1):13–23.
75. Nickoloff BJ, Qin JZ, Chaturvedi V, Denning MF, Bonish B, Miele L. Jagged-1 mediated activation of notch signaling induces complete maturation of human keratinocytes through NF-kappaB and PPARgamma. Cell Death Differ 2002;9(8):842–55.
76. Kopan R, Goate A. A common enzyme connects notch signaling and Alzheimer's disease. Genes Dev 2000;14(22):2799–806.
77. Curry CL, Reed LL, Golde TE, Miele L, Nickoloff BJ, Foreman KE. Gamma secretase inhibitor blocks Notch activation and induces apoptosis in Kaposi's sarcoma tumor cells. Oncogene 2005.
78. Paris D, Quadros A, Patel N, DelleDonne A, Humphrey J, Mullan M. Inhibition of angiogenesis and tumor growth by beta and gamma-secretase inhibitors. Eur J Pharmacol 2005;514(1): 1–15.
79. Haruki N, Kawaguchi KS, Eichenberger S, Massion PP, Olson S, Gonzalez A, Carbone DP, Dang TP. Dominant-negative Notch3 receptor inhibits mitogen-activated protein kinase pathway and the growth of human lung cancers. Cancer Res 2005;65(9):3555–61.
80. Itoh F, Itoh S, Goumans MJ, Valdimarsdottir G, Iso T, Dotto GP, Hamamori Y, Kedes L, Kato M, ten Dijke Pt P. Synergy and

antagonism between Notch and BMP receptor signaling pathways in endothelial cells. Embo J 2004;23(3):541–51.
81. Chappell WH, Green TD, Spengeman JD, McCubrey JA, Akula SM, Bertrand FE. Increased protein expression of the PTEN tumor suppressor in the presence of constitutively active Notch-1. Cell Cycle 2005;4(10).
82. Kamakura S, Oishi K, Yoshimatsu T, Nakafuku M, Masuyama N, Gotoh Y. Hes binding to STAT3 mediates crosstalk between Notch and JAK-STAT signalling. Nat Cell Biol 2004;6(6):547–54.
83. Sjolund J, Manetopoulos C, Stockhausen MT, Axelson H. The Notch pathway in cancer: differentiation gone awry. Eur J Cancer 2005;41(17):2620–9.

ARTICLE IN PRESS

YMVRE-03744; No. of pages: 11; 4C: 4

Available online at www.sciencedirect.com

ScienceDirect

Microvascular Research xx (2007) xxx–xxx

Microvascular Research

www.elsevier.com/locate/ymvre

Regular Article

Regulation of multiple angiogenic pathways by Dll4 and Notch in human umbilical vein endothelial cells

Laura S. Harrington [a], Richard C.A. Sainson [a], Cassin Kimmel Williams [a], Jennifer M. Taylor [b], Wen Shi [a], Ji-Liang Li [a], Adrian L. Harris [a,*]

[a] *Cancer Research UK, Molecular Oncology Laboratories, Weatherall Institute of Molecular Medicine, John Radcliffe Hospital, Headley Way, Oxford, OX3 9DS, UK*

[b] *Wellcome Trust Centre for Human Genetics, University of Oxford, Roosevelt Drive, Oxford, OX3 7BN, UK*

Received 19 February 2007; revised 15 June 2007; accepted 15 June 2007

Abstract

The Notch ligand, Dll4, is essential for angiogenesis during embryonic vascular development and is involved in tumour angiogenesis. Several recent publications demonstrated that blockade of Dll4 signalling inhibits tumour growth, suggesting that it may constitute a good candidate for anti-cancer therapy. In order to understand the role of Dll4 at the cellular level, we performed an analysis of Dll4-regulated genes in HUVECs. The genes identified included several angiogenic signalling pathways, such as VEGF, FGF and HGF. In particular we identified downregulation (VEGFR2, placenta growth factor PlGF) of VEGF pathway components resulting in the overall effect of limiting the response of HUVEC to VEGF. However extensive upregulation of VEGFR1 was observed allowing continued response to its ligand PlGF but the soluble form of the VEGFR1, sVEGFR1 was also upregulated. PlGF enhanced tubulogenesis of HUVEC suggesting that downregulation of PlGF and upregulation of VEGFR1 including sVEGFR1 are important mechanisms by which Dll4 attenuates PlGF and VEGF signalling. Dll4-stimulated HUVECs had impaired ERK activation in response to VEGF and HGF indicating that Dll4 signalling negatively regulates these pathways. Dll4 expression reduced vessel sprout length in a 3D tubulogenesis assay confirming that Dll4 signalling inhibits angiogenesis. Altogether, our data suggest that Dll4 expression acts as a switch from the proliferative phase of angiogenesis to the maturation and stabilisation phase by blocking endothelial cell proliferation and allowing induction of a more mature, differentiated phenotype. The regulation of sVEGFR1 provides a novel mechanism for Dll4 signalling to regulate cells at distance, not just in adjacent cells.
© 2007 Published by Elsevier Inc.

Keywords: Dll4; Notch; cDNA microarray; HUVEC; Sprout formation; Angiogenesis

Introduction

Notch signalling has recently been implicated in vascular development and homeostasis since genes encoding components of Notch signalling are mutated in two human diseases (Alagille Syndrome and CADASIL (Cerebral Autosomal Dominant Arteriopathy with Subcortical Infarcts and Leukoencephalopathy)) which exhibit vascular defects (Karsan, 2005; Shawber and Kitajewski, 2004). Furthermore, many Notch receptors and ligands are expressed in cells of the vasculature (Iso et al., 2003a; Villa et al., 2001). Finally studies of transgenic mice have revealed an essential early role for Notch signalling in angiogenesis (Iso et al., 2003a).

Notch signalling is an evolutionarily conserved intercellular signalling pathway mediated by membrane-tethered receptor–ligand interactions between adjacent cells (Artavanis-Tsakonas et al., 1999; Lai, 2004). Receptor–ligand binding induces sequential cleavages of the Notch receptor, the last of which is performed by the γ-secretase complex, releasing the Notch intracellular domain (NICD) which translocates to the nucleus (Artavanis-Tsakonas et al., 1999; Lai, 2004). In the nucleus NICD typically interacts with RBP-Jκ (recombination signal binding protein Jκ) leading to the transcription of Notch target genes such as members of the Hes and Hey families of

* Corresponding author. Fax: +44 1865 222431.
E-mail address: aharris.lab@cancer.org.uk (A.L. Harris).

0026-2862/$ - see front matter © 2007 Published by Elsevier Inc.
doi:10.1016/j.mvr.2007.06.006

Please cite this article as: Harrington, L.S., et al., Regulation of multiple angiogenic pathways by Dll4 and Notch in human umbilical vein endothelial cells, Mucrovasc. Res. (2007), doi:10.1016/j.mvr.2007.06.006

UNCORRECTED PROOF

ARTICLE IN PRESS

transcriptional repressors (Iso et al., 2003b). In mammals there are four Notch receptors (Notch1–4) and 5 Notch ligands: two serrate-like ligands named Jagged1 and Jagged2 and three delta-like ligands (Dll) named Dll1, 3, 4.

We and others have shown that Dll4 is expressed specifically at sites of vascular development and angiogenesis and is confined to arterial ECs (Benedito and Duarte, 2005; Claxton and Fruttiger, 2004; Mailhos et al., 2001; Shutter et al., 2000). Dll4 expression is particularly critical for angiogenesis as haploinsufficiency of Dll4 leads to embryonic lethality in mice due to vascular defects (Duarte et al., 2004; Gale et al., 2004; Krebs et al., 2004) demonstrating the essential role of Dll4 in angiogenesis during development.

Thus Dll4 expression is essential for normal angiogenesis during development but Dll4 expression in adults is confined to areas of physiological angiogenesis such as in the ovary around developing follicles and areas of pathological angiogenesis such as tumour vasculature (Mailhos et al., 2001). Recent evidence suggests that Dll4 expression is upregulated in tumour endothelium and that this correlates with tumour vessel maturation and remodeling (Hainaud et al., 2006; Patel et al., 2006). In addition Dll4 expression is induced by hypoxia, a common feature of tumour development known to induce angiogenesis (Mailhos et al., 2001) making Dll4 an attractive anti-tumour target. Indeed recent papers have demonstrated that blockade of Dll4 signalling promotes non-productive angiogenesis thus inhibiting tumour growth (Noguera-Troise et al., 2006; Ridgway et al., 2006) though the mechanistic basis for this remains unclear. In the present study we performed a cDNA microarray screen to identify Dll4 regulated genes in order to understand the function of Dll4 signalling in physiological and pathological angiogenesis.

Materials and methods

Cell culture, cells and reagents

HUVECs were isolated from fresh human umbilical cords by infusion with 0.2% collagenase. Single donor HUVECs were used between passages 3 and 7 and were cultured in M199 media supplemented with 20% fetal calf serum (FCS: Sigma-Aldrich, St. Louis, MO), 12 mM L-glutamine, 50 mg/L ECGS (endothelial cell growth supplement; BD Biosciences Bedford MA, USA), 10 units/mL heparin (Sigma) and an antimycotic/antibiotic (Gibco). The Phoenix amphotropic viral packaging cell line (gift from Garry Nolan) was cultured in DMEM supplemented with 10% FCS, 12 mM L-glutamine and penicillin/streptomycin. Recombinant human Dll4 extracellular domain (rDll4) was purchased from R&D Systems (Minneapolis, USA). The γ-secretase inhibitor DAPT (Calbiochem) was dissolved in DMSO (Sigma) and used at a final concentration of 2 μM.

Retroviral packaging and infection

The retroviral vector and full length human Dll4 construct have been previously described (Williams et al., 2006). Low passage, 50% confluent HUVECs were infected using 0.4-μm filtered virus containing supernatant supplemented with 4 ng/mL polybrene. After 5 h at 37 °C an equal volume of normal HUVEC culture media was added. Infection efficiencies were from 60% to 90%.

Microarray analysis

Microarray analysis was performed in triplicate and each replicate used HUVECs from a different donor. Total RNA was extracted from HUVECs using TRI-reagent (Sigma) followed by DNase I treatment (DNase-free; Ambion) according to the manufacturer's instructions. First and second strand cDNA synthesis was performed using Superscript dscDNA Synthesis Kit (Invitrogen) and 10 μg of total RNA. Clean-up of double stranded cDNA was carried out using Phase Lock Gels, 2 mL light (Eppendorf), followed by synthesis of labeled cRNA with the BioArray High Yield RNA Transcript Labeling Kit (ENZO, Affymetrix). Purification of cRNA and quantification was done with RNeasy Mini Kit (Qiagen), followed by cRNA Fragmentation using 30 μg cRNA and Fragmentation Buffer (200 mM Tris-acetate pH 8.1, 500 mM MKOAc, 150 mM MgOAc). Hybridisation Cocktail for human HG-U133A Affymetrix GeneChip® utilised the Gene Chip Eurkaryotic Hybridisation Control Kit (ENZO, Affymetrix) and hybridisation, washing, staining, and scanning of the chip was performed according to the manufacturer's instructions. Data was labeled as MIAME compliant. Raw signal files were background corrected and normalised using the gcrma modification of the rma normalisation procedure (Irizarry et al., 2003) available from the Bioconductor project (www.bioconductor.org) for the R statistical language. Log2 ratios of Dll4 signal to control signal were generated for each probeset. A list was generated that contained those probesets for which an average absolute fold change of at least 1.5 was observed between Dll4 and control samples. Where a gene was represented by more than one probeset the average signal value was used. This list was used to generate a list of statistically significant ($P \leq 0.01$) probesets with the eBayes approach (Smyth, 2004) as implemented in the limma package (Smyth and Speed, 2003) of BioConductor. Visualisation of this gene list was performed using the hierarchical clustering algorithm with euclidean distance and single linkage. Enrichment analysis was conducted using the DAVID algorithm and significance of enrichment is measured using the Fisher's Exact Test for each GO term relative to the background of the Affymetrix HG-U133A chip.

Quantitative real time PCR (Q-PCR)

Reverse transcription was performed using 1 μg total DNase 1-treated RNA and the High Capacity cDNA Archive Kit (Applied Biosystems). The resulting cDNA was used for Q-PCR using the Exiqon system (Roche, Basel, Switzerland). Briefly Q-PCR reactions were set up in triplicate using the Corbett Research Roto Gene RG-3000 robot (Corbett, Sydney, Australia). Each 25 μl reaction contained the equivalent of 25 ng reverse transcribed cDNA, 0.4 μM of each oligonucleotide, 12.5 μl of 2× Absolute QPCR master mix (AbGene, Epsom, UK) and 0.25 μl of the appropriate Exiqon probe. GAPDH or Flo2 were used as reference genes to normalise results. The cycling conditions used were: 95 °C for 10 min followed by 40 cycles of 95 °C for 15 s and 60 °C for 60 s. The relative quantitation was performed as previously described (Patel et al., 2005). The differences between Q-PCR experimental groups were analyzed using one sample Student's *t* test and $p < 0.05$ was considered significant.

Oligonucleotides

Gene	Forward 5′–3′	Reverse 5′–3′
GAPDH	AGCCACATCGCTCAGACAC	GCCCAATACGACCAAATCC
Flo2	CTCAGCTTCACCATCAAGGAC	TCAGCATCTCTCTGCACCAC
Sulfatase1	CCAATGCTTCCCAACACATA	GCATTGGTCCTGTGTACTGC
Elastin	CACTGGGGTATCCCATCAAG	GTGGTGTAGGGCAGTCCATAG
PCDH12	GGAGGAGCTCACTGTGGATT	CTGATGCAGCAAGGACAGC
INHBA	CTCGGAGATCATCACGTTTG	CCTTGGAAATCTCGAAGTGC

Please cite this article as: Harrington, L.S., et al., Regulation of multiple angiogenic pathways by Dll4 and Notch in human umbilical vein endothelial cells, Mucrovasc. Res. (2007), doi:10.1016/j.mvr.2007.06.006

ARTICLE IN PRESS

SDC1	CCAGTCAGCTCCCAGCAG	CCCCGAGGTTTCAAAGGT
CDH11	ACCAAAGTTTCCGCAGAGC	TGGATCTTTAGCTTTCACTCTTCC
STAT1	AAAGTATTACTCCAGGCCAAAGG	CCAGTTCCTTTAGGGCCATC
Biglycan	CAGCCCGCCAACTAGTCA	GGCCAGCAGAGACACGAG
SNAI2	GAACAAAACACAGGAGAATGTATTAAA	GCCAGGAATGTTCAAAGCTAA
VCAM1	TGGACATAAGAAACTGGAAAAGG	GATTTCTGGATCTCTAGGGAATGA
RASSF2	TGAAGGCCAGAATTTACAGCTC	CCCTCCACAATGAACTCGTC
FBLN5	CTGCCCTCCAGGCTACATC	CCTGTGCTCACATTCGTTGA
NRP2	GGACCCCCAACTTGGATT	ATGGTTAAAAAGCGCAGGTC
SEMA5A	ATGGAGATCGCCAACTGTTC	TAGTGCTGCAGGGAGACCA
VEGFR1	CAGCATACCTCACTGTTCAAGG	CCACACAGGTGCATGTTAGAG
MET	ACCAAAATGGCTACACACTGG	CATTCAATGGGATCTTCGTGA
Hey2	CCAGCAGTGCATCAGTATGTC	CAGGCACTTACGAAACACGA
PlGF	GGCTGTTCCCTTGCTTCC	CAGACAAGGCCCACTGCT
Jagged1	TGGGCTTTGAGTGTGAGTGT	CCCCGTGGGAACAGTTATTA
Notch3	CAATGCTGTGGATGAGCTTG	AAGTGGCTTCCACGTTGTTC
RGC32	CAGACTCTACCCCAGCTCTTCT	GCTCTTTTGTGTCTCCTAATTTAGCTT
Dll4	CCCTGGCAATGTACTTGTGAT	TGGTGGGTGCAGTAGTTGAG

rDll4-coated tissue culture plates

Tissue culture plates were coated with 0.2% gelatine (w/v) in PBS containing 1 μg/mL rDll4 or BSA as a control (Williams et al., 2006) and incubated at 4 °C for 24 h before use. Plates were warmed to 37 °C and the coating solution aspirated prior to seeding 2×10^5 HUVECs per well in 6-well plates. RNA, protein (as per serum stimulation of HUVECs below) or conditioned media were harvested 48 h later.

γ-Secretase treatment

2×10^5 HUVECs were seeded in the presence of 2 μM DAPT or an equivalent amount of DMSO vehicle. The media containing DAPT or DMSO control was replaced after 24 h (except when used for ELISA). RNA, protein (as per stimulation of HUVECs below) or conditioned media was harvested after 48 h.

Western blotting

Proteins were separated by SDS-PAGE using standard techniques. Antibodies were purchased from the following companies: Notch1IC, MET, STAT1, phospho-ERK and total ERK antibodies (Cell Signalling), Jagged1, Notch3, VEGFR2, Snai2 (Santa Cruz), β-tubulin, β-actin, VEGFR1 antibodies (Sigma). The anti-Hes1 antibody was a gift from Tetsuo Sudo, Toray Industries, Japan. Anti-mouse and anti-rabbit HRP conjugated secondary antibodies were from DAKO while anti-goat HRP was from Perbio.

$VEGF_{165}$, HGF and PlGF stimulation of HUVECs

2×10^5 HUVECs per well were seeded into BSA control or rDll4-coated 6-well plates. After 43 h the media was replaced with starvation media (DMEM with 0.5% FCS). 5 h later the media was replaced with starvation media (unstimulated) or starvation media supplemented with 20 ng/mL $VEGF_{165}$ or HGF for 2 or 10 min or 10 ng/mL PlGF for 2.5, 5 and 10 min. Cells were lysed in RIPA buffer (Sigma) supplemented with Complete protease inhibitor cocktail (Roche) and phosphatase inhibitor cocktails I and II (Sigma). Following centrifugation (13,000 rpm, 5 min at 4 °C) the supernatant was collected. Equal amounts of protein were separated by SDS-PAGE as described above.

In vitro 3D-tubulogenesis fibrin gel bead assay

The fibrin gel bead assay was previously described (Nakatsu et al., 2003). HUVECs were infected with retrovirus encoding for GFP (empty vector control) or full-length Dll4 as described above and subsequently placed in the fibrin gel bead assay. To investigate the effect of PlGF, HUVEC were placed in the fibrin gel bead assay and treated 2 days later with vehicle- or 10 ng/mL or 50 ng/mL PlGF-containing EGM-2, replacing the media every other day for a total of 5 treatments. A Zeiss Axiovert S100 microscope using 10x and 20x objectives attached to a Hamamatsu C4742-95 camera was used to capture images. Image acquisition software used was OpenLab 3.5 and Image J software (NIH) was used for the analysis of sprout length (Nakatsu et al., 2003).

Soluble VEGFR1 ELISA

2×10^5 HUVEC were seeded on BSA or rDll4-coated plates as described above except that EGM-2 media was used. ELISA for human sVEGFR1 (R&D Systems) was performed according to the manufacturer's instructions using the conditioned media (diluted 1 in 10 in EGM-2 media) from HUVECs cultured on BSA- or rDll4-coated plates in the presence of DMSO or DAPT for 48 h. Total ng of sVEGFR1 were normalised to the amount of cellular protein in mg to account for differences in proliferation.

Results

Exogenous Dll4 enhances Notch signalling in HUVECs

HUVECs were chosen for this study because of their capacity to express low levels of Dll4 mRNA as detected by RT-PCR (Patel et al., 2005) and to induce Dll4 expression following hypoxia and VEGF stimulation (Hainaud et al., 2006; Liu et al., 2003; Mailhos et al., 2001; Patel et al., 2005). Transduction of HUVECs with Dll4-encoding retrovirus increased Dll4 expression at the mRNA and protein levels as previously reported (Williams et al., 2006).

Identification of Dll4 target genes by microarray analysis

In order identify genes and processes regulated by Dll4 signalling that are responsible for its role in regulating angiogenesis we performed cDNA microarray analysis in triplicate comparing Dll4-retrovirally-infected HUVECs to control empty vector-infected HUVECs. Analysis of the microarray data revealed 104 candidate genes that were statistically significantly up or downregulated by an average of more than 1.5 fold in Dll4-infected HUVECs compared to control-infected HUVECs ($p<0.01$; Fig. 1 and Supplementary

Please cite this article as: Harrington, L.S., et al., Regulation of multiple angiogenic pathways by Dll4 and Notch in human umbilical vein endothelial cells, Mucrovasc. Res. (2007), doi:10.1016/j.mvr.2007.06.006

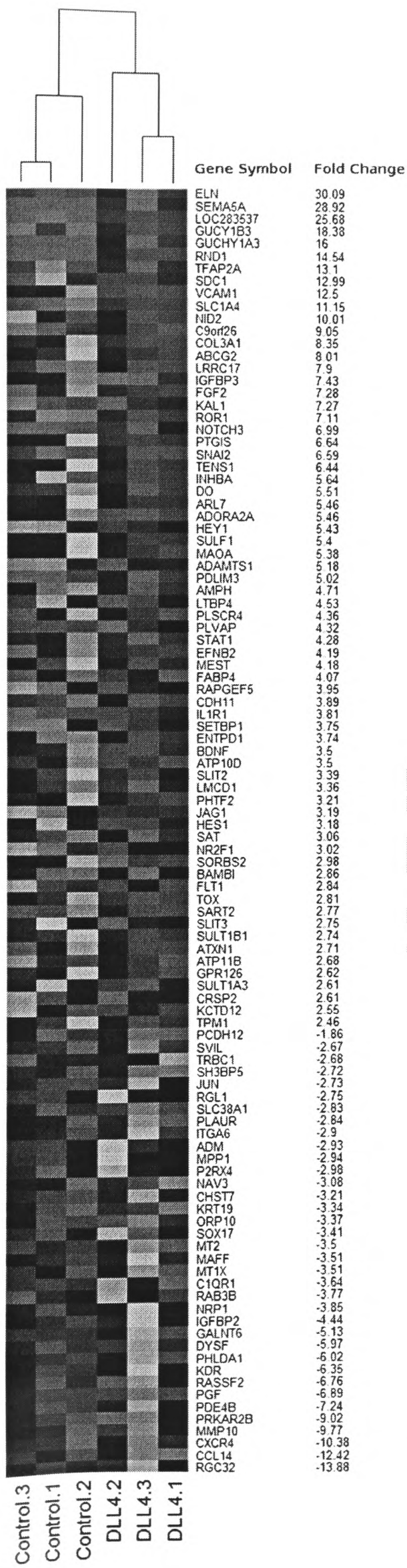


Table 1). Table 1 shows that Dll4 regulated a wide variety of genes including components of cell signalling pathways important for angiogenesis such as the VEGF, FGF and hepatocyte growth factor (HGF) signalling pathways. Indeed the list of 104 genes is significantly enriched for GO terms of angiogenesis ($p=0.00012$), and angiogenesis-associated processes, including proliferation ($p=0.018$) and cell adhesion ($p=0.029$). The gene functional classification algorithm within DAVID produced a cluster of angiogenesis related GO terms that had a geometric mean significance of enrichment of ($p=0.0012$). Dll4 upregulated more genes than it downregulated.

Validation of candidate Dll4 target genes by Q-PCR

Using Q-PCR we analysed the mRNA levels of candidate genes in Dll4-infected HUVECs compared to empty vector-infected HUVECs for a panel of 14 genes up-regulated in the microarray analysis and 5 genes that were down regulated. Genes were chosen from the list of 104 genes and also a longer list of genes regulated by Dll4 by 1.5 fold or more (Supplementary Table 2). Q-PCR results for the 19 genes tested confirmed the microarray data (Table 1). As expected using HUVECs from different donors the magnitude of gene expression changes by Q-PCR was not always similar but the average fold induction or repression of genes by Dll4 was at least 1.5 fold matching that of the microarray.

Dll4 target genes are regulated by immobilised Dll4

In order to confirm the regulation of genes by Dll4 signalling by an alternative non-viral approach HUVECs were cultured on dishes coated with recombinant human Dll4 extracellular domain (rDll4) or with BSA as a control. Immobilisation of the Notch ligand is thought to mimic the tethering of the ligand on the cell surface enabling Notch signalling which soluble ligands usually fail to do as has been shown for Delta1 (Varnum-Finney et al., 2000). This approach activated Notch signalling as demonstrated by the accumulation of the cleaved active N1IC in HUVECs cultured on rDll4 for 48 h (Fig. 2B).

Q-PCR validation of a subset of the candidate genes by this method showed that all 12 genes tested were up-regulated and all 5 were downregulated in HUVECs cultured on rDll4 compared to those cultured on BSA-coated dishes (Table 1). This was in complete agreement with the cDNA microarray and Q-PCR results from retroviral-infected HUVECs. In addition this suggests that the regulation of these genes is via Notch receptor cleavage rather than via Dll4-ICD as the recombinant protein lacks the ICD.

Fig. 1. A heat map to show genes differentially regulated by Dll4 expression in HUVECs. The heatmap and dendrogram show clustering of samples based on the log2 expression ratio of 104 probesets. Clustering is based on manhattan distance metric and single linkage. Heatmap colours represent log2 ratio of −5 (green) to 5 (red).

Please cite this article as: Harrington, L.S., et al., Regulation of multiple angiogenic pathways by Dll4 and Notch in human umbilical vein endothelial cells, Mucrovasc. Res. (2007), doi:10.1016/j.mvr.2007.06.006

ARTICLE IN PRESS

Table 1
Genes involved in angiogenesis-related signalling pathways and biological processes identified as Dll4 target genes by microarray analysis and Q-PCR validation

Genes (UniGene number)	Microarray ($n=3$)	Infection	rDll4-coated plates
Signalling pathways			
VEGF			
NRP1 (Hs.131704)	−3.9	ND	ND
NRP2 (Hs.471200)	−2.7	−1.9 [0.2] (3)	−1.6 [0.1] (3)
PlGF (Hs.252820)	−6.9	−3.3 [0.6] (4)	−2.8 [0.6] (4)
VEGFR1 (Hs.507621)	2.8	2.6 [0.4] (3)	3.9 [0.5] (3)
VEGFR2 (Hs.479756)	−6.3	ND	ND
FGF			
FGF2 (Hs.284244)	7.3	ND	ND
HGF			
MET (Hs.132966)	−1.9	−1.9 [0.3] (3)	−2.3 [0.1] (3)
Notch			
Notch 3 (Hs.8546)	7.0	9.7 [4.2] (5)	3.1 [0.2] (3)
Hey2[§] (Hs.14427)	1.2	14.8 [6.0] (3)	12.9 [0.3] (3)
RASSF2 (Hs.379970)	−6.8	−2.1 [0.4] (4)	−2.2 [0.4] (3)
Jagged1 (Hs.224012)	3.2	1.5 [0.1] (5)	2.6 [0.3] (3)
Proliferation			
Fibulin5 (Hs.332708)	3.0	5.8 [1.4] (3)	3.4 [0.3] (3)
Inhibin βA (Hs.28792)	5.6	5.0 [0.7] (5)	8.1 [0.9] (4)
STAT1 (Hs.470943)	4.3	1.8 [0.1] (5)	ND
Migration and adhesion			
CDH11 (Hs.116471)	3.9	2.3 [0.2] (5)	ND
CXCR4 (Hs.421986)	−10.4	ND	ND
PCDH12 (Hs.439474)	−1.9	−6.2 [1.3] (5)	−7.0 [1.0] (5)
Snai2 (Hs.360174)	6.6	3.9 [0.5] (5)	4.9 [1.2] (4)
VCAM1 (Hs.109225)	12.5	15.0 [4.7] (4)	8.8 [2.3] (4)
Vessel guidance			
RND1 (Hs.124940)	14.5	ND	ND
Sema5A (Hs.321637)	28.9	22.6 [6.8] (3)	15.1 [3.9] (3)
Slit2 (Hs.558436)	3.4	ND	ND
Slit3 (Hs.145601)	2.8	ND	ND
Differentiation and morphogenesis			
Elastin (Hs.252418)	30.1	143 [49] (5)	60.0 [33.6] (4)
EphrinB2 (Hs.149239)	4.2	ND	ND
Integrin β3 (Hs.218040)	−1.6	ND	ND
Extracellular matrix-associated			
Biglycan (Hs.821)	2.3	5.5 [1.3] (5)	6.7 [1.0] (4)
Collagen, typeIII, alpha1 (Hs.443625)	8.4	ND	ND
Matrix metalloprotease 10 (Hs.2258)	9.8	ND	ND
SDC1 (Hs.224607)	13.0	8.5 [2.2] (5)	6.0 [1.2] (4)
Sulfatase1 (Hs.409602)	5.4	23.3 [8.2] (5)	8.8 [4.1] (4)

Genes identified as Dll4 targets by cDNA microarray analysis categorized according to the signaling pathway or biological process in which they play a role. The average fold change in mRNA levels according to the microarray analysis is shown. In addition the table shows a comparison between the average fold change in mRNA levels of 20 genes identified by microarray analysis to be differentially regulated by Dll4 signalling either in Dll4-expressing HUVECs compared to empty vector control-infected HUVECs (infection) or HUVECs cultured on Dll4-coated plates compared to HUVECs cultured on BSA-coated plates as a control (rDll4-coated plates). The average fold change relative to expression in the corresponding control cells is shown. *ND*, not determined. *Parentheses*, number of independent experiments performed on HUVECs from separate donors. *Square brackets*, S.E.M. All results are significant with $p<0.05$. [§]While Hey2 mRNA was not regulated by more than 1.5 fold in the microarray, Q-PCR results demonstrate that it is upregulated by Dll4 signalling using both approaches.

Dll4 signalling regulates Hes1, Jagged1, MET, VEGFR1, Snai2 and STAT1 proteins

In order to determine whether Dll4-induced mRNA changes were reflected at the protein level we performed western blotting for some of the confirmed targets and found that levels of Hes1 protein were higher in HUVECs expressing Dll4 by retroviral infection and in HUVECs cultured on rDll4-coated plates compared to control (Fig. 2A). Since the Q-PCR validation by both approaches to induce Dll4 signalling yielded similar results as did the western blotting for Hes1 (Fig. 2A) we then tested the protein expression of STAT1, Jagged1, VEGFR1, snai2 and MET in HUVECs cultured on rDll4-coated plates compared to control. In HUVECs cultured on rDll4-coated plates, Notch signalling was activated and this correlated with higher levels of STAT1, Jagged1, Snai2 and full length VEGFR1 proteins and a lower level of MET protein compared to control (Fig. 2B). These protein expression changes correlated with the mRNA level changes induced by Dll4.

In addition we used the γ-secretase inhibitor DAPT to prevent Notch signalling and investigated its effect on Dll4-induced regulation of elastin (the most upregulated gene by Q-PCR), PCDH12 (the most down-regulated gene by Q-PCR) and two other candidates. DAPT treatment inhibited the Dll4-induced upregulation of elastin, sulfatase-1 and snai2 and downregulation of PCDH12 at the mRNA level (Fig. 2C). DAPT treatment inhibited Dll4 activation of Notch signalling as demonstrated by the reduced accumulation of NICD in HUVECs cultured on Dll4-coated plates in the presence of DAPT (Fig. 2D). Furthermore DAPT treatment reduced the protein expression changes of VEGFR1, VEGFR2, MET, snai2 and STAT1 induced in HUVECs cultured on rDll4-coated plates (Fig. 2D).

Dll4-Notch signalling regulates the levels of soluble VEGFR1

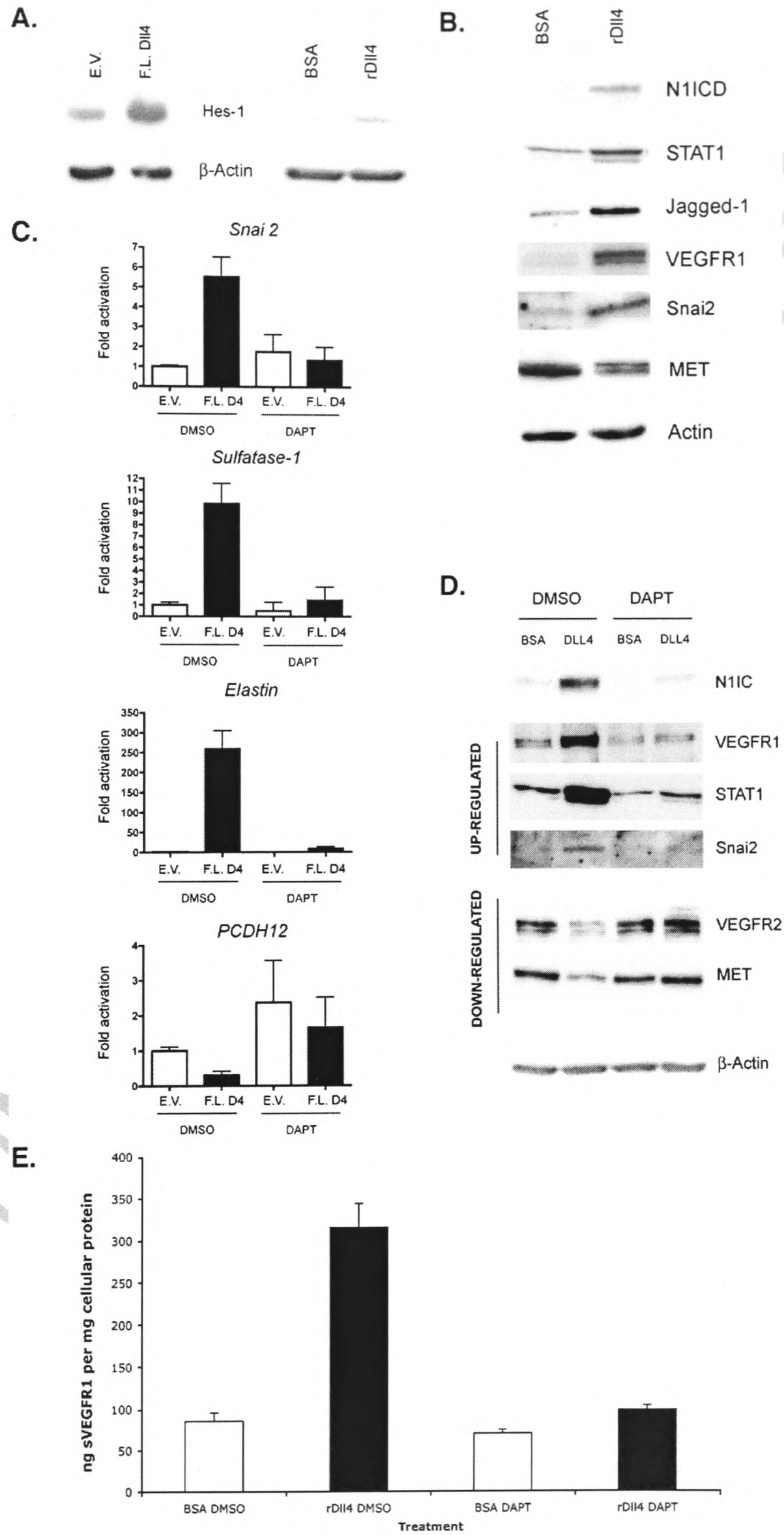
Since Dll4 signalling upregulated the levels of full length VEGFR1 protein in HUVEC, the effect of Dll4 signalling on the levels of the inhibitory soluble alternative splice variant of VEGFR1 (sVEGFR1) in the conditioned media of HUVEC cultured on BSA or rDll4-coated plates was measured by ELISA. The levels of sVEGFR1 were elevated in the conditioned media of HUVEC cultured on Dll4-coated plates compared to those cultured on BSA by 3.5 fold (Fig. 2E). Treatment with DAPT inhibited the Dll4-induced elevation of sVEGFR1 levels confirming that Notch signalling is necessary for rDll4 to upregulate sVEGFR1.

ERK activation in response to $VEGF_{165}$ and HGF is impaired by Dll4 signalling

Since Dll4 signalling altered the gene expression of several genes involved in VEGF signal transduction (Fig. 2; Table 1) we explored the effect of Dll4 signalling on the ability of HUVECs to respond to $VEGF_{165}$ stimulation. We investigated the phosphorylation of ERK as ERK lies downstream of

Please cite this article as: Harrington, L.S., et al., Regulation of multiple angiogenic pathways by Dll4 and Notch in human umbilical vein endothelial cells, Mucrovasc. Res. (2007), doi:10.1016/j.mvr.2007.06.006

ARTICLE IN PRESS



Please cite this article as: Harrington, L.S., et al., Regulation of multiple angiogenic pathways by Dll4 and Notch in human umbilical vein endothelial cells, Mucrovasc. Res. (2007), doi:10.1016/j.mvr.2007.06.006

ARTICLE IN PRESS

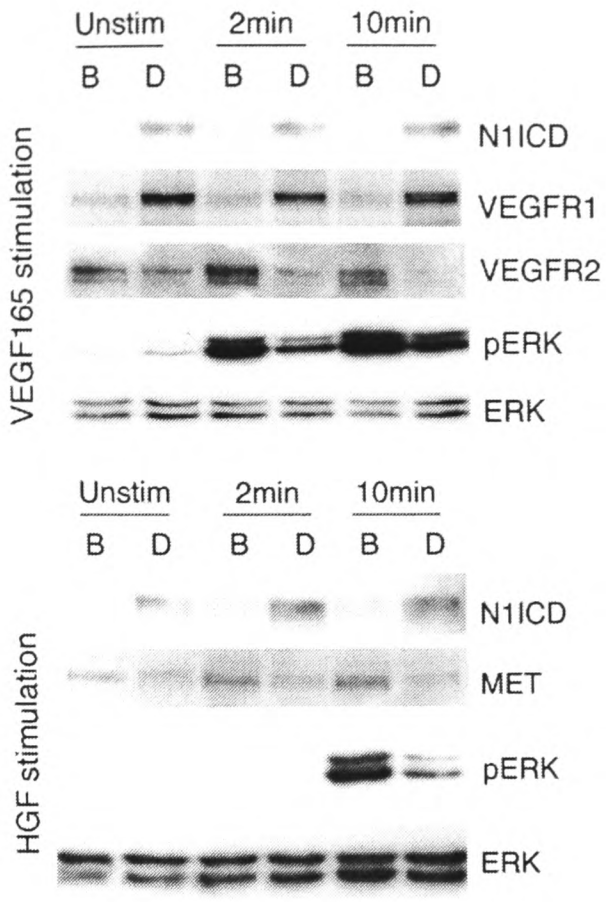


Fig. 3. Activation of ERK by $VEGF_{165}$ and HGF stimulation is impaired in HUVECs cultured on rDll4-coated plates. HUVECs were cultured on Dll4-coated plates for 48 h. 5 h prior to harvesting the cells were starved and then left unstimulated or stimulated with the indicated growth factor (20 ng/mL) for 2 min or 10 min. Activation of ERK is indicated by detection of phosphorylated ERK p42/44 with a phospho-specific antibody and was attenuated in HUVECs cultured on rDll4-coated plates. The blot was stripped and reprobed with total ERK as a loading control. One experiment representative of two is shown.

VEGFR activation. HUVECs cultured on rDll4-coated plates for 48 h prior to starvation and stimulation with 20 ng/mL $VEGF_{165}$, had an impaired ability to phosphorylate and therefore activate ERK (Fig. 3). In addition, in a similar experiment, ERK activation in response to 20 ng/mL HGF stimulation was also impaired demonstrating that the decreased level of MET protein following Dll4 stimulation reduced the ability of HUVEC to respond to HGF (Fig. 3).

Dll4 effects on sprout length in a 3D-tubulogenesis assay

We investigated the effect of Dll4 expression in a 3D-tubulogenesis assay that recapitulates crucial steps characteristic of *in vivo* angiogenesis such as vessel elongation, vessel branching and lumen formation (Nakatsu et al., 2003). In the present study, expression of Dll4 clearly inhibited sprout formation (Fig. 4A). Indeed, HUVECs infected with Dll4-encoding retrovirus only formed short vessels (Fig. 4A) which were about 50% of the length of mock or GFP-encoding empty vector control-infected HUVECs (Fig. 4B). These experiments demonstrated that increased Dll4-induced Notch signalling attenuated tubulogenesis.

PlGF enhances tubulogenesis

In order to investigate whether modulation of VEGF signalling pathway components in the tubulogenesis assay may contribute to the Dll4-induced phenotype described above, we examined the effect of PlGF in this assay. As shown in Fig. 5A, PlGF treatment led to enhanced tubulogenesis. PlGF is downregulated by Dll4 signalling, which has the opposite effect on tubulogenesis in this assay (Fig. 4), suggesting that downregulation of PlGF by Dll4 may contribute to Dll4-induced attenuation of tubulogenesis.

Dll4 signalling enhances PlGF-induced ERK activation

Since Dll4 signalling increased levels of the full-length VEGFR1 receptor the ability of PlGF, the ligand for VEGFR1, to activate ERK in HUVECs cultured on Dll4-coated plates compared to BSA-coated plates was investigated. PlGF-stimulated activation of ERK was enhanced in HUVEC cultured on rDll4-coated plates and was also more prolonged (Fig. 5B).

Discussion

Dll4, the most recently identified Notch ligand, is essential for angiogenesis during embryonic vascular development. Like VEGF, haploinsufficiency of Dll4 is embryonic lethal, demonstrating its importance for successful angiogenesis (Duarte et al., 2004; Gale et al., 2004; Krebs et al., 2004). Recent reports have shown that blockade of Dll4 decreases tumour growth but increases vessel density in contrast to the previously accepted dogma that increased vessel density is associated with increased tumour growth (Noguera-Troise et al., 2006; Ridgway et al., 2006). However the underlying mechanisms by which Dll4-mediated Notch signalling contributes to the control of multiple signalling pathways to coordinate such

Fig. 2. Gene expression changes induced by Dll4 are reflected at the protein level and are inhibited by the γ-secretase inhibitor DAPT. (A) Protein extracts from infected HUVECs or HUVECs cultured on BSA- or Dll4-coated plates for 48 h were separated by SDS-PAGE and immunoblotted. The levels of Hes1 protein (30 kDa) were increased following Dll4 stimulation by both approaches. (B) Culture of HUVECs on Dll4-coated plates compared to BSA-coated plates for 48 h led to an upregulation of STAT1 (84/91 kDa), Jagged1 (150 kDa), full length VEGFR1 (220 kDa), snai2 (30 kDa) and a downregulation of MET protein (145 kDa). (C) Control empty vector retroviral infected cells (E.V.) or full length Dll4-retroviral infected HUVECs (F.L.D4) were cultured for 2 days in the presence of 2 μM DAPT or the equivalent amount of DMSO as a control. DAPT prevented the Dll4-induced mRNA expression changes of elastin, Snai2, sulfatase-1 and PCDH12. One experiment representative of three is shown. mRNA expression changes are represented as a fold change relative to expression in E.V. cells in DMSO. (D) HUVECs were cultured on BSA or rDll4-coated plates for 48 h in the presence of 2 μM DAPT or the equivalent amount of DMSO. DAPT prevented the Dll4-induced changes in protein levels of VEGFR1, VEGFR2, STAT1, MET and Snai2. Blots representative of three independent experiments are shown. (E) HUVECs were cultured on BSA or rDll4-coated plates for 48 h in the presence of 2 μM DAPT or the equivalent amount of DMSO. HUVECs cultured on rDll4-coated plates for 48 h secreted 3.5-fold more sVEGFR1 into the conditioned media than the control HUVEC per mg cellular protein and this was inhibited by DAPT treatment. Error bars represent standard deviation. One experiment representative of two is shown.

Please cite this article as: Harrington, L.S., et al., Regulation of multiple angiogenic pathways by Dll4 and Notch in human umbilical vein endothelial cells, Mucrovasc. Res. (2007), doi:10.1016/j.mvr.2007.06.006

UNCORRECTED PROOF

ARTICLE IN PRESS

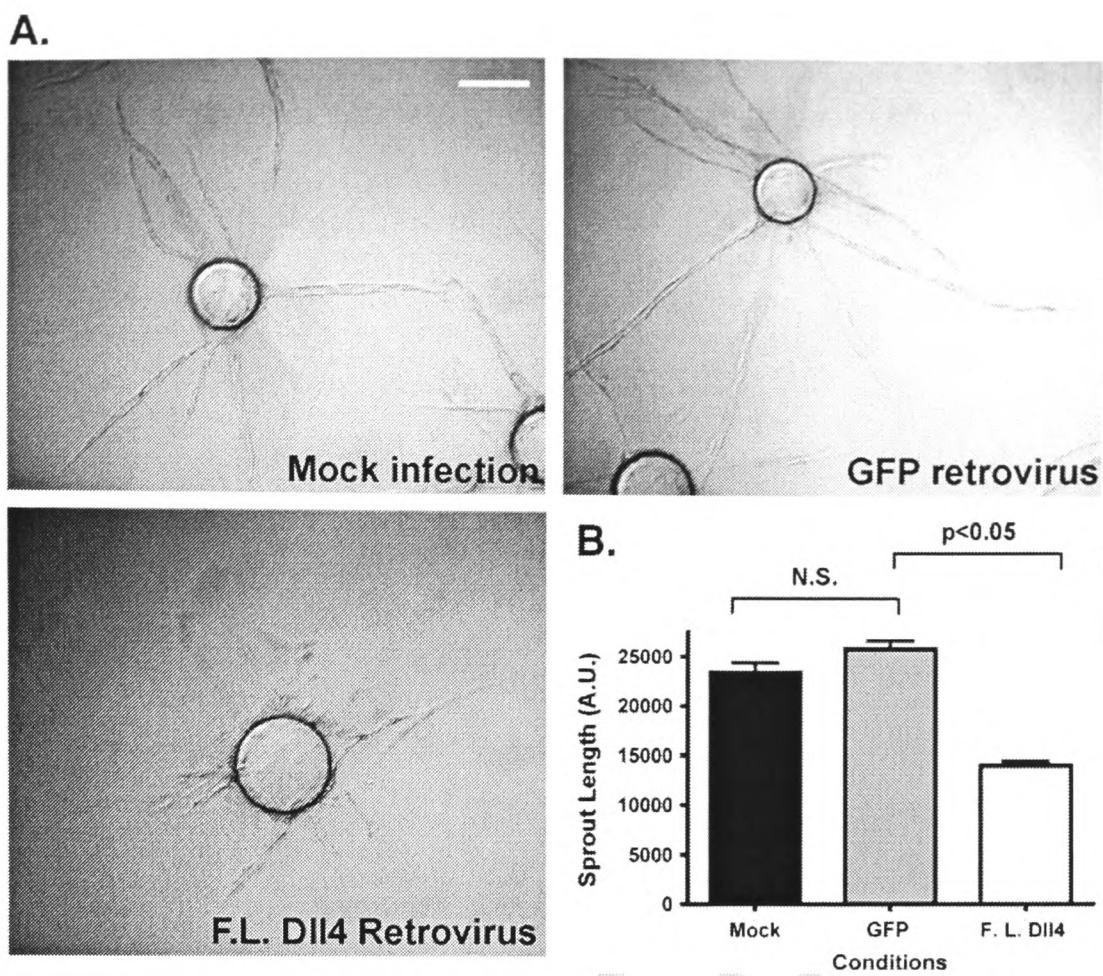


Fig. 4. Ectopic expression of Dll4 inhibits angiogenesis. Single donor HUVECs were infected by retrovirus to express GFP or full-length Dll4 and were compared to mock infected cells for their ability to form tubes in an *in vitro* 3D-tubulogenesis assay. (A) Phase contrast images show a decrease in vessel length (at day 10) following exogenous expression of Dll4. Scale bar represents 100 μm. (B) Quantification of vessel length in arbitrary units (a minimum of 100 sprouts was quantified). Results from one experiment representative of three independent experiments are shown.

complex vascular processes remains unclear. We have recently shown that Dll4 signalling increases tumour growth and decreases vessel density but the resulting vessels are larger and better perfused (Li et al., submitted). We therefore suggest that Dll4 signalling may bring to an end the initial proliferative phase of angiogenesis thus accounting for the decreased vessel number and trigger a maturation phase to refine and stabilise vessels to improve vascular function. This idea is supported by recent *in vivo* data in Dll4+/− mice and using pharmacological inhibitors of Dll4-Notch signalling which demonstrate enhanced angiogenic sprouting and increased vascular proliferation when Dll4 levels or signalling is reduced in the retina or whole embryos (Hellstrom et al., 2007; Lobov et al., 2007; Scehnet et al., 2007; Suchting et al., 2007). However it is unclear how Dll4 regulates these processes and investigating downstream mechanisms was the purpose of this study. Here we identify Dll4-regulated genes which may constitute the mechanism by which Dll4 signalling coordinates such events.

The validity of using a microarray screen to identify Dll4 target genes is demonstrated by the fact that we have identified previously known Notch target genes such as Hey1, and Hes1 (Iso et al., 2003b) consistent with other reports (Patel et al., 2005; Williams et al., 2006).

Dll4 is highly expressed in tumour endothelium and is induced by VEGF and hypoxia (Hainaud et al., 2006; Liu et al., 2003; Mailhos et al., 2001; Patel et al., 2005). Dll4 signalling is known to decrease levels of VEGFR2 and the VEGF co-receptor NRP1 (Williams et al., 2006) but here we demonstrate that Dll4 signalling regulates several more components of VEGF signalling including NRP2 and PlGF (downregulated) and VEGFR1 (upregulated). These findings support recent *in vivo* data where VEGFR2 expression was elevated and VEGFR1 expression was decreased in the retina of Dll4+/− mice compared to wild type controls (Suchting et al., 2007).

By sequestration of VEGF away from VEGFR2 through higher receptor–ligand affinity (Ferrara et al., 2003), VEGFR1 can act as a negative regulator of VEGF action by inhibiting proliferation. Furthermore we have shown here that the inhibitory soluble splice variant of VEGFR1, sVEGFR1, is also upregulated in response to Dll4 contributing to the impairment of VEGF signalling. PlGF can stimulate angiogenesis possibly by displacing VEGF from VEGFR1 (Ferrara et al., 2003). Indeed we have shown enhanced tubulogenesis induced by PlGF in the 3D tubulogenesis assay in agreement with a previous report of PlGF-induced tubulogenesis using primary microvascular endothelial cells (Cai et al., 2003). Here we also show that the increased levels of full length VEGFR1 receptor following Dll4 signalling can enhance ERK activation in response to PlGF thereby indicating that the down regulation of PlGF by Dll4 is an important part of the programme of gene expression changes of VEGF pathway components induced by Dll4 resulting in impaired VEGF signalling. The inhibition of tubulogenesis by Dll4 in the 3D tubulogenesis assay (Fig. 4) is opposite to the effect of PlGF in the same assay suggesting that downregulation of PlGF contributes to this Dll4 phenotype.

Please cite this article as: Harrington, L.S., et al., Regulation of multiple angiogenic pathways by Dll4 and Notch in human umbilical vein endothelial cells, Mucrovasc. Res. (2007), doi:10.1016/j.mvr.2007.06.006

ARTICLE IN PRESS

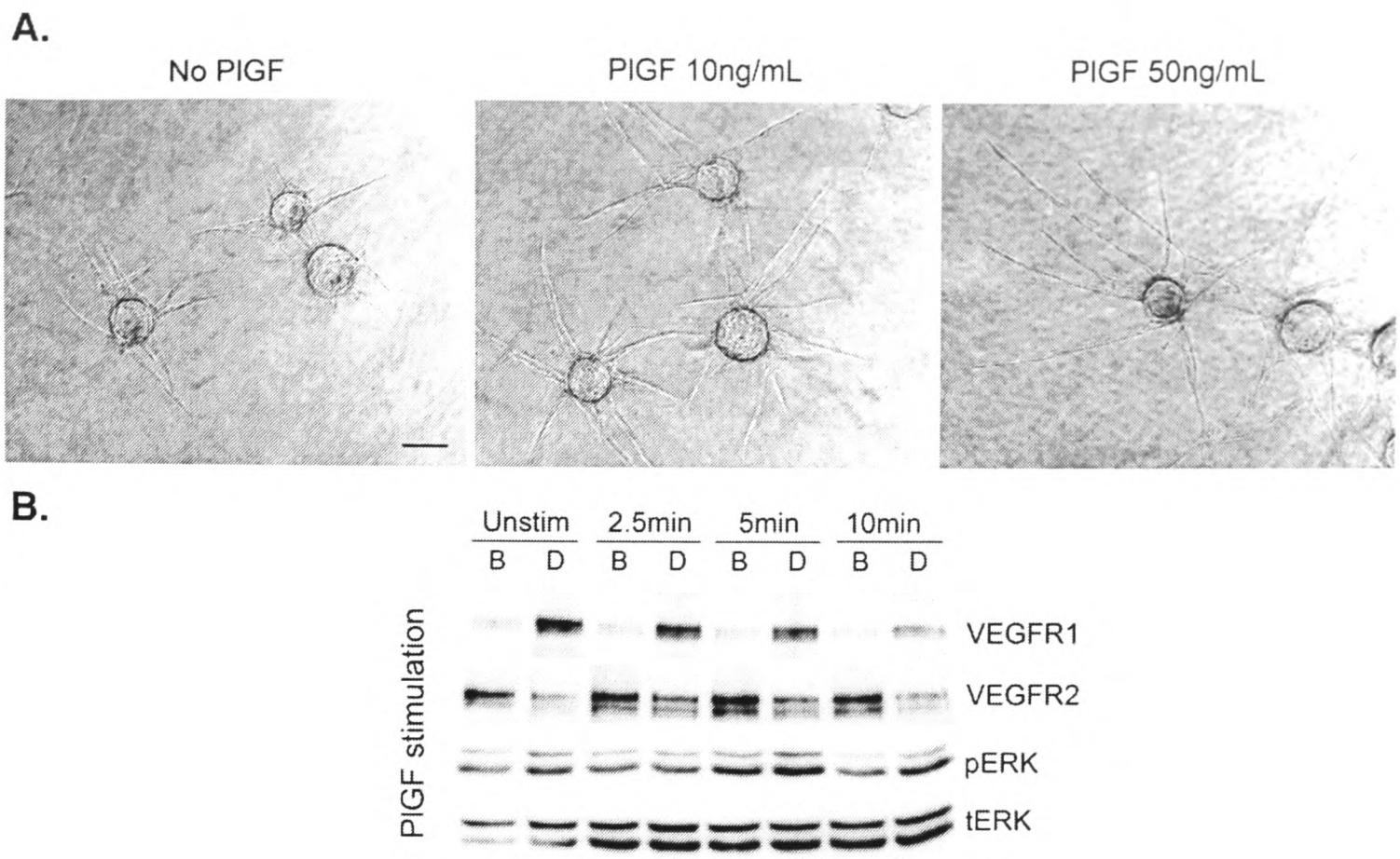


Fig. 5. PlGF enhances tubulogenesis and ERK activation in HUVECs cultured on rDll4-coated plates. (A) HUVECs placed in the 3D tubulogenesis assay were treated 2 days later with vehicle, 10 ng/mL or 50 ng/mL PlGF-supplemented media changing the media every other day for 5 treatments. PlGF treatment led to enhanced tube formation. Scale bar, 100 μm. (B) HUVECs were cultured on BSA- or rDll4-coated plates for 48 h and starved for 5 h prior to stimulation with fresh starvation media supplemented with 10 ng/mL PlGF for the indicated times. PlGF stimulation resulted in enhanced and prolonged ERK activation in HUVECs cultured on rDll4-coated plates compared to control. One experiment representative of three is shown.

Thus these data describe an efficient negative feedback loop whereby Dll4 is induced by VEGF but then reduces the ability of EC to respond to VEGF by regulating multiple components of the VEGF pathway. We demonstrate that all these changes result in impaired activation of ERK in response to $VEGF_{165}$ stimulation in HUVEC cultured on Dll4-coated plates. That this impairment of ERK signalling might contribute to the reduced sprout length in the 3D-tubulogenesis assay is supported by the observation that inhibition of ERK activation reduced tube formation in a similar collagen gel tubulogenesis assay (Yang et al., 2004).

The upregulation of sVEGFR1 by Dll4-Notch signalling is particularly important as its levels could be monitored in serum making it a potentially useful diagnostic tool to identify patients who may benefit from anti-Dll4 therapy and to monitor their response to such therapy. In addition, regulation of the expression of sVEGFR1 by Dll4 raises the possibility that rather than only influencing angiogenesis via signalling to adjacent cells, Dll4 may have an impact on angiogenesis over greater distances by regulation of such soluble factors. Although exogenous PLGF showed some enhancement of signalling associated with full length VEGFR1 upregulation, this was not as extensive as the upregulation of VEGFR1, and it is possible that secreted sVEGFR1 limited this response, although fresh medium was used to stimulate the cells.

Notch signalling is known to inhibit ECs proliferation (Noseda et al., 2004; Sainson et al., 2005; Williams et al., 2006). Results from the cDNA microarray indicate further mechanisms by which Dll4 may limit EC proliferation for example by upregulating the levels of fibulin5 and STAT1 which are known to be involved in reducing EC proliferation (Albig et al., 2006; Battle et al., 2006). A reduction in EC proliferation could contribute to the reduced sprout length phenotype in the 3D tubulogenesis assay and lead to the reduced vessel number in Dll4-expressing tumours *in vivo* (Noguera-Troise et al., 2006; Li et al., submitted).

Activation of the HGF receptor, MET, induces cell proliferation, migration and tubulogenesis and branching morphogenesis and HGF regulates angiogenesis *in vivo* (Rosario and Birchmeier, 2003). A constitutively active form of the Notch4 receptor has been shown to inhibit MET expression in MDA-MB-435β4 cells (Stella et al., 2005) but here we demonstrate that Dll4 signalling downregulated MET mRNA and protein. Furthermore we showed that this Dll4-induced reduction of MET protein impairs the ability of HUVEC to respond to HGF stimulation and activate ERK. These results suggest that Dll4 signalling can negatively modulate key angiogenic pathways.

Dll4 is specifically expressed in arterial ECs (Benedito and Duarte, 2005; Claxton and Fruttiger, 2004; Mailhos et al., 2001) leading to the hypothesis that it is involved in the differentiation of ECs as they mature and that tumour vasculature is arterial in nature. Our data showed that Dll4 signalling downregulated the venous-specific gene NRP2 and upregulated genes associated with arterial vessels such as ephrinB2 (Iso et al., 2006) and elastin which is necessary for the elasticity of arterial vessels. Such a hypothesis is reminiscent of but reciprocal to the role of the orphan nuclear

Please cite this article as: Harrington, L.S., et al., Regulation of multiple angiogenic pathways by Dll4 and Notch in human umbilical vein endothelial cells, Mucrovasc. Res. (2007), doi:10.1016/j.mvr.2007.06.006

ARTICLE IN PRESS

receptor, COUP-TFII, which suppresses Notch signalling and arterial markers such as NRP1 to regulate venous cell fate (You et al., 2005).

Only four genes from our microarray were also regulated by Hey2 overexpression in HUVECs (Chi et al., 2003). The small degree of concordance may reflect differences in array technologies and relative degrees of expression of the constructs but emphasises potential specificity as Dll4 regulates genes independently of one downstream factor, Hey2.

In conclusion, in order to understand the molecular mechanisms behind the effects of Dll4 on EC biology, elucidation of the signal transduction pathways regulated specifically by Dll4 in ECs is essential. Here we report the use of a microarray screen to systematically identify novel Dll4 targets. In accordance with our *in vitro* 3D tubulogenesis assay and recent *in vivo* data, we suggest that Dll4 limits EC proliferation and angiogenesis and triggers the maturation and differentiation of vessels possibly via the novel Dll4 targets identified herein. Elucidation of the functions of these targets in angiogenesis is the focus of our ongoing work.

Acknowledgments

Cancer Research UK; EU 6thFramework Angiotargeting.

Appendix A. Supplementary data

Supplementary data associated with this article can be found, in the online version, at doi:10.1016/j.mvr.2007.06.006.

References

Albig, A.R., Neil, J.R., Schiemann, W.P., 2006. Fibulins 3 and 5 antagonize tumor angiogenesis in vivo. Cancer Res. 66, 2621–2629.

Artavanis-Tsakonas, S., Rand, M.D., Lake, R.J., 1999. Notch signaling: cell fate control and signal integration in development. Science 284, 770–776.

Battle, T.E., Lynch, R.A., Frank, D.A., 2006. Signal transducer and activator of transcription 1 activation in endothelial cells is a negative regulator of angiogenesis. Cancer Res. 66, 3649–3657.

Benedito, R., Duarte, A., 2005. Expression of Dll4 during mouse embryogenesis suggests multiple developmental roles. Gene Expr. Patterns 5, 750–755.

Cai, J., Ahmad, S., Jiang, W.G., Huang, J., Kontos, C.D., Boulton, M., Ahmed, A., 2003. Activation of vascular endothelial growth factor receptor-1 sustains angiogenesis and Bcl-2 expression via the phosphatidylinositol 3-kinase pathway in endothelial cells. Diabetes 52, 2959–2968.

Chi, J.T., Chang, H.Y., Haraldsen, G., Jahnsen, F.L., Troyanskaya, O.G., Chang, D.S., Wang, Z., Rockson, S.G., van de Rijn, M., Botstein, D., Brown, P.O., 2003. Endothelial cell diversity revealed by global expression profiling. Proc. Natl. Acad. Sci. U. S. A. 100, 10623–10628.

Claxton, S., Fruttiger, M., 2004. Periodic Delta-like 4 expression in developing retinal arteries. Gene Expr. Patterns 5, 123–127.

Duarte, A., Hirashima, M., Benedito, R., Trindade, A., Diniz, P., Bekman, E., Costa, L., Henrique, D., Rossant, J., 2004. Dosage-sensitive requirement for mouse Dll4 in artery development. Genes Dev. 18, 2474–2478.

Ferrara, N., Gerber, H.P., LeCouter, J., 2003. The biology of VEGF and its receptors. Nat. Med. 9, 669–676.

Gale, N.W., Dominguez, M.G., Noguera, I., Pan, L., Hughes, V., Valenzuela, D.M., Murphy, A.J., Adams, N.C., Lin, H.C., Holash, J., et al., 2004. Haploinsufficiency of delta-like 4 ligand results in embryonic lethality due to major defects in arterial and vascular development. Proc. Natl. Acad. Sci. U. S. A. 101, 15949–15954.

Hainaud, P., Contreres, J.O., Villemain, A., Liu, L.X., Plouet, J., Tobelem, G., Dupuy, E., 2006. The role of the vascular endothelial growth factor-delta-like 4 ligand/Notch4-Ephrin B2 cascade in tumor vessel remodeling and endothelial cell functions. Cancer Res. 66, 8501–8510.

Hellstrom, M., Phng, L.K., Hofmann, J.J., Wallgard, E., Coultas, L., Lindblom, P., Alva, J., Nilsson, A.K., Karlsson, L., Gaiano, N., et al., 2007. Dll4 signalling through Notch1 regulates formation of tip cells during angiogenesis. Nature.

Irizarry, R.A., Hobbs, B., Collin, F., Beazer-Barclay, Y.D., Antonellis, K.J., Scherf, U., Speed, T.P., 2003. Exploration, normalization, and summaries of high density oligonucleotide array probe level data. Biostatistics 4, 249–264.

Iso, T., Hamamori, Y., Kedes, L., 2003a. Notch signaling in vascular development. Arterioscler. Thromb. Vasc. Biol. 23, 543–553.

Iso, T., Kedes, L., Hamamori, Y., 2003b. HES and HERP families: multiple effectors of the Notch signaling pathway. J. Cell. Physiol. 194, 237–255.

Iso, T., Maeno, T., Oike, Y., Yamazaki, M., Doi, H., Arai, M., Kurabayashi, M., 2006. Dll4-selective Notch signaling induces ephrinB2 gene expression in endothelial cells. Biochem. Biophys. Res. Commun. 341, 708–714.

Karsan, A., 2005. The role of notch in modeling and maintaining the vasculature. Can. J. Physiol. Pharmacol. 83, 14–23.

Krebs, L.T., Shutter, J.R., Tanigaki, K., Honjo, T., Stark, K.L., Gridley, T., 2004. Haploinsufficient lethality and formation of arteriovenous malformations in Notch pathway mutants. Genes Dev. 18, 2469–2473.

Lai, E.C., 2004. Notch signaling: control of cell communication and cell fate. Development 131, 965–973.

Liu, Z.J., Shirakawa, T., Li, Y., Soma, A., Oka, M., Dotto, G.P., Fairman, R.M., Velazquez, O.C., Herlyn, M., 2003. Regulation of Notch1 and Dll4 by vascular endothelial growth factor in arterial endothelial cells: implications for modulating arteriogenesis and angiogenesis. Mol. Cell. Biol. 23, 14–25.

Lobov, I.B., Renard, R.A., Papadopoulos, N., Gale, N.W., Thurston, G., Yancopoulos, G.D., Wiegand, S.J., 2007. Delta-like ligand 4 (Dll4) is induced by VEGF as a negative regulator of angiogenic sprouting. Proc. Natl. Acad. Sci. U. S. A. 104, 3219–3224.

Mailhos, C., Modlich, U., Lewis, J., Harris, A., Bicknell, R., Ish-Horowicz, D., 2001. Delta4, an endothelial specific notch ligand expressed at sites of physiological and tumor angiogenesis. Differentiation 69, 135–144.

Nakatsu, M.N., Sainson, R.C., Aoto, J.N., Taylor, K.L., Aitkenhead, M., Perez-del-Pulgar, S., Carpenter, P.M., Hughes, C.C., 2003. Angiogenic sprouting and capillary lumen formation modeled by human umbilical vein endothelial cells (HUVEC) in fibrin gels: the role of fibroblasts and Angiopoietin-1. Microvasc. Res. 66, 102–112.

Noguera-Troise, I., Daly, C., Papadopoulos, N.J., Coetzee, S., Boland, P., Gale, N.W., Lin, H.C., Yancopoulos, G.D., Thurston, G., 2006. Blockade of Dll4 inhibits tumour growth by promoting non-productive angiogenesis. Nature 444, 1032–1037.

Noseda, M., Chang, L., McLean, G., Grim, J.E., Clurman, B.E., Smith, L.L., Karsan, A., 2004. Notch activation induces endothelial cell cycle arrest and participates in contact inhibition: role of p21Cip1 repression. Mol. Cell. Biol. 24, 8813–8822.

Patel, N.S., Li, J.L., Generali, D., Poulsom, R., Cranston, D.W., Harris, A.L., 2005. Up-regulation of delta-like 4 ligand in human tumor vasculature and the role of basal expression in endothelial cell function. Cancer Res. 65, 8690–8697.

Patel, N.S., Dobbie, M.S., Rochester, M., Steers, G., Poulsom, R., Le Monnier, K., Cranston, D.W., Li, J.L., Harris, A.L., 2006. Up-regulation of endothelial delta-like 4 expression correlates with vessel maturation in bladder cancer. Clin. Cancer Res. 12, 4836–4844.

Ridgway, J., Zhang, G., Wu, Y., Stawicki, S., Liang, W.C., Chanthery, Y., Kowalski, J., Watts, R.J., Callahan, C., Kasman, I., et al., 2006. Inhibition of Dll4 signalling inhibits tumour growth by deregulating angiogenesis. Nature 444, 1083–1087.

Rosario, M., Birchmeier, W., 2003. How to make tubes: signaling by the Met receptor tyrosine kinase. Trends Cell Biol. 13, 328–335.

Sainson, R.C., Aoto, J., Nakatsu, M.N., Holderfield, M., Conn, E., Koller, E., Hughes, C.C., 2005. Cell-autonomous notch signaling regulates endothelial

UNCORRECTED PROOF

Please cite this article as: Harrington, L.S., et al., Regulation of multiple angiogenic pathways by Dll4 and Notch in human umbilical vein endothelial cells, Mucrovasc. Res. (2007), doi:10.1016/j.mvr.2007.06.006

ARTICLE IN PRESS

cell branching and proliferation during vascular tubulogenesis. FASEB J. 19, 1027–1029.

Scehnet, J.S., Jiang, W., Ram Kumar, S., Krasnoperov, V., Trindade, A., Benedito, R., Djokovic, D., Borges, C., Ley, E.J., Duarte, A., Gill, P.S., 2007. Inhibition of Dll4-mediated signaling induces proliferation of immature vessels and results in poor tissue perfusion. Blood 109, 4753–4760.

Shawber, C.J., Kitajewski, J., 2004. Notch function in the vasculature: insights from zebrafish, mouse and man. BioEssays 26, 225–234.

Shutter, J.R., Scully, S., Fan, W., Richards, W.G., Kitajewski, J., Deblandre, G.A., Kintner, C.R., Stark, K.L., 2000. Dll4, a novel Notch ligand expressed in arterial endothelium. Genes Dev. 14, 1313–1318.

Smyth, G.K., 2004. Linear models and empirical bayes methods for assessing differential expression in microarray experiments. Stat. Appl. Genet. Mol. Biol. 3 (Article3).

Smyth, G.K., Speed, T., 2003. Normalization of cDNA microarray data. Methods 31, 265–273.

Stella, M.C., Trusolino, L., Pennacchietti, S., Comoglio, P.M., 2005. Negative feedback regulation of Met-dependent invasive growth by Notch. Mol. Cell. Biol. 25, 3982–3996.

Suchting, S., Freitas, C., le Noble, F., Benedito, R., Breant, C., Duarte, A., Eichmann, A., 2007. The Notch ligand Delta-like 4 negatively regulates endothelial tip cell formation and vessel branching. Proc. Natl. Acad. Sci. U. S. A. 104, 3225–3230.

Varnum-Finney, B., Wu, L., Yu, M., Brashem-Stein, C., Staats, S., Flowers, D., Griffin, J.D., Bernstein, I.D., 2000. Immobilization of Notch ligand, Delta-1, is required for induction of notch signaling. J. Cell Sci. 113 (Pt. 23), 4313–4318.

Villa, N., Walker, L., Lindsell, C.E., Gasson, J., Iruela-Arispe, M.L., Weinmaster, G., 2001. Vascular expression of Notch pathway receptors and ligands is restricted to arterial vessels. Mech. Dev. 108, 161–164.

Williams, C.K., Li, J.L., Murga, M., Harris, A.L., Tosato, G., 2006. Up-regulation of the Notch ligand Delta-like 4 inhibits VEGF-induced endothelial cell function. Blood 107, 931–939.

Yang, B., Cao, D.J., Sainz, I., Colman, R.W., Guo, Y.L., 2004. Different roles of ERK and p38 MAP kinases during tube formation from endothelial cells cultured in 3-dimensional collagen matrices. J. Cell. Physiol. 200, 360–369.

You, L.R., Lin, F.J., Lee, C.T., DeMayo, F.J., Tsai, M.J., Tsai, S.Y., 2005. Suppression of Notch signalling by the COUP-TFII transcription factor regulates vein identity. Nature 435, 98–104.

UNCORRECTED PROOF

Please cite this article as: Harrington, L.S., et al., Regulation of multiple angiogenic pathways by Dll4 and Notch in human umbilical vein endothelial cells, Mucrovasc. Res. (2007), doi:10.1016/j.mvr.2007.06.006